جامعة البحرين
المكتبة
LIBRARY
University of Bahrain

UNIVERSITY OF READING

Task Space Robot Hand Manipulation and Optimal Distribution of Fingertip Force Functions

A Thesis Submitted For the Degree of Doctor of Philosophy

By

Ebrahim Abdulla Al-Gallaf

Department of Cybernetics

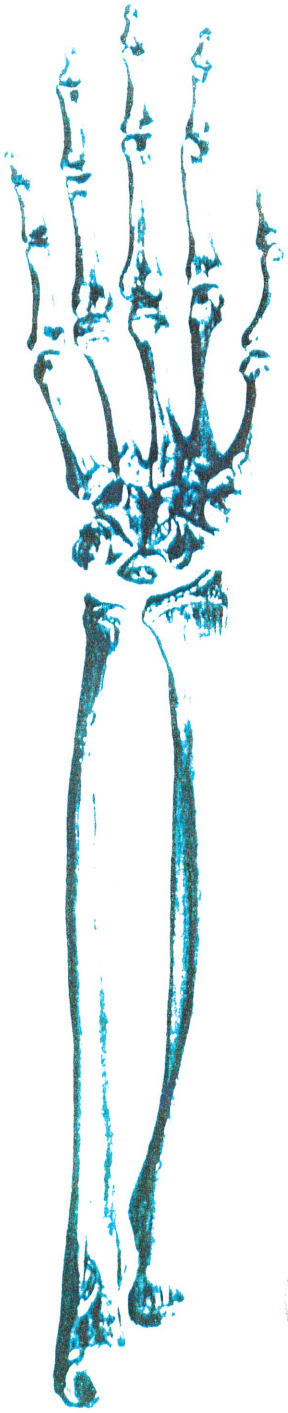
School of Engineering and Information Sciences,

Whiteknights,

University of Reading

May 1994.

GIFT هَدِيَّة



جامعة البحرين
الحكيم
LIBRARY
University of Bahrain

ABSTRACT

This research frame work investigates the aspects of manipulation, based on a four digit, anthropomorphic robot hand (built for research purposes and designated as the Cybhand). The thesis has looked in detail at three aspects of task-space object manipulation, where position and force control, are acting simultaneously on the object.

Firstly, a force feedback control system was constructed. Force sensing was achieved by sensing the tension in tendons.

The second aspect, of object manipulation and force distribution, investigates the techniques involved in generating torques to move the hand and to grasp an object in an optimal way. Optimization of the contact forces was achieved, by the employment of nonlinear constraints inequality, with a quadratic cost function to reduce the grasping energy. This method has proven its advantage in reducing the computation time required to converge to an optimal force function. Use of optimization has been based on the computation of the dynamic model of the entire hand, and compared with the four fingered null-space solution or *internal forces optimization.*

The third aspect deals with the singularity problem. The research has investigated the problem of an *ill-conditioned* hand configuration, when the entire hand Jacobian becomes a singular matrix, resulting in infinite forces applied to the object. *Robust singularity inversion* techniques were employed to invert the matrix of the multiple contact system. Using *singular value decomposition* techniques, it has been shown that :

i) the manipulability measure of each finger can be utilized to invert the hand Jacobian.

ii) the manipulability measure of a single finger is enough to be employed if certain kinematic conditions are satisfied.

ACKNOWLEDGEMENTS

I would like to take this opportunity to thank Professor Kevin Warwick for his guidance and encouragement through the course of this research.

I am very grateful to my supervisor, Mr. Aurther Allen, for his help, he has always had endless patience and managed to put me back on the right course when necessary.

I would like to take this opportunity to thank family, colleagues and friends who helped and encouraged me during my research. In particular, (I would like to thank) my mother Mrs Moza AL-Gallaf for her moral, patience and financial support, and (thanks to) all the members of my family, especially to my young nephew Hamad AL-Gallaf.

Thanks to Dr. Mike Usher, the postgraduate tutor, for his help in conducting the requirements of the course, to the secretaries Liz Lucas and P. Mason for their help, to all the staff, friends and colleagues in the department for their support, to Les Comley, John Dickens, Chris King, (for his help in the mechanical work-shop), to Nigle Archer and Leo Kiernan (my first year friends), Darren Wenn, Neil Glover, and Grant Foster and thanks to the other colleagues with 'no life' who provided companionship during the twilight hours.

Also thanks to Dr. Sallie Vaughn of the Maths department for helping me under-stand the NAG optimization library and thanks to Dr. Colin Bridgewater. Finally thanks to all members of Cybernetics whose companionship I will always remember.

TABLE of CONTENTS

CHAPTER ONE : *MANIPULATION BASED on ROBOTS HANDS.*

(1.1) INTRODUCTION ---------- 1-2

(1.2) ROBOTICS HANDS ---------- 1-6

(1.3) GENERAL PURPOSE ROBOT HANDS and DESIGN TECHNIQUES ---------- 1-9

(1.4) OBJECT MANIPULATION by FINGERTIPS MOTION ---------- 1-13

(1.5) GRASP STIFFNESS and COMPLIANCE MOTION ---------- 1-27

(1.6) GRASP STABILITY and SYNTHESIS ---------- 1-33

(1.7) ARTICULATED SYSTEMS DYNAMICS ---------- 1-35

(1.8) INTRODUCTION to the RESEARCH ---------- 1-37

CHAPTER TWO : *THE DEVELOPMENT of a FOUR FINGERED ROBOT HAND.*

(2.1) INTRODUCTION ---------- 2-2

(2.2) HUMAN HAND ---------- 2-3

(2.3) SYSTEM STRUCTURE ---------- 2-4

(2.4) THE DESIGN of the ARTICULATED HAND ---------- 2-5

CHAPTER THREE : *MODELLING of CYBHAND KINEMATICS*

(3.1) INTRODUCTION ---------- 3-2

(3.2) FRAME ASSIGNMENTS ---------- 3-3

(3.3) FORWARD KINEMATICS FORMULATION ---------- 3-4

(3.4) INVERSE KINEMATICS ---------- 3-7

(3.5) FINGER JACOBIAN J_Θ ---------- 3-10

(3.6) CONFIGURATION SPACE and TIP MAPPING ---------- 3-16

(3.7) OBJECT-HAND KINEMATICS ---------- 3-26

(3.8) EFFECT of FOUR CONTACT FINGERTIPS ---------- 3-31

CHAPTER FOUR : *HAND POSITION and FORCE CONTROL*

(4.1) INTRODUCTION ---------- 4-2

(4.2) HAND HARDWARE DESCRIPTION ---------- 4-3

(4.3) JOINT FORCE CONTROL ---------- 4-10

CHAPTER FIVE : *OPTIMIZATION of STATIC GRASPING FORCES*

(5.1) INTRODUCTION ---------- 5-2

(5.2) GRASPING THEORY ---------- 5-3

(5.3) OBJECT-HAND CLOSED DYNAMIC SYSTEM ---------- 5-9

(5.4) FORCE DISTRIBUTION PROBLEM ---------- 5-10

(5.5) EMPLOYMENT of NONLINEAR CONSTRAINTS
in FORCE OPTIMIZATION ---------- 5-28

(5.6) STATIC GRIPPING of OBJECTS ---------- 5-34

CHAPTER SIX : *COORDINATED DYNAMIC CONTROL and OPTIMIZATION of FINGERS DYNAMIC MANIPULATION FORCES.*

(6.1) INTRODUCTION ---------- 6-2

(6.2) HAND-OBJECT MOTION ---------- 6-3

(6.3) OBJECT-HAND DYNAMICS ---------- 6-4

(6.4) OBJECT MOTION with CONTACT FORCES ---------- 6-10

(6.5) CARTESIAN ROBUST-SINGULARITY- INVERSE (RSI) ---------- 6-16

(6.6) DYNAMIC FORCES COMPUTATION BASED
on OPTIMIZATION APPROACH ---------- 6-25

(6.7) COMPARISON BETWEEN LINEAR and NONLINEAR
FORCE OPTIMIZATION ---------- 6-39

CHAPTER SEVEN : *PARALLEL COMPUTATION APPROACH of CONSTRAINED MOTION.*

(7.1) INTRODUCTION ---------- 7-2

(7.2) NATURE of PARALLEL COMPUTATION ---------- 7-3

(7.3) ASPECTS of PARALLEL COMPUTATION
of the HAND DYNAMICS ---------- 7-4

(7.4) HAND DYNAMICS ---------- 7-14

(7.5) PARALLEL REQUIREMENTS
COMPUTATION of J_h and J_h^{-1} ---------- 7-14

(7.6) PARALLEL REQUIREMENTS for LINEAR
and NONLINEAR CONSTRAINTS OPTIMIZATION ---------- 7-16

CHAPTER EIGHT : ***CONCLUSIONS REMARKS and FURTHER RESEARCH***

(8.1) INTRODUCTION ---------- 8-2

(8.2) THE HAND DESIGN ---------- 8-3

(8.3) HAND KINEMATICS ---------- 8-4

(8.4) EMPLOYMENT of FORCE FEEDBACK ---------- 8-5

(8.5) FORCE COMPUTATION AND OPTIMIZATION ---------- 8-6

(8.6) CONSTRAINED DYNAMICS and SINGULARITY PROBLEM ---------- 8-7

(8.7) PARALLEL COMPUTATION of HAND DYNAMICS ---------- 8-8

(8.8) GENERAL AREA of RESEARCH ---------- 8-8

APPENDIX A-1 ---------- A1-1
APPENDIX A-2 ---------- A2-1
APPENDIX A-3 ---------- ---------- A3-1
APPENDIX A-4 ---------- A4-1
APPENDIX A-5 ---------- A6-1

REFERENCES ---------- REF -1

Nomenclature

L : *Lagrangian* function of one finger.

f_{tip} : A vector of all fingertips forces $f_{tip}^{T} = [f_{1tip} \;\; f_{2tip} \;\; f_{3tip} \;\; f_{4tip}] \in \Re^{12\times1}$

F_b : Resultant force and moment vector of the grasped object $\in \Re^{6\times1}$.

G : Grip transform of an object (*or grip matrix*) $\in \Re^{6\times12}$.

$U\Sigma V$: Three matrices of *singular value decomposition* of a matrix of Jacobian.

$r_i^T = [x_i, \; y_i, \; z_i]$: vector from object centre of mass to an *ith* point of contact.

$\ddot{\Theta}_c$: Constrained acceleration of the hand-object including *differential Jacobian*, $\in \Re^{12\times1}$

Θ_h : Joint space vector of the entire hand $\in \Re^{12\times1}$

m_o : Object mass.

E : An identity matrix of appropriate dimension, $\in \Re^{n\times n}$

θ_{ij} , $\dot{\theta}_{ij}$, $\ddot{\theta}_{ij}$: *jth* joint position , velocity, and acceleration in the *ith* finger

M_i, N_i and C_i ; Inertia, centrifugal and coriolis and gravity matrices of *ith* finger.

J_i : Definite matrix representing a particular finger Jacobian $\in \Re^{3\times3}$

μ_i : Frictional constant at the *ith* point of contact.

f_x, f_y, f_z : Three forces at a particular point of contact.

H_c : Contact matrix defining the transmitted forces $\in \Re^{3\times6}$.

η : *Null space* of the grip transform $\in \Re^{12\times6}$.

λ : Vector of of internal forces magnitudes $\in \Re^{6\times1}$

$[\upsilon_b ; \omega_b]$: An object linear and rotational velocity vectors $\in \Re^{6\times1}$

J_h^R : Robust singularity inverse of hand Jacobian.

B_g : Matrix of decomposition into grasping forces.

CHAPTER ONE

INTRODUCTION TO MANIPULATION BASED ON ROBOTICS HANDS

(1.1) INTRODUCTION

Manipulation using robotics began less than thirty years ago when the first computer controlled machine was demonstrated. Since that time scientists and engineers have designed hundreds of different manipulators and shown different applications. To day's industrial robots usually consist of six-jointed arms with a simple gripper or "*end-effector*" for grasping objects. In a typical application, robots are fixed firmly to the floor or to the wall and commanded by a computer to perform physical operations on the environment they are facing. Most robotic manipulators are competent only to perform the simplest functions; there are many instances of spray painting and welding robots programmed to perform certain pre-defined tasks.

Some robots can be programmed to move about the environment in a predefined strategy in order to perform simple tasks. There are some cases of complex robotic assembly, but these usually involve extensive fixtures and special tooling. Even the simplest assembly operations, such as getting and putting involve a complex sequence of motions and sensory operations. As the reliability and precision of industrial robots have increased, they have been applied to a variety of unusual tasks. Many of these applications involve dangerous or unpleasant working conditions, exacting quality control requirements, or other features that make it especially desirable to use robots in place of human workers.

The manipulation of different objects can be achieved by the use of different grippers or tools which require the robot arm to change its end-effector for different objects. This solution of providing robots with an array of grippers or gripper-adaptors, is practical in many instances but has drawbacks: it becomes expensive to keep an inventory of grippers, the robot slows down if it pauses frequently to change grippers and, if tactile and force sensors are added, it becomes difficult to make connections

between the gripper and the wrist. Furthermore, a significant proportion of the cost of operating a manipulator is in the development of specialized end-effectors for each task.

Another approach to improve object manipulation is to employ a robot arm with an articulated end-effector attached to its last link. Articulated end-effectors can be designed to have a kinematic structure similar to the human hand, and hence a kinematically similar robotics hand can be achieved. A universal gripper would be able to grasp every part the robot might encounter. Recent universal gripper designs have used the human hand as a source of inspiration.

To understand manipulation using multi-fingered hands, it is necessary to appreciate how objects move when humans touch and push them. Specifically, articulated hands are devices with two or more powered joints that can grip and manipulate objects. Articulated hands appear to offer some solutions to a number of problems found in object manipulation using conventional end-effectors. In fact, research has been directed towards the design and control of complex end-effectors to increase the *dexterity* and *adaptability* of a robot. The main issue has been operating robot manipulators (mostly in manufacturing environments) with a device that consists of the palm and fingers of actively powered joints. It would be convenient to think of a robot manipulator as a machine that performs tasks simply by adapting its task planning, however, the state of the art in robot hand design is still far away from this ambition.

The future view of robot hands carries within it the wide spectrum of applications both in the domestic and the industrial fields. Robot hands are being planned to be employed in surface cleaning in hostile environments where compliance of the fingers

links is an important issue. Robot hands are the essentials of tele-robotics and space applications where different dynamic parameters govern the motion of the hand. In addition to this, they are employed in object manipulation and assembly tasks where forces have to be controlled. On the other side of hand application comes the technology and aspects of hand designs. Four fingered robot hands can enhance an object stability, however, complicated control designs are required.

Although multi-fingered robotics hands offer certain advantages over conventional robotics grippers in tasks which require dextrous manipulation, they are much more complex mechanical systems and their design and control must take into consideration the forces which can be generated during grasping and manipulation. One of the problems which is of considerable interest is that of finding the finger-object contact forces and the actuator torques necessary to effect a prescribed motion of the hand-object system. In addition to that, when an object is grasped such that the hand becomes redundantly-actuated the contact force equations do not have a unique solution. The kinematics of a mechanical hand handling an object vary discretely with time. Each joint in the kinematic chain is driven by an actuator which is controlled to effect a certain motion between the links which it couples.

When the number of actuators in the kinematic chain exceeds its degree of freedom (DOF) , the system is known to be *redundantly actuated* with a certain redundancy. As more fingers come into contact with the grasped object, the DOF of the system decreases. If all the finger actuators remain powered, then more actuators are powered than there are degrees of freedom, which can lead to the generation of large forces within the system, or the crushing of the grasped workpiece.

Rather than attempting to avoid redundant actuation by turning off certain actuators,

it is desirable to exploit it by optimizing the forces the hand exerts on the grasped object and / or the force distribution within the hand. Once a set of optimum forces is found, it can be used as a set point in a force controller loop. Thus, the finger-object contact forces can be reduced, reducing chances of slippage and crushing. Also, a redundantly actuated robotics hand has the advantage of increasing the object manipulability and allows greater safety in case of breakdown of individual actuators.
In order to find an optimal solution to the force distribution on an object, several techniques have been implemented, one being, the *Quadratic Optimization Algorithm* (QOA), which has certain features that allow the minimization of the objects internal forces based on linearizing the frictional cone constraint present at the contact.

Hence, for accurate modelling of the nonlinear contact cone, it is necessary to investigate the aspects of computing the fingertip forces using optimization methods.

Employing the nonlinear friction cone constraints affect static, dynamic grasping, and reduce the number of constraints especially when a real time control is required.

Furthermore, robot hands are complicated mechanical devices which need to be instructed from a higher level of control. One aspect of instructing a robot hand motion is under hand-camera coordination. From static grasping, STANSFIELD [1991] coordinated a robot hand to produce stable grasping of known objects. For dynamic manipulation, the concept of transforming the object's cartesian motion from camera coordinate to the joint space coordinate is constrained by the fact the object may move within singular configuration of the hand. As will be further discussed, at singular configuration the entire hand Jacobian is not invertible and so hand-camera coordination can not be achieved. Other methods of inverting the hand Jacobian can be

achieved using certain measures of dexterity.

(1.2) ROBOTICS HANDS

1.2.1) MULTI-DEGREES OF FREEDOM GRIPPERS

Efforts have been directed towards multi-fingered robot hands because:

(*i*) Parallel jaw grippers can assume a limited range of configurations, since having only one degree of freedom in a hand limits the choice of grasping configurations, SALISBURY [1984].

(*ii*) It is unreasonable to expect large, massive links in a robot arm to be able to cover a large working volume and simultaneously have high bandwidth and sensitivity, SALISBURY [1984].

(*iii*) Multi-fingered hands provide for a unique sensing modality; the cooperation of position, force and tactile and proximity sensors provides an opportunity for obtaining information about the mechanical and physical attributes of objects and tasks.

(*iv*) There is need for mechanical interfacing between the end-effector and the arm due to (*a*) Robot oscillation. (*b*) Robot programming errors. (*c*) Unexpected environmental forces and displacements. (*d*) Part fixing errors, SALISBURY and CRAIG [1982].

(*v*) Dexterous hands can be used in direct human control, e.g where they are utilised in hazardous locations, as in ROHLING and HOLLERBACH [1993].

(*vi*) The versatility of robot hands arises from the fact that fine motion manipulation can be accomplished through relatively fast and small motions of the fingers, so they can be used for different objects, ZEXIANG *et al.* [1989].

(*vii*) Contemporary industrial robots are not suited to operating in unstructured environments, so the range and complexity of the tasks they can perform is limited. Multi-fingered hands have the potential for improving on this deficiency, their continued development holds the prospect of the application of robot technology to a wider variety of manufacturing tasks, MCAREE *et al.* [1991].

1.2.2) A GENERAL VIEW OF MANIPULATION SCIENCE

In a manufacturing environment, the use of the hand to obtain an effective grasp and the manipulation of the grasped object to achieve a given task are objectives which have led to a division of manipulation science into. : {1} Task Planning. {2} Hand design. {3} Grasping issues. {4} Hand Control. {5} Hand Sensing, as illustrated in Fig [1.1]. Furthermore each topic is further sub-divided into a number of concerns, some are related to others depending on a specific task requirement.

TASK PLANNING This develops a sequence of homogeneous manipulations for the hand to execute the task while providing the necessary transition of grips. Since most tasks require a number of different grasps, task planning is required to develop the necessary hand motions. In order to perform these tasks the robot must be able to change from one grip to another, possibly using a very different intermediate grip. Change must be done in real time without losing control of the object, MISHRA *et al.* [1989].

HAND DESIGN The human hand is protypical of a general purpose manipulator. Do we have to begin our design so that we end with an anthropomorphic hand? Do we need different designs to execute specific tasks? How many fingers are needed? What size should each finger be? How many joints per finger? Do we need hands designed to execute specific tasks? These questions need to be considered while

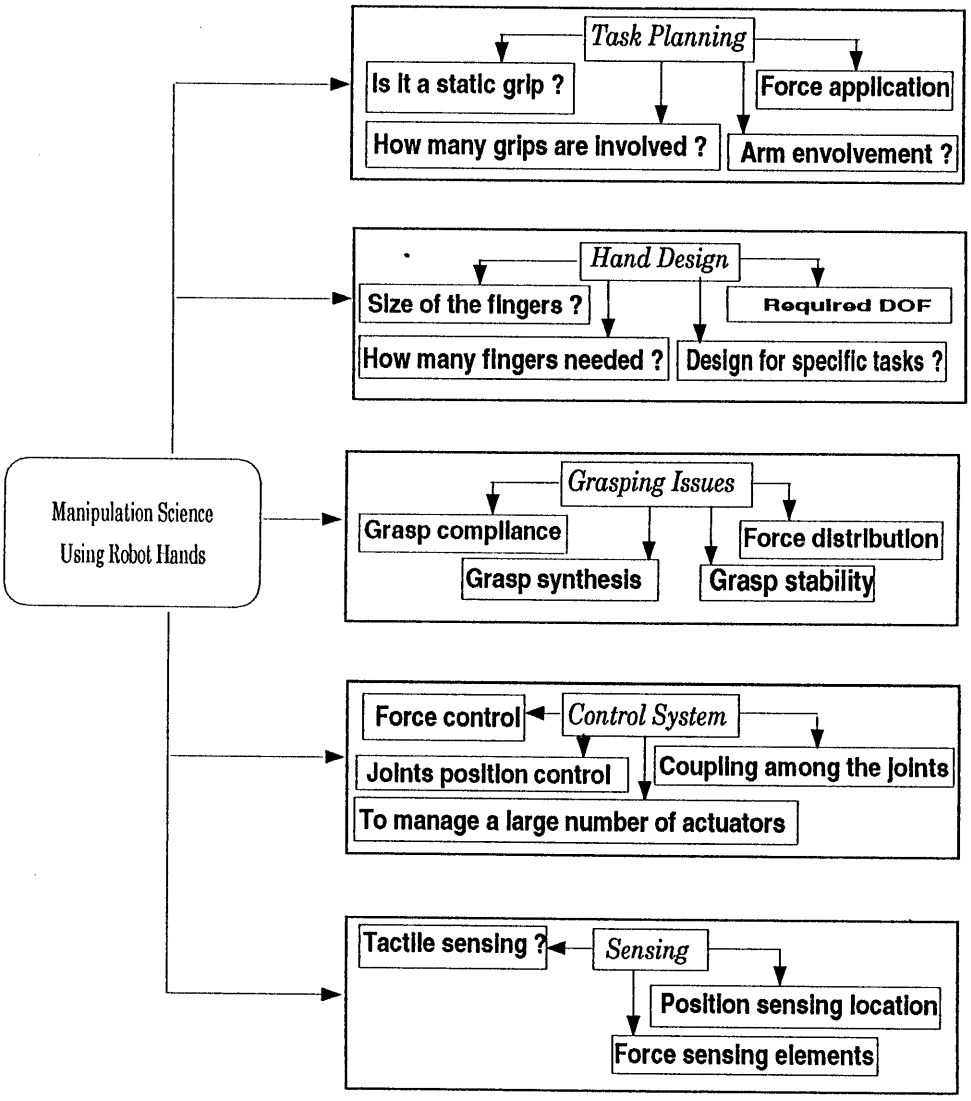


Figure 1.1 : Subdivision of Manipulation Based on Robot Hands.

designing multi-fingered robot hands.

GRASPING ISSUES Grasping is an important topic into which researchers have put a lot of effort. Grasping of objects by a multi-fingered robot hand is more complicated than the manipulation of an object rigidly attached to the end of a six-axis robotic arm for three reasons : (*i*) The kinematic relations between finger joint motion and object motion are complicated. (*ii*) The hand has to firmly grasp the object during its motion. (*iii*) The two complementary issues of position and force trajectories. While manipulating an object under a pre-defined strategy, some joints have to follow a force trajectory, the others follow a position trajectory, and switching from one state to another is not an obvious task, AL-GALLAF *et al.* [1991].

CONTROL SYSTEM It is the control which deals with hardware such as motors, sensors,. . , etc. , and higher software levels including the task planning. A control system should be built to manage a large number of actuators at the same time, and to adapt its strategy according to a given task. How the control system has interacted with previously considered issues is a vital problem that determines the dexterity achievement of a robot hand.

SENSING In some previous hand designs, sensing was considered as a part of the hand mechanical design. This is because consideration should be given to where various sensing elements should be fixed, what size of area they are to be fitted in, and how electrical conductors are passed to them. Tactile sensing is a branch of sensing which provides the hand control system with full updated information of the interaction between the hand and the environment it is facing.

As an attempt to survey some works in this area, the next section has been divided into two main sub-sections. The first gives a brief survey of some designed general

purpose manipulators, while the second discusses some grasping issues related to robotic hands.

(1.3) GENERAL PURPOSE ROBOT HANDS AND DESIGN TECHNIQUES.

A large variety of grippers have been designed for industrial use. These special purpose devices use not only fingers, but suction cups, magnetic tentacles, and adhesives to achieve their gripping function, MASON and SALISBURY [1985]. Some attempts have been made to design grippers that can actively move the grasped object and manipulate it in a pre-defined manner, notable amongst these are:

1) ASADA and HANAFUSA , GRUPEN *et al.* [1989].

2) OKADA manipulator, OKADA [1979].

3) Stanford/JPL hand, SALISBURY and CRAIG [1982].

4) LIAN Manipulator, GRUPEN *et al.* [1989].

5) Utah/MIT hand, JACOBSEN *et al.* [1984].

6) Belgrade hand, GRUPEN *et al.* [1989].

7) WABOT-2 Arm, SUGANO and KATO [1987].

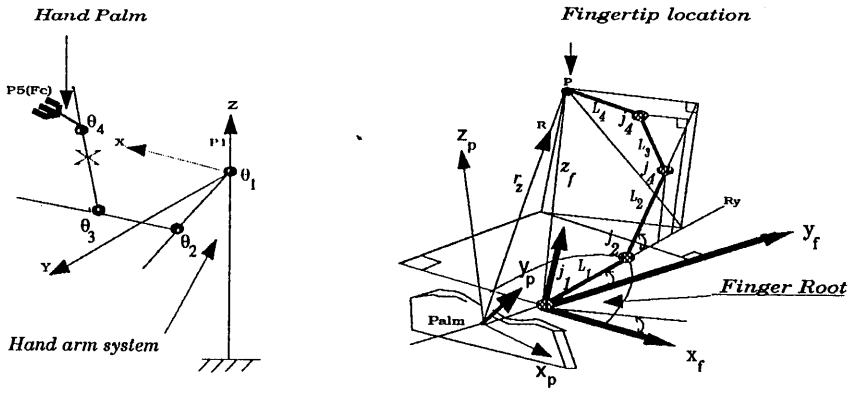
8) Southampton Glovebox, CROWDER [1991-a].

9) Micro-actuator robotic hand, KOICHI *et al.* [1991].

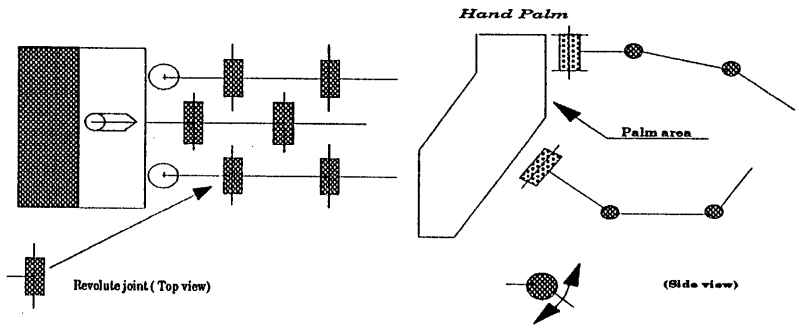
10) MONASH Dextrous gripper, RUSSELL [1990].

1.3.1) OKADA MANIPULATOR [1979]

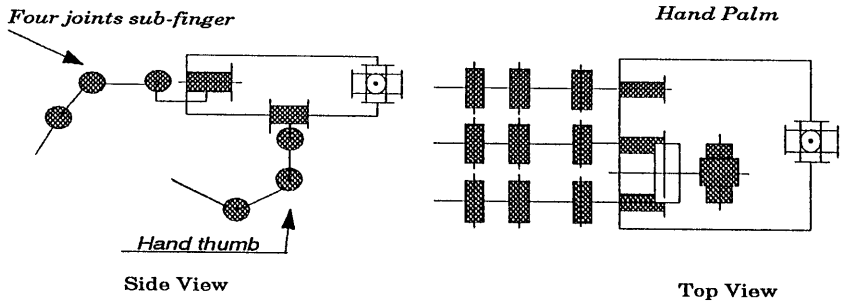
OKADA developed an industrial object handling system which consisted of an arm/wrist with five degrees of freedom attached to an eleven degree of freedom robot hand, as shown in Fig [1.2-a]. There are three fingers, each has four degrees of freedom, whereas the thumb has only three degrees of freedom. OKADA's hand itself is a



a



b



c

Figure 1.2 : Examples of Multi-fingered Robots Hands Design.
a : OKADA HAND.
b : STANFORD / JPL HAND.
c : UTAH / MIT HAND.

simple prototype of the human hand. The finger has been designed to have a circular shape, since the circular cross section is suitable to suppress the rapid change of the grasping condition which arises during complicated finger motion, OKADA [1979]. To make the finger flexible and the finger subsystem more compact, cables, hoses and signal lines of sensors are made to pass through the finger tubes. Motors for driving the finger's joints are located within a trunk separated from the fingers. The bending angle of each joint and the corresponding torque are indirectly detected from a potentiometer and the value of the motor current in the trunk. The finger control consists of a hybrid position/torque servo implemented in hardware. OKADA has demonstrated the ability of the hand by to grasp and manipulate an object by gathering data in terms of set points (defining fingertip positions) under the manual mode of position control.

1.3.2) STANFORD / JPL HAND [1982]

The Stanford/JPL hand was motivated by anthropomorphic attention and kinematic and control concerns. The final hand design was based on a number of analytical and intuitive procedures. A simulation of the hand was used to optimize relative finger locations, link lengths and joint range motions.

Each finger consists of three joints, as illustrated in Fig [1.2-b], the first and the second joints have ranges of 90°, while the last joint has a range of +/– 135 °. In order to power closely spaced joints Salisbury located 12 motors at a distance from the hand and transmitted forces through teflon coated steel cables (or tendons) passing through sheathes of close wound springs. Although joints could be actuated with ten tendons and motors, the system was divided into three modular three degree of freedom fingers actuated by four tendons.

To ensure accurate sensing and control of forces a cable tension mechanism is placed on each cable where it enters a finger. A cantilever beam supports an idler pulley around which the cable is deflected. Sensing the strain at the base gives an inference of cable tension. Incremental optical encoders placed directly on motor shafts are used to obtain position and velocity information of each joint in the hand. A fingertip sensor has also been developed by SALISBURY with an ability to determine location, magnitude and direction of a force exerted through a point contact. The line of action of a force can be determined if the resultant forces and moments are known by the sensor.

Control System Implementation : Since tendons are used to produce joint motions, joint displacements are related to tendon displacements by constants representing pulley radii. The tendon position and joint displacement are related to each other by a constant matrix which represents the finger pulley radii. Thus, controlling a joint angular position needs the control of tendon displacement. The hand has been controlled in a parallel fashion through the use of 12 microprocessor based tendon position controllers. A VAX 11/750 communicates with the 12 tendon controllers to enable coordination of joint and finger motions.

1.3.3) UTAH / MIT HAND [1986]

The biological model of the Utah hand has provided evidence that such a design is efficient for very complicated manipulation. The MIT hand has three four-degree-of-freedom fingers and one four-degree-of-freedom thumb and is the most determined attempt towards a truly anthropomorphic hand, Fig [1.2-c]. Since the hand is used for biological and tele-operation research, the outset design is comparable to the human hand. The hand is energized by extremely fast pneumatic cylinders through polymeric tendons. The MIT hand is actuated antagonistically using a *2N* tendon strategy that requires a system of 32 independent tendons and actuators. It is suita-

ble for object compliance control since the antagonistic arrangement allows the joint stiffness to be controllable. The control system of the Utah hand implements two reflex motions which are observed in the human hand. {1} Proximal stiffening and {2} Distal curling. Being closely modelled on the human hand it can be used as slave apparatus in a tele-operation system.

1.3.4) MICRO-ACTUATOR ROBOTICS HANDS

A flexible micro-Actuator robotic hand has been developed by KOICHI *et. al* [1991]. The hand was driven by an electro-pneumatic (or electro-hydraulic) system by actuating four Flexible Micro-Actuators (FMA). The FMA has several distinctive features that make it suitable for robot hand design. {1} It is easy to miniaturize, because of its uncomplicated structure. {2} It has a high power density. {3} Although it is small in size, it has many degrees of freedom which are suitable for robot mechanisms. {4} It operates smoothly and gently because of its frictionless mechanism. The FMA was made of fibre-reinforced rubber, and its deformation was regulated by electro-pneumatic means.

There are three interior chambers whose individual internal pressures are controlled independently through elastic tubes. When the internal pressure in the three chambers is raised equally, the FMA stretches in the axial direction. Meanwhile, when the pressure of only one chamber is increased, the FMA deflects in a direction opposite to the pressurized chamber. The KOICHI hand design consists of four links, $12mm$ in diameter, of FMA and it is capable of pinch, pair-pinch, and grip of grasping modes.

The hand has 12 degrees of freedom, since each FMA link has three degrees of freedom: pitch, yaw, and stretch. Gripping force of the hand is controlled by the force exerted by the individual FMA links. This is done by adding more compression to the

links in the contact surface. The micro-actuator hand is appropriate for non-industrial areas such as medicine, biology and agriculture. Examples of these are soft grips for handling fragile items such as eggs, fruit or glasses, and micro-robots for inspecting the body or supporting micro-surgery, KOICHI *et al.* [1991]. The introduced hands mechanisms have shown the anthropomorphic design pattern continues to be the dominant approach to general purpose manipulators. The fundamental challenge to this technology is the control of the complex multi-fingered hands. The attempt by KOICHI to introduce the micro-actuator is an indication that the coming challenge is the use of muscle type fingers with less mechanical design.

(1.4) OBJECT MANIPULATION BY FINGERTIPS MOTION

1.4.1) PHYSICALLY ACTING FORCES ON AN OBJECT

When an object is to be moved in a three dimensional space by the fingertips motion, it is essential to overcome the external forces acting on that object. Some externally acting forces are motion dependent e.g. the object's inertia. To manipulate an object using a robot hand or a multi-arm system, chain forces have to be applied to the grasped object in such a way that they generate the desired external object force, including the object weight, without sliding or breaking contact. Fig [1.3] illustrates the physical forces and moments acting on an object including those applied by the fingertips. Once an object is in motion with respect to a reference frame, the forces acting can be represented by the NEWTON-EULER equation which is defined by Eq. 1.1.

$$\begin{bmatrix} m_o E & 0 \\ 0 & I_b \end{bmatrix} \begin{bmatrix} \dot{v}_b \\ \dot{\omega}_b \end{bmatrix} + \begin{bmatrix} -m_o g \\ \omega \times I_b \omega \end{bmatrix} = \begin{bmatrix} F_o \\ N_o \end{bmatrix} \qquad (1.1)$$

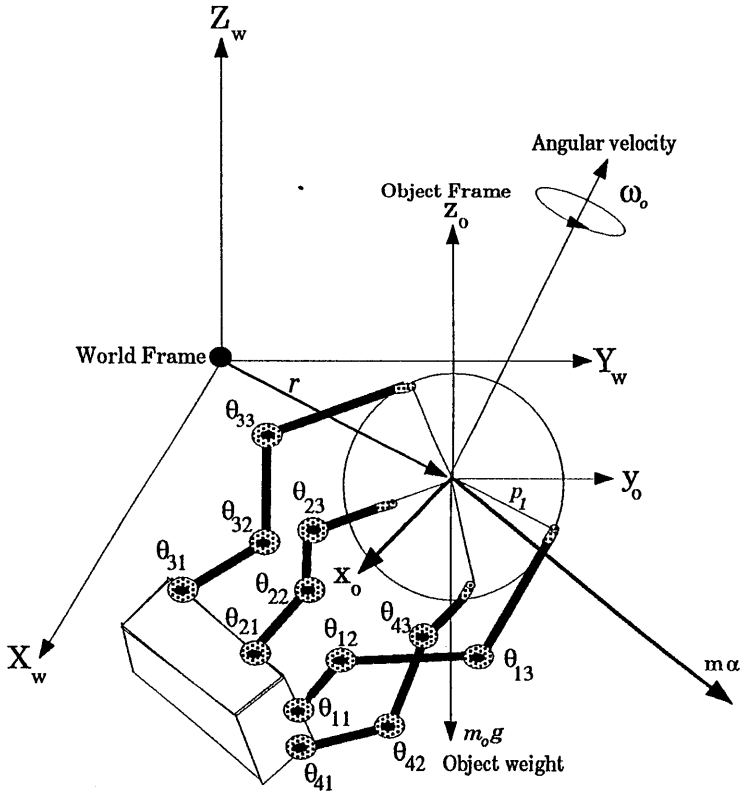


Figure 1.3 : An Object Manipulation and Externally Acting Forces.

In Eq. 1.1 $m_o E \in \Re^{3\times 3}$ is the diagonal object mass matrix, I_b is the object inertia matrix expressed in the base frame (I_o is the constant object inertia matrix expressed in the object frame), and $[F_o ; N_o]$ are the force and moment applied at the object centre of mass. The force control distribution problem is the determination of the fingers contact forces (in order) to keep the object in equilibrium or to follow a defined trajectory while overcoming the acting forces expressed by the Newton-Euler equation.

1.4.2) THE GRIP JACOBIAN (TRANSFORM G)

Once n fingers are brought in contact with an object, the mapping of each fingertip force or velocity to the overall object is carried out through the use of the *grip transform*, or *grip Jacobian*. The role played by the grip transformation, G, in controlling manipulation with a multi-fingered system is analogous to the function performed by the joint Jacobian matrix in robot arms. The resultant force and moment vectors applied to an object are represented by :

$$F_o = \sum_{i=1}^{n} f_i + m_o g \quad \text{and} \quad N_o = \sum_{i=1}^{n} n_i + \sum_{i=1}^{n} p_i \times f_i \tag{1.2}$$

Under the assumptions of *frictional point contact* and no change in the closed kinematic topology with the object, the external object force F_b can be represented by the following equation.

$$F_b = G f_{tip} \tag{1.3}$$

In the above equation, $F_b \in \Re^{[6\times 1]}$ is the external object force vector which is represented by :

$$F^T_b = [f_x, f_y, f_z, m_x, m_y, m_z] \tag{1.4}$$

$\in \Re^{[(n\times 3)\times 1]}$ fingertip force magnitude vector f_{tip} is given by $f_{tip} = (f_{tip1}, f_{tip2}, f_{tip3}$

, . ., $f_{tipn})^T$ where $f_{tipi} = (f_{ix}, f_{iy}, f_{iz})^T$. Also in Eq. 1.3, the $\in \Re^{[6\times(n\times 3)]}$ grasping matrix G is defined by:

$$G = \begin{bmatrix} E & E & E \ldots E \\ P_1 & P_2 & P_3 \ldots P_i \end{bmatrix} \quad \text{where} \quad P_i = \begin{bmatrix} 0 & -z_i & y_i \\ z_i & 0 & -x_i \\ -y_i & x_i & 0 \end{bmatrix} \tag{1.5}$$

$E \in \Re^{[3\times 3]}$ identity matrix and (x_i, y_i, z_i) in Eq. 1.5 represents the position vector from the origin of the object reference frame to the *ith* contact location, Fig [1.3].

1.4.3) CLOSED CHAIN SYSTEM THROUGH THE LOAD OBJECT

A multi-fingered robotics hand forms a closed-kinematic loop, where the responses of individual chains are tightly coupled with one another through the load object. If the desired object trajectory is expressed as $U_d(t) \in \Re^6$, then the required resultant force F_b to be applied to the object for producing the force required to overcome the physically acting forces, is given by :

$$F_b = Q_o + I_o[\ddot{U}_d + K_1(\dot{U}_d - \dot{U}) + (K_2(U_d - U)] \tag{1.6}$$

In Eq. 1.6 K_1 and $K_2 \in \Re^{6x6}$ are constants and U_d is the required object trajectory. Thus to manipulate an object requires each robotics finger to apply a force vector to the object which will produce the desired motion. By referring to Fig [1.4], the finger acceleration vector $\ddot{a}$ at the *ith* contact point can be expressed in terms of the required object acceleration as, NAKAMURA *et. al* [1987] :

$$\ddot{a}_i = \ddot{a} + \dot{\omega} \times p_i + \omega \times (\omega \times p_i) \tag{1.7}$$

where

$$[\ddot{a}\ \dot{\omega}]^T = \ddot{U} = \ddot{U}_d + K_1(\dot{U}_d - \dot{U}) + K_2(U_d - U) \tag{1.8}$$

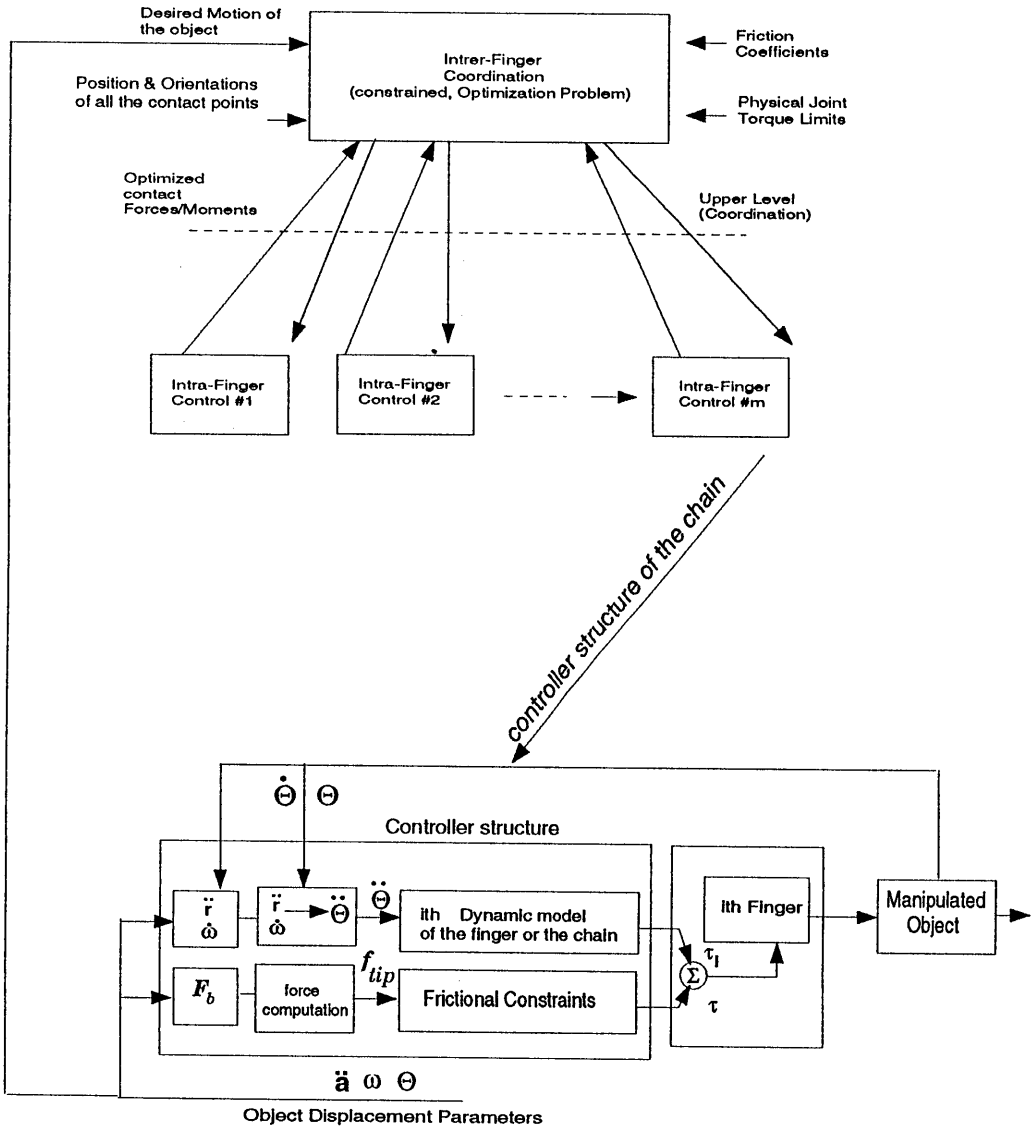


Figure 1.4 : Aspects of Multi-fingered Hands Control :
High Level Computation Requirements and Low Level Coordinated Servo System.

Each robotics finger is required to apply a force f_i to the object according to Eq. 1.6 and to produce a motion of $\ddot{a}_i$ according to Eq. 1.7 ; the two formulations constitute the concept of force distribution on a manipulated object which is represented by the controllers diagrams in Fig [1.4]. If the object's size and weight are small compared to the hand inertia, then it is essential for the dynamic effects of chains to be involved in the force distribution computation. Given $\ddot{a}_i$ as in Eq. 1.7, an inverse dynamic process is done to evaluate the required torque of each chain τ_i. Furthermore, at the points of contacts, the contact forces are filtered according to the type of contact that exist assigned as H_c, where H_c is a matrix defining the contact wrenches.

Assuming that the motion control of the fingers is achieved by any control schemes that exist for controlling multi-fingered hands, hence the following sections will concentrate on the calculation of the contact forces and the various methods of implementation. To achieve an object tracking operation, the joints acceleration has to be evaluated by the controller so that joint torques are within their limits. Furthermore the contact forces should be chosen to satisfy the frictional constraints between the fingertips and the object.

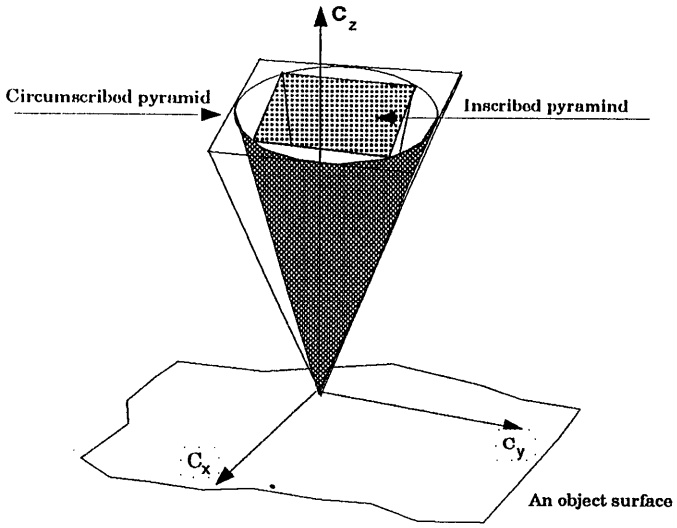
Main Constraints :

At the point of contact, a finger acts on the grasped object by a given force vector, such force vector will be filtered according to the contact type, e.g. three force components for a point contact, Fig [1.5].

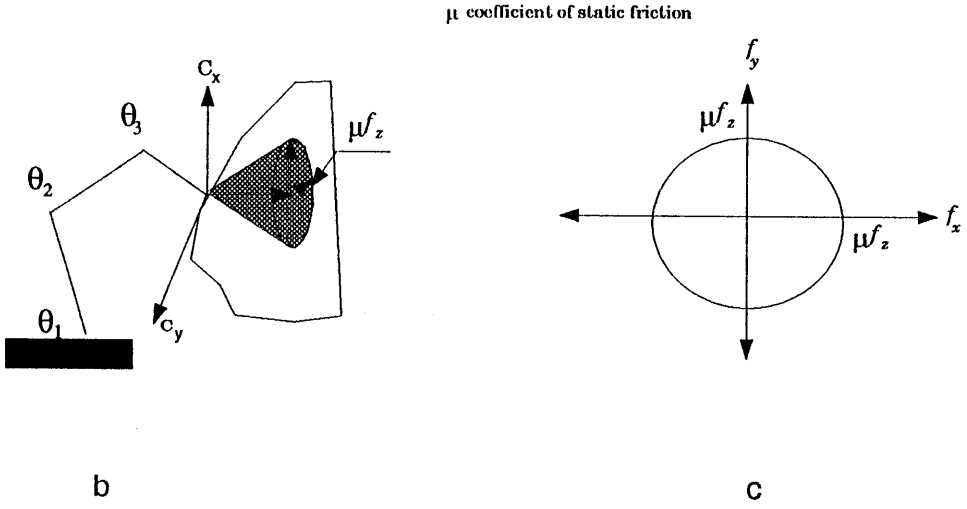
(*A*) *Frictional Constraint* :

Suppose the shape of the grasped object is represented by surface equation $S(X, Y, Z) = 0$, where $S(X, Y, Z) > 0$ denotes the inside of the object, then the inner unit normal vector at a point of contact p_i is given by :

$$e_{ni} = Grad\, S(P_i) \;/\; |\, Grad\, (P_i)\,| \quad \in \Re^{[3\times 1]} \tag{1.9}$$



a



b c

Figure 1.5 : a : Circumscribed and Inscribed Pyramids Approximation of Cone Nonlinearity.
b : Side View of the Acting Frictional Cone Inside an Object.
c : Top View of Linearity Approximation.

where $|*|$ is the Euclidean norm of a vector. Referring to Fig [1.5-a], the applied force at the *ith* point of contact is constrained by the maximum static frictional condition which is given as :

$$e_{ni}^{T} \cdot f_{tipi} \geq (1 / \sqrt{(1 + \mu_i^2)}) \, |f_{tipi}| \qquad (1.10)$$

In order to avoid slippage of the grasped object and maintain contact forces, the contact must satisfy the frictional constraints between the object and the fingertip. Thus Eq. 1.11 can be rewritten in another form as given in CHENG and ORIN [1991]. If f_z is the normal force component at the contact frame, then :

$$\sqrt{(f_x^2 + f_y^2)} \leq -\mu f_z \qquad (1.11)$$

The above given equation represents a nonlinear relation interpreted by what is known as the friction cone. To simplify the force computation algorithms, a friction pyramid is inscribed within the desired friction cone. A set of linear inequality constraints can be used instead of the cone nonlinear representation as shown in Fig [1.5-a].

In addition to the above set of equations, soft fingertips give torsional friction constraints which are described by the following two inequalities

(B) Maximum developed torque constraint :

If the torque vector produced by a single finger is given by τ_a, then the contact forces at the fingertip are related to the torque vector by the Jacobian transpose of the finger, thus:

$$\tau_a = J^T H_c \qquad (1.12)$$

Having found the required joint space torque vector to achieve given contact forces, it is essential to limit the joint torques within the physical torque limits of the chain sub-system. Given the above position and force control strategy, the problem of force distribution on an

object can be narrowed to the development of efficient computational algorithms suitable for real time implementation. Several attempts have been reported for multi-fingered robotics hands from these :

1.4.4) SALISBURY HAND GRIP JACOBIAN G^{-T}

When external forces are acting on an object (e.g. the weight of the object), it is essential to compensate for such forces, as well as the internal forces acting on the object so that the object remains in equilibrium and does not slip., SALISBURY [1985], has defined the grip transform for three fingered hands assuming the contact to be a point contact with friction. The grip transform maps a set of forces and moments acting on the fingers, to external and internal forces acting on the object. In the force domain f_{tip} is found by $f_{tip} = G^{-T}F_b$ where F_b is the object resultant force and f_{tip} are fingertip forces. Additionally G^{-T} maps the fingertip velocities to the body's resultant velocities V_b about a frame fixed to the body's centre of gravity.

An object velocity vector given by $V_b^T = [\, \upsilon_x, \upsilon_y, \upsilon_z, \omega_x, \omega_y, \omega_z, \xi_1, \xi_2, \xi_3 \,]$ is related to the tips velocities by $V_b = G\upsilon_f$ where υ_f are fingertip velocities. The grip transform for a three fingered hand is, CUTKOSKY [1986]:

$$G^{-T} = \begin{bmatrix} 1 & 0 & 0 & 1 & 0 & 0 & 1 & 0 & 0 \\ 0 & 1 & 0 & 0 & 1 & 0 & 0 & 1 & 0 \\ 0 & 0 & 1 & 0 & 0 & 1 & 0 & 0 & 1 \\ 0 & -r_z & r_y & 0 & -r_z & r_y & 0 & -r_z & r_y \\ r_z & 0 & -r_x & r_z & 0 & -r_x & r_z & 0 & -r_x \\ -r_y & r_x & 0 & -r_y & r_x & 0 & -r_y & r_x & 0 \\ r_{x12} & r_{y12} & r_{z12} & -r_{x12} & -r_{y12} & -r_{z12} & 0 & 0 & 0 \\ r_{x13} & r_{y13} & r_{z13} & 0 & 0 & 0 & -r_{x13} & -r_{y13} & -r_{z13} \\ 0 & 0 & 0 & r_{x23} & r_{y23} & r_{z23} & -r_{x23} & -r_{y23} & -r_{z23} \end{bmatrix} \quad (1.13)$$

The vectors r_{12}, $-r_{12}$, r_{13}, $-r_{13}$, r_{23}, and $-r_{23}$ are formed from 3 element vectors r_{ij}

which point from finger point of contact *ith* to finger point of contact *jth* on the grasp plane. G provides a basis for applying forces and controlling small motions with an articulated hand, MASON and SALISBURY [1985]. However, for different types of contacts, such as soft finger types, the matrix will not be an axle matrix and inversion in real time may not be computationally feasible. Also the computed finger force may not satisfy the contact conditions, and sliding or breaking might occur once the fingers are brought into contact.

1.4.5) FORCE DISTRIBUTION BASED ON THE GENERALIZED INVERSE

Most force control research effort entails the decomposition of fingertip force into two components by using the pseudo-inverse of a coefficient matrix, grip transform G in this case, that relates the resultant force exerted on the object to the fingertip force. When a resultant force F_b is known the fingertip force which results is determined by

$$f_{tip} = G^{+}F_b + [E - G^{+}G]\,\lambda \qquad (1.14)$$

in G^{+} is the pseudo-inverse of the grasp transform as further discussed in Appendix [A1], and $\lambda \in \Re^k$ is an arbitrary constant vector chosen to satisfy contact constraints. Sometimes the solution obtained using generalized inverse does not satisfy the contact constraint. If this is the case appropriate internal forces need to be added. Internal forces are forces added to the object without disturbing the grasp equilibrium, they are added to satisfy the contact constraints.

KERR and ROTH [1986] and NAKAMURA *et. al* [1987] determined the fingertips forces by first finding the finger manipulation force, hence they obtained the internal force from linear and nonlinear programming methods. But the use of optimization to find internal forces involves a numerical procedure. With non-linear inequality con-

straints, even if mathematically well-defined, a closed form solution is not easily found.

1.4.6) FORCE COMPUTATION WITHOUT THE GRIP JACOBIAN

HOLLERBACH and NARASIMHAN [1986] introduced the concept of calculating fingertip forces without the use of the grip transform G. The algorithm was a fast and an efficient way to compute the mapping from a desired external force on a grasped object, to the joint torques for three and four fingered hands. Furthermore, they extended their algorithms to a four fingered hand, where it is not an easy task to calculate fingertip forces under soft contact type assumptions. The developed algorithm has included the mapping from a fingertip location to the joint space vector of a chain or a finger.

1.4.7) GRASPING AND MANIPULATION FORCES DECOMPOSITION

YOSHIKAWA and NAGAI [1991] have developed algorithms in which they divided fingertip forces into grasping and manipulation forces for three and four fingered robotics hands. The decomposition of a given fingertip force into grasping and manipulating forces is significant when the grasping and manipulating forces are chosen as controlled variables in a force control loop.

Furthermore, if the hand changes its action from a manipulating action in a given environment (where external forces are acting on the object) to another environment, the fingertip forces have to be changed by changing the manipulating forces only and keeping the grasping forces constant. For a three fingered hand system an expression of the grasping forces $F_g^T \cong [f_{g1}\ f_{g2}\ f_{g3}] \in \Re^{9\times 1}$, and ith contact forces $f_{gi}^T = [f_{ix}, f_{iy}, f_{iz}]$ is given by:

$$F_g = B_g h_g \tag{1.15}$$

where :

$$B_g \cong \begin{bmatrix} 0 & e_{12} & e_{13} \\ e_{23} & 0 & e_{21} \\ e_{32} & e_{31} & 0 \end{bmatrix}$$

$e_{i(i+1)} \cong \Upsilon_{i+2} \cdot e_{i(i+1)}$, and

$e_{i(i+2)} \cong -e_{(i+2)i}$ for $i = 1,2,3$

The h_g vector is chosen so that fingertip forces satisfy the contact and frictional constraints, and can be expressed as $h^T_g \cong [h_{g1}, h_{g2}, h_{g3}]$. The e_{ij} are the unit vectors directed from points of contact, e.g. from c_i to c_j on the grasp plane which include the three contact points, as shown in Fig [1.3]. Υ_i is the grasping mode which depends on each finger's position around the object.

In a similar way the manipulating forces have been defined as $F_m = B_m h_m$ where

$$B_m \cong \begin{bmatrix} 0 & (1-k_2)e_{13} & k_3 e_{12} & e_{10} & 0 & 0 \\ k_1 e_{23} & 0 & (1-k_3)e_{21} & 0 & e_{20} & 0 \\ (1-k_1)e_{32}k_2 & e_{31} & 0 & 0 & 0 & e_{30} \end{bmatrix} \tag{1.16}$$

and $h^T_m = [\, h_{m1}, h_{m2}, h_{m3}, h_{m4}, h_{m5}, h_{m6}]$. The concept of manipulating forces has been defined as a fingertip force fulfilling the following three conditions:

(1) It produces the specified object resultant force F_b. (2) It is not in the backward direction of the grasping force. (3) It is orthogonal to the grasping force elements. Such computation of grasping and manipulating forces can be determined off-line,

suggesting that the burden of real-time computation is decreased. YOSHIKAWA and NAGAI [1991] have shown an analogous argument can be developed for two-fingered hands with planar motion. The analysis of YOSHIKAWA and NAGAI is quite geometric for the determination of the internal , grasping, and manipulation forces. The developed analysis is for three finger frictional grips in space and does not seem to generalize to other cases.

1.4.8) OPTIMAL FINGERTIPS FORCES

Fig. [1.4] has shown a two-level hierarchical control scheme for a multiple-chain robotic system (e.g. a multi-fingered robotics hand). The function of the upper-level coordinator is to gather all the essential information so as to formulate the corresponding force distribution problem, and then to solve this constrained computational problem so that best solutions for the contact force/moment vectors $(\boldsymbol{H}_c)_k$, *for* $k = 1$ *to* m, are produced. The best contact force/moment vectors are then the set-points for the lower level subsystems. After all the contact force/moment vectors have been determined and optimised, the terms $\boldsymbol{J}^T\boldsymbol{H}_{ck}$ are fixed and known and the dynamics of each finger are decoupled. In considering the optimization procedures in the top level of Fig [1.4], several researches have developed optimal schemes for the force distribution problem using a variety of objective functions.

The literature indicates the use of numerical optimization algorithms and the involvement of numerical procedures .

However, finding suitable λ that satisfy the (*i*) directional constraints and (*ii*) static friction constraint, has been formulated as a standard non-linear programming problem. If the friction coefficient between the object and the fingertip material is designated as μ, then the optimization problem can be stated as given by YOUNG and STARR [1989] : find λ_i, $i = 1,2,3$ so as to minimize the following objective

equation for the case of a three fingered hand:

$$(|\boldsymbol{F}_{g1}| - |\boldsymbol{F}_{g2}|)^2 + (|\boldsymbol{F}_{g1}| - |\boldsymbol{F}_{g3}|)^2 \qquad (1.17)$$

subject to the frictional contact constraint given by :

$$(\boldsymbol{F}_{gi} \cdot \boldsymbol{F}_{gi}) - (1+\mu^2)(\boldsymbol{F}_{gi} \cdot \boldsymbol{n}_i)^2 \leq 0 \qquad i = 1, 2, 3$$

and subject to a force directional constraint given by :

$$-(\boldsymbol{F}_{gi} \cdot \boldsymbol{n}_i) \leq 0 \qquad i = 1, 2, 3$$

to prevent the trivial solution which might occur once λ is zero, then

$$\lambda^T \eta^T \eta \lambda = 1$$

1.4.9) DEVELOPED OPTIMIZATION ALGORITHMS

KERR and ROTH [1986] noted the under-determined force problem in robots hands and proposed a linear programming approach *'simplex algorithm'* to determine the optimal internal force as that with the minimum norm under approximated frictional constraints to satisfy the inherent inequalities. It has been formulated as a linear programming problem to maximize:

$$\boldsymbol{F}(\lambda_d) = d \qquad (1.18)$$

according to $\quad [\,|\boldsymbol{AN}_i| - 1\,]\,\lambda_d \geq (\boldsymbol{P} - \boldsymbol{AC}_p)$

The dynamic effects of the fingers were assumed to be small and they were neglected. However the dynamic effects may well be significant in hands for micro-manipulation in which the finger inertia is comparable to the target object.

Nonlinear programming based on *'Lagrange multiplier method'* has been implemented by NAKAMURA *et al.* [1987] to solve the force distribution problem for systems of multiple manipulators and robot hands. Minimum norm contact forces fulfilling friction constraints were designated as the optimal so that stable grasp without crushing may be assumed. The proposed algorithm was to determine the resultant force taking the dynamics of the object

into consideration. The optimal forces to minimize the internal forces are these $min \mid \mathbf{H} \mid$ where $\boldsymbol{H}_{min}$ is used in the pseudo-inverse of the grasp transform. Thus $f_{tip} = F_b + \eta\lambda_{min}$, and η is the null space of grip transform $\boldsymbol{G}$. However, the problem of transient discontinuity was not considered, this is most likely to arise when the algorithm is to be used in real time manipulation tasks.

CHENG and ORIN [1990] used the *' Compact dual LP '* formulation to allow real time implementation of linear programming. The concept behind the Compact-Dual LP formulation is the reduction of constraint matrices, thus increasing the speed of convergence to the optimal solution.

The technique was developed by : {1} removing the equality constraints from the original LP formulation to obtain the compact-primal formulation, {2} solving the corresponding dual to obtain the compact -dual formulation.

The Compact-Dual LP formulation for force distribution is :

$$\begin{aligned} &\textit{Minimize} && \boldsymbol{B}_o^T\, \boldsymbol{U} \\ &\textit{Subject to} && \boldsymbol{A}^T\, \boldsymbol{U} = \boldsymbol{C}^T \end{aligned} \tag{1.19}$$

where $\boldsymbol{U} \geq 0 \quad \boldsymbol{B}_o = \boldsymbol{B} - \boldsymbol{A}\,\boldsymbol{G}_p, \quad \boldsymbol{A}_o = \boldsymbol{AN}, \quad$ and $\quad \boldsymbol{C}_o = \boldsymbol{CN}$

where $\boldsymbol{B}_o$ is the boundary-value vector of the inequality constraints, $\boldsymbol{A}_o$ is the matrix of in-equality constraints, $\boldsymbol{C}_o$ is the cost vector for the objective function, and $\boldsymbol{N}$ a matrix that maps the partial vector for free variables of $\boldsymbol{G}$ onto the null space of $\boldsymbol{G}$. The obstacles inherent in a linear programming approach to the force distribution problem are :

{1} It cannot be used to minimise the internal forces of a grasp.

{2} It can initiate undesirable discontinuities into the solution.

{3} Most variables must be separated into two components to bypass the non negativity con-

straints, thereby enlarging the size of the system.

{4} The altered *simplex method* tends to take more steps to achieve a solution than a Quadratic programming algorithm approach.

NAHON and ANGELES [1992] applied ' Quadratic-programming formulation ' to solve the constrained optimization problem that arises in closed kinematics hands. It was a continuation of the pseudo-inverse solution to involve inequality constraints, thereby minimizing the internal force in the system. The quadratic-optimization problem is solved using the algorithm developed by GOLDFRAB and IDNANI [1983]. The suggested Quadratic programming formulation can be summarized as follows:

$$\begin{aligned} &\textit{minimize} \quad f_{tip} && c^T f_{tip} + \tfrac{1}{2} f_{tip}{}^T W f_{tip} \\ &\textit{subject to} && G f_{tip} = F_b \\ & && A_2 f_{tip} \leq b_2 \end{aligned} \tag{1.20}$$

In the above given quadratic formulation c^T is a vector of contact wrenches at each contact in the grasp system. Internal forces are minimized through the minimization of the actuator torques, since c^T equals $[\tau^T J^T \cdots \cdot \tau^T J^T_i]$ where J is the *ith* chain Jacobian. W is an $\in \Re^{[n \times n]}$ positive-definite weighting matrix, and G and A_2 are matrices defining the physical system equality and inequality respectively. In terms of discontinuities the algorithm has shown smoother results over time rather than the LP methods which exhibit severe discontinuities, due to their non-uniqueness. The algorithm is able efficiently to include both linear equality and inequality constraints inherent in the under-determined force problem. In terms of speed of convergence, the algorithm is fast enough (e.g. 38 ms in SUN 3/80 machines for a task of 2 s in time) to provide set points for a real-time force/motion controller, with changes in constraints and no initial prediction to start its solution search.

1.4.10) FORCE COMPUTATION BASED ON SCREW THEORY

YOUNG and STARR [1989] have developed an algorithm for the computation of fingertip forces which can be used for an object manipulation grasped by a three fingered hand. An optimization scheme is achieved only at the beginning of the task to obtain the optimal contact forces on the grasp plane. Once the grasped object is displaced with respect to the hand palm, the initial internal forces are updated using the screw theory to accommodate the new object orientation.

From the required object forces F_b and moments N_b and the modelling of the fingertip as a point contact with friction, fingertip forces are calculated using :

$$f_{tipi} = [f_{xi},\ f_{yi},\ f_{zi}] \quad \text{where} \quad i = 1, 2, 3 \qquad f_1 = F_b - f_{tip1} - f_{tip2} \tag{1.21}$$

$$\text{and} \quad [f_2\ \ f_3]^T = G^T_m (G_m G^T_m)^{-1} [M_e\ \ F_e]^T$$

In the above three equations F_o and N_o are the equivalent force and moment respectively which are found using :

$$F_e = 1/3\, F_b \times [(r_2 - r_1) + (r_3 - r_1)] \tag{1.22}$$

$$M_e = M_b - r_1 \times F_r$$

where

$$G_m = \begin{bmatrix} 0 & z_1 - z_2 & y_2 - y_1 & 0 & z_1 - z_3 & y_3 - y_1 \\ z_2 - z_1 & 0 & x_1 - x_2 & z_3 - z_1 & 0 & x_1 - x_3 \\ y_1 - y_2 & x_2 - x_1 & 0 & y_1 - y_3 & x_3 - x_1 & 0 \\ x_2 - x_1 & y_2 - y_1 & z_2 - z_1 & x_3 - x_1 & y_3 - y_1 & z_3 - z_1 \end{bmatrix}$$

where G_m is the modified grip transform having a smaller dimension than the grip transform itself, thus speeding up the execution time of the manipulation task.

Given the difficulty of measuring and tracking contact normals, screw displacement theory has been used to find the object *rotational matrix* $\boldsymbol{R}_{ot}$. The contact normals $\boldsymbol{N}$, and the grasping forces were updated during an object manipulation from initial grasping forces and initial contact normals with the rotational partition given by :

$\boldsymbol{N} = \boldsymbol{R}_{ot} \times \boldsymbol{N}_i$ $\quad$ $\boldsymbol{N}_i$ = contact normal at the initial state,

$\boldsymbol{f}_g = \boldsymbol{R}_{ot} \times \boldsymbol{f}_{gi}$ $\quad$ $\boldsymbol{f}_{gi}$ = initial grasping force determined at the initial grasping stage.

(1.5) GRASP STIFFNESS AND COMPLIANCE MOTION

In section 1.4.1 it was shown how fingertip forces are calculated to achieve a given object resultant force. As a part of the subject, in this sub-section we shall concentrate on the concept of an object compliance motion. Assume a robot hand is applying a set of contact forces using one of the developed algorithms presented in section 1.4.1, if the object is to comply in a pre-defined manner then it is required to specify the directions of the object motion.

Compliance of an object determines the first order of link displacements that will occur when a set of forces is imposed on the object. In general a grasp compliance or its inverse, the grasp stiffness have been investigated by several researchers. From these :

1.5.1) AUGMENTED GRIP TRANSFORM G^{-T} IN COMPLIANCE CONTROL

SALISBURY [1985] augmented the resultant force and torque on an object with internal grasp forces so that an invertible $\Re^{9\times9}$ stiffness matrix is obtained. The joint stiffness matrix is:

$$\boldsymbol{K}_\Theta = \boldsymbol{J}_\Theta{}^T \boldsymbol{G}^T \boldsymbol{K}_c \boldsymbol{G} \boldsymbol{J}_\Theta \qquad (1.23)$$

In Eq. 1.23, $\boldsymbol{K}_c$ is the augmented stiffness matrix specified by the user, which is defined by:

$$\boldsymbol{K}_c = diag\,[\,K_x,\ K_y,\ K_z,\ g_x,\ g_y, g_z,\ K_1,\ \ldots\ \ldots\ \ldots, K_p\,] \qquad (1.24)$$

The first six diagonal elements are the translational and rotational stiffness of the grasped object, while the last p elements account for the internal stiffness. $\boldsymbol{J}_\Theta$ is a block diagonal matrix where the matrices along the diagonal are the specific finger Jacobians. Therefore, to apply a generalized force to the object , the finger joint torques are given by $\tau_a = (\boldsymbol{J}_\Theta{}^T \boldsymbol{G}^T \boldsymbol{K}_c \dot{\boldsymbol{G}}\, \boldsymbol{J}_\Theta)\delta\Theta$, where $\delta\Theta$ is the object displacement vector from a pre-defined frame position, SALISBURY [1985]. The augmented $\boldsymbol{K}_c$ matrix is defined by the user to obtain the finger joint space vector required to achieve a desired stiffness of the object itself.

1.5.2) NON AUGMENTED GRIP TRANSFORM [G].

NGUYEN [1990] has addressed the stiffness and stability of planar and three dimensional objects grasp by virtual springs corresponding to force components, or wrenches, at the finger-object contacts.

However, he does not address the relation of virtual springs to joints of an actual robotics hand. CUTKOSKY and KAO [1989] examined the effective stiffness of a grasped object and showed that it is not only due to the servo parameters but also due to fingertip models and changes in the grasped geometry, thus :

$$\boldsymbol{K}_p = -\,\delta\boldsymbol{F}_p \,/\, \delta\boldsymbol{X}_p \qquad (1.25)$$

That resulting contact stiffness matrix $\boldsymbol{K}_p$ can be seen as an instantaneous static relationship between contact forces and compliant deflections. For n finger in contact

with an object, the object stiffness is the overall contribution of all fingers, KAO and CUTKOSKY [1992], therefore K_b can be expressed as;

$$K_b = \sum_{i=1}^{n} Z_i^T K_{pi} Z_i \tag{1.26}$$

where Z_i is $\in \Re^{6\times6}$ transformation matrix that relates motions at two points.
If the control of the fingers is coupled so that K_{pi} are not independent, K_p is defined for all the fingers. In this case the concatenated object transformation matrices J_c, and object stiffness matrix K_p that depend on the type of contact are related to object stiffness K_b by:

$$K_b = Z^T K_p Z \tag{1.27}$$

Since an object stiffness is a function of the servo parameters, hence K_{pi} in Eq. 1.27 is a matrix associated with each finger-object contact, SHIMOGA and GOLDENBERG [1992]. This matrix can be computed as a function of the finger joint stiffness, the structural compliance in the fingers and the type of contact at the fingertips. Consideration of such physical parameters formulate the finger stiffness matrix at the *ith* point of contact, thus K_{pi} can be expressed as :

$$K_{pi} = H_c^T (H_c (Y + C_s) H_c^T)^{-1} H_c \tag{1.28}$$

C_s is the structural compliance (e.g. compliance in the tendons), H_c is the concatenated type of contact. Y is the concatenated servo compliance which is expressed as a function of the joint parameters and fingers Jacobian. If the servo stiffness parameters are given by K^{-1}_{Θ} then Y can be rewritten as $Y = J_{\Theta} K^{-1}_{\Theta} J_{\Theta}$. Substituting Y in Eq. 1.28 results in K_p expressed as :

$$K_p = H_c^T (H_c ((J_{\Theta} K^{-1}_{\Theta} J_{\Theta}) + C_s) H_c^T)^{-1} H_c \tag{1.29}$$

CUTKOSKY has drawn the following conclusions regarding the stiffness control of an object grasped by a robot hand :

(*i*) Since K_p is made as a function of the fingers Jacobians J_Θ, therefore it is position dependent and must be updated along with the Jacobian as the fingers move.

(*ii*) The eigenvalues evaluation of the stiffness matrix in the body coordinate, K_b , can readily indicate the stiffest and softest directions of an object motion. Furthermore if the eigenvalues are all positive, this confirms that the grasp is stable.

(*iii*) If K_b has the full rank property, the grasp is a force-closure and it can resist forces and moments from any direction, CUTKOSKY and KAO [1989].

(*iv*) K_b depends on the hand configuration. It changes with changes in the location of the contact points on the object resulting in changes in the cartesian transformation matrix, Z_i.

(1.6) GRASP STABILITY AND ITS SYNTHESIS

1.6.1) GRASP POTENTIAL FUNCTION

HANAFUSA and ASADA [1977] proposed the notion of stability by centring a robot hand with elastic fingers and rollers on fingertips on an object mass centre, and examining for grasps that are stable with respect to rotation and then to translation. They developed a planar three-fingered hand capable of implementing an analytical grasp algorithm. For a desirable hand position two conditions have been drawn : (*i*) Horizontal plane stability which amounts to obtaining a local minimum for the potential function of the grasp, $V(x,y,\theta)$. (*ii*) The friction due to the finger forces must be large enough to support the weight of the object. When the grasp state energy reaches a local minimum, that means the external force disturbed the object from its required position has been mastered by the elastic field produced by the fingers.

The introduction of grasp stability by HANAFUSA and ASADA was limited to simplified model of the fingers. Their analysis works for limited cases of no friction, since friction at the fingertips is an essential factor to be accounted for in robotics hands.

For a three dimensional case, NGUYEN [1990] has made some assumptions for obtaining analytical conditions for which a grasp is in stable equilibrium, using the potential function of the grasp. He modelled contacts as frictionless point contacts, hard finger contacts, or soft finger contacts with friction. Fingers are modelled as virtual springs, where each virtual spring is a set of independent linear and angular springs independently controlled. The main objective was to obtain from the potential function analytical conditions for which a grasp is in equilibrium. The potential function of the grasp equals the sum of the potential functions from all n forces at contacts, AL-GALLAF *et al.* [1992] ;

$$U_p = \sum_{i=1}^{n} \tfrac{1}{2} \boldsymbol{K}_i \sigma_{ci}^2 \tag{1.30}$$

and n is the number of linear and angular springs corresponding to n wrenches defined by SALISBURY [1985], σ_{ci} is the compression of a linear spring $\boldsymbol{K}_i$ due to the object twist. Expanding U_p, the potential function of an object with n wrenches acting is given by:

$$U_p = \tfrac{1}{2} \; [\sigma_{c1}, \sigma_{c2}, \ldots \sigma_{cn}] \begin{bmatrix} K_1 & 0 & 0 & 0 \\ 0 & K_2 & 0 & .. \; 0 \\ 0 & 0 & 0 & 0 \\ 0 & 0 & 0 & .. \; K_n \end{bmatrix} \begin{bmatrix} \sigma_{c1} \\ \sigma_{c2} \\ . \\ \sigma_{cn} \end{bmatrix} \tag{1.31}$$

The compression σ_{ci} of a linear spring $\boldsymbol{K}_i$ due to a twist of the grasped object is equal to the original compression σ_{cio} plus the dot product of the line of action of the spring and the twist move of the object. As the object is displaced by a slight twist, $\boldsymbol{t} = [\delta, \boldsymbol{d}]$, the current position of the points of contacts of the *ith* finger is $\boldsymbol{P}_{ni}$ where $\boldsymbol{P}^T_{ni}$ is expressed by :

$$\boldsymbol{P}^T_{ni} = rot\,[\,\delta x,\ \delta y,\ \delta z\,]\,\boldsymbol{P}^T_i + \boldsymbol{d}^T \tag{1.32}$$

and $rot\,[\delta x, \delta y, \delta z] = I + [\delta x] + \frac{1}{2}\{[\delta\delta^t] - [\delta \cdot \delta] I\}$, expanding $rot(A)$:

$$rot(A) = \begin{bmatrix} 1 & 0 & 0 \\ 0 & 1 & 0 \\ 0 & 0 & 1 \end{bmatrix} + \begin{bmatrix} 0 & -\delta_x & \delta_y \\ \delta_z & 0 & -\delta_x \\ -\delta_y & \delta_x & 0 \end{bmatrix} + \begin{bmatrix} -[\delta^2_y+\delta^2_z] & \delta_x\delta_y & \delta_z\delta_x \\ \delta_x\delta_y & -[\delta^2_z+\delta^2_x] & \delta_y\delta_z \\ \delta_z\delta_x & \delta_y\delta_z & -[\delta^2_x+\delta^2_y] \end{bmatrix} \tag{1-33}$$

A linear spring $\boldsymbol{K}_i$ exerts a pure force on the grasped object if and only if its tip $\boldsymbol{P}_i$ is displaced along the direction $\boldsymbol{K}_i$, where $\boldsymbol{K}_i$ is the direction of the spring oriented with the normal of the surface of contact, NGUYEN [1990]. The effective compression σ_{ei} is given by the addition of its initial compression σ_{cio} and the dot product of the line of action of the spring and the twist displacement of the object, i.e., $\sigma_{cio} + \boldsymbol{K}_i \cdot (\boldsymbol{P}_i - \boldsymbol{P}_{io})$. For an angular spring model, the twist has the same angular part, but a different linear part so, $\boldsymbol{t} = \{\delta, (\boldsymbol{d} - [\boldsymbol{P}_i \times \delta])\}$, and the angular displacement is then given by :

$$\begin{aligned} \sigma_{ci} &= \boldsymbol{k}_i \cdot \delta \\ &= [0, \boldsymbol{K}_i] \cdot \{(\boldsymbol{d} - (\boldsymbol{P}_i \times \delta)), \delta\}. \end{aligned} \tag{1.34}$$

Finally the potential function is found by substituting in Eq. 1.33 values of σ_{ci}, resulting in a grasp potential function:

$$U_p = \sum_{i=1}^{n} \frac{1}{2} \boldsymbol{K}_i \sigma^2_{ci} \tag{1.35}$$

A grasp is then in equilibrium when the gradient of its potential function is zero.

(1.7) Articulated Systems Dynamics

The computation of the dynamics of articulated systems and robot manipulators has received considerable attention in the research media. For accurate control of articulated robots it is necessary to have a full knowledge of the dynamic model of a robot hand for the purpose of defining a control strategy. Model based control of robot arms and articulated systems need computation of the dynamic model in real time where the sampling rate requirements have to be met. Hence, parallel computation approaches have been defined. It has been shown that the solution of the dynamic problem incurs a heavy computational load. This computation of the highly coupled dynamic equations has always posed a bottleneck in real-time dynamic control of robot manipulators and robot hands when the dynamics of the links are of considerable variation with respect to the dynamics of the object. However, the recent advances in the *VLSI* technology make it possible to implement new computational algorithms that compute the dynamics whilst meeting real-time constraints with considerable cost-perfomance ratio improvement.

1.7.1) Computational Approach

There have been two main approaches for the on-line computation of the inverse dynamics problem. The first approach is to reduce the complexity of the model whilst recognising that the robot performance suffers as a consequence. BEJCZY [1974] employed this approach where he neglected the coriolis and centripetal effects by assuming low speed operation of the robot itself. However, ignoring these terms will result in a noticable vibration and overshooting of the robot arm at high speed. The second approach is to employ a stand-alone computation system for the computation of the dynamic model, but this may lead to an increased development cost, LUH *et al.*

[1980].

1.7.2) Parallel computation Approach.

One approach towards reasonable computational results that lies between the complete use of the dynamic model and the high speed of computation is the of parallel computation approach. The pioneering work of LUH and LIN [1982] based on a generalisation of the branch-and-bound algorithm exhibits several significant limitations such as the not consideration of the recursive structure of the Newton-Euler (NE) and the sequential dependencies of the algorithm.

ORIN *et al.* [1985] proposed a pipeline design for the (NE) that eliminates some of the performance degradation problems associated with inter-processor communications which appear in the computation of the (NE) using parallel processing techniques. LATHROP [1985] proposed two parallel algorithms using special purpose processors. The first, a linear parallel algorithm which is related to the method developed by LUH and LIN [1982]. The second is a logarithmic-parallel algorithm based on the partial sum technique. Both approaches exhibit massive buffering which degrades the performance and causes complicated inter-task communication, and hence no practical implementation of the scheme had been made.

CHEN *et al.* [1988] presented two methods, the A* algorithm combined with a heuristic function derived from the Fernanadez and Bussel bound, and the dynamical highest level first most immediate successors first (*DHLF/MISF*). The efficiency of the work was only demonstrated by simulation results.

However, most of the previous attempts did not involve implementation on an actual parallel processing system. Results are usually presented in terms of the number of

A* is a minimum cost graph search algorithm.

multiplications and additions and their theoretical equivalent of processor clock cycles. This way, of measuring the efficiency of parallel algorithms has been shown to be inaccurate, ZOMAYA [1992]. The different task allocations are executed by a parallel-processor system. Hence, the results do not represent only the processing-time of multiplication and addition but also the delays caused by the communication between different processors and software development.

(1.8) INTRODUCTION to the RESEARCH

The main objectives of this research are the investigation of the joint force sensing and control, force distribution and cartesian based object manipulation of a four fingered robot hand.

For investigating these issues a four fingered robot hand has been designed, where its kinematic and dynamic models have been used extensively to formulate the force optimization and control even at ill conditioned hand configuration, where the hand Jacobian determinant is zero.

From the mechanical point of view, the project shows how remotely located joints are actuated by the routing of the transmission tendons through the fingers themselves. Although multiple-degrees of freedom grippers have the advantage of enhancing object manipulability, such mechanical systems need a large number of actuators to be driven, controlled, and supervised in a prescribed manner. Twelve motion processors (capable of producing a trajectory motion and performing a digitized PID controller action in real time) have been utilized in this project.

Above the low level layer comes the interfacing level both in position and force loops which are supervised by one master processor. The above described system is an example of a multi-degrees of freedom system which is governed by kinematic relations and equations. The

kinematic structure is the most important topic, since it relates both high level task planning with low levels of the hand controller.

Finger Jacobian, hand Jacobian, manipulability measure and differentials mode of motion are examples of the hand kinematics investigated in this thesis. Force control on an object, for compensating the external forces acting on the object e.g. the weight, is the subject which receives considerable attention in this project. Force control in a pre-defined trajectory describes the fine motion of the fingers while the fingertips interact with the environment through the grasped object. An effective scheme for specifying fingers motion should provide for the specification of trajectories for the manipulated object to follow.

With regard to the first issue of this research, for controlling a joint in a force mode, a force sensing is required. An applied force to an object by the fingertip is sensed by the knowledge of tension in the tendons using strain gauges. The sensed force is used to close the loop for achieving force control in the distal joints.

With regard to the *second* issue of this research, while discussing the force distribution and control of a robot hand we either discuss static grasping or dynamic manipulation which require forces to be applied to the grasped object.

In particular, there are two main approaches of force balance computation, the algebraic approach, and the numerical approach. The use of the numerical approach in force computation involves the use of optimization techniques where either linear or nonlinear constraint has to be solved for. The research has shown the possibility of applying the nonlinear constraint optimization which indeed has the advantage of reducing the overall computational requirements. First the concept of extending the internal forces optimization to a four fingered hand will be discussed and then will be compared with a novel method of employing

nonlinear constraints optimization for dealing with the nonlinear model of the frictional cone of the four contacts. Other research work has used the linear model of the frictional cone constraints, however, within this thesis it will be shown how the use of nonlinear constraints optimization will give an equivalent solution with less computational requirements.

With regard to the *third* issue of this research, a cartesian based motion of an object is an essential aspect of manipulation in robot hands due to the use of these hands in coordinated systems (*such as eye-hand system*). However, robot hands usually have finger kinematics with a maximum of four DOF, which makes it difficult to avoid singular configurations of the hand, if the task is defined in a cartesian coordinate system. The research investigates the use of other techniques of inverting the hand Jacobian. The application of the RSI method needs a measure of how ill the work space is, hence the dexterity measure of one finger, as shown, is enough to describe the performance of the entire hand, providing certain kinematic conditions are satisfied.

The problem of using a robust inverse method for overcoming the *ill* hand configuration is that, the dexterity measure of the entire hand has to be investigated, since we are dealing with multiple Jacobian rather than a single one as in a six degrees of freedom robot arm. The thesis shows how the dexterity measure of one finger is used to invert the entire hand Jacobian if certain conditions are satisfied. For the investigations of the hybrid dynamic based controller (*which uses the inverse hand Jacobian*), we are working under three assumptions stated as : (*i*) The physical lengths of the finger links are identical. (*ii*) The joint space vectors of the four fingers are also equal, and the four fingers start their motions at the same instant with the same joint displacements. (*iii*) The entire hand Jacobian is a block diagonal matrix, thus all the off diagonal elements are zero .

Finally as a side issue, since the computation of optimal contact forces either for static or

dynamic motion, the use of RSI and constrained object-hand motion will require large amount of computations. Aspects of implementing these computations using parallel approach will be discussed. First by observing the computation requirement of manipulation and then sub-dividing the entire constrained equation into smaller sub-tasks.

CHAPTER TWO

THE DEVELOPMENT of a FOUR FINGERED ROBOT HAND.

(2 .1) INTRODUCTION

A gripper, hand or an end-effector is the apparatus mounted at the distal end of a robot arm enabling it to pick up workpieces, hold, manipulate, transfer, place and release them accurately in discrete positions. Thus the gripper is the all-important mechanical interface between the robot arm and its environment, without which in most circumstances, the robot cannot function effectively irrespective of the degrees of sophistication it may otherwise possess.

End effectors range from general purpose devices such as pneumatic grippers to special tools for applications from arc welding and spray painting to the handling of silicon wafers in a corrosive acid environment RICHARD *et al.* [1989]. Some end-effectors might be very delicate, e.g. multi-fingered robot hands, where they are involved in fine manipulation and the extraction of object physical attributes.

Thus, a multi-degree of freedom gripper in conjunction with other sensory modalities can be used to measure the three-dimensional character of the environment, support an object recognition system and perform alternately as a delicate and powerful manipulator. In this research study a four fingered robot hand with its supporting sensing (position and force) has been designed and used as test equipment for the implementation of force control on a defined workpiece. In an effort to present the hand mechanics and the mechanism of motion, this chapter has been divided into four sections.

The first, section (2.2) presents a simplified biological structure of the human hand since it is considered to be the prototype of an ideal multi-degrees of freedom gripper, whereas section (2.3) presents the physical hand-control system structure. The designed hand structure, force sensing and routing of the tendons will be discussed in section (2.4).

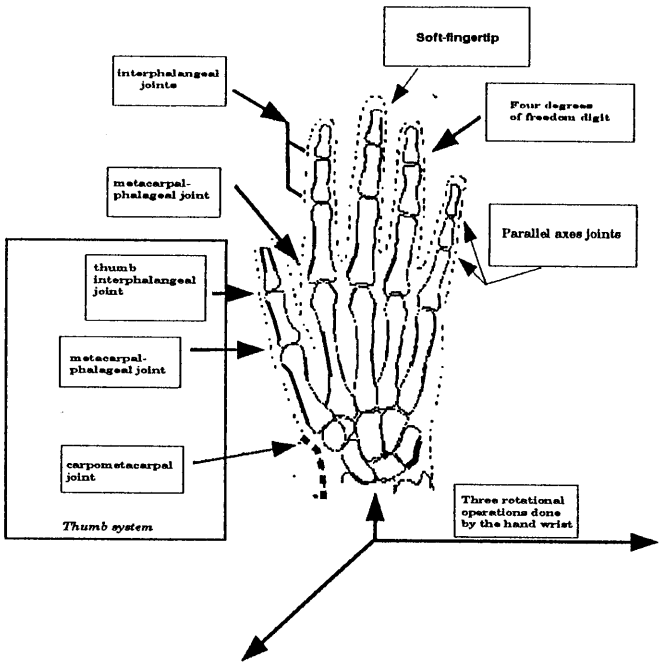
(2.2) THE HUMAN HAND

2.2.1) The Biological Structure of the Human Hand

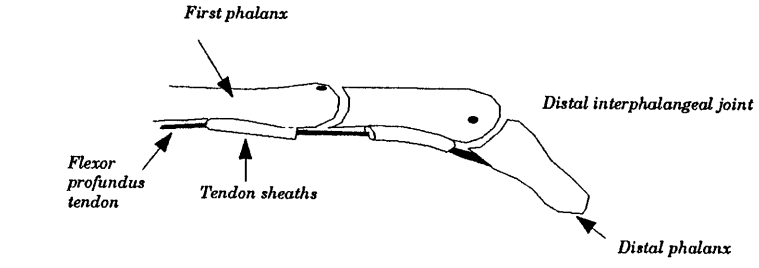
The design of a multi-degrees of freedom mechanical manipulator or, in particular, a multi-fingered robot hand is usually motivated by a definite class of tasks. One strategy of developing a general-purpose manipulator is to emulate those virtues of the human hand which make it such a versatile end-effector. Fig [2.1] presents the skeletal pattern of the human hand.

The human hand consists of the wrist, palm, thumb and fingers. The palm and fingers of the human hand has twenty degrees of freedom; two in the knuckles, one in each of the other finger joints, three in the thumb and one in the palm, CROWDER [1991-b]. Each of the four fingers of the human hand has three joints, the most proximal to the hand palm of which is called the metacarpal-phalangeal, GRUPEN *et al.* [1989]. It has two degrees of freedom and is capable of adduction-abduction over an extent of approximately 30° and flexion-extension of approximately 120° . The next two joints of the human finger are the interphalangeal joints. These are hinge joints with only one degree of freedom each and a range of motion of approximately 90°.

In Fig [2.1-a], the thumb is a more complex mechanism, the proximal joint is called the carpometacarpal joint and contains two degrees of freedom. The first degree of freedom is adduction-abduction with a range of motion of approximately 90°. The second degree of freedom operates the joint in flexion extension with a range of motion of somewhat less than 90°. The next joint of the thumb is the metacarpal-phalangeal joint whose predominant DOF is that of flexion-extension from the plane of the palm toward the palm over a range of



a



A simplified drawing of a flexor tendon acting through sheaths and across joints

b

Figure 2.1 : a : Structure of the Human Hand Including the Thumb Mechanism.
b : Details of One Finger Tendon Transmission System.

about 60°. The last (distal) joint of the thumb is the interphalangeal joint. This joint is a simple hinge joint with one degree of freedom which allows a range of motion of about 90°.

The human muscles can only apply force by contracting. They can not extend by their own effort, and thus, they can not push. Muscles are extended by the contraction of other muscles. Two sets of muscles act on the human hand : (*i*) Extrinisics which are located in the forearm, and (*ii*) the less forceful Intrinisics which are located within the hand itself. Most of the dexterity and flexibility of the hand can be attributed to the action of the intrinsic muscles. Some muscles act directly on the bones, and others act through tendons.

Flexors, shown in Fig [2.1-b], are used to close the fingers to grip an object, extensors are used to open the hand again. In the human hand, a flexor connects the distal phalanx (*which is the bone at the tip of the finger*) to muscle, and it transmits the force and excursion produced by the muscle to the finger. This tendon is held close to the intermediate bones by sheaths, in which they maintain the position of the tendon relative to the phalanges. With reference to the human hand structure, the human hand is many things in addition to being just a gripper. It is sensory organ designed as much for palprebility as for manipulation. An understanding of human hand biology paves the way for the designed robots which emulate the human function. The rest of the Chapter concentrates on the aspects of a four fingered hand design and the mechanism used to position and apply force to a grasped object.

(2.3) SYSTEM STRUCTURE

Fig [2.2] shows a simple block diagram of the structure of the research set up. It composes of five units. The first is the master controller (*which includes the SUN and PC/XT machines*), within such environment task definition is developed. In the first unit an appropriate supervisory software has been developed to facilitate the communication with

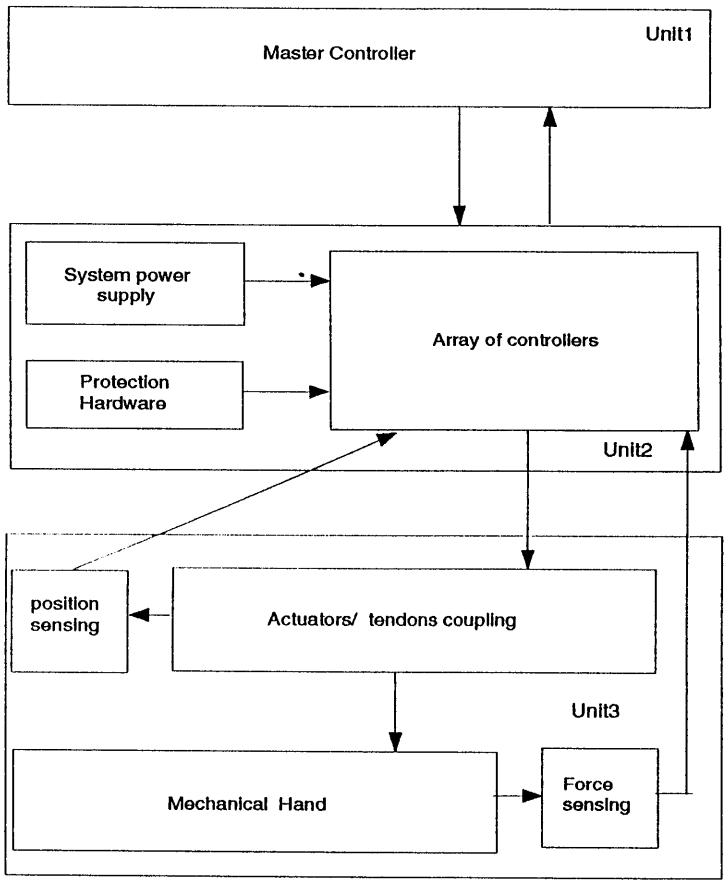


Figure 2.2 : Full Layout of the Designed Hand-Control System.

the various functions of the hand. The second unit is the controllers array box; motion and force control hardware aspects are mainly located within this unit. The third unit is the mechanical hand and the drive box used for actuation. Within this chapter the subject of hand design will be further expanded, whereas kinematic and dynamic modelling are discussed in the coming chapters.

(2.4) THE DESIGN OF THE ARTICULATED HAND

2.4.1) Four Fingers Hand

Three photographs representing the Cybhand system mechanical design are shown in Plate [2.1] to Plate [2.3].

Plate [2.1] illustrates the hand four fingers and how they have been configured around the hand palm. The last joint of a finger sub-system has its tendons routed over the medial and the third joints supporting pulleys. This sort of tendon routing introduces what is known as the mechanical coupling among the joints in one finger.

Plate [2.2] shows some inside details of the hand driving package (for one finger), e.g. the incremental encoders and the tendons routing tubes through which tendons are led to the corresponding joints in the fingers.

Plate [2.3] is the hand palm where the four fingers roots are attached, it can be modified to circular palm or other shapes for specific applications.

The question of why a four fingered hand has been adopted is explained elsewhere. In addressing this issue from kinematics and applied wrenches to a grasped object, Chapter Three discusses the *quality measures* of how a four fingered hand increases the quality measure over a less number of fingers hand.

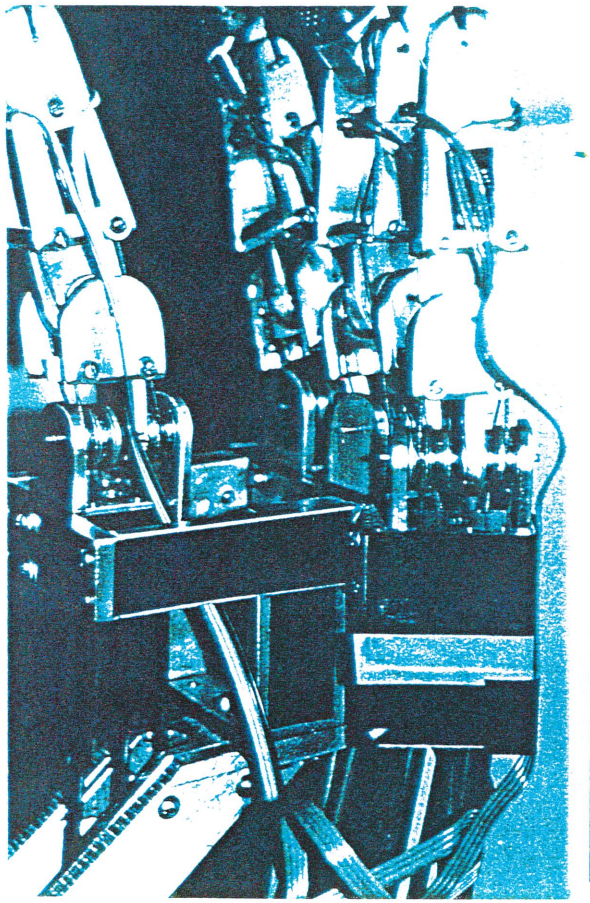


Plate [2.3] : Hand Palm.

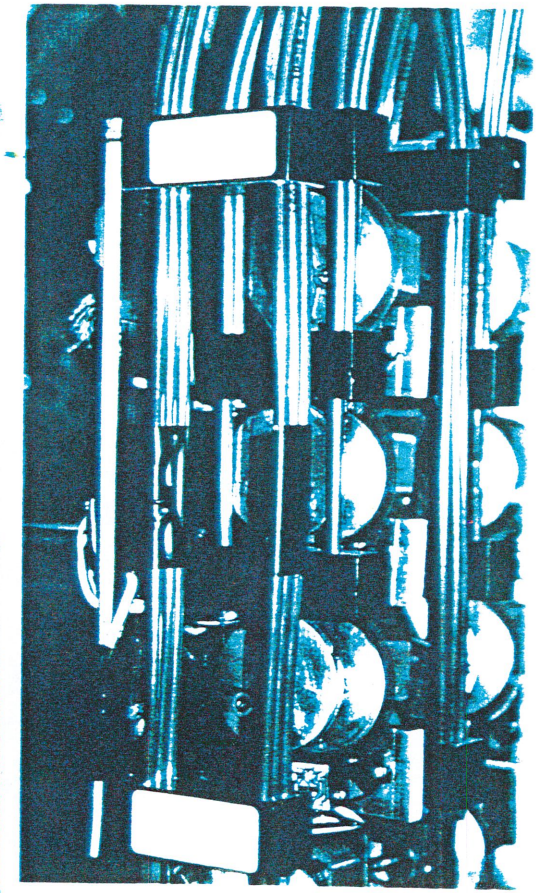


Plate [2.2] : One Finger Drive.

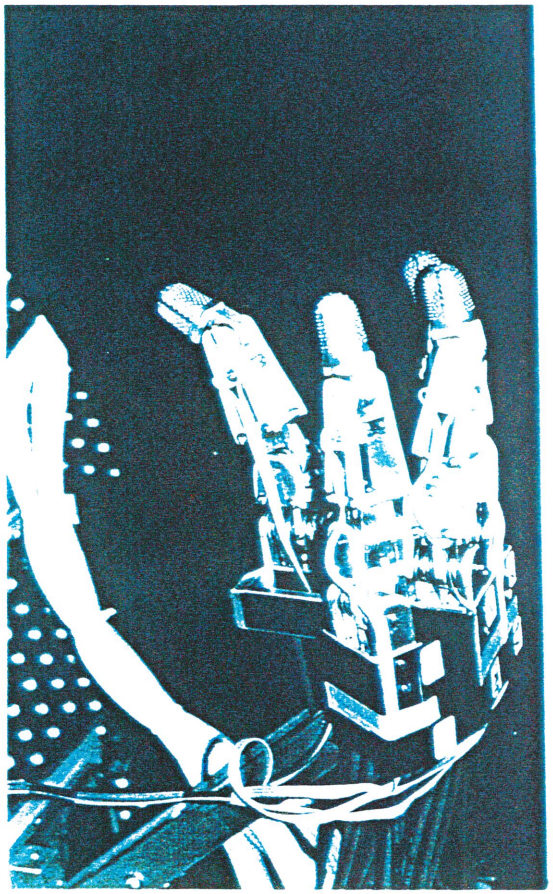


Plate [2.1] : Cybhand

Kinematics of human hands allow the performance of actions such as warping, pinching, picking, gripping, searching etc. In a similar way, the hand system is desired to have satisfactory handling functions for performing various flexible motions required to accomplish defined tasks with grasped workpiece.

2.4.2) One Finger Mechanical Structure

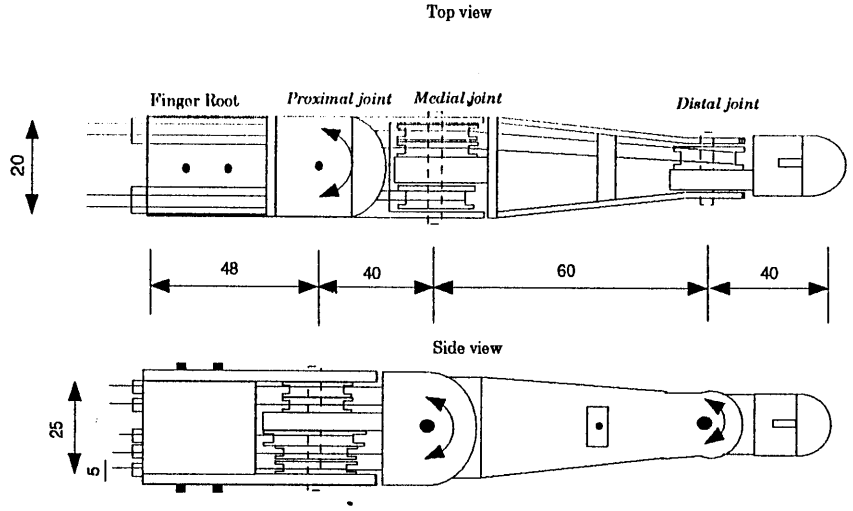
The construction of a finger with three degrees of freedom (DOF) is shown in Fig [2.3-a]. Each finger has a first joint (proximal joint) for lateral flexional motion at its proximal point, and two parallel axis joints (the medial and distal) to provide curling action. The first joint which is not anthropomorphic, is perpendicular to the other axes and provides the side to side motion of the finger. The hand includes four fingers, each digit containing three joints. The two distal joints of the fingers are capable of excursions from –90° to +90°, whereas the first joint is capable of +/–30° motions as shown in Fig [2.3-b]. The hand also includes up to 36 low friction pulleys for the purpose of tendon routing, AL-GALLAF *et al.* [1993-b].

2.4.3) Contact Nature and Transmitted Forces

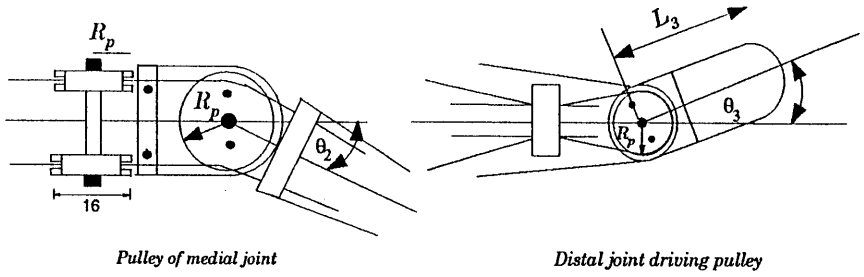
The shape of the fingertip part is an important element for the determination of a supporting area between the finger and the grasped object to be manipulated, since the smoothness of the manipulation depends on the form of this area.

The fingertip is designed mechanically to have a circular shape, since the circular cross section is the most suitable to suppress the rapid change of the grasping condition which arises during complicated finger motion, OKADA [1979]. Before discussing about a given grip and its properties to be studied and investigated, it is essential to consider the frictional interaction between the fingertips and the object being grasped.

What will be concentrated on is the mechanics of constraint and an object freedom that take



a



b

scale in mm

Figure 2.3 : a : Top and Side Views of One Finger Mechanical Structure.
b : Tendon Routing for the Medial and Distal Joints.

effect when two bodies come into contact. The type of contact which causes either *forces* or *forces and moments* to be transmitted to the objects and consequently the relative motion between the two bodies is determined by the geometric and frictional properties of the contact. Table [2.1] shows SALISBURY's three contacts types (point, line, plane) and their frictional properties which can be experienced by a surface, SALISBURY [1982].

Contact Type	*Remaining Degrees of Freedom*	*Absorbed DOF*
No contact	6	The workpiece is *free* to translate and rotate
Frictionless point contact	5	1
Frictionless line contact	4	2
Friction point contact	3	Normal and side motions are absorbed
Frictionless plane contact	3	3
Soft finger	2	4
Friction line contact	1	5
Planar contact with friction	0	All the DOF are absorbed, *immobilization*

Table [2.1] : SALISBURY's Types of Contacts .

The constraints imposed by each type of contact are characterized in terms of the degrees of freedom allowed and in terms of screw systems of motion and force related with each contact type.

Hence, for all the analysis done through out this thesis, the type of contact between the fingers and the grasped object has been considered to be a point contact with friction. From the mechanical point of view, a point contact with friction transmits a three wrench system and reduces an object degree of freedom from six to three.

Fig [2.4] shows a model of a fingertip type considered as friction type of contact which rolls around the point of contact with no slip, hence no torque is transmitted to the object due to this rolling. For static and dynamic grasping, the orientation of the surface where the object is in contact with the fingertip is an important matter in computing the distribution of forces in the entire hand.

For further details in the adopted contact type, Fig [2.5] shows the transmitted forces to the object itself due to a point contact. In the figure, the point of contact with friction forces are shown, where it is assumed that the fingertip is free to rotate in all directions about the contact point so that only forces are transmitted. At the point of interaction with the object, the normal force f_z produces a force f_t, which is tangential to the surface of contact and having a magnitude of μf_z. The tangential force f_t is decomposed into f_x and f_y, which are two orthogonal components with respect to a frame fixed at the contact location.

Since the interaction is a static problem, besides satisfying the condition for static equilibrium and not exceeding the conditions that bound μf_z, the direction of the tangential forces are unconstrained by the columb friction law.

For selecting those elements of a general six-element force/moment vector that are transmitted through the contact, the contact selection matrix $\boldsymbol{H}_c$ is defined for frictional point contact as :

$$\boldsymbol{H}_c = \begin{bmatrix} 1 & 0 & 0 & 0 & 0 & 0 \\ 0 & 1 & 0 & 0 & 0 & 0 \\ 0 & 0 & 1 & 0 & 0 & 0 \end{bmatrix} \tag{2.1}$$

The twist 3-system contains all zero pitch twists through the point of contact. The reciprocal wrench 3-system is composed of all zero wrenches through the point of contact, HSU *et al.* [1989]. Most of the analyses consider the point contact with friction, since it is the

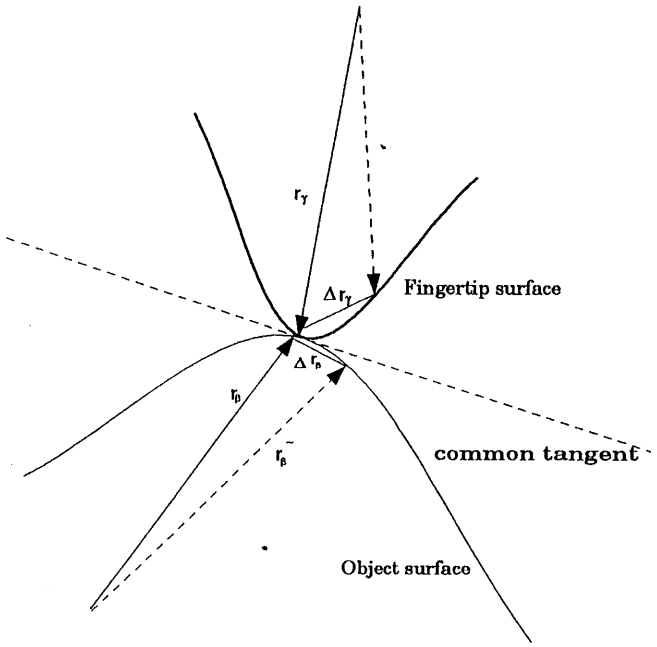
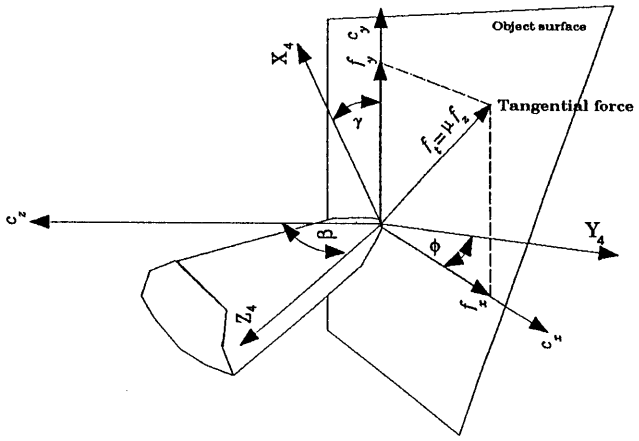


Figure 2.4 Rolling Contact.



β , γ , *and* ϕ *represent the finger tip rotation at the point of contact*

c_x c_y c_z : object contact frame

X_4 Y_4 Z_4 : fingertip frame

Figure 2.5 : Frictional Point of Contact and the Associated Resistance to Motion.

simplest to deal with mathematically, specially when making use of the grip transform, although quite a few consider the soft finger model that models a human finger, MCAREE *et al.* [1991]. The tangential force can be of any direction over the contact area depending on the direction where the normal force is acting.

The main difference between the soft finger type and a frictional point contact in terms of mathematical simplicity is the fact that : the use of soft finger type produces an extra rotational wrench which has to be modelled mathematically as an extra column in the grip transform as will be further discussed in Chapter Five. This extra column will enlarge the grip transform to be a $\in \Re^{[6\times 12]}$, thus increasing the complexity of the system.

2.4.4) Hand Drive Mechanism

The most straight forward choice of an actuator location for robot hands is at or near the finger joint it drives. However, because of difficulties in mounting joint actuators in each finger in recently presented designs, OKADA [1979] and SALISBURY [1985], have utilized a remote drive approach. Mechanical motions are transmitted to finger joints using tendons routed over frictionless pulleys. In direct-drive hand, joints axes are directly coupled to rotors of high-torque electric motors, therefore, no transmission mechanism is included between the motors and their loads. Because of this, the drive system has excellent features, no backlash, small friction, and high stiffness, ASADA *et al.* [1983]. From the modelling point of view, the simple mechanism allows a clear and precise model of each finger dynamics in the hand which is of special importance not only for accurate positioning control, but also for compensating interactive and nonlinear toques at high speed manipulation, AL-GALLAF *et al.* [1991].

2.4.5) Remotely Driven Hand

The employment of remotely located actuators is characterized by :

(*i*) A considerable reduction in hand weight.

(*ii*) Since space around the actuator is not a primary constraint, large position sensors could be mounted.

(*iii*) Utilizing robotics hands in under water and radioactive environments requires protection of the hand actuators. It is usually simpler to protect a drive box containing a number of actuators rather than to protect each joint actuator separately.

(*iv*) Locating actuators away from the hand avoids routing of electrical connectors to each joint.

(*v*) Allows the joints to be smaller, and reduces the load applied to the actuators from prior links.

(*vi*) Tendons provide smooth control at low speeds, however , they can stretch and exhibit hysteresis characteristics, thus reducing control accuracy, DOLL *et al.* [1988].

2.4.6) Direct Drive Hand

Contrary to this, direct drive hands are characterized by:

(*i*) Mathematical computations used in force and position control are reduced, especially when the hand is to implement a task that consists of a number of hand configurations.

(*ii*) Backlash and tendons stretch non-linearities are avoided, which reduces the complexity of the control system.

(*iii*) No mechanical coupling (due to transmission tendons) among finger joints, since every joint is controlled individually, however dynamic coupling is present.

(*iv*) The ratio of torque to current in direct drive actuator can vary considerably with rotor position and resulting in ripple torque, HOLLERBACH *et al.* [1993].

2.4.8) Hand Internal Sensors (Position and Force)

For the Cybhand mechanical design, incremental encoders have been employed for position sensing since they are suitable for interfacing to the used motion processors.

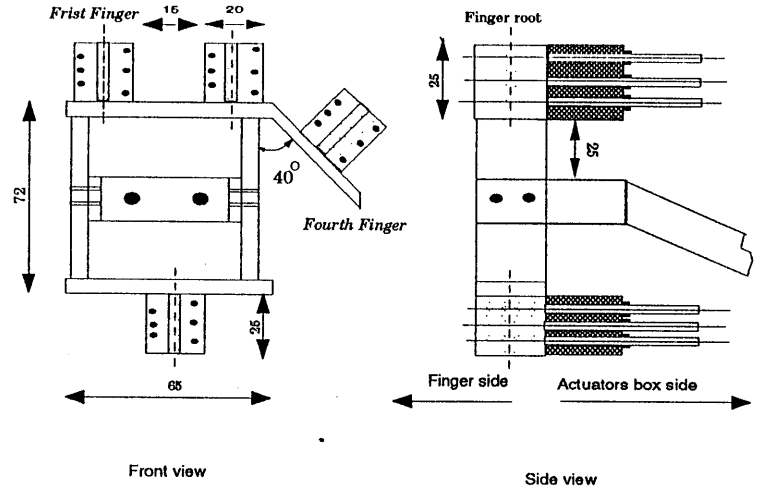
(A) Position Sensing :

The configuration of the fingers around the hand palm and tendon routing are shown in Fig [2.6-a]. For control purposes, Fig [2.6-b] illustrates one type of hand internal sensing which is : the position sensor. In the figure the position sensing has been based on the use of incremental encoders. An optical encoder for sensing angular displacement of a joint is located at each actuator driving pulley with an incremental encoder disk of 200 line/rev line resolution, AL-GALLAF [1994-c].

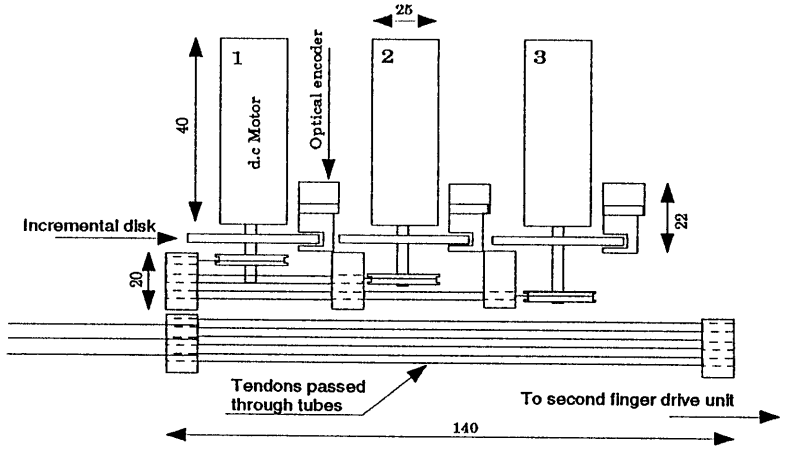
(B) Force Sensing :

The other type of hand sensing is the joint torque sensing based on detecting the change in tendon tension, as given in Appendix [A2]. Force sensing can be implemented either at the fingertip as in DOLL *et al.* [1988] and MAEKAWA *et al.* [1992] or at the joints as in JACOSON [1986]. Fingertip force sensing is useful in obtaining either tactile information or fingertip force both with high accuracy and high sensitivity. For the achievement of force control on an object it is required to transmit joints torques to fingertips force, since fingertip forces are related to the joint torque through the Jacobian J^T. Here the mechanism of force sensing is explained, whereas, the forces distribution problem will be formulated in Chapter Five.

From the mechanical design of one finger, because of the small size and insufficient space to mount the actuator inside the fingers, tendons have been used to transmitt the actuator torques and motion. The transmission system includes some significant compliance and friction in parts of the system such as the tendons and the gears. Therefore it is difficult to achieve a fine force control without of any force feedback. Employing force feedback would require the ability of the control system to sense the applied force to an object. Such force sensing is to be discussed in the coming section.



a



b

scale in *mm*

Figure 2.6 : a : Front and Side Views of Fingers Location Around the Hand Palm.
b: One Finger Drive System.

2.4.9) Applied Torque and Sensed Voltage Relation.

Construction

The overall torque sensor has been based on the use of a pair of strain gauges located on a cantilever beam. The pulley with cantilever beam are positioned in order to perturb the path of the tendon such that tendon tension imposes a moment on the cantilever beam. An aluminium type strain gauge bridge detects beam strain and provides a linear output for tendon tensions from 0 to 100 mN. The supporting electronics for both the position and tendon tension sensors are within the low level control unit as further discussed in AL-GALLAF [1994-c]. Such type of force sensing electronics will be further discussed while investigating the closed loop position and force servo mechanisms.

Within this section the mechanism of sensing an applied force to the fingertip is discussed. Furthermore, in Chapter Five it will be elaborated in the mechanism of computing the appropriate fingertip forces used in the force feedback to keep the object is static equilibrium against externally applied forces (*such as the weight of the object*).

Force sensing at the fingertip limits the control speed because of the required coordinate transformation of the sensed data from the sensor local frame to the joint frame. This approach has the disadvantage of making it difficult to measure the exact forces applied to the fingertip without using a six-axis force sensor. On the hand, joint torque allows higher servo rates, hence higher gain and bandwidth joint in the torque control. In accordance to the finger structure given in Appendix [A2], the basic structure of the sensor consists of two idler beams of a given beam stiffness, k_{s1} and k_{s2}, determined by the material and the physical dimension of the beam itself, where the two beams are fixed to a Π shaped holder. The torque produced by the fingertip is in proportion to the difference in the tensions at both ends of the driving pulley thus :

$$\tau_{drive} = \Re_p (T_1 - T_2) \qquad (2.2)$$

where $\Re_p$ *is* the radius of the distal joint driving pulley. When an external torque is applied to the driving pulley $\Re_p$, the vertical component V_f dimensional force acting on the cantilever beam is proportional to the tendon tension T_1 or T_2, such force can be expressed by, as given in Appendix [A2] :

$$V_{f1} = 2\, T_1\, Sin\,(\beta_1) \tag{2.3}$$

Further arrangement of variables gives :

$$V_o = G_a\, V_{ref}\, \frac{\kappa\,\tau}{(1-\kappa^2\,\tau^2)} \tag{2.4}$$

where

$$\kappa = \frac{12\,\sin(\beta)\,\chi}{\Re\, E_s\, W\, t^2}$$

Using the Table of sensor parameters given in Appendix [A2] and back substituting in Eq. 2.4, we are left with a numerical value of κ that equals to 0.0425 *v/Nm*. Hence a relationship has been established between an applied fingertip force F_a to the amount of torque acting in the driving pulley. This relationship is expressed as : $V_o = 6.80\, F_a$. From Eq. 2.4, the voltage generated from the sensor is entirely related to the acting torque on driving pulley. For certain beam physical parameters, the sensor voltage is made controllable by further adjusting the instrumentation amplifier gain G_a. For the constructed sensor, some experimental results have been gathered and compared with analytically obtained results.

Furthermore, Eq. 2.4 suggests that, the relation between V_o and the applied force exhibits nonlinear characteristics due to the existance of $[\kappa\,\tau\ /\ (1-\kappa^2\,\tau^2)\ ]$ term, however this nonlinearity can be approximated by ignoring the squared terms κ^2 due to its negligible value with respect to unity.

2.4.10) Results and Analysis

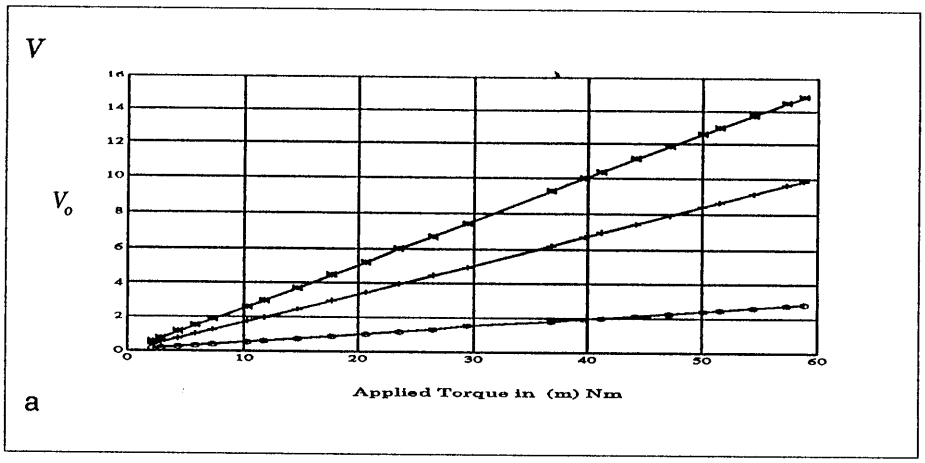
Having considered the relationship between an externally applied fingertip force acting at the fingertip to the generated voltage due to the beam strain in the previous section, within this section some experimental results will be shown and discussed.

An experimental test has been achieved for qualifying the voltage generated as a function of some externally applied force. Three sets of readings were obtained, where each set of reading corresponds to a given beam stiffness k_s.

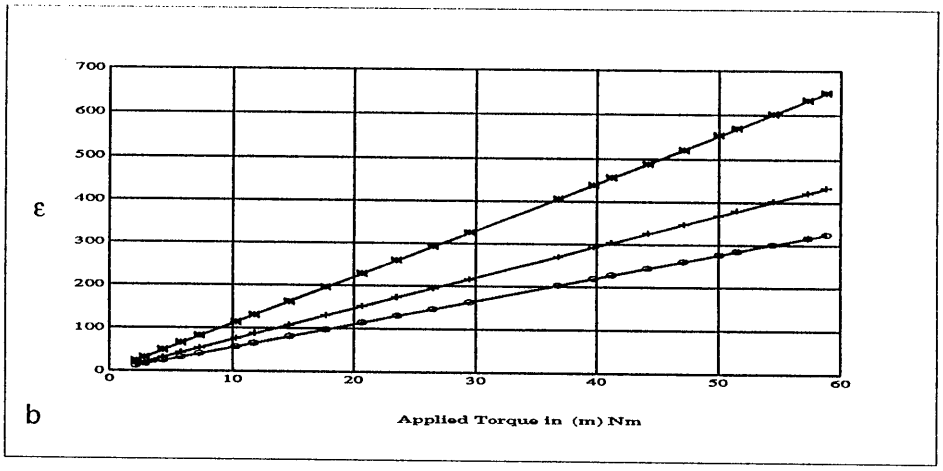
Fig [2.7-a] shows three linear relations between a known applied fingertip force and the corresponding sensed output voltage (a quantity used later for force feedback) for three different cantilever beams of different widths W, ($4\times10^{-3}\,m$, $6\times10^{-3}\,m$, and $8\times10^{-3}\,m$). For this experimental work, a force of known value was applied at a defined location in fingertip. This force produces a torque acting at the driving pulley, converted to measured voltage by Eq. 2.4.

The first is that when the sensor was having a beam stiffness of, k_s, $1568\,N/m$. Due to the fact small force applied will produce a considerable amount of strain ε , the generated voltage is highly comparable with the results when the beam stiffness of $2352\,N/m$.
The second line is when the beam stiffness has been increased to $k_s = 2352\,N/m$ by increasing the beam width to $6\times10^{-3}\,m$. The line shows higher beam stiffness, the generated voltage will be less due to the higher stiffness of the beam to the tendon displacement.

The third line is where the beam stiffness has been further increased by the increase in the beam thickness, up to $8\times10^{-3}\,m$. The generated voltage is even smaller than those in the previous cases. The type of beam characteristics (when $k_s = 3136\,N/m$) is useful when



* : Beam Stiffness of 1568 N/m,
\+ : Beam Stiffness of 2352 N/m,
o : Beam Stiffness of 3136 N/m.



* : Beam width of 4mm
\+: Beam width of 6mm
o: Beam width of 8mm.

Figure 2.7 : a : Measured Sensor Voltage for an Applied Torque.
b : Strain Acting on Cantilever Beam as a Function of Applied Torque.

the sensor is required to sense a large amount of applied force an the fingertip, since the sensor will be able to generate voltage for higher beam deformation , (thus a higher applied force).

Fig [2.7-b] shows the calculated strain of one beam in the sensor due to the previously applied forces. Due to the dependece of beam strain on the beam width, three lines of relations have been obtained, corresponding to the three lines in Fig [2.7-a]. The graph shows clearly how the beam strain (which is main factor in in the force sensor) changes with its width. The constructed torque sensor will be used in Chapter Four for closing a force feedback loop used to control the amount of pressure on an object for static grasping.

SUMMARY

Chapter Two has discussed the design aspects of the four fingered hand. It started with a brief look at the human hand and the sensory origins. Tendons routing, finger mechanical structure and sensing elements have been the main concepts presented.

The mechanical drive system and force sensor structure are the main concepts presented here, with a brief discussion on the contact interaction between the fingers and the object.

Sensor stiffness and the associated generated voltage have been shown (in association with Appendix [A2]) the main elements for designing force feedback sensor.

CHAPTER THREE

MODELLING of CYBHAND KINEMATICS

(3.1) INTRODUCTION

Kinematics is the relationship between the positions, velocities, and acceleration of the links of an articulated system, such as an arm, finger or leg.

Hand kinematics is the science of finger motion which treats those motions without regard to the forces that cause them. The study of the hand kinematics refers to all the geometrical and time-based properties of the motion. Within articulated hands, to deal with complex geometry a number of coordinate frames need to be affixed at various points of the mechanism and the relationship between these attached frames described. Hand kinematics is mainly utilised by the High Level Task planning for producing certain displacements within the hand working-space.

Given required fingertip locations in a defined cartesian space, we need to find values for the joint variables which will achieve this required position and orientation. The results of the hand inverse kinematics based either on Denavit-Hartenberg notation of frame assignment, DENAVIT and HARTENBERG [1955], hand geometrical structure, or by using an algebraic solution for the reduction to polynomial, are used by the hand task planning routines for the generation of a programmed sequence of motion.

This chapter has been classified into seven main sections. Section (3.2) concentrates on the frame assignment strategy at all the joints in a finger sub-system. Section (3.3) introduces the concept of the forward kinematics, and the inverse kinematics are given in section (3.4). Section (3.5) concentrates on the derivation of finger JACOBIAN, and the use of its determinant function to interpret some of the dexterity measures of the fingers is given in section (3.6). Section (3.7) provides the notation of the hand-object kinematics relations of contact which will be utilised later for transforming forces from contact frames to the

entire object frame. Finally section (3.8) presents the grasp quality measure associated with a four fingered hand using the singular value decomposition of the grasp transform.

(3.2) FRAME ASSIGNMENTS

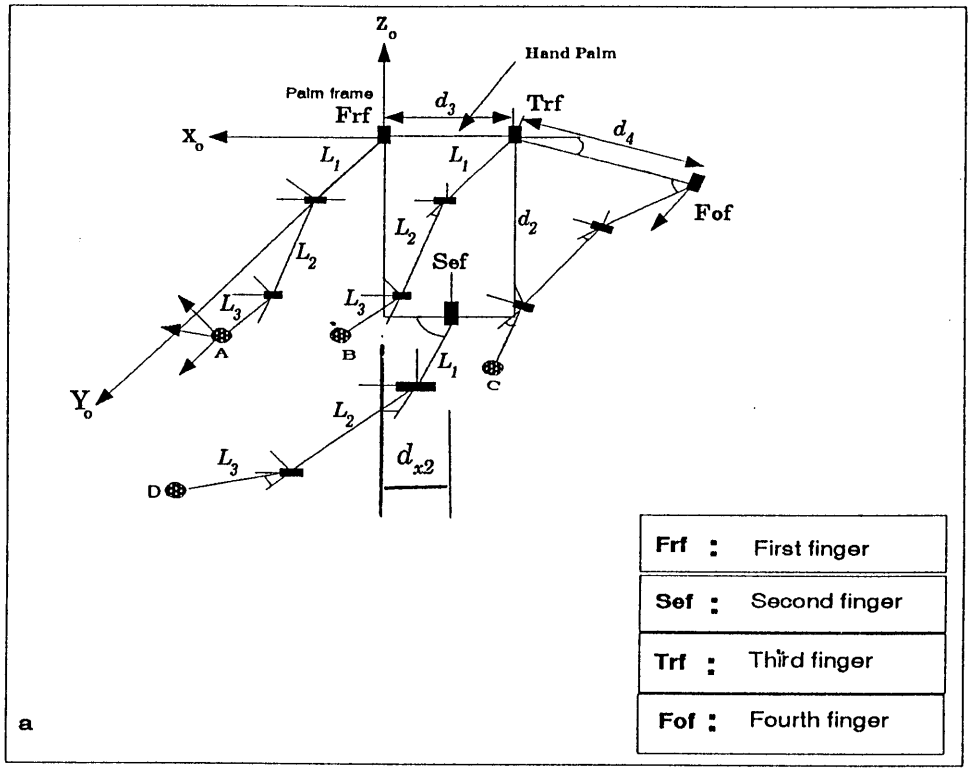
In order to deal with and handle the complicated geometry of multifingered robots hands, coordinate frames are affixed at the various locations of motions of the mechanism, Fig [3.1-a]. Relations are then developed between these frames. A succession of coordinate transformations, each defined by a particular transformation matrix, can be expressed by the matrix product or composition of the individual transformation matrices.

As was indicated in Chapter Two, each finger is a three degrees of freedom open chain comprising three rigid links (*Proximate, Medial, and Distal*) connected by three revolute pairs which are designated as the Proximal , Medial, and Distal joints respectively as shown in Fig [3.1-b]. The significance of links in articulated systems is that they maintain a fixed relationship between the fingers joints at each end of the link.

Four frames have been assigned to the finger sub-system , three of which are located at the joints and one at the fingertip where the finger makes contact with the workpiece. Defining the following links parameters in accordance to the hand fingers physical lengths.

Kinematics Links Parameters					
Joint	θ_i	α_i	a_i	d_i	Joint Range
Proximal	θ_1	90	L_1	0	- 30 to + 30
Medial	θ_2	0	L_2	0	- 90 to + 90
Distal	θ_3	0	L_3	0	- 90 to + 90

Table [3.1] : Associated kinematic links parameters.



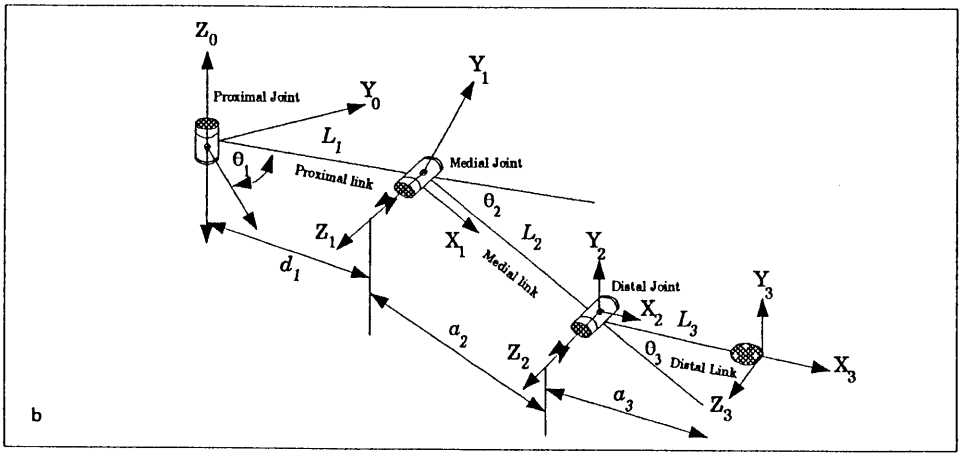


Figure 3.1 : a : Whole Hand Kinematics Frames Assignments.
b : Cybhand One Finger Link Frame Assignments.

(3.3) FORWARD KINEMATICS FORMULATION

While describing the hand kinematics two main factors come into consideration, "Are the fingers coupled from the kinematics point of view and is the issue of palm and proximal phalanges grasping considered? " In the observation of human grasping and manipulation, one frequently notes the fundamental role played by the inner parts of the hand (in particular the links) to enhance both the stability of the grip and the versatility of operation. If this enhanced dexterity and versatility is to be transferred to robot hands, then the object has to be grasped by the hand fingers links rather than by the fingertips prehension. However, if this is to be achieved then the complexity of the problem from the kinematics and dynamics point of view will be enlarged due to the involvement of all the links contacts. The whole hand contact system has already been discussed by BICCHI and PRATTICHIZZO [1992], where they assumed the object is manipulated by the entire hand links.

Hence , at this stage, it is made clear that the manipulation assumed here is a fingertip prehension rather than the use of the hand palm and proximal phalanges to enhance the grasp strength.

In this sub-section we are concerned with the kinematic's of one finger structure. First, the forward kinematics is evaluated which is based on the frame assignment given in section (3.2). Following this, the inverse kinematics process is performed using both the geometric and algebraic approaches.

3.3.1) Individual Fingers Kinematics

First Finger:

The ${}^{0}T_{3}$ is formed by matrix multiplication of all the individual link matrices, while forming this product some sub-results will be derived which will be useful while solving the

inverse kinematics problem in section (3.4). By multiplying

$$ {}^{0}T_{3} = \begin{bmatrix} n_x & o_x & a_x & P_x \\ n_y & o_y & a_y & P_y \\ n_z & o_z & a_z & P_z \\ 0 & 0 & 0 & 1 \end{bmatrix} \qquad (3.1) $$

where the ${}^{0}T_{3}$ entries have been calculated as :

$$ \begin{aligned} n_x &= C_1C_{23} & o_x &= -C_1S_{23} & a_x &= S_1 & P_x &= C_1\,[L_3\,C_{23} + L_2C_2 + L_1] \\ n_y &= S_1C_{23} & o_y &= -S_1S_{23} & a_y &= -C_1 & P_y &= S_1\,[L_3\,C_{23} + L_2C_2 + L_1] \\ n_z &= S_{23} & o_z &= C_{23} & a_z &= 0 & P_z &= L_3S_{23} + L_2S_2 \end{aligned} \qquad (3.2) $$

In order to compute the right hand three columns of ${}^{0}T_{3}$, we require eight transcendental function calls, three multiplications and six additions are required. The first column of ${}^{0}T_{3}$ can be obtained as the vector cross product of the second and third columns. If the joint coordinates are given, the position and orientation of the fingertip are obtained by evaluating these equations to obtain ${}^{0}T_{3}$, thus describing the position and orientation of the fingertip in terms of the variables (θ_1, θ_2, θ_3). While describing the kinematic for the fingers, it is necessary to define their kinematics with respect to a fixed cartesian frame in the hand palm. Such frames are essential factors for an object manipulation that will be utilized later in Chapter Six. To define the fingertips of the four fingers to the fixed cartesian frame, a permanent palm frame has been established at the base of the first finger sub-system, illustrated in Fig [3.1-a].

Second Finger:

Each of the fingers is related to the hand palm reference coordinate (attached to the root of the first finger) by transformations which are designated by d_2, d_3, and d_4 for the second,

third , and fourth fingers respectively. Due to the position of the second finger in the hand palm, the fingertip location with respect to the hand palm is defined by the kinematics equation that is obtained by multiplying the finger transformation matrix ${}^{0}T_{3}$ by the transformation matrix which represents the displacement of that finger from the origin of the palm coordinate frame. If the displacement of the second finger is denoted by $[-d_{x2}, 0, -d_{2}]$, the location of the second finger with respect to the hand frame is defined by :

$$T_s = \begin{bmatrix} C_1C_{23} & -C_1S_{23} & S_1 & P_x - d_{x2} \\ S_1C_{23} & -S_1S_{23} & -C_1 & P_y \\ S_{23} & C_{23} & 0 & -d_2 + P_z \\ 0 & 0 & 0 & 1 \end{bmatrix} \tag{3.3}$$

Third Finger :

$$T_t = \begin{bmatrix} C_1C_{23} & -C_1S_{23} & S_1 & P_x - d_3 \\ S_1C_{23} & -S_1C_{23} & -C_1 & P_y \\ S_{23} & C_{23} & 0 & P_z \\ 0 & 0 & 0 & 1 \end{bmatrix} \tag{3.4}$$

Fourth Finger:

$$T_f = \begin{bmatrix} .76C_2S_{23} + .64S_{23} & -.76C_1S_{23} + .64C_{23} & .76S_1 & .7P_x + .64P_z - d_4 \\ S_1C_{23} & -S_1C_{23} & -C_1 & P_y \\ -.64C_2S_{23} + 0.76S_{23} & .64C_2S_{23} + .76C_{23} & -.64S_1 & -.64P_x + .76P_z \\ 0 & 0 & 0 & 1 \end{bmatrix} \tag{3.5}$$

Eq. 3.2 to Eq. 3.5 constitute the kinematics model of the four fingers, they specify how to compute the position and orientation of frame 3 relative to frame 0 in each finger. These are the basic equations for all kinematics analysis of the hand which are investigated with-

in this chapter.

(3.4) INVERSE KINEMATICS

In order to describe a finger position, the reverse problem must be considered, that is, given P_x, P_y, and P_z in Eq. 3.2, what are the corresponding joint coordinates?

In section (3-3), the problem of computing the position and orientation of the fingertip frame ${}^0T_3$ was considered relative to the frame fixed at the hand palm, given the joint angles of the finger. In this section the problem of inverse kinematics is presented.

Expressed another way, the inverse kinematics problem is given a frame or a homogeneous ${}^0T_3$ matrix in the reachable subset, solve for the corresponding values of the joint variables that would result in simillar ${}^0T_3$ matrix numerical values. In contrast to the direct kinematics problem, the inverse kinematics problem does not have a general analytical solution. Given the desired position and orientation of the fingertip relative to the finger root, how do we compute the set of joint angles which will achieve this desired result within a constrained kinematic system ?

The cartesians upon which to base a decision vary, but a reasonable choice would be the closest solution. A finger will be considered kinematically solvable if the joint variable can be determined by an algorithm which allows one to determine all the sets of joint variables associated with a given position and orientation. We shall restrict our attention to closed form solution methods.

In this context "closed form" means a solution method based on analytic expressions or on the solution of a polynomial. Within the closed form solutions two methods of obtaining a

solution are distinguished : The algebraic and geometric solutions.

3.4.1) Algebraic Approach

According to Eq. 3.2 and the frame assignment given in Fig [3.1-b], we wish to solve for the joint space vector $\Theta_i^T = [\theta_{1i}\ \theta_{2i}\ \theta_{3i}]$ given a cartesian numeric coordinate of a given fingertip posture.

If we equate the ${}^0A_3$ matrix with the numeric matrix we shall end up with:

$$\underbrace{\begin{bmatrix} \Re_{11} & \Re_{12} & \Re_{13} & \Re_{14} \\ \Re_{21} & \Re_{22} & \Re_{23} & \Re_{24} \\ \Re_{31} & \Re_{32} & \Re_{33} & \Re_{34} \\ 0 & 0 & 0 & 1 \end{bmatrix}}_{T_{symbolic}} = \underbrace{\begin{bmatrix} n_x & o_x & a_x & P_x \\ n_y & o_y & a_y & P_y \\ n_z & o_z & a_z & P_z \\ 0 & 0 & 0 & 1 \end{bmatrix}}_{T_{numeric}} \tag{3.6}$$

Equating the individual elements of the two matrices, that gives :

$$\begin{aligned} P_x &= C_1 [L_3 C_{23} + L_2 C_2 + L_1] \\ P_y &= S_1 [L_3 C_{23} + L_2 C_2 + L_1] \\ P_y / P_x &= S_1 / C_1 \\ \theta_1 &= TAN^{-1}(P_x / P_y) \end{aligned} \tag{3.7}$$

Also from P_z

$$P_z = L_3 S_{23} + L_2 S_2 \tag{3.8}$$

Divid by $Cos(\theta_2)$

$$P_z / C_2 = \frac{L_3\ S_{23} + L_2 S_2}{C_2}$$

$$(P_z - L_3 S_{23} / C_2) = L_2\, Tan(\theta_2)$$

$$Tan(\theta_2) = (P_z - L_3 S_{23}) / (L_2 C_2) \tag{3.9}$$

However, what is the value of $COS(\theta_2)$ in Eq. 3.9 ?

From $$P_x = L_3C_1O_z + C_1L_2C_2 + C_1L_1$$

$$L_2C_2 = (P_x - L_3o_zC_1 - C_1L_1)/(C_1)$$

$$L_2C_2 = [(P_x/C_1) - L_3o_z - L_1]$$

$$\theta_2 = Tan^{-1}\frac{(P_z - L_3n_z)}{(P_x/C_1 - L_3o_z - L_1)} \qquad (3.10)$$

$$\theta_3 = Tan^{-1}(n_z / o_z) - \theta_2 \qquad (3.11)$$

The use of the above kinematics equations requires the use of the orientation and position vectors. These vectors may not have been provided for or calculated previously, unless they have been computed numerically. The initial solution is that which corresponds to a known orientation vectors.

3.4.2) Geometric Approach

A geometric approach for solving the inverse kinematic problem is the method of decomposing the spatial geometry of the finger into several plane geometry problems. Joint space vectors can be solved for using the tools of plane geometry. Fig [3.2-a] shows the geometric configuration of one finger. Applying rules of geometry for that finger shape gives the following equations describing the joint space vector in terms of the given P_x, P_y, P_z fingertip vector. From Fig [3.2-a], and for the triangle OIM :

$$Tan(\theta_1) = P_y / P_x$$

$$\theta_1 = Tan^{-1}(P_y / P_x) \qquad (3.12)$$

From Fig [3.2-a], since $P_q = P_r - L_1$,

$P_r^2 = P_x^2 + P_y^2$ and $P_t^2 = P_z^2 + P_q^2$

$$\theta_z = Tan^{-1}(P_z / P_q)$$

Having found θ_z then $\theta_z = \theta_z - W_a$

$$\theta_3 = 180° - Cos^{-1}((P_t^2 - L_2^2 - L_3^2) / (-2L_2L_3)) \qquad (3.13)$$

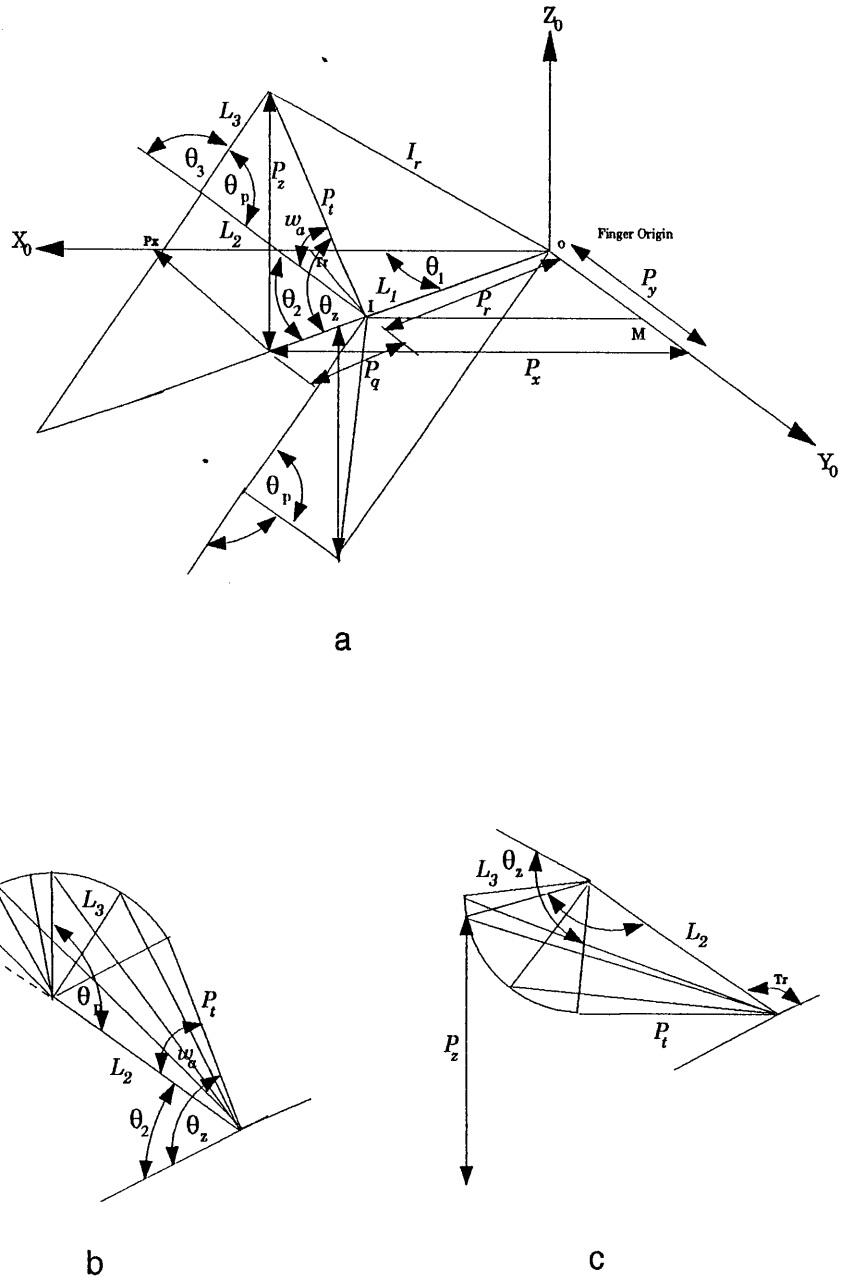


Figure 3.2 : a : 3-D Geometry Associated with One Finger.
b : Trajectery of Possible Solutions for an Up Motion Finger.
c : Trajectery of Possible Solutions for a Down Motion Finger.

$$W_a = C^{-1}((L_3^2 - P_t^2 - L_2^2) / (-2P_t L_2))$$

Using the geometric model of the finger is a simple and quick approach to obtaining the joint space vector. One drawback of this method is that : at certain finger posture the geometric configuration of the finger fails to give a solution. Fig [3.2-b-c] show certain configurations of the fingertip where the solution is not well defined and hence multiple solutions may appear. However as θ_p gets large enough, the fingertip location P_t goes to a position with respect to θ_z and T_r angles where the cosine rule used in Eq. 3.13 is not applicable. To obtain a reasonable solution, the hand controller source code has been designed in such a way as, to get the inverse kinematic for the finger model using the geometric approach. After the joint space vector has been obtained, the orientation vectors are evaluated since they constitute the columns of the well known Jacobian matrix of a finger J_Θ. Generally, both the geometric and algebraic approaches of solutions fail to give definite solution. Once the finger is in singular configuration, θ_3 is null as will be proved analytically in the coming section.

(3.5) FINGER JACOBIAN J_Θ

A Jacobian is a matrix of differentials, and in the case of an articulated system, differential changes in the location of the end of the finger are caused by differential changes in joint variables. The number of rows in a Jacobian is determined by the number of degrees of freedom in cartesian space required by the task which is, in turn, determined by the degrees of mobility of the task.

From a mathematical point of view JACOBIAN is a multi-dimensional form of the derivative of a function of several variables. Since the Jacobian is a differential form of matrix, then it is possible to obtain the elements of that matrix using the chain rule as far as the functions of independent variables.

For the finger Jacobian J_Θ, there are a number of methods which have been developed for the Jacobian calculation, examples of which are :

(*i*) Waldron Algorithm, (*ii*) Renand Algorithm,

(*iii*) Orin and Shrader Algorithm, SAMASON *et al.* [1991].

(*iv*) Paul's Algorithm, PAUL [1981].

Since the position of the fingertip is characterized by the relative positioning of a frame f_{i+1} linked to the fingertip with respect to a reference frame f_o, the velocity of the fingertip is a vector in the tangent space of the frame space, which is related by the Jacobian matrix J_Θ

Singularities of the Jacobian . Due to the fact the Jacobian is a position dependant, in some finger configurations the matrix becomes not full of rank. When this occurs the Jacobian rows and column vectors are linearly dependent, thus do not span the $\in \Re^{(3\times 1)}$ vector space of X. Therefore , there exists at least one direction in which the fingertip cannot be moved no matter how the joint velocities $\dot{\theta}_1$ through $\dot{\theta}_3$ are chosen.

3.5.1) Computation of the Jacobian

All the methods developed for the computation of the Jacobian share the same common method of solution and hence only differ from each other where the components of the matrix are expressed.

Calculation by differentiation :

The Jacobian for fingers can be computed by differentiating its forward kinematic transform given by Eq. 3.2. Differentiation Eq. 3.2:

$$\begin{bmatrix} \partial x \\ \partial y \\ \partial z \end{bmatrix} = J_\Theta \begin{bmatrix} \partial\theta_1 \\ \partial\theta_2 \\ \partial\theta_3 \end{bmatrix} = \begin{bmatrix} (\partial P_x/\partial\theta_1) & (\partial P_y/\partial\theta_2) & (\partial P_z/\partial\theta_3) \\ (\partial P_y/\partial\theta_1) & (\partial P_y/\partial\theta_2) & (\partial P_z/\partial\theta_3) \\ (\partial P_z/\partial\theta_1) & (\partial P_z/\partial\theta_2) & (\partial P_z/\partial\theta_3) \end{bmatrix} \begin{bmatrix} \partial\theta_1 \\ \partial\theta_2 \\ \partial\theta_3 \end{bmatrix} \quad (3.14)$$

This results in the following Jacobian :

$$J_{\Theta} = \begin{bmatrix} -\Psi S_1 & -C_1[L_2S_2 + L_3S_{23}] & -C_1L_3S_{23} \\ \Psi C_1 & S_1[L_3S_{23} + L_2S_2] & -S_1L_3S_{23} \\ 0 & L_3C_{23} + L_2C_2 & L_3C_{23} \end{bmatrix} \qquad (3.15)$$

where $\Psi = (L_3 C_{23} + L_2C_2 + L_1)$

3.5.2) Jacobian in the Velocity Domain

[A] *Derivation of Finger Jacobian Matrix in Terms of D-H Matrices.*

In Eq. 3.15 the Jacobian is defined with respect to the reference frame, frame (0) at the finger root. However, for our purpose it has been assumed that the points of contact are stationary on the grasped object and another algorithm can be implemented based upon the kinematic model of the finger. Such algorithm is based on the method shown by PAUL [1981]. Since all joints are revolute, the three columns of the matrix are given by :

$$\begin{aligned} A^3d_i &= (-n_xP_y + n_yP_x)\,i \quad (-o_xP_y + o_yP_x)\,j \quad (-a_xP_y + a_yP_x)\,k \\ A^3\delta_i &= n_z i \qquad o_z j \qquad a_z k \end{aligned} \qquad (3.16)$$

While using such an algorithm, it is necessary to evaluate the orientation vectors of a particular finger posture, which are assumed to be known by using the geometric finger model and the forward transformation matrix.

Paul's algorithm can be used to calculate the Jacobian of an n degrees of freedom manipulator, where each degree of freedom corresponds to one joint. Thus, each column in the Jacobian is a vector which describes the differential motion of a joint. A revolute joint has a differential rotation around the axis of rotation Z axis:

$$
\begin{aligned}
\partial P_x/\partial\theta_n &= J_{1n} = {}^{n-1}n_y\,{}^{n-1}P_x - {}^{n-1}n_x\,{}^{n-1}P_y \\
\partial P_y/\partial\theta_n &= J_{2n} = {}^{n-1}o_y\,{}^{n-1}P_x - {}^{n-1}o_x\,{}^{n-1}P_y \\
\partial P_z/\partial\theta_n &= J_{3n} = {}^{n-1}a_y\,{}^{n-1}P_x - {}^{n-1}a_x\,{}^{n-1}P_y \\
\partial\delta_x/\partial\theta_n &= J_{4n} = {}^{n-1}n_z \\
\partial\delta_y/\partial\theta_n &= J_{5n} = {}^{n-1}o_z \\
\partial\delta_z/\partial\theta_n &= J_{6n} = {}^{n-1}a_n
\end{aligned}
\tag{3.17}
$$

To relate the position of the fingertip of a finger (defined in Cartesian coordinates) to the joint angles of the fingers of a finger, one may make use of the forward solution and obtain the fingertip matrix ${}^0T_3$. PAUL [1981] presented a method that relates differential changes in joint variables to the differential changes in the tip position and orienation.

$$
{}^0T_3 = \begin{bmatrix}
C_1C_{23} & -C_1S_{23} & S_1 & C_1[L_3C_{23}+L_2C_2+L_1] \\
S_1C_{23} & -S_1S_{23} & -C_1 & S_1[L_3C_{23}+L_2C_2+L_1] \\
S_{23} & C_{23} & 0 & L_3S_{23}+L_2S_2 \\
0 & 0 & 0 & 1
\end{bmatrix}
\tag{3.18}
$$

$$
{}^1T_3 = \begin{bmatrix}
C_{23} & -S_{23} & 0 & L_3C_{23}+L_2C_2 \\
S_{23} & C_{23} & 0 & L_3C_{23}+L_2S_2 \\
0 & 0 & 1 & 0 \\
0 & 0 & 0 & 1
\end{bmatrix}
\tag{3.19}
$$

$$
{}^2T_3 = \begin{bmatrix}
C_3 & -S_3 & 0 & L_3C_3 \\
S_3 & C_3 & 0 & L_3S_3 \\
0 & 0 & 1 & 0 \\
0 & 0 & 0 & 1
\end{bmatrix}
\tag{3.20}
$$

Further application of Paul's algorithm using the relation defined by Eq. 3.17 gives :

First column of $\boldsymbol{J}_\Theta$

$$\begin{aligned} \partial x_1 &= \Psi S_1 C_1 C_{23} - S_1 C_{23} & \partial x_1 &= 0 \\ \partial y_1 &= \Psi[C_1 S_1 S_{23} + S_1 C_1 S_{23}] & \partial y_1 &= 0 \\ \partial z_1 &= -C_1^{\,2}\Psi - S_1^{\,2}\Psi & \partial z_1 &= -\Psi \end{aligned} \qquad (3.21)$$

$$\delta x_1 = S_{23} \qquad \delta y_1 = C_{23} \qquad \delta z_1 = 0 \qquad (3.22)$$

Second column of $\boldsymbol{J}_\Theta$

$$\begin{aligned} \partial x_2 &= S_{23}[L_3 C_{23} + L_2 C_2] - C_{23}[L_3 S_{23} + L_2 S_2] & \partial x_2 &= L_2 S_3 \\ \partial y_2 &= C_{23}[L_3 C_{23} + L_2 C_2] + S_{23}[L_3 S_{23} + L_2 S_2] & \partial y_2 &= L_3 + L_2 C_3 \\ \partial z_2 &= 0 \end{aligned} \qquad (3.23)$$

$$\delta x_2 = 0 \qquad \delta y_2 = 0 \qquad \delta z_2 = 1$$

Third column of $\boldsymbol{J}_\Theta$

$$\begin{aligned} \partial x_3 &= L_3 C_3 S_3 - L_3 S_3 C_3 & \partial x_3 &= 0 \\ \partial y_3 &= L_3 C^2_{\ 2} + L_3 S^2_{\ 3} & \partial y_3 &= L_3 \\ \partial z_3 &= 0 \end{aligned} \qquad (3.24)$$

$$\delta x_3 = 0 \qquad \delta y_3 = 0 \qquad \delta z_3 = 1$$

Hence $\boldsymbol{J}_\Theta$ can be written as :

$$\boldsymbol{J}_\Theta = \begin{bmatrix} 0 & L_2 S_3 & 0 \\ 0 & L_3 + L_2 C_3 & L_3 \\ -\Psi & 0 & 0 \end{bmatrix} \qquad (3.25)$$

Eq. 3.25 has been verified using MATHEMATICA software using the Velocity Cross Product method used by FU *et al.* [1987].

Since each finger has a three degrees of freedom mechanism responsible for producing translational differentials motion at the fingertip, the Jacobian matrix can be rewritten in terms of differentials motion of the fingertip.

3.5.3) Jacobian in the Force domain

In the force domain the Jacobian transpose of a finger J^T maps Cartesian forces acting at the fingertip into equivalent joint torques. If the Jacobian is expressed with respect to frame the finger root, then *ith* force vector f_{tipi} acting at the fingertip may be transformed to the corresponding joints torques as follows :

$$\tau_i = J_\Theta^T f_{tipi} \tag{3.26}$$

where the column vector τ_i has entries corresponding to torques of force depending on the type of joint and column vector, f_{tipi} has entries of force relating to the degrees of freedom chosen. For a six-degree-of-freedom situation, it consists of three forces corresponding to the x, y, z directions and three torques (*or moments*) corresponding to rotations about the $x, y,$ and z frames of the hand. Eq. 3.26 is one of the fundamental equations to be used in force distribution since it is required to map the fingertip forces to their corresponding torques at the finger. For the finger kinematics driven by Eq. 3.2 , the joint torques are related to the contact forces through only the upper sub-matrix of the Jacobian J_Θ^T with a size $\in \Re^{[3\times3]}$

$$\tau_i = \begin{bmatrix} 0 & 0 & -\Psi \\ L_2S_3 & L_3+L_2C_3 & 0 \\ 0 & L_3 & 0 \end{bmatrix} \begin{bmatrix} f_x \\ f_y \\ f_z \end{bmatrix} \tag{3.27}$$

Eq. 3.27 is based on the use of the Jacobian expressed with respect to the contact coordi-

nate, a coordinate which might not be allied with an object contact frame. When the Jacobian has to be expressed with the contact coordinate, it has to be multiplied by a rotation matrix that defines the rotation of the fingertip coordinate to those at the contact point.

(3.6) THE CONFIGURATION SPACE and TIP MAPPING

A taxonomy study concluded that "the choice of one particular grasp over all others is primarily determined by the characteristic of the task that must be accomplished ", CUTKOSKY [1989]. It is important factor to understand the grasp and motions of the fingers in the defined task in order to understand the motions of the workpiece.

Manifolds geometry arise naturally as the configuration spaces of mechanical linkages HUNT *et al.* [1992]. The central idea is to think of each configuration of a mechanism as a point in a higher dimensional space. For the cybhand design, because each joint is a revolute, the configuration space of the finger is identified with the cartesian product of three circles, $C = \boldsymbol{S}_1 \times \boldsymbol{S}_2 \times \boldsymbol{S}_3$ which is a three tours. Each finger configuration corresponds to a point on the three tours and is uniquely specified by a triple of angles representing the forward kinematic relation of each finger. Knowledge of the joint space angles (θ_1 , θ_2 , θ_3), e.g. configuration of the finger linkage, determines a location for the fingertip $\boldsymbol{I}$ in the ambient three-space which we fully specify by a triple point $\boldsymbol{I} = (I_1, I_2, I_3)$. From the forward kinematics equation represented by Eq. 3.2, it is clear the triple point $\boldsymbol{I}$ is a function of the three joint angles namely.

$$\boldsymbol{I}^T = \quad [\ \Psi C_1 \quad \Psi S_1 \quad L_3 S_{23} + L_2 S_2\ ] \tag{3.28}$$

The region of ambient three-space that the point $\boldsymbol{I}$ can reach is known as the reachable workspace of the finger. For the four fingered hand, the contact geometry represents a

polygon, if the contacts are stationary with respect to the object frame and reachable by the workspace of the entire hand, then the size of the polygon remains constant during the manoeuvre of the object as long as the fingers do not slide. Each point of the polygon is defined by Eq. 3.28 for a particular grasp geometry.

3.6.1) Jacobian Function

The determinant function :

Numerous dexterity and manipulability indices, such as the condition number of the Jacobian, MASON and SALSIBURY [1985], have been proposed for the analysis and the design of robotics manipulators. The determinant function of the Jacobian designated by D, can be used to describe the dexterity of the finger at a given finger configuration. For a one finger case; the Jacobian was defined in terms of finger x, y, and z components.

$$\boldsymbol{J}_{\Theta} = \begin{bmatrix} -\Psi S_1 & -C_1 [L_3 S_{23} + L_2 S_2] & -C_1 L_2 S_{23} \\ \Psi C_1 & -S_1 [L_3 S_{23} + L_2 S_2] & -S_1 L_3 S_{23} \\ 0 & L_3 C_{23} + L_2 C_2 & L_3 C_{23} \end{bmatrix} \tag{3.29}$$

Note that the first column of $\boldsymbol{J}_{\Theta}$ describes the direction in which the tip moves if only the proximal joint θ_1 is actuated. Similarly, the second and third columns of $\boldsymbol{J}_{\Theta}$ describe the respective directions of tip motion when the medial θ_2 or distal joint θ_3 are independently actuated. When the tip map is singular, the tip (*instantaneously*) loses one or more of these DOF. Instead of finding the finger singularities using a recursive method as achieved by BURDICK [1992], the determinant function can be used to describe the status of the finger at a particular posture. Through appropriate manipulation of the rows and columns of the Jacobian matrix, Eq. 3.29, as described in Appendix [A3-1], the determinant D is found to be, AL-GALLAF and WARWICK [1994-d]:

$$D = -\Psi L_2 L_3 S_3 \tag{3.30}$$

By the inverse function theorem, the tip I is singular once D is zero. There are three occasions when $D = 0$: (*i*) when L_2 or L_3 are zero which is not considered here, since the lengths of the links are constant, and are of non-zero values. (*ii*) When either S_3 or Ψ is zero. (*iii*) When both condition (*i*) and condition (*ii*) occur at the same time.

Furthermore :

(*i*) $S_3 = 0$ when the finger is straight or folded back on itself and shown in Fig [3.3-a].

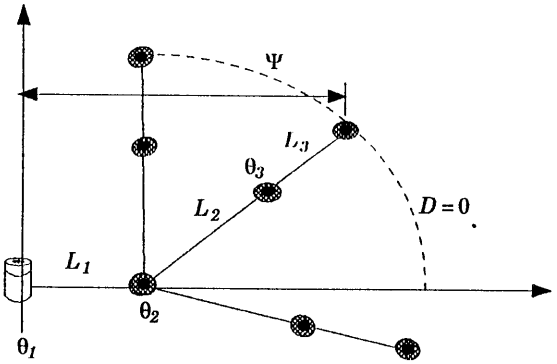
(*ii*) $\Psi = 0$ when the tip T lies on the proximal axis as shown in Fig [3.3-b].

(*iii*) Special configuration types 1 and types 2 occur simultaneously, Fig [3.3-c]. The columns of the Jacobian J_Θ now span the two-dimensional linear space of vectors available for infinitesimal displacements of I. Furthermore, when the finger linkage is in configuration 3, the tip loses two DOF's and the columns of J_Θ all belong to the same dimensional vector space. Finally it is clear that for this particular finger design, the finger does not lose more than two DOFs.

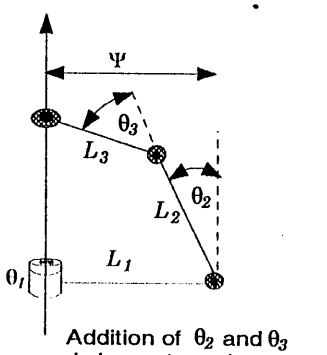
Due to the physical limitations on the joints motions, the fingertip of the linkage will not be located within a configuration when Ψ is zero, hence we are left with the possibility of losing one DOF when the distal joint is of zero value.

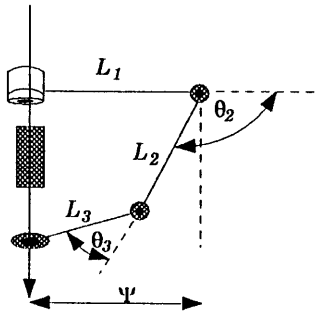
The determinant of the Jacobian D can be used to describe the dexterity at a given configuration. The value of D coincides with the oriented volume of the parallelepiped defined by the column vectors of the Jacobian J_Θ.

For each configuration, the magnitude of D relative to the absolute maximum value that it can take gives a measure of the sensitivity of the finger at that configuration. When it is large high tip velocities are achievable, but the mechanical advantage of the linkage is low. When it is small the mechanical advantage of the linkage improves, but achievable fingertip speeds decrease.

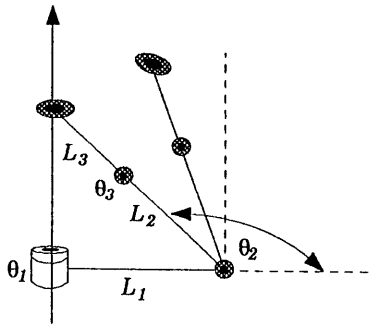


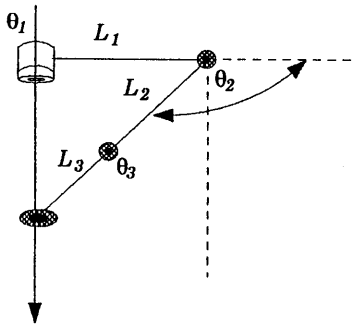
a





b





c

Figure 3.3 : a : Trajectory of Singular Posture for Type 1 Configuration.
b : Singular Posture Over the Z-axis, Type 2 Configuration.
c : A Finger in Singularity Approching Another Singularity, Type 3 Configuration.

Singularity is also an important factor in the force domain. It has been mentioned that when the Jacobian is *ill-conditioned,* it is difficult to solve. As the Jacobian is an important matrix for robot hands due to its use in the force domain, singularities also cause problems for force control. However, the Jacobian transpose is used in the inverse force transform and not the inverse Jacobian itself as in the inverse velocity transform. In force domain near singular position, the applied force in the singular directions can vary greatly with no effect on the torque. As the finger gets away from singularity, the dexterity changes with finger configuration. The motion and force domain qualities change with the dexterity.

Consider a simple human example of pressing two objects together; the natural position adopted is to press with the forearms in a straight line and the hands close to the chest. It would be unusual to press with the hands extended away from the chest; the mechanical advantage is low.

Since the determinant function of a finger Jacobian $D = -\Psi L_2 L_3 S_3$, is independent of the proximal joint angle, it can be projected onto a mesh plot to observe how it changes with configuration. In the mesh plot, each of the medial and distal joints are varied over their entire range of motion. The two mesh plots are for the same determinant function seen from two different view points.

3.6.2) Continuous Measure for Kinematic Dexterity

The degree of manipulability, which we shall designate as M_o, provides information about the equality of kinematic structure in executing tasks described by the manipulation variable. If DOM degenerates and becomes less than the DOF, then there exist some directions in which the fingers cannot move. Hence it is necessary to measure the manipulability M_o as the hand undergoes a continous motion.

Relationship with Condition Number

The condition number of a matrix can be used to evaluate the property of the linear equations.

As has been mentioned before, the Jacobian becomes a rank defect once it is in singular configuration. The measure of how close the finger to singularity can be based in a number of techniques. Here, for the purpose of analysing the singularity problems associated with the finger design, we shall use the condition number of the Jacobian in addition to the *countor plot* of this matrix $\boldsymbol{J}_{\Theta}$.

Singular Value Decomposition

The singular value decomposition theory of a matrix has received considerable attention in robotics in general, since this theory may be used in solving the problem of operation in singular configurations, KIEFFER [1992] and KLEMA and LANB [1980]. The main drawback of this theory is its high computational complexity when compared with other schemes such as "Gaussian elimination " or the "Analytical inverse kinematic solution". Within this section, the information extracted from the SVD of the Jacobian will be used to invert the hand Jacobian.

With regard to the analysis of the SVD of a finger Jacobian, it has been found that, the eigenvectors of $\boldsymbol{J}_{\Theta}^{T}\boldsymbol{J}_{\Theta}$ are the right singular vectors of $\boldsymbol{J}$ (matrix $\boldsymbol{V}$), whereas the eigenvectors of $\boldsymbol{J}_{\Theta}\boldsymbol{J}_{\Theta}^{T}$ are the left singular vector of $\boldsymbol{J}_{\Theta}$ (matrix $\boldsymbol{U}$). The eigenvalues of $\boldsymbol{J}_{\Theta}\boldsymbol{J}_{\Theta}^{T}$ are equal to the squared singular values of $\boldsymbol{J}_{\Theta}$. This conclusion will be utilized in this Chapter and Chapter Six since it gives the information for advanced inversion of the Jaccobian. Appendix [A3-2] gives a symbolic expression for the singular of the finger Jacobian values obtained using MATHEMATICA Package, WOLFRAM [1988]. Due to it's relation with the condition number, the condition number of γ of the Jacobian denotes the ratio of the largest and the smallest singular values: namely:

$$\gamma = \frac{\sigma_1}{\sigma_p} \tag{3.31}$$

If the Jacobian matrix has a small condition number, then it is said to be well conditioned, whereas if the finger Jacobian has a large condition number, then it is said to be ill conditioned. With reference to Appendix [A3-2], the ratio can be expressed as :

$$\gamma = \frac{\Psi^2}{[L_2^2 + 2L_3^2 + 2L_2L_3C_3 - \chi^2\ ]/2} \tag{3.32}$$

where $$\chi = \sqrt{(L_2^2 + 2L_3^2 + 2L_2L_3C_3 + 2L_2L_3S_3)}$$

Eq. 3.32 simply reveals, the finger condition number γ will approach high value once the value of 0_3 is zero.

3.6.3) Results and Analysis

For further analysis of Eq. 3.32, we shall investigate these issues under the assumption that θ_2 and θ_3 are changed from negative to positive values, which is a valid assumption in any manipulation task .

Fig [3.4] shows the condition number of the Jacobian matrix for changes in the finger joint space vector of θ_2 , and θ_3 both from -50 to $+50$. Since Eq. 3.30 reveals that the Jacobian Determinant is a function of θ_2 and θ_3 only, then it is obvious from the graph that the condition number of J_Θ approaches high value indicating that it is ill conditioned over the period when θ_3 is of zero value .

The singular value decomposition of the Jacobian matrix J_Θ can be represented by :

$$J = U \Sigma V^T \tag{3.33}$$

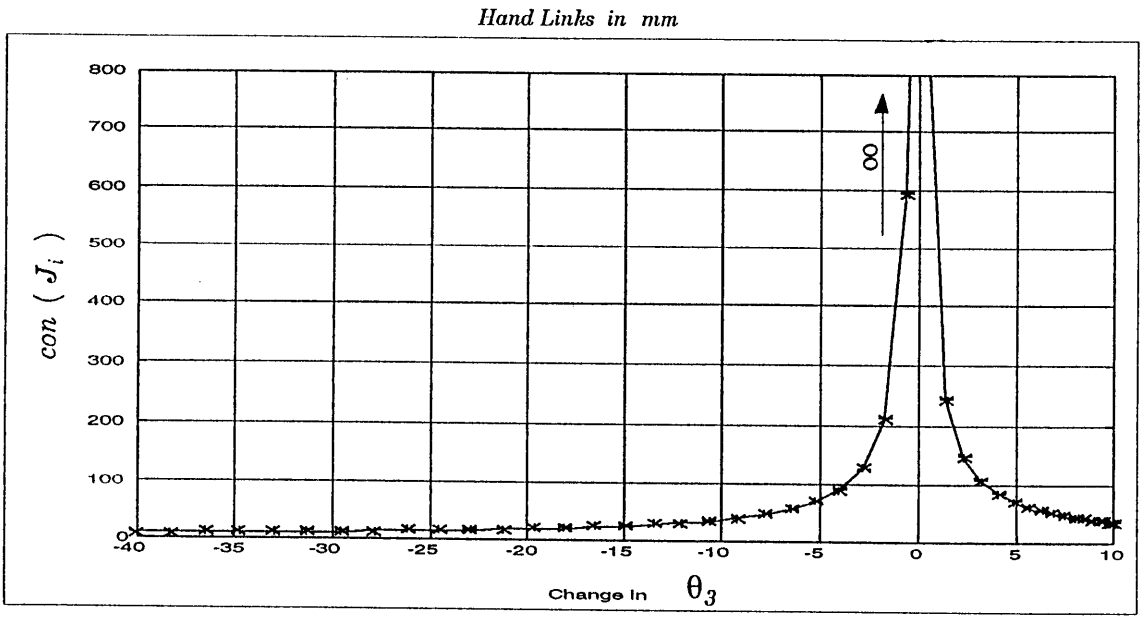


Figure 3.4 : The Condition Number of a Finger Jacobian.

where U and V are two orthogonal matrices, and Σ is expressed by the singular values to be known. Thus Σ is expressed by :

$$\Sigma = diag\,(\,\sigma_1, \ldots\ldots, \sigma_3\,) \text{ and } \sigma_1 \geq \sigma_2 \geq \sigma_3 \geq 0 \qquad (3.34)$$

Further analysis using the singular value decomposition of the Jacobian matrix, as given in Eq. 3.33, reveals that when one singular value drops to the smallest value then the determinant function is zero, resulting in difficulty in inverting J_Θ.

In order to have a better understanding of how a finger Jacobian approaches singularity, Fig [3.5] shows the three singular values of one finger Jacobian expressed over a defined manipulation task (*as shown in Chapter Six*).

In Fig [3.5-c], σ_3 the third singular value drops to zero over a particular period of time , as expressed by the analytical expressions given in Appendix [A3-2]. Since a fingertip frame is to be aligned with the object contact frame, some of the singular values are exchanged in such a way that the zero singular value becomes σ_1 or σ_2. However, even if the finger Jacobian is expressed with reference to a particular object surface, this will still result in singular configuration of J_Θ as far as θ_3 is of zero value.

The singular configuration of the Jacobian matrix is further analysed here using the mesh plot for the purpose of defining a Robust Inverse of the Jacobian utilised later in Chapter Six.

Fig [3.6-a] shows the mesh plot of the Jacobian matrix for defined changes in the joint space vector and Fig [3.6-b] is the determinant function of the hand Jacobian (*a function of all fingers Jacobians*). The mesh plot shows clearly that the determinant value of the Jacobian drops to zero when the third joint angle is zero. The change in the

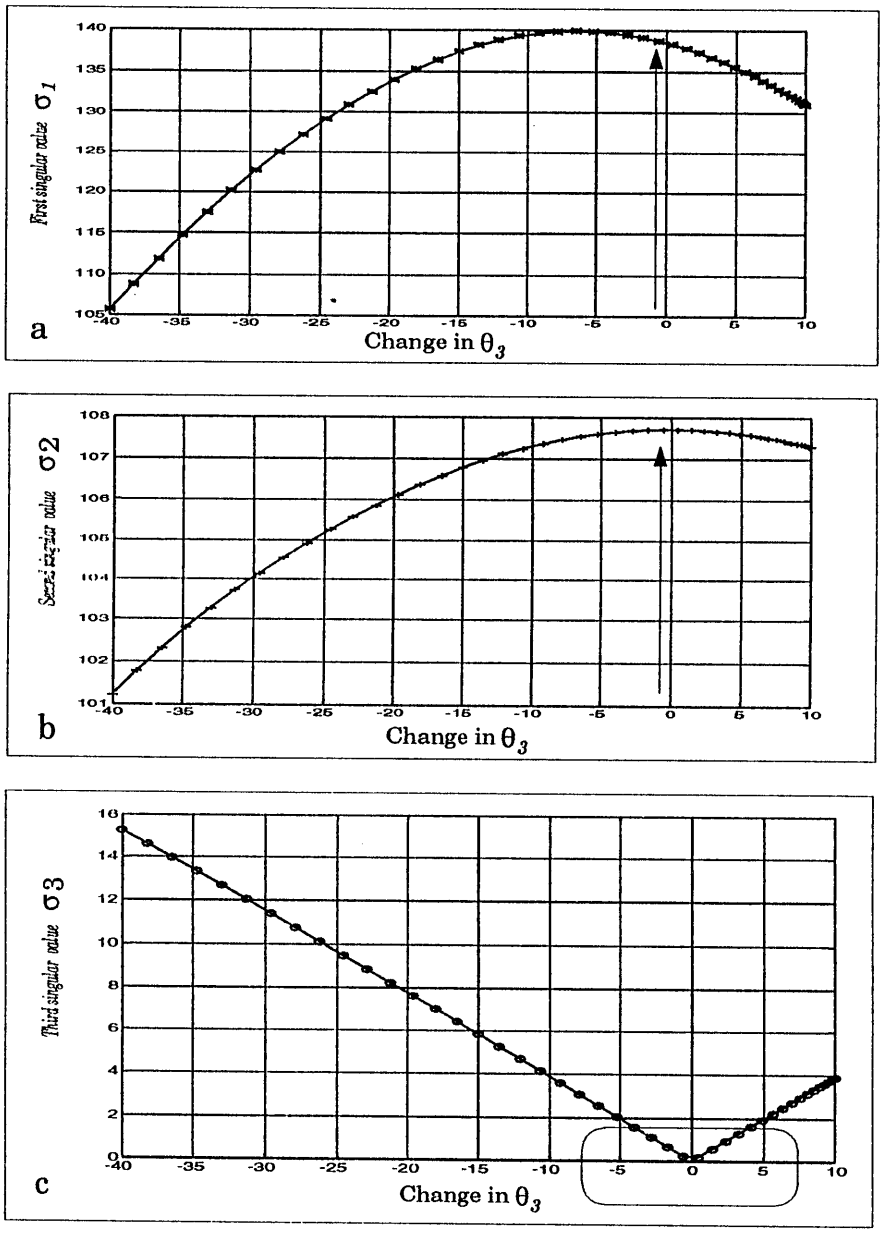
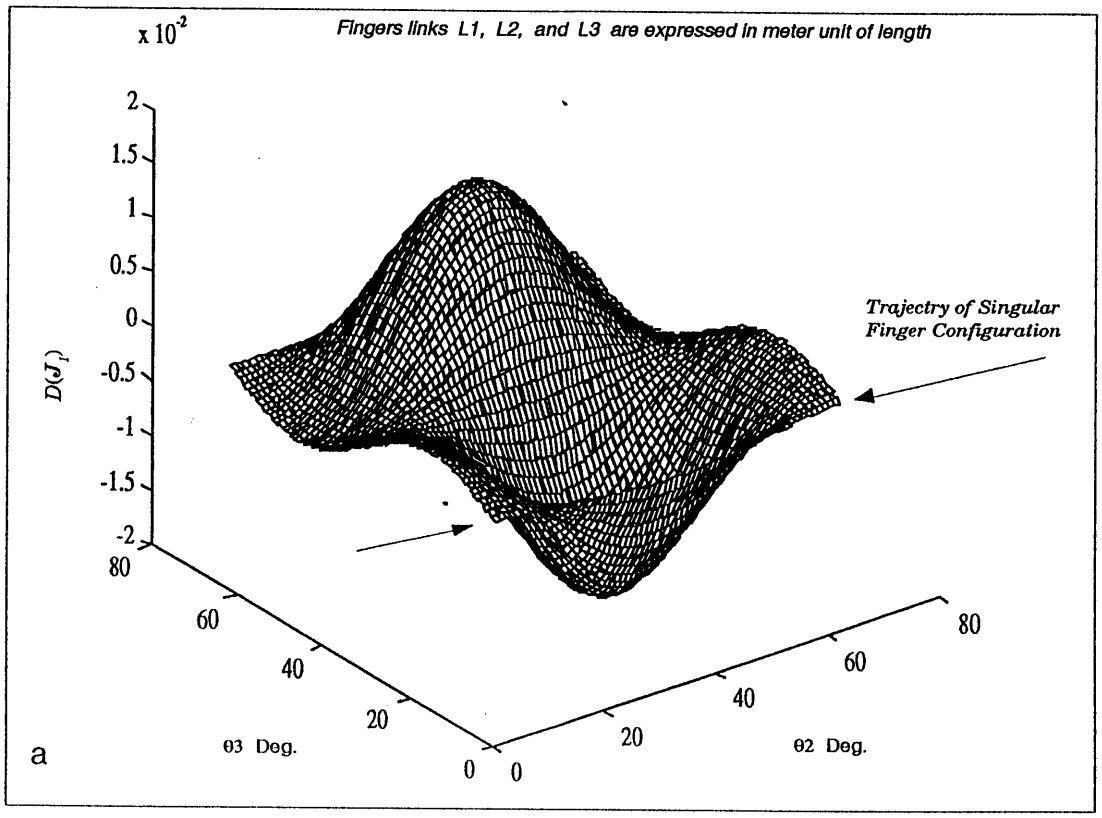


Figure 3.5 : a : First Singular Value of a Finger Jacobian.
b : Second Singular Value.
c : Third Singular Value.



Finger links in mm

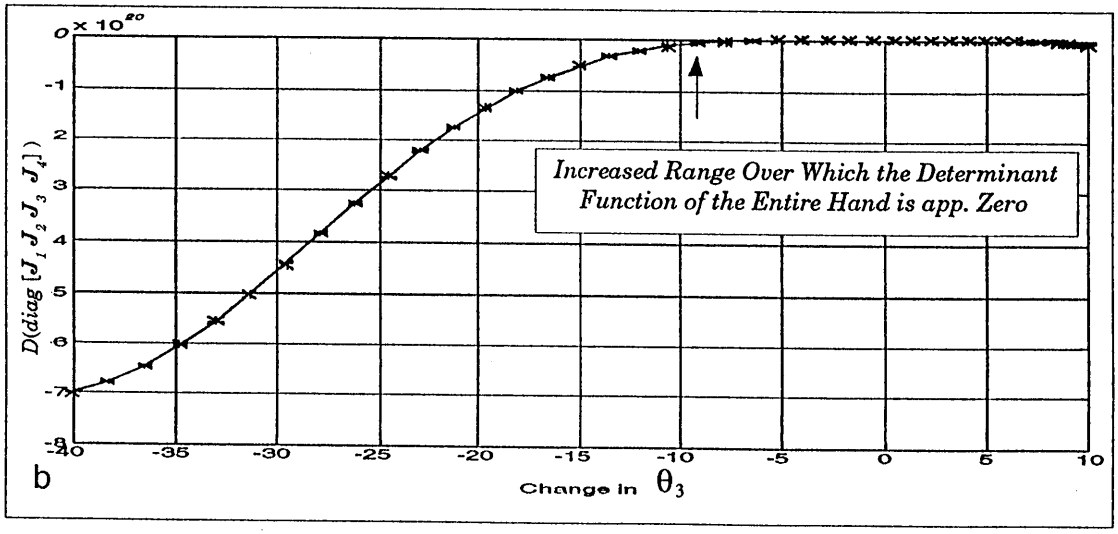


Figure 3.6 : a : Finger Determinant Function (using 3-D mesh plot)
b : Determinant Function of Hand Jacobian as a Function of the Distal Joints.

dexterity of a finger is a useful tool for characterising how well the finger performs in a particular posture. When θ_3 is $\neq 0$, determinant value is mainly dependent in the combinational values of θ_2 and θ_3.

3.6.4) Multiple Jacobian and Associated Determinant

In the previous analysis regarding the singular posture of one finger, it has been shown that the determinant function of the first finger approaches zero once the distal joint is of zero value. In Chapter Six, while discussing the dynamic motion of the hand, the concatenated Jacobian of the four fingers is of great importance for mapping the contact location motion parameters with the corresponding joint space parameter vectors. The entire hand Jacobian, designated as $\boldsymbol{J}_h$, can be expressed as follows, ZEXIANG *et al.* [1989], SCHNEIDER [1992]:

$$\boldsymbol{J}_h = diag\,[\,\boldsymbol{J}_{\Theta 1}\;\; \boldsymbol{J}_{\Theta 2}\;\; \boldsymbol{J}_{\Theta 3}\;\; \boldsymbol{J}_{\Theta 4}\,] \tag{3.35}$$

Furthermore, the inverse of the hand Jacobian plays a crucial role while an object motion is expressed in cartesian based coordinate. However, due to the singularity problem associated with one finger, the determinant function of the hand Jacobian $\boldsymbol{J}_h$ falls to zero resulting in an infinite value of $\boldsymbol{J}_h^{-1}$. The corresponding determinant function for the four fingers in performing the same task used in Fig [3.4] is shown in Fig [3.6-b]. The concept remains the same, the determinant function goes to zero in the interval of which θ_3 is of zero value.

Assumptions Based on the Kinematic Constraints :

At this stage while inverting $\boldsymbol{J}_h$ in Eq. 3.35, we are working under the three main assumptions : (*i*) The physical lengths of the fingers link are identical, i.e finger lengths are equal due to identical kinematic structure. (*ii*) The joint space vectors of the four fingers are also equal, since the four fingers start their motions at the same instant with the same joint displacements. In particular, $\theta_3 = \theta_{i3}$, $i = 1,..,4$ where θ_{i3} is the angle of θ_3 for the *ith* joint.

(*iii*) The entire hand Jacobian J_h is a block diagonal matrix, thus all the off diagonal elements are zero .

One Finger Case :

The analysis of the determinate function of one finger has already been discussed in the previous section, where the mapping from the joint space is projected into the corresponding 3D plot and its corresponding countor, this is shown clearly in Plate [3.1].

Two Fingers Case :

The concatenated hand Jacobian for two fingers $J_h = diag\,[J_1\ J_2]$, where the determinant function of J_h in this case has been computed using MATHEMATICA software and is equal to $D = L_2^{\,2} L_3^{\,2} \Psi^2 S_3^{\,2}$. This determinant function results in a 3D plot shown in Plate [3.2], where the still zero value of θ_3 (*distal joint*) results in singularity. Furthermore, the number of singular values has doubled to six , thus increasing the complexity of the problem if the links are not identical .

Three Fingers Case :

When the hand Jacobian is expressed in terms of the three fingers, the determinant function has been found to be $D = -L_2^{\,3} L_3^{\,3} \Psi^3 S_3^{\,3}$. This results in the increase in the dimensionality of the singular values of J_h in addition to the 3D plot shown in Plate [3.3]. This Plate shows that the determinant function still goes to zero once the distal joint is of zero value.

Four Fingers Case :

The addition of the fourth finger Jacobian to the three fingers will result in the determinant function being $D = L_2^{\,4} L_3^{\,4} \Psi^4 S_3^{\,4}$. Here we arrive at the case being analysed, where the hand Jacobian J_h is expressed in terms of the four fingers. The addition of the fourth

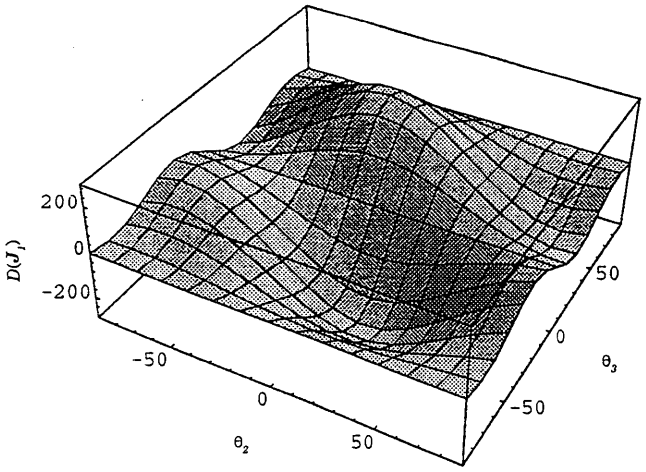


Plate 3.1 : One Finger Determinant Function

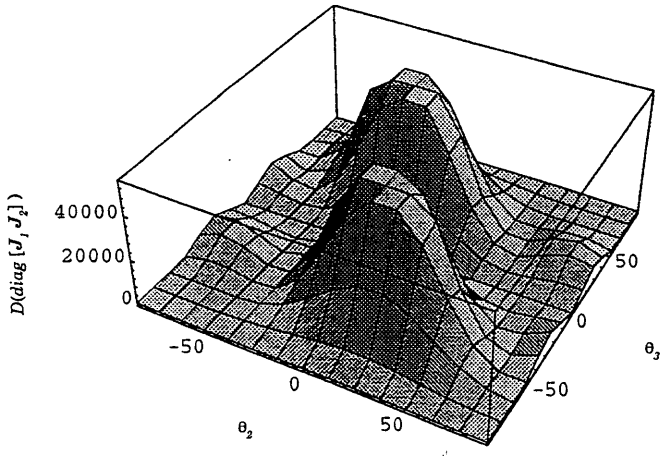


Plate 3.2 : Two Fingers Determinant Function

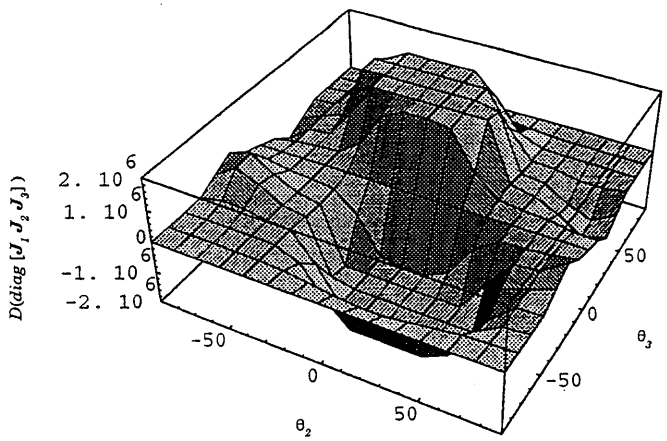


Plate 3.3 : Three Fingers Determinant Function

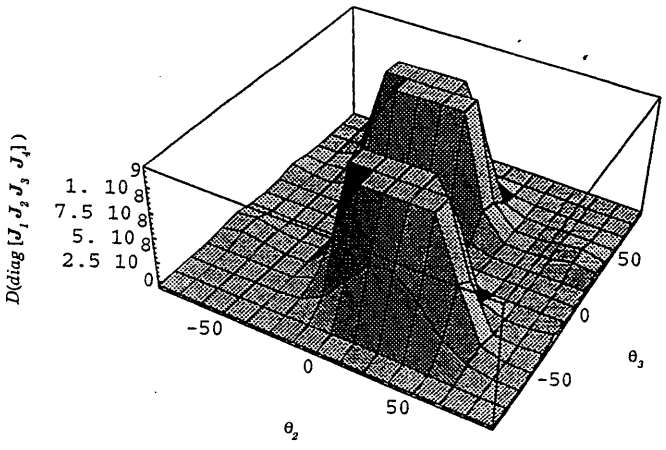


Plate 3.4 : Four Fingers Determinant Function

finger still produces a zero determinant function when the distal joints are of zero values as shown in Plate [3.4]. However, determinant function is close to zero (but not zero) over a wide spread of changes in θ_2 and θ_3. This effect can be seen in Fig [3.6-b], which shows the determinant function of the entire hand for changes in θ_2 and θ_3. The result of Fig [3.6-b] indicates that the inversion of the hand Jacobian J_h will be singular once θ_3 is zero and the matrix is close to singularity over a wide range of changes in θ_2 and θ_3.

Singularity in the Multiple Contact System :

Basically we are interested in inverting J_h, meanwhile, the determinant of J_h has shown that : determinant function goes to zero over a wide range due to the concatenating of the four fingers. One approach of inverting J_h even at singular position is to employ the Robust Singularity Inverse (RSI) with variable scaling factor (this is explained further in Chapter Six and Appendix [A-1]). The variable scaling factor used by NAKAUMARA is the dexterity measure of the manipulator which is a function of the six conventional joint positions. The dexterity measure in our sense is the dexterity measure of one finger.

The dexterity measure of the entire hand Jacobian J_h cannot be used as a variable scaling factor in the RSI due to the complexity of this measure if the three assumptions are invalid, since it will be expressed in terms of the individual fingers Jacobian (*although it has been simplified in our case by the assumptions stated earlier*). The other reason for not employing the dexterity measure of the entire hand is the not smoothness of the function $D = L_2^4 L_3^4 \Psi^4 S_3^4$. If the dexterity measure of one finger , Plate [3.1] , is compared with the dexterity measure of the four fingers hand Jacobian , Plate [3.4], we observe that the changes in Plate [3.1] are smooth as θ_2 and θ_3 are changed, as compared with that in Plate [3.4] because of the appearance of S_3^4 in the function.

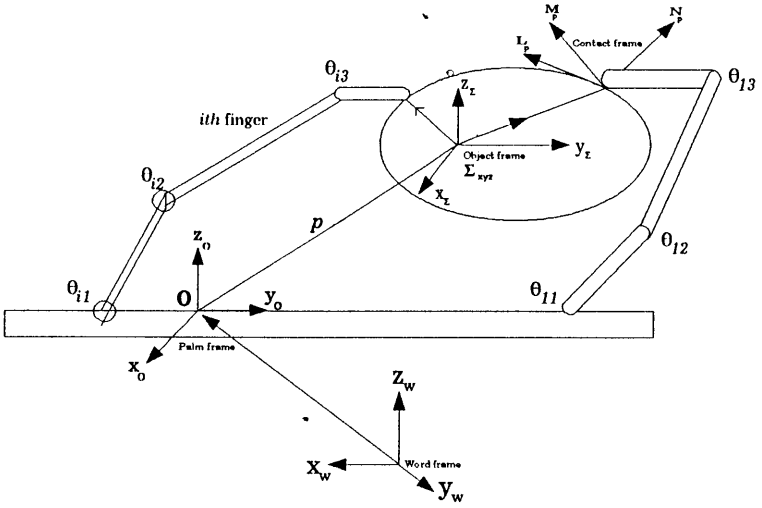
Furthermore, it has been shown by MATHEMATICA software that the dexterity measure of the various four fingers are still the same as the function of the L_2, L_3, Ψ, and S_3. This result suggests that if the dexterity measure to be used as the scaling factor in the RSI then one finger dexterity measure is enough for scaling the RSI of the entire hand Jacobian J_h, provided that the three stated assumptions are satisfied in this design. If the three assumptions are not satisfied, then the dexterity measure of one finger will be different from the other due to the change in the values of joint space vectors. In this analysis, the nature of the hand Jacobian, which is block diagonal, has made the problem much simpler, since inverting a block diagonal matrix consisting of sub-matrices is like inverting the individual matrices and concatenating them later after inversion as developed by OGATA, OGATA [1987].

(3.7) OBJECT-HAND KINEMATICS

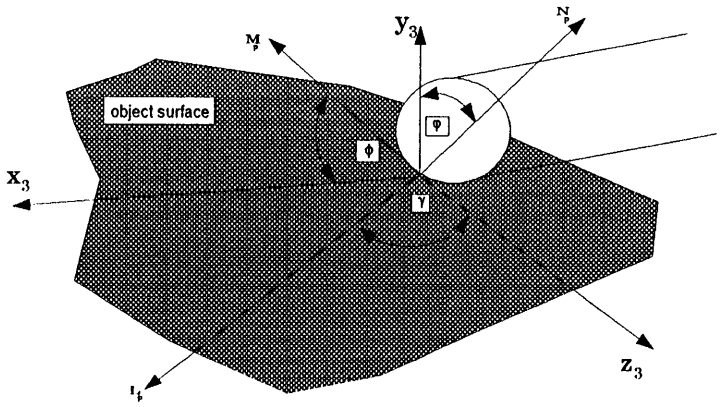
3.7.1) Associated Frames.

What has been discussed about coordinate frames in sections (3.3) and (3.4) concentrated on the kinematic relations of the fingers as multi-degrees of freedom bodies. The analysis of this sub-section will be concerned with relative motions between a grasped object and one or more fingers in contact with an object. Such contact kinematic relations will be utilised later in Chapter Five while formulating the force control on an object. Each finger makes contact with the workpiece at its tip only. The four grasp points become four points attached to the grasped object. During manipulation these four points must remain at the vertices of an invariant polygon which is inscribed in the work piece itself.

With reference to Fig [3.7-a], let $O_{(x,y,z)}$ be a coordinate frame system that is immovable with respect to the palm of the hand. Also let $\Sigma_{(x,y,z)}$ be a coordinate frame system implant in the object used for manipulation.



a



(φ γ φ) angles of rotations between the contact frame and the fingertip frame

b

Figure 3.7 : a : Kinematics of Hand-Object System.
b : The Kinematics of the Point of Contact and the Assosicated Rotations of Frame to Coinside with The Object Surface.

We also attach a coordinate frame $P_{(L, M, N)}$ at the centre of the pressure distribution at each contact. As the object moves each $P_{(L, M, N)}$ at each contact point frame moves with its associated contact and is arranged so that L and M lie in the local tangent plane and N is normal to the object surface. The instantaneous position of each contact with respect to the $\Sigma_{(X, Y, Z)}$ object frame is given by $\boldsymbol{p}^T = [r_L \; r_M \; r_N]$ expressed in the object frame, as shown in Fig [3.1-a]. Furthermore, let a fixed frame be attached away from the hand palm and fixed at a world location. This frame is designated as $W_{(x,y,z)}$.

In Fig [3.7-b], the contact coordinate at the *ith* fingertip velocity point $P_{(L, M, N)}$ by itself has a given orientation with respect to the object frame $\Sigma_{(X, Y, Z)}$ frame given by (ϕ_L, φ_M, γ_N) representing successive rotations about the *LMN* axis in standard notation.

In terms of the object motion it is necessary to relate its motion parameters to the motion parameters of the hand servo system. Later, in Chapter Six, while discussing *manipulation* and *dynamic forces* for an object motion, relation between the object motion and the corresponding joint space vectors will be further elaborated based on these kinematic relations. For any two of these four coordinate frames, say Σ_Σ, O_o, where $_\Sigma$, $_o$ are subscripts to describe the frames, we denote the position vector $\boldsymbol{p}_{o\Sigma}$ and an orientation matrix $\boldsymbol{A}_{o\Sigma}$. The translational and rotational velocity of Σ_Σ relative to O_o are expressed as :

$$\upsilon_{\Sigma o} = \boldsymbol{A}^T_{\Sigma o} \boldsymbol{p}_{\Sigma o}$$

and

$$\omega_{\Sigma o} = S^{-1} (\boldsymbol{A}^T_{\Sigma o} \dot{\boldsymbol{A}}_{\Sigma o}) \qquad (3.6)$$

where S is a *scew-matrix* operation in a vector and the vector $[\upsilon_{\Sigma o}, \omega_{\Sigma o}]^T$ is $\in \Re^6$ is the generalized velocity of frame Σ_Σ to frame O_o. In a similar way, the three frames, contact, object and palm frames system p, Σ, and O respectively, are related to each other by translational and rotational velocities and are given by:

$$\upsilon_{\rho o} = \boldsymbol{A}^{T}_{\rho\Sigma}(\upsilon_{\beta\alpha} + \omega_{\beta\alpha} \times \boldsymbol{P}_{\rho\Sigma}) + \upsilon_{\rho\Sigma}$$
$$\omega_{\rho o} = \boldsymbol{A}^{T}_{\rho\Sigma}\omega_{\Sigma o} + \omega_{\rho\Sigma} \tag{3.37}$$

Using this relation and considering the fact that the frame coordinate at the point of contact is fixed in orientation to the frame at the centre of mass Σ_{Σ}, the velocity of the point of contact can be given relative to the object frame relative to a fixed coordinate at the hand O_o palm by :

$$\begin{bmatrix} \upsilon_{\rho o} \\ \omega_{\rho o} \end{bmatrix} = \begin{bmatrix} \boldsymbol{A}^{T}_{\rho\Sigma} - \boldsymbol{A}^{T}_{\rho\Sigma} & S(\boldsymbol{P}_{\rho\Sigma}) \\ 0 & \boldsymbol{A}^{T}_{\rho\Sigma} \end{bmatrix} \begin{bmatrix} \upsilon_{\Sigma o} \\ \omega_{\Sigma o} \end{bmatrix} \tag{3.38}$$

$$= \boldsymbol{T}_{\rho\Sigma} \begin{bmatrix} \upsilon_{\Sigma o} \\ \omega_{\Sigma o} \end{bmatrix} \tag{3.39}$$

In other words, the velocity of the grasped or manipulated object represented by a body frame o a local frame within the object at the point of contact $\boldsymbol{P}$ and a palm frame is related to the constant transformation matrix $\boldsymbol{T}_{\rho\Sigma}$ which by itself is a function of the object geometry and the location of the object within the hand palm coordinate frame. These kinematic relations are of significant value while expressing the motion of the fingertips with respect to the hand palm.

In a similar way, dual to the generalized velocity of the grasped object is the generalized force (or wrench) exerted to the object. Relative to the object coordinate frame Σ_{Σ}, a generalized force can be written as :

$$F_b = \begin{bmatrix} F_o \\ \\ N_o \end{bmatrix} \tag{3.40}$$

where N_o is a $\in \Re^3$ the torque about the origin of $\Sigma_{(x,y,z)}$, and F_o a $\in \Re^3$ is a linear force. A wrench can also be expressed relative to the local frame $P_{(L,M,N)}$, and the relation between F_{bi} at contact and F_b at the object frame is given by:

$$\begin{bmatrix} F_o \\ \\ N_o \end{bmatrix} = \begin{bmatrix} A_{\rho\Sigma} & 0 \\ \\ S(P_{\rho\Sigma})A_{\rho\Sigma} & A_{\rho\Sigma} \end{bmatrix} \begin{bmatrix} F_{oi} \\ \\ N_{oi} \end{bmatrix} \tag{3.41}$$

$$= T_{\rho\Sigma} \begin{bmatrix} F_{oi} \\ \\ N_{oi} \end{bmatrix} \tag{3.42}$$

This relation explains the fact that a fingertip will apply a general six dimensional force vector to the object. However, the type of contact then determines the transmitted forces to the object surface. Since the chosen type of contact in this research does not transmit associated torques, i.e. N_{oi} in Eq. 3.41 is zero, the object resultant force F_b will be a function of F_o, $A_{\rho\Sigma}$, and $S(P_{\rho\Sigma})A_{\rho\Sigma}$ only. Put in another form F_b will be a function of the first three columns of the $T_{\rho\Sigma}$ matrix using the twist space rather than the wrench space of the object.

The same result will be shown in Chapter Five while deriving the grip transform matrix. In particular the first three columns of the $T_{\rho\Sigma}$ matrix constitute the associated three columns of the grip transform as far as the contact does not transmit torques to the object

through the contact (i.e. frictional point contact).

3.7.2) Forces and Contact kinematics

In general a fingertip (*of any fingertip shape of contact , e.g. frictional flat*) in contact with an object applies a six-dimensional vector of forces and moments, KUMAR [1993]. Thus :

$$\boldsymbol{f}^{T}_{p} = [f_L \;\; f_m \;\; f_n \;\; m_L \;\; m_M \;\; m_n] \tag{3.43}$$

at contact. According to the geometrical design of the fingertip given in Chapter Two (rounded fingertip), some of the moments about the L and M components are zero since the fingertip is free to rotate about these axes. At the point of contact the contact type which exists determines the forces which are transmitted to the object. For a point contact, it is assumed that the fingertip is free to rotate in all directions about the contact points, so that forces are transmitted only through the contact. Grasping is an operation in which each finger of the robot hand contacts an object so, by a given force, the object loses its freedom.

In general, an object (*solid body*) has six degrees of freedom in a three-dimensional space. However, if one finger of the robot hand contacts the object at one point (a point contact with friction) and if this point is assumed to be fixed, then the object has lost three degrees of freedom. Three rotational degrees of freedom still remain for the object. With the finger in a general configuration and with all the joints free, the workpiece has six DOF. Locking one of the joints reduces the freedom of the connection to five. Locking two revolute joints in a finger leaves the workpiece with four freedom. With all three actuators locked, the workpiece is free in spherical rotation about $\boldsymbol{T}_a$.

We define a contact selection matrix $\boldsymbol{H}_c$, as that which selects those elements of a general

six-element force/moment vector that are transmitted through the contact. The equivalent force and moment in the $B_{(xyz)}$ frame resulting from the *ith* contact force, F_{pi}, is $\boldsymbol{F}_{bi} = \boldsymbol{P}^{T}_{b}$ $\boldsymbol{f}_{pi}$ where $\boldsymbol{P}^{T}_{b}$ is defined as $\in \Re^{[6\times6]}$ cartesian transformation matrix that relates linear velocities at two separate points, B and P on the same rigid body and expresses them and the angular velocity of the body in frames with different orientations.

Considering the fact that the $\boldsymbol{H}_{c}$ matrix at point of contact will filter out some of the transmitted forces, then the $\boldsymbol{f}_{p}$ equation given in Eq. 3.43 can be expressed as follows for a point contact with friction:

$$\boldsymbol{f}^{T}_{p} = [\dot{f}_{L} \;\; f_{m} \;\; f_{n} \;\; 0 \;\; 0 \;\; 0] \tag{3.44}$$

In order to perform the force control on an object, it is essential to relate the contact forces acting at the object surface, Eq. 3.44 , to the joint torque as expressed by Eq. 3.26. However, that equation expresses the forces expressed with respect to the tip force as far as the Jacobian is expressed with reference to the finger base frame. In order to apply the force optimization algorithm, it is essential to relate the Jacobian to the contact coordinate which by itself is oriented to the object centred frame. A further rotation at the contact point is required by pre-multiplying the Jacobian by a rotation matrix that transforms the fingertip coordinate frame to the contact coordinate frame.

(3.8) EFFECT of FOUR CONTACTS

Previous research on an object restrained by the effect of three fingertips contact has been discussed by Salisbury, MASON and SALISBURY [1985], where it has been shown that a three finger grasp will produce a stable grasp as long as the grip transform is a *full rank* matrix. Since a grasp stability depends on the configuration of the contacts around the

object in addition to the forces transmitted through the contact to the object, the effect of a fourth fingertip contact on an object can be viewed from the extra terms columns added to the grip transform. If the quality measure is applied to a three and four fingered hands under a point contact with friction contact, the effect of the extra frictional forces acting at the four point of contact can be further examined using the SVD.

It is not a trivial mathematical task to decompose the grip transform of a four fingered hand into the three $U\Sigma D$ matrices in a symbolic form using a symbolic singular value decomposition. Meanwhile, two, three, and four finger numerical grasps will be examined based on the use of largest singular value of a particular grasp configuration $\delta(G_i)$, thus:

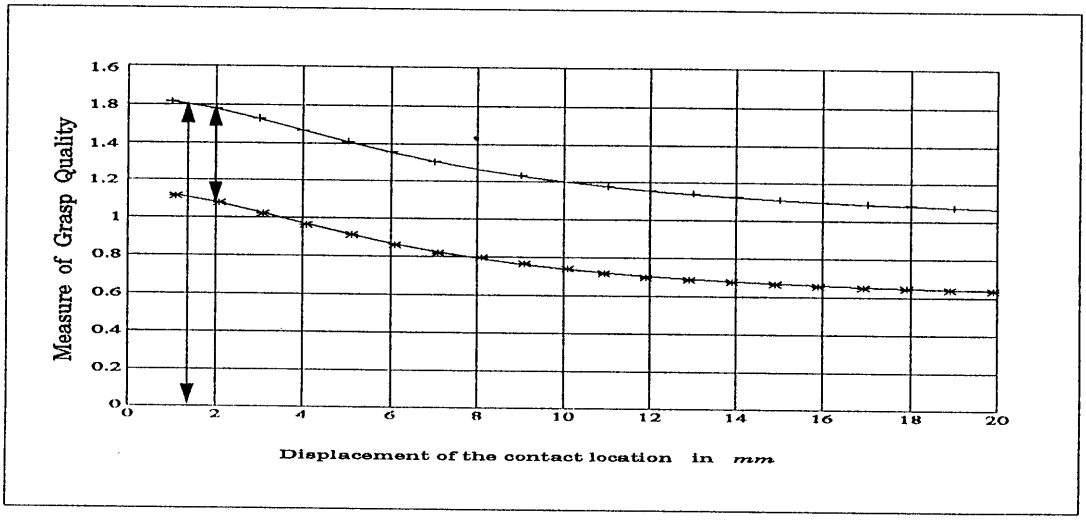
$$G_4 \geq G_3 \geq G_2 \quad if \quad \delta(G_4) \geq \delta(G_3) \geq \delta(G_2) \tag{3.45}$$

For a given grasp configuration in a defined object, certain points of contact are changed over the object surface while the object coordinate remains fixed.

Fig [3.8] shows the grasp quality measure , *smallest singular values* of GG^T, for a two, three, and four fingers grasp. For this particular grasp configuration, a two fingered grasp has shown the worst case of quality measure. The three fingered hand has raised the quality of grasp to a better level of quality measure.

The effect of a four fingered hand gives higher measure of quality. Although perturbation in the grasp configuration is small, the four fingered grasp has preserved the highest singular value among the two and three contact grasp.

The effect of a four fingered grasp can be seen from motion or force domains. From force



+ : *Four Fingers Grasp,*
* : *Three Fingers,*
\- : *Two Fingers.*

Figure 3.8 : Stability Measure Using Singular Value Decomposition.
For a two, three and Four Fingers Grasp With Changes in Contact Locations.

domain point of view, the object stability will be physically enhanced because of the extra wrenches added to the object by the four contacts and hence extra distribution of forces around the object itself. These extra forces can be seen from the extra columns being added to the grip transform. However, from control point of view, the four fingers system adds complexity to the system because of the amount of coordination required.

Summary

Chapter three has presented the concept of finger, hand, object kinematics. To deal with the complicated structure of multifingered hand structure, frames were affixed to the different parts of the mechanism. The chapter started with the concept of homogeneous transformation which plays an important role in the kinematic characterisation of robots and articulated mechanisms. Based on the homogeneous transformation and the Denavit-Hartenberg parameters a special $\in \Re^{[4\times 4]}$ matrix expression of the relationship between two adjacent links was introduced for one finger structure.

Also dealt with in this chapter is the concept of inverse kinematics and the employment of two methods of solutions : the algebraic approach and the geometric approach both of which are characterized by a number of issues concerning the existence of solutions.

This chapter has looked at aspects of finger differential motion and the use of finger Jacobian. Since the Jacobian matrix of the whole hand plays an important role in the manipulation of an object (as will be seen in chapter six), two solutions have been addressed: the vectorial rotation method and the Pauls's algorithm method. The chapter then moved to the concept of finger determinant function and its use to derive the manipulability measure of one finger. This measure is of important use when discussing the use of robust singularity inverse of the whole hand Jacobian .

The aspect of having a four contact in an object has been examined and its effect of an increased grasp quality of measure over a two and three contact grasp shown.

Finally the chapter has looked at the quality measure of a four fingered grasp and concluded that, a four fingered grasp increases the stability of grasping due to the extra forces applied to an object.

CHAPTER FOUR

CYBHAND POSITION AND FORCE CONTROL.

(4.1) INTRODUCTION

Most computer controlled systems used in robotics have distributed processors which are dedicated to specific tasks. For a six degrees of freedom arm six processors are usually dedicated for the production of digitally controlled motion, hence parallel motion of all the DOF is achieved. All of these DOF are then managed by a single master processor, DANIEL *et al.* [1988]. Multi-processors are special distributed processors which may be utilized to share the computational load for the same task, for providing redundancy in computation or for sharing the multi-axis controllability load in a system. For multifingered robot hands, a few dedicated hardware structures have been used in practice examples of which are found in VENKATAVAMAN *et al.* [1987], NARASIMHAN *et al.* [1989] and KRIGMAN *et al.* [1985].

For the CYBHAND multifingered robot hand, due to the large number of actuators to be managed by the supervisory software controller, the design adopted here comprises of up to 12 motion processors for the purpose of tendon displacement control. Furthermore, each distal joint in the system is also digitally force controlled. The control aspect of the joints has been divided into two main areas of investigation: the first (described within this chapter) is concerned with treating them as if they were independent joints where other link motions are not affecting.

The overall hardware level for position and force control with their associated interfacing circuitry and management software will be the main concepts presented in this chapter. Specific items of CYBHAND kinematics already presented in Chapter Three will be incorporated at this stage for producing a desired motion with respect to a specified cartesian coordinate frame. Due to the large number of actuators and the need to have a user friendly software interface, supervisory software has been implemented for the purpose of hand programming and coordinating the various units in the hand hardware.

Smooth fingertip cartesian motion is an essential capability for robots in general , therefore for achieving an n path cartesian point fingertip motion, the motion is required to be such that the fingertip passes near to defined "via points " without stopping.

Further discussed in this chapter is the cartesian motion of the overall hand which can be produced by the implementation of the cartesian motion of the individual finger at the task planning level. The aspect of higher level commands and coordination are to be presented since they formulate the basis for any coordination task definition.

In addition, this chapter discusses the hardware configuration which incorporates the controllers in addition to the sensory feedback elements for both position and force. Force sensing, presented in Chapter Two, is used to obtain a signal in proportional to the amount of pressure a fingertip applies to an environment. Such signal is utilized in this chapter for closing the force loop and achieving a digitally controlled force joint.

This chapter has been divided into two main sections. Section (4.2) presents the concept of controlling the hand joints with the associated required hardware. Section (4.3) concentrates on aspects of the force controller with the associated physical parameters used to describe the behaviour of the system.

4.2) HAND HARDWARE DESCRIPTION.

4.2.1) PCAMS-CYBHAND Hardware Interfacing

In general, computer architecture for the few designed articulated hands to be operated under computer control has received little attention. For the CYBHAND mechanical hand design presented in Chapter Two, a hardware design has been implemented so that concurrent motion of the joints in the hand is possible. The approach taken here is to divide the hardware into four main block controllers, where each individual block has been

dedicated for the control of the three joints of one finger, as shown in Fig [4.1]. The controller hardware configuration is based on the use of the National Semiconductor product, the LM628 motion processors. Twelve motion processors have been employed for the overall hand control where a single processor was dedicated to an individual DOF in the hand.

Overall supervisory software for the CYBHAND is achieved on an Amstrad/386 machine (which we shall designate as PCAMS) communicating with four main control blocks via 18 (each of 8-bit) hardware ports. An optional serial interface between the hand controller and a SUN/3.0 Unix system has also been employed for the purpose of enhancing the co-ordination between the CYBHAND and a PUMA 560 ARM controller. From the software viewpoint the control of the hand takes place at different computational levels.

The hierarchical nature of the system leads inherently to a bottom-up supervisory software design. One level of concurrency exists within the hand hardware controller. At this low level, the LM628 processors control programs are concurrently controlling the joints motions to achieve the desired cartesian motion of the fingertip. The full schematic/wiring design system of one finger contoller is discussed in AL-GALLAF [1994-c].

4.2.2) One Joint Controller Structure

The complete loop for one joint controller consists of one motion processor, LM 628, 8 bit D/A converter, power amplifier, in addition to the digital optical encoder mounted in the actuator driving box. For the purpose of describing the complete closed loop system, the following section concentrates on the structure of one joint controller exploited for the finger control.

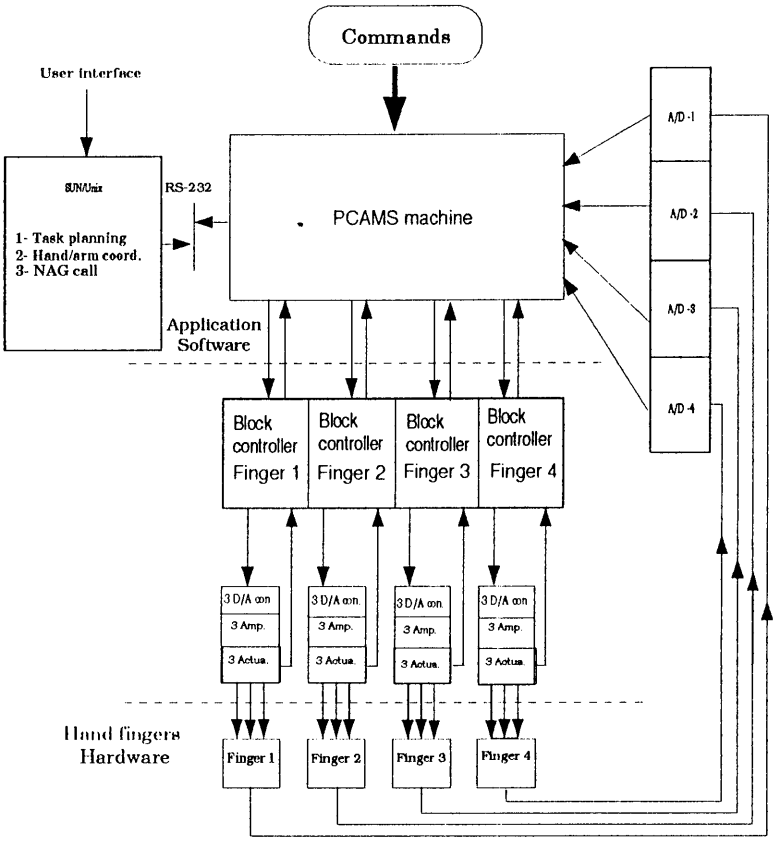


Figure 4.1 : Three Levels of Control for the Cybhand.

4.2.3) Digital Control of a Single Axis

In Chapter Six we shall discuss the implementation of an object manipulation which requires the position and force control of associated joints in the motion. However, such control considers the coupling effects among the links which is usually described as dynamic model of the hand.

The implementation of one joint control can be simplified. That is because the control input for *ith* joint depends only on locally measured variables, not on the variables of the other joints. Moreover, the computations are easy and do not involve solving the complicated derived nonlinear hand inverse dynamics, as given in Appendix [A5]. Contrary to this, from the manipulation and exertion of forces points of view, independent force joint control has to be added for defining the grasping forces during the object motion.

The PID control action in analog controllers is given by, KVIKELS and FASSAMS [1984] :

$$u(t) = k\,[\, e(t) + (1/T_i) \int e(t)\,dt + T_d\,(de(t)/dt)\,] \qquad (4.1)$$

where $e(t)$ is the input to the controller, $u(t)$ is the output of the controller. From OGATA [1988], the digitized form of Eq. 4.1 is expressed by :

$$u(z) = [k_p + k_{ip}/(1-z^{-1}) + k_d(1-z^{-1})]E(z) \qquad (4.2)$$

where $k_p = k$ proportional gain

$k_{ip} = kT/T_i$ integral gain

$k_d = kT_d/T$ derivative gain

For the CYBHAND, the numerical values of the actuator parameters are obtained from

the data sheets in addition to experimental verification. The parametric data for the motor unit and the gearing box are listed in Table [A4-1] in Appendix [A4].

From the block diagram shown in Fig [4.2], a simplified dynamical model of the *ith* joint with the electric actuator may be written as, VENKATARAMAN and DJAFERIS [1987]:

$$(J_a + J_m + n^2{}_i J_L)\,\ddot{\theta}_i + \frac{(B_a + B_m + k_b k_i)\,\dot{\theta}_i}{R} = \frac{k_i}{Rv_i} - n_i d_i$$

$$i = 1, 2, 3 \qquad (4.3)$$

where J_a is the actuator motor inertia, B_a the rotor damping constant, k_i is the torque constant, k_b is the generated back-emf constant, R is the armature resistance, and n is the gear ratio for *ith* joint seen from actuator side (n = /1440) .

The d.c actuator shaft is mechanically connected to an actuator-gear-load assembly of n gear reduction. The relationship among the mechanical components is described by Laplace transform as follows, LUH [1983] :

$$\tau_a(s) = [J_T s^2 + B_T s]\,\theta(s) \qquad (4.4)$$

where J_T and B_T are now the *effective* inertia and the *effective* damping coefficients of the actuators shafts including the inertia of the joint.

Closing the loop :

A joint controller in the hand closes the loop inside the motion processor. The trajectory position for the control loop is calculated by the trajectory planning in the chip itself, and is given to the controller in terms of the number of pulses received by the chip. Hence

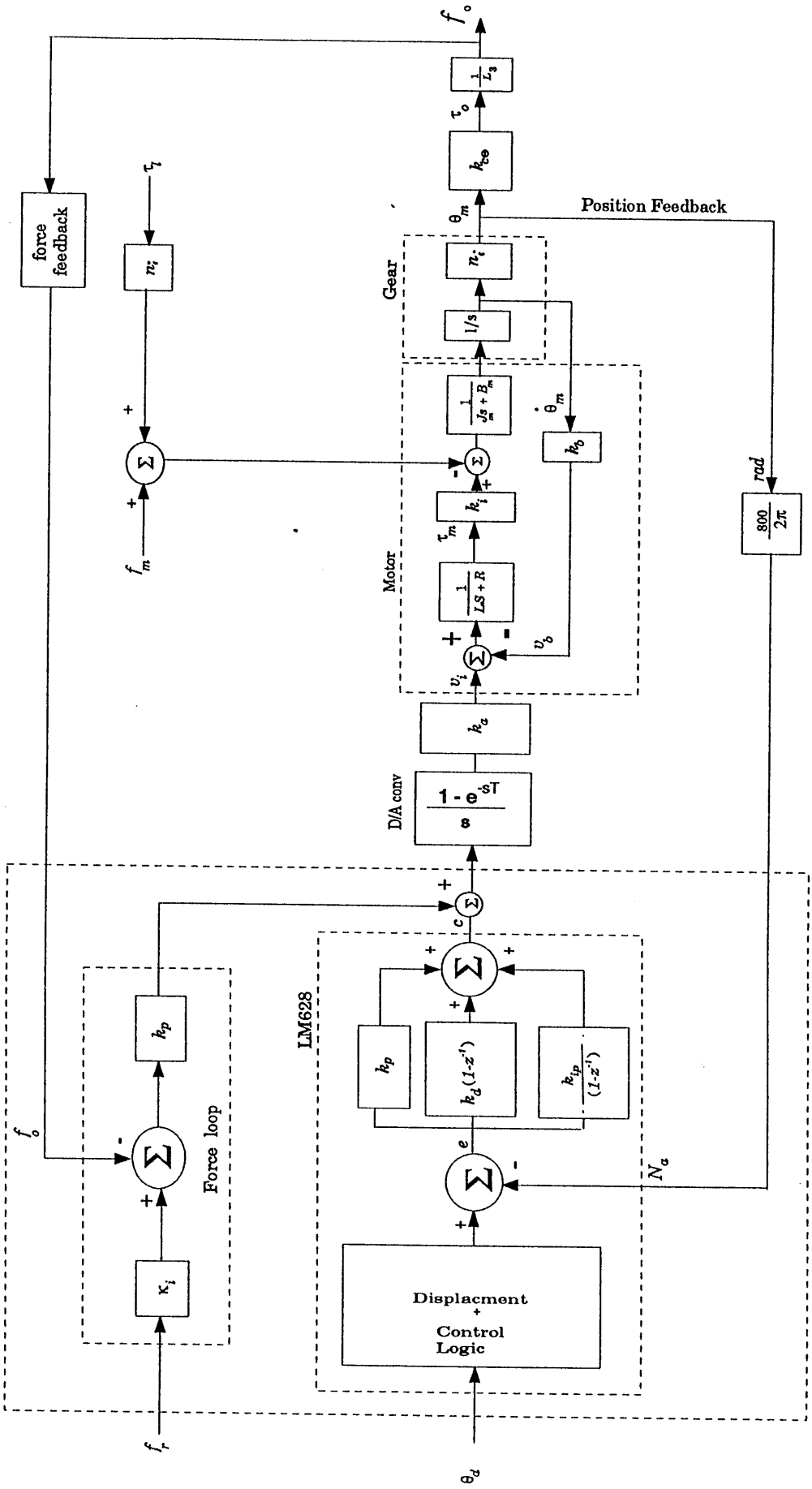


Figure 4.2 : One Joint Closed Loop Digital Control System.

a conversion has to be done from *rad* to number of pulses, which is given as :

$$con = (800\,\theta_m / 2\pi).$$

In accordance to the block diagram shown in Fig [4.2], the transfer function between the input and output points $\theta_d(s)$ and $\theta_m(s)$ is :

$$\frac{\theta_m(s)}{\theta_d(s)} = \frac{nk_\Theta k_{PID}\, k_i\, RJ_T}{s^2 + \dfrac{(RB_T + k_i k_b)}{RJ_T}\, s + \dfrac{nk_\Theta k_{PID}\, k_i}{RJ_T}} \qquad (4.5)$$

Eq. 4.5 is an *nth* order system (*depending in the structure of the controller itself*) which should be theoretically always stable as far the location of the poles in the *s* plan. When k_{PID} consists only of the proportional term and by the application of control theory analysis for a second order system, Eq. 4.5, shows that the system is stable and the poles are located in the left hand side of the *s* plane.

The investigations have been supported by the employment of CAD departmental interactive control packages (CYCLOID), with facilities provided to aid the design including Nyquist diagram, Modulus frequency response and Step response, ALLEN and MITCHELL [1986]. The two evaluated roots are : ($s_1 = -28.3$) and ($s_2 = -5.15$) as far the proportional gain is kept equal to 100.

In this analysis, the obtained closed loop transfer function, Eq. 4.5, is useful only when the controller is designed using analog design techniques. However, the finger joints are being controlled digitally rather than in analog way. Hence, what will be presented at this stage is a brief discussion in how the joint controller behaves as a function of the controller parameters.

In the Z domain, the sampling process plays an important role in determining the system stability. Modelling the D/A converter as $(1 - e^{-Ts})/s$, hence the corresponding Z transform of the D/A and actuator system can be expressed togather as :

$$\frac{\theta_m(z)}{\theta_o(z)} = \frac{z^2}{(z - 0.95)(z - 0.9)} \qquad (4.6)$$

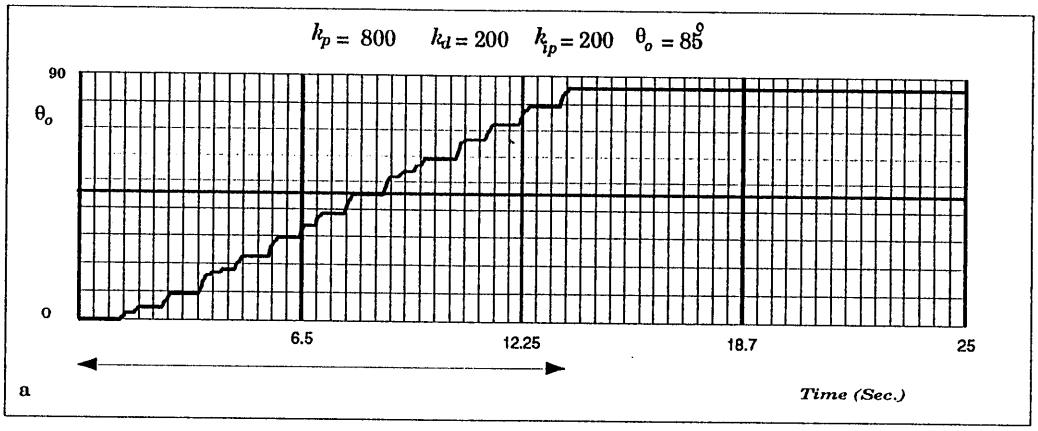
From Eq. 4.6 it can be observed that : the system transfer function is having two poles with their magnitudes are within the unit circle of stability. Eq. 4.6 has shown that the resulting poles of the new discrete form of the transfer function and they are related to the sampling rate T of the processors. Poor sampling rate does drive the poles to be out of the unit circle, thus instability occurs.

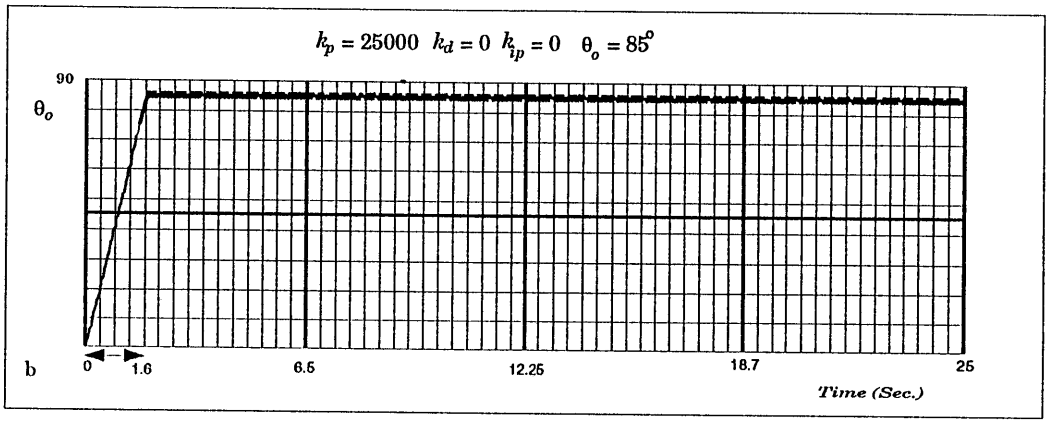
In addition, the poles of Eq. 4.6 are as well function of the variable factor in the system, the scaler value of the proportional gain k_p. The inclusion of the other PID controller parameters results in added poles and zero to the transfer function itself.

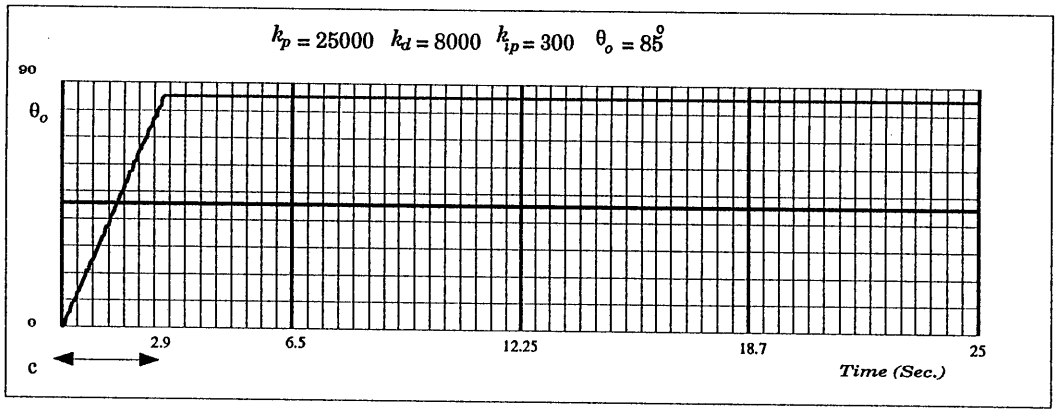
Adjusted Gains Full PID :

In Fig [4.3-a] the employment of low controller parameters has shown to produce a joint performance which is not desirable due to the amount of friction and stiction that have to be overcome. The use of adjusted parameters control law have the effect of making the response behaviour better.

The effect of the adjusted full PID control action can be seen in Fig [4.3-b]. From the shown step response it is clear that : the choice of low proportional gain in addition to the integral and derivative has the effect of decreasing the corresponding rise time as compared with the result for a purely high proportional gain. Furthermore, the addition of an integral term in the controller overcomes the frictional effect at interval of time when the







Parameters expressed in processor numerical format

Figure 4.3 a : Real Time Measurements for Distal Joint Motion at Low PID Parameters.
b : Oscillating around the Final Position Due to High Proportional.
c : Step Response for a Distal Joint with Full PID Control Action.

integral controller builds up. Thus we find a better control combination that has a much smoother response. Keeping the controller parameters of high values drives the system to the instability margins as shown in Fig [4.3-c].

4.2.3) N Configuration Hand Motion

The direct implementation of a defined manipulation task requires the hand to move from one configuration to an n configuration in the three dimensional working space. A defined n stage manipulation task with each joint in the hand to move at various defined velocities and acceleration necessitates the use of a higher dimension data structure.

A motion of the object is produced by the motion of the fingertips at the points of contact, consequently points of contact motions are generated by the specification of n direction of motion. For an object to be moved within the work-space of the hand the principle axes of motions have to be defined in addition to the cartesian fingertip paths. If the fingertips paths are specified as $H, K, L, U,$ for the four fingers, then for four segments path the cartesian points given to the hand controller software are:

Config	1	2	3	4
First finger	$H = [H_1$	H_2	H_3	$H_4]$
Second finger	$K = [K_1$	K_2	K_3	$K_4]$
Third finger	$L = [L_1$	L_2	L_3	$L_4]$
Fourth finger	$U = [U_1$	U_2	U_3	$U_4]$

(4.7)

where each finger segment vector consists of an array $\in \Re^{[6x1]}$ representing a finger joints positions and velocities. In accordance to the specified path coordinates the hand controller creates a [4x4] array of records. At the final stage of the records creation, the hand controller holds four by four of records containing cartesian motion information of four

segment paths for each finger in the hand which will be ready to be loaded in the four hardware block controllers.

(4.4) JOINT FORCE CONTROL

Employment of Force Sensor for Force Feedback :

In the last section we have concentrated on the control of the fingers free motion, which is mainly utilised for the fingertip positioning action using the records of the associated data structure. Within this section the concept of a digitally force controlled joint will be implemented for the purpose of controlling an overall object resultant force. The hardware structure concerning one force controller is given in AL-GALLAF [1994-c].

Since the concept of controlling a force in a joint is mainly utilised when the hand is in contact with an object, the hand task planning level also involves the option of fingertip force control. The force sensor mechanical structure used at this stage has been fully described in Appendix [A2], hence it will be used in this section for closing the force feedback loop.

The implementation of force control requires the continuous reading of the sensor output with the progress in time. Fig [4.4] shows a joint torque sensor enclosed in a closed loop system (which has been incorporated with the position controller in Fig [4.2]) where the feedback signal is based on strain instead of torque.

The strain gauges sensed signals are buffered through an independent linear amplifier which are interfaced directly to the PCAMS machine through A/D channels. A counter interrupts the controller software at a fixed rate, hence a digitized sensor output is read, new control signal based on proportional control is computed and applied to the actuator

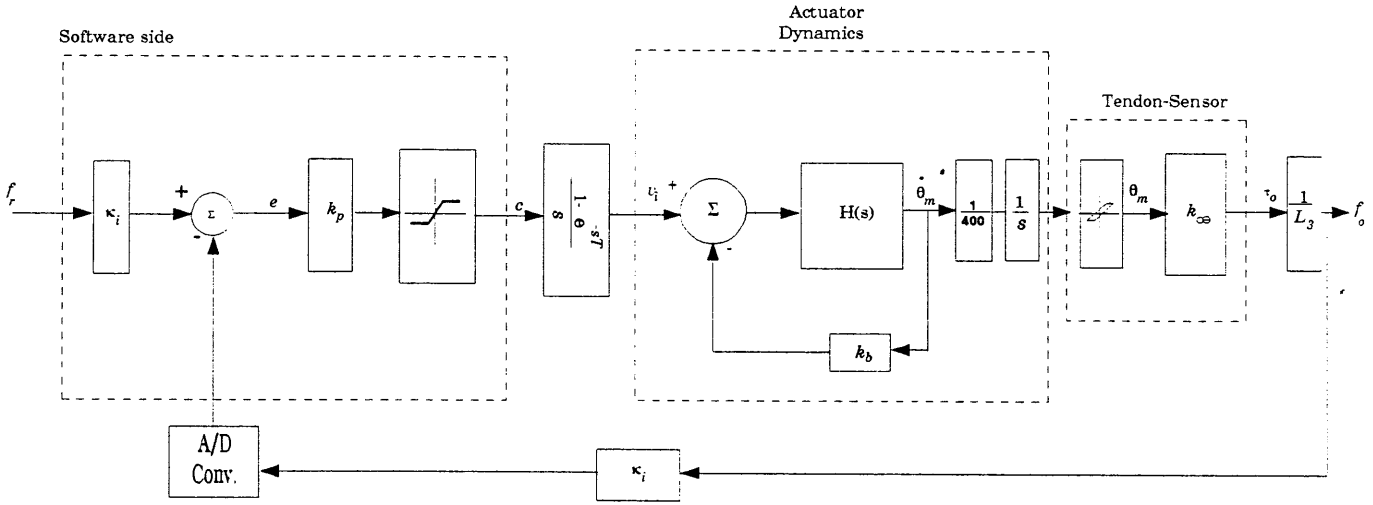


Figure 4.4 : One Joint Force Closed Loop Control System.

through a D/A converter. The actual sampling frequency produced by the counter and used for the digital controller implementation is 500 *Hz.*
In this research the moment of inertia of the finger link element is negligible in comparison with the motor shaft inertia after gearing, which is a valid assumption for robotic hands due to the light weight of the finger links with respect to the produced actuator torque KANEKO *et al.* [1992]. A distal joint is driven by the d.c servo motor with a gear system, and a tension differential type torque sensor is mounted to measure the joint torque.

While discussing the physical implementation of a force control of a joint, the mechanism of transmission at the joint plays an important role in the performance of the servo system itself. The problem of closing a joint force control feedback loop is the non-ideal transmission and drive system, i.e. presence of stiction, cogging, coulombic friction, together with higher order resonance modes in the system, ELOSEGUI *et al.* [1990].

The tension sensor signal is feedback to the torque servo mechanism system (after filtering) through an A/D converter in such a way that the signal feedback gain can be changed by software as well in hardware. The tendon diameter of 0.8 *mm* (with a measured stiffness of 100 000 *N/m*) maintains linear stiffness up to 2.5*N* tension which is sufficient for the hand setup.

To analyse the experimental results which will be shown in the next sub-section, we first formulate an ideal torque response, where ideal means that the finger joint and actuator are connected through a straight line tendon. In case of high reduction gear, this enables us to neglect the feedback torque from the gear output shaft to the motor rotor. Conventional robotics fingers have a tendon-sheath driving system, tendon-sheath lengths seem to be designed in the range of 300-1000 *mm* to avoid the nonlinear effects resulting from friction and compliance.

Furthermore, using a longer tendon also amplifies the nonlinearity of the transmission. A tension change at the end of the tendon is transmitted to the end through deformation and movement along the length of the tendon, and thus a larger tendon tension will make it more difficult to transmit a change of tendon tension.

Given two tendon tension T_1 and T_2 when the actuator is starting to rotate in a given direction to increase or decrease a joint torque, the two tendon tensions around the joint pulley will not change until the actuator rotates by a certain angle. This is the effective backlash angle and the hysteresis of the sensor which to be considered.

4.3.1) Performance of Joint Force Control.

An important factor of consideration in multifingered hands force control is the equivalent rotational stiffness $k_{s\Theta}$, since it relates the change in joint torque with changes in joint displacement $\Delta\theta$ and has to be computed for a rotational system. In particular, the equivalent rotational stiffness $k_{s\Theta}$ is derived in Appendix [A4-1] for the torque sensor :

$$k_{s\Theta} = D_\Theta \left[\cos\alpha - \sin(\alpha)\,\sin(\beta)\,\tan(\alpha+\beta)\right]k_s \tag{4.8}$$

where

$$D_\Theta = \frac{1}{(8\,\sin(\beta)\,\sin(\alpha+\beta))} \tag{4.9}$$

and k_s is the beam stiffness.

For that particular sensor design $k_{s\Theta}$ has been found to be = 102.3 *Nm/rad* for a beam stiffness k_s of 2352 *N/m*. Based on the assumption that the link inertia is ignored with respect to the actuator, an ideal actuator characteristic is conventionally governed by Eq. 4.10, where τ_a is the actuator input torque expressed at the output shaft of the gear box

$$J_T\ddot{\theta} + B_T\dot{\theta} = \tau_a \tag{4.10}$$

For the implementation of a proportional control system , then the following law is considered :

$$\tau_a = k_p(\tau_r - \tau_f) \tag{4.11}$$

where k_p is the controller gain, τ_r desired behaviour, and τ_f is the finger joint torque. Eq. 4.11 represents the ideal mechanism of controlling a joint torque.

In examining the real physical construction of the sensor, the transmission system of a joint, and the compliance of the object to be grasped, add complexity to the force control system which have to be considered. There is variation in the dynamics of the finger due to its configuration dependence, however such changes are masked by the actuator dynamics.

The grasped object physical characteristics of compliance plays an important role in the response of the force controller. There exists the following relationship between τ_f and θ, the angular displacement of the driving pulley which is given by :

$$\tau_f = k_{c\Theta}\,\Delta\theta \tag{4.12}$$

where $k_{c\Theta}$ is a compound rotational stiffness of the mechanical system which can be expressed in terms of the sensor equivalent rotational stiffness $k_{s\Theta}$, the equivalent of the environment $k_{e\Theta}$, (whether the grasped object is rigid or compliant), and finally in terms of the stiffness of the tendon $k_{t\Theta}$.

The compound rotational stiffness $k_{c\Theta}$ is a dependent factor on $k_{s\Theta}$, $k_{e\Theta}$ and $k_{t\Theta}$ and it is expressed by :

$$\frac{1}{k_{c\Theta}} = \frac{1}{k_{s\Theta}} + \frac{1}{k_{t\Theta}} + \frac{1}{k_{e\Theta}} \tag{4.13}$$

From Eq. 4.11 and Eq. 4.12 , the relation between τ_f and τ_r can be expressed as:

$$\frac{\tau_f}{\tau_r} = \frac{k_{c\Theta} k_p}{J_a s^2 + B_a s + k_{c\Theta} k_p} \tag{4.14}$$

Eq. 4.14 shows that the torque response of the closed loop system is controllable by $k_{c\Theta}$ and k_p factors. However the behaviour of the torque servo system does not remain uniform even for constant gains k_p, because $k_{c\Theta}$ involves varying quantities like $k_{e\Theta}$ and $k_{t\Theta}$.

For instance $k_{t\Theta}$ increases from a very stiff environment while it decreases for a compliant object surface. Furthermore, $k_{t\Theta}$, the tendon stiffness might change if a greater stretching force is applied to its ends. From the above issues, the behaviour is expected to have non uniform characteristics. However, the behaviour could be further simplified by taking into account the fact that the CYBHAND has been categorized to be grasping a rigid object, hence $k_{e\Theta}$ is having a very high value. $k_{t\Theta}$ is quite a high quantity for the routed tendon due to the short length of the tendon and the use of high stiffness tendon characteristics (100 000 N/m).

The equivalent rotational stiffness, $k_{s\Theta}$, is having a smaller numerical value with respect to the other stiffness parameters in Eq. 4.13, and hence it dominates the behaviour of the force controller. Furthermore, the equivalent rotational stiffness, $k_{s\Theta}$ by itself is a function of the physical construction of the sensor and the its location in the finger.

Having considered such assumption, Eq. 4.13 is totally dominated by the equivalent

rotational stiffness, $k_{s\Theta}$ which is by the sensor physical parameters.

In analysing the force feedback control system shown in Fig [4.4], the Laplace transform of the transfer function has been obtained where it can be expressed as :

$$\frac{F_o(s)}{F_r(s)} = \frac{\dfrac{nk_{c\Theta}\kappa_i k_p k_i}{RJ_T}}{s^2 + \dfrac{(RB_T+\kappa_i k_b)\,s}{RJ_T} + nk_\Theta k_{c\Theta}\kappa_i k_p k_i\,(RJ_T)} \qquad (4.15)$$

where κ_i is the conversion ratio from force to volt as was given in Chapter Two.
Once again, analysing the Eq. 4.15 from the s domain shows that, the force closed loop is having two poles located at $s_1 = -16.7 + j4.0$ and $s_2 = -16.7 - j4.0$ at a value of proportional gain equal to $k_p = 1.2$.

For improving the response time of the system, by employing a control design software, the gain has been moved to 1.65 resulting in a damping ratio of 0.966 instead of 0.72, thus increasing the response rise time. Furthermore, using the same concept of converting the s domain transfer function to the Z domain and including the effect of $k_{c\Theta}\kappa_i$, the system has stable characteristics where the three poles of the discrete time transfer function have been found located within the unit circle. The two poles are found as : $z_1 = 0.85$ and $z_2 = 0.98$ while the sampling frequency was taken as 500 Hz.

Result and Analysis :

For experimental testing of the force closed loop system, the fingertip is to apply an amount of force to a solid surface of an object, where the sensor output are loaded to graphics software for observing the real time response.

The controller software provides proportional gain only, hence the responses are achieved for changes in the forward gain.

Due to the dependence of the response on the controller gain, three different controller gains have been used. The first when k_p = 2 unit, resulting in a faster response as shown in Fig [4.5-a]. The response was noisy due to the fact, the force sensor was detecting the vibration in the beam itself due to the tendon sliding. After a one *sec.* time, the commanded force was dropped to zero resulting in zero force applied to the object surface. This response decreases as the value of this gain is reduced to k_p = 1.5, as shown in Fig [4.5-b]. In reducing the forward gain, the rising time of the controller to reach the desired applied force decrease, and the effect of friction can be seen at the start of the response.

Finally, Fig [4.5-c] shows the corresponding response when the force controller was commanded to a changing force. The amount of force applied by the fingertip on the surface is then made controllable by changing the fingertip force to the corresponding joint acting torque, hence to voltage.

In studying the force control on an object, each fingertip is required to apply the appropriate amount of force to the object in such away the object is not damaged. The selection of these forces depends on the physical weight of the object and the characteristics of the achieved task, hence force distribution problem will be discussed in Chapter Five.

SUMMARY

The Software coordination of a twelve degrees of freedom articulated system is not an obvious task to be implemented for the control of object motion. This chapter has focused on a developed software for supervising and controlling the designed hand. The software

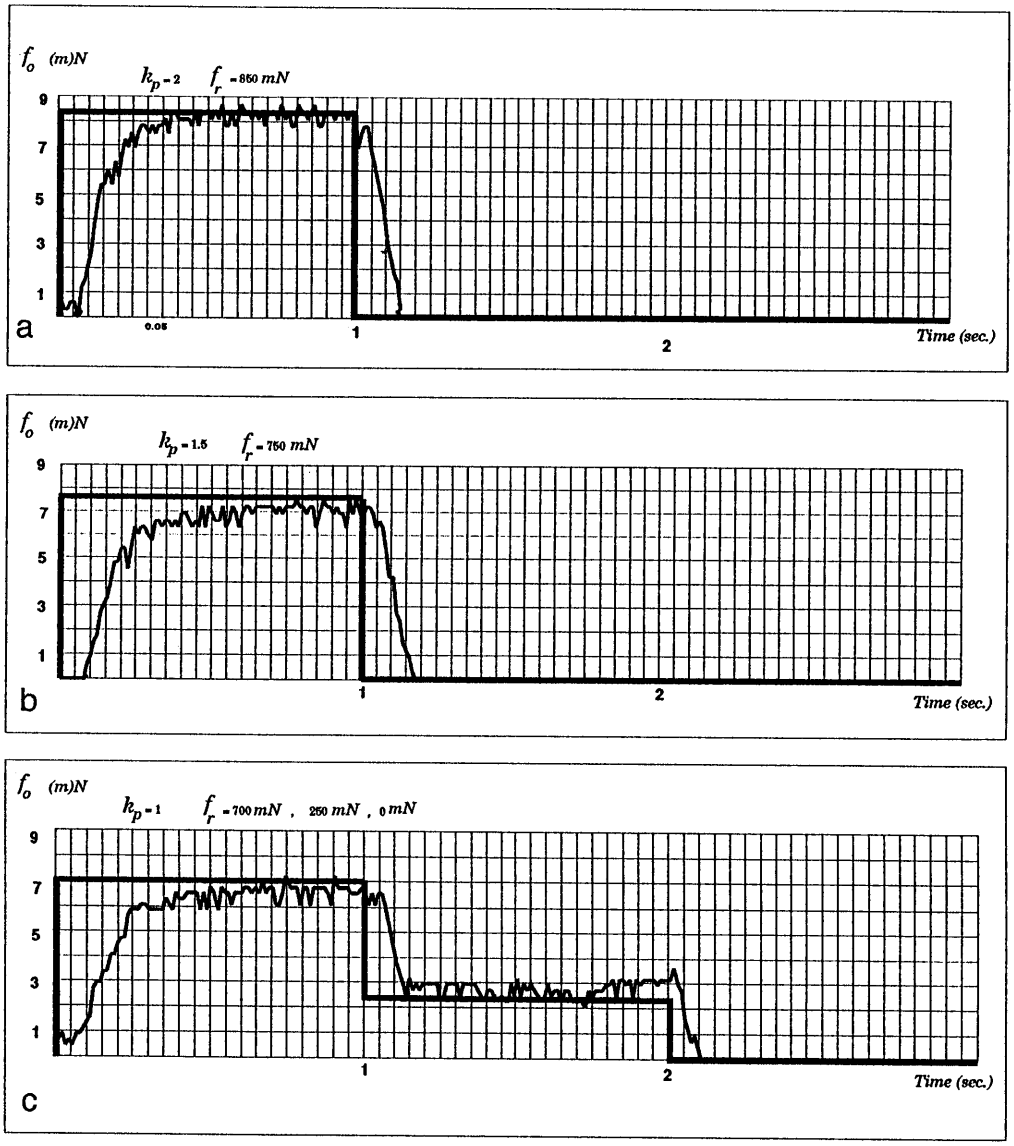


Figure 4.5 : a : Force Step Response.
b : Reduced Gain.
c : Change in Force Response.

links high level hand commands to the low-level motion processor instructions.
An n cartesian motion of the hand would involve the motion of the kinematically modelled hand.

The Chapter has combined results obtained from Chapter Two concerning the force sensor based on tension measurements to close a force control loop that enables the hand to apply fingertip forces to grasp an object.

While discussing the physical implementation of a force closed loop in robot hand, the mechanisum of the drive plays an impotant role in the performnce of the system. The force closed loop system has been shown to be critical to the enviroment where the robot hand is acting. Proportional controller has been achieved to overcome the friction present at the driving actuators in addition to the friction due to the tendon routing.

CHAPTER FIVE

OPTIMIZATION of STATIC GRASPING FINGERTIPS FORCE FUNCTION

(5.1) INTRODUCTION.

In Chapter Four the free motion of the fingers using the kinematic modelling of the entire hand was considered. However, not much emphasis was given to the aspects of the interaction between the fingertips and a grasped object. In this chapter the aspects of forces interaction between the fingertip and the object will be discussed, based on how these forces are selected in an optimal manner to satisfy certain objectives.

To determine if a particular grasp on a body imposes sufficient constraint to immobilize it completely, we must go beyond the simple freedom counting of Grubler's equation. Since each contact between a grasped object and a finger reduces the object's freedom, the associated forces to be applied are of significance in producing stable force closure grasps. The concept of grasping and the associated theory based on the force optimization will be clearly defined in this chapter.

When a multifingered hand grasps an object, each finger applies a normal force associated with a tangential force. A full restraint of an object then means that the overall system of contact forces is applied in definite directions so that the object is constrained. The purpose of this chapter is to discuss the grasping theory in a simple form. Concepts will be used to introduce the optimal grasping theory based on the internal forces optimization, and the employment of nonlinear constraints optimization technique.

The theory behind the optimization and how the problem is formulated will also be discussed within this Chapter. If the optimized variables, which are the contact forces in our case, are to be arranged in a specific format, then the quadratic formula will result. The current quadratic optimization theory is mainly concentrated on the inequality constraints as developed by GOLDFARB and ADNANI [1983]. However, the force formulation has been further developed to include the equality constraints as well. Nonlinear constraints

optimization, developed by GILL *et al.* [1984] can be applied in robot hand forces computation as long as the equality and inequality linear constraints are arranged in a form accepted by the optimization code. Hence, in this chapter we shall discuss the implementation of force optimization of the real fingertip forces instead of optimizing the internal forces, as developed by NAHON and ANGELES [1992] and NAKAMURA *et al.* [1987].

Chapter five has been classified into six sections as follows : Section (5.2) presents the concept behind the grip transform formulation. Object-hand force balance is discussed in section (5.3), whereas the distribution of forces between the fingertips is elaborated in section (5.4). Section (5.5) presents the technique of applying the nonlinear constraints optimization. Finally static grasping of objects is given in section (5.6).

(5.2) GRASPING THEORY.

5.2.1) A Single Contact Finger

The effect of several contacts on a body can be viewed either from a motion or a force point of view, MASON and SALISBURY [1985]. In terms of motion, each acting contact limits the body to executing a particular system of twists. When several contacts are imposed simultaneously on a body, the net motion twist system available to the body will be the interaction of the twist system allowed by each contact alone.

Consider four fingers in contact with a common object shown in Fig [5.1]. With the body coordinate $\Sigma_{x\text{-}y\text{-}z}$ shown in the figure attached to its centre mass a matrix of representation of each contact can be represented as a map from the applied independent contact to the wrench space of the object. Consider Y_{ci} to be the map representing the three applied finger forces at each finger, namely the normal force f_z and two orthegonal friction forces f_x and f_y, to the body wrench:

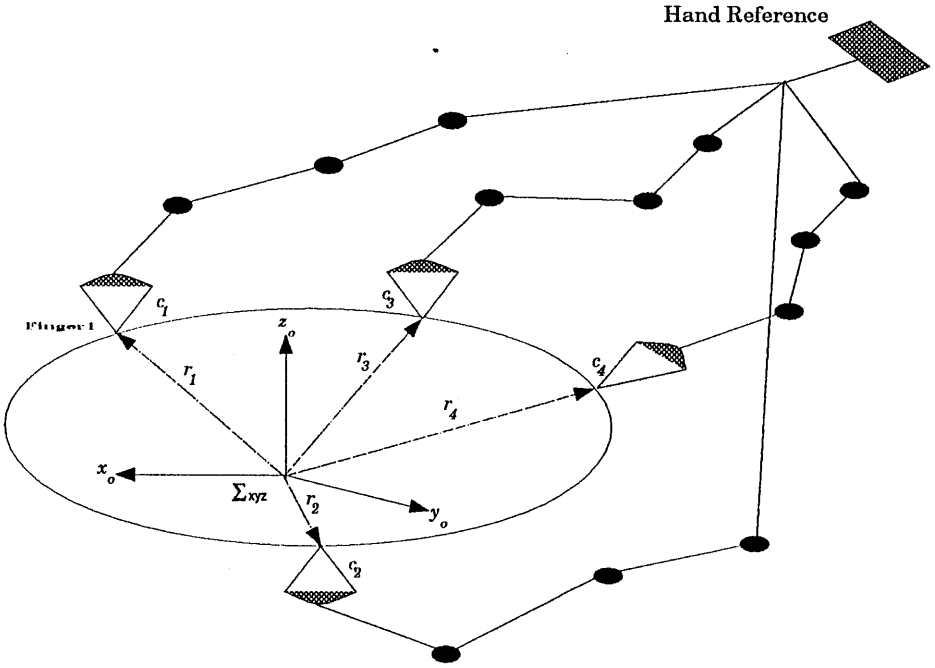


Figure 5.1 : Grip Transform Formulation from Contact Vectors.

$$Y_{ci}(f_{xi}, f_{yi}, f_{zi}) = \begin{bmatrix} f_{n1} & f_{n2} & f_{n3} \\ f_{n1} \times r_{xi} & f_{n2} \times r_{yi} & f_{n3} \times r_{zi} \end{bmatrix} \begin{bmatrix} f_{xi} \\ f_{yi} \\ f_{zi} \end{bmatrix} \tag{5.1}$$

$$Y_{ci}(f_{xi}, f_{yi}, f_{zi}) = \begin{bmatrix} 1 & 0 & 0 \\ 0 & 1 & 0 \\ 0 & 0 & 1 \\ 0 & r_{zi} & -r_{yi} \\ -r_{zi} & 0 & r_{xi} \\ r_{yi} & -r_{xi} & 0 \end{bmatrix} \begin{bmatrix} f_{xi} \\ f_{yi} \\ f_{zi} \end{bmatrix} \in \Re^{[6\times 1]} \tag{5.2}$$

where f_{n3} is the unit normal to the contact surface at the *ith* contact point, f_{n1} and f_{n2} are the unit tangents to the object surface. In a similar way we define the grasp of a rigid body by a multifingered robot hand as a group of contacts, depending on the used type of contact. If the fingertip has been modelled as a soft finger type, then there will be an extra column in Eq. 5.2 representing the torsional torque due to the deformation of the fingertip, KERR and ROTH [1986].

Four Contacts :

From this we move to the case of a four contacts hand. Each finger contacts the object at one point (*i.e. fingertip prehension*), and each defines a contact map $Y \in \Re^{12}$. Hence the grasp of a rigid body at a particular configuration by a robot hand with four fingers is a map of $G \in \Re^{[6\times 12]}$ given by :

$$G(f_{x1}, f_{y1}, \ldots\ldots, f_{z4}) = Y_{c1}(f_{x1}, f_{y1}, f_{z1}) + \ldots + Y_{c4}(f_{x4}, f_{y4}, f_{z4}) \tag{5.3}$$

However, while formulating the grip transform, the basic relation of forces in the manipulation of a rigid object by a four-fingered hand, and a representation of the internal force, will be given under the following assumptions :

(*i*) The four contact points are not located on a straight line.

(*ii*) The mechanism of each finger is such that each fingertip can exert a normal force to the object only in the direction perpendicular to the object surface.

5.2.2) Grip Transform Formulation *G*

In order to formulate the grip transform, the effect of the four fingertip contacts have to be considered. For instance, Fig [5.1] has shown the four contacts of a multifingered robot hand under assumptions (*i*) and (*ii*). In the figure, $\sum_{x,y,z}$ is the object coordinate frame fixed to the object, and c_i is the contact point of the *ith* finger. For the case of four fingers contacting an object, the grasp transform can be obtained in terms of the acting fingertips forces as, FEARING [1986] :

$$Gf_{tip} = \begin{bmatrix} \sum_{i=1}^{4} f_{tipi} \\ \\ \sum_{i=1}^{4} (f_{tipi} \times r_i) \end{bmatrix}$$

$$Gf_{tip} = \begin{bmatrix} f_{tip1} + f_{tip2} + f_{tip3} + f_{tip4} \\ \\ f_{tip1} \times r_1 + f_{tip2} \times r_2 + f_{tip3} \times r_3 + f_{tip4} \times r_4 \end{bmatrix} \tag{5.4}$$

where f_{tipi} in Eq. 5.4 is four fingers force mapping. Extracting G from Eq. 5.4 gives :

$$
\boldsymbol{G} = \begin{bmatrix}
1 & 0 & 0 & 1 & 0 & 0 & 1 & 0 & 0 & 1 & 0 & 0 \\
0 & 1 & 0 & 0 & 1 & 0 & 0 & 1 & 0 & 0 & 1 & 0 \\
0 & 0 & 1 & 0 & 0 & 0 & 0 & 0 & 0 & 0 & 0 & 0 \\
0 & r_{z1} & -r_{y1} & 0 & r_{z2} & -r_{y2} & 0 & r_{z3} & -r_{y3} & 0 & r_{z4} & -r_{y4} \\
-r_{z1} & 0 & r_{x1} & -r_{z2} & 0 & r_{x2} & -r_{z3} & 0 & r_{x3} & -r_{z4} & 0 & r_{x4} \\
r_{y1} & -r_{x1} & 0 & r_{y2} & -r_{x2} & 0 & r_{y3} & -r_{x3} & 0 & r_{y4} & -r_{x4} & 0
\end{bmatrix} \tag{5.5}
$$

as the grasp transform for a four finger hand under frictional point contact $\boldsymbol{G} \in \Re^{[6\times12]}$.

Force Domain and transmitted wrenches :

In the case where the contacts are to apply a force $\boldsymbol{f}_{tip}$ on the body in the direction at point of contact c, the wrench system associated with each point is :

$$T(c) = [n(c), \; c \times n(c)]$$

Corresponding to a set of finger-contacts, we have a system of 12 wrenches :

$$[\, \boldsymbol{G}_1, \ldots \boldsymbol{G}_k, \; \boldsymbol{G}_{k+1}, \ldots \ldots \boldsymbol{G}_{12} \,]$$

Under the assumption that the magnitude of these wrenches is given by the scalars (f_1,... f_k,...f_n), we call such a system of wrenches and the wrench-magnitude a grip $\boldsymbol{G}$. This grip generates an external six dimensional object wrench.

Breaking Eq. 5.5 into up to 12 columns (called $\boldsymbol{G}_i$) where each column represents the individual force vector associated with the contact. The twelve forces, are balanced to produce a resultant force in the object itself. This force vector of the object is designated here as $\boldsymbol{F}_b$. $\boldsymbol{F}_b$ is given by :

$$F_b = \sum_{i=1}^{12} G_i f_{tip}$$

Put in a matrix form, ROMDHANE and DUFFY [1990] :

$$\begin{bmatrix} f_x \\ f_y \\ f_z \\ m_x \\ m_y \\ m_z \end{bmatrix} = [G_1\ G_2\ G_3, \ldots\ldots G_{12}] \begin{bmatrix} f_{x1} \\ f_{y1} \\ f_{z1} \\ . \\ . \\ . \\ f_{z4} \end{bmatrix}$$

$$F_b = G f_{tip} \tag{5.6}$$

Eq. 5.6 reveals an important physical meaning used in robot hands. The resultant force vector of an object F_b is equal to the vectorial summation of the individual fingertips forces. Hence, the force computation problem is how these forces are computed in such a way that resultant force vector equals the external force vector of the object itself, YOUNG and STARR [1989].

From another point of view, each fingertip applies an external wrench vector of $\in \Re^{[6\times 1]}$ to the grasped object, and exerts a set of independently controllable wrenches w_{ij} through the point of contact. This force vector is then filtered at the contact point depending on the contact type. In Eq. 5.2 the normal force to the contacted surface is unisense, whereas the other generated two tangential forces can be bidirectional. Thus a linear combination of all finger wrenches that yield the desired external wrench can to found, HOLLERBACH and NARASIMHA [1986]. In other words :

$$F_b = \sum_{i=1}^{4} \sum_{j=1}^{3} x_{ij} w_{ij}$$

where x_{ij} is the corresponding wrench intensity and the summation is for a four fingered grasp. But $\Sigma \Sigma x_{ij} w_{ij}$ can be written in terms of the grip transform itself, hence, more compactly, KUMAR and WALDRON [1988] :

$$F_b = G f_{tip} \tag{5.7}$$

Use of Grip Transform :

Furthermore, the grip transform is a useful operator matrix for the description of an object location. A small displacement of the *ith* contact point is represented by the following kinematic equation :

$$\delta c_i = \delta r - r_i \times \delta\Omega \tag{5.8}$$

where δr and $\delta\Omega$ are the small translational displacement of the object mass centre and the small angular displacement of the object respectively, and r_i is the three columns matrix of the grip transform. G representing the position vector from the mass centre of the object to its *ith* contact point, the matrix representation of the above equation for the entire hand is then given by :

$$\delta c = G^T \delta X \tag{5.9}$$

where $\delta X^T = [\delta r_x \;\; \delta r_y \;\; \delta r_z \;\; \delta\Omega_x \;\; \delta\Omega_y \;\; \delta\Omega_z] \in \Re^6$

and $\delta c^T = [\, \delta c_1 \;\; \delta c_2 \;\; \delta c_3 \;\; \delta c_4] \in \Re^{12}$

The above given equations are significant while discussing the issues of object motion and the velocities of points of contacts, since they represent the constraints of hand-object dynamics which can be stated as : " the velocity of motion at the fingertips is equal to the rate of change of the object contacts ".

(5.3) OBJECT-HAND CLOSED LOOP DYNAMIC SYSTEM.

Once the grasped object dynamic is coupled with the dynamic of the fingers in the hand, the hand-object is in a closed loop kinematic where the position and orientation of the object is completely specified by the position and orientation of the fingers. Within this section, the dynamic of an object will be considered which is entirely based on the Lagrange formulation.

5.3.1) Dynamics of the Reference Member (Grasped Object)

The dynamic of the object is basically derived from the Lagrange equation of motion for a single link. This can be expressed as a summation of the forces due to the linear and angular displacement of the object itself. The motion equations of the object are represented by the following Lagrange equations of the solid structure of the object as formulated by COLE *et al.* [1992] :

$$\boldsymbol{F}_b = \begin{bmatrix} \dot{m}_o \upsilon_o - m_o g \\ \dot{\boldsymbol{I}}_o \omega_o + \omega_o \times \boldsymbol{I}_o \omega_o \end{bmatrix}$$

$$\begin{bmatrix} m_o \boldsymbol{I} & 0 \\ 0 & \boldsymbol{I}_o \end{bmatrix} \begin{bmatrix} \dot{\upsilon}_o \\ \dot{\omega}_o \end{bmatrix} + \begin{bmatrix} -m_o g \\ (\omega_o \times I_o \omega_o) \end{bmatrix} = \begin{bmatrix} \boldsymbol{E}_3 & \boldsymbol{E}_3 & \boldsymbol{E}_3 & \boldsymbol{E}_3 \\ S(r_1) & S(r_2) & S(r_3) & S(r_4) \end{bmatrix} \begin{bmatrix} f_{tip1} \\ f_{tip2} \\ f_{tip3} \\ f_{tip4} \end{bmatrix} \qquad (5.10)$$

The above equation forms the basis for the calculation of the contact forces for force equilibrium achievements, where m_o is the total mass vector, $[\upsilon_o, \omega_o]$ is the linear and angular velocity vector of the object at its centre of mass and $\boldsymbol{I}_o$ is the inertia matrix of the grasped object about its centre of mass.

What is required for the force distribution problem is the calculation of the fingertip forces so that the object remains stable either during rest or at motion. Eq. 5.10 represents an undetermined equation of force distribution, hence multiple solutions are obtained. However, the obtained solutions have to be selected so that certain constraints are satisfied. These constraints represent the physical limits in the hand and the interaction force directions.

To grasp an object (in static), the hand must generate the resultant force as given by Eq. 5.10. The distribution of the resultant force into individual fingertip forces is the main issue. For a contact with constraint surfaces to be maintained, force control should be applied in the constrained directions (namely, the normal directions of the constraint surfaces), whereas position control in moving the fingertip should be applied in the unconstrained directions (*namely, the tangential directions of constraint surfaces*).

In dynamic coordinated manipulation, the force control is required in three-dimensional space, where an object is manipulated by work done by the fingertips. In addition to this, the force distribution must consider both the static and dynamic equilibrium condition of the task. Static equilibrium is needed to generate the desired fingertip force at the contact point without the fingertip motion. Whereas, dynamic equilibrium serves to maintain contact with the object by accelerating the fingertip to follow the motion of the contact point, an issue to be further elaborated in Chapter Six.

(5.4) FORCE DISTRIBUTION PROBLEM

A grasp achieves equilibrium when the distributed sum of the forces and sum of moments are zero, PONCE *et al.* [1993]. Force distribution problems can be applied either for the static grasping of an object to hold against the gravity force effect, or for the dynamic case where the four fingers are used to manipulate an object in a pre-defined way. This

chapter concentrates on the static grasping of an object where the velocity of the object is zero.

While solving the force distribution problem in robot hands, two main cases have to be considered. The first is that concerned with the dynamic model of the hand object system as in the dynamic case, whereas the second is concerned with the dynamic effects of the hand and solves only the object dynamics. Proceeding with static grasping would require the controller to calculate joint torques to hold the hand links stable in addition to generating a torque vector for grasping the object.

Force balance (*distribution*) problems are characteristics of articulated systems which have to be solved, in particular robot hands depend on frictional material for the grasping of objects. The basic problem of controlling these systems is that of coordination of forces during the motion. Because the fingers share the same object, this global coordination problem is usually under-specified and involves redundancy. Moreover, since friction constraints for preventing slippage and the physical limits of the joint actuators often need to be considered and not violated, this problem is also a constrained redundancy. The main theme of the problem is to compute the appropriate actuator torques which generate fingertip forces to produce either a static equilibrium or stable grasping during dynamic motion of the hand-object:

$$\tau_a = C_i + J_{\Theta i}^{T} G^{-1} F_b \qquad (5.11)$$

In Appendix [A5] the model of the hand dynamics equation has been derived based on the Lagrange dynamics. There are three necessary conditions for a stable grasp. First, the object must be in equilibrium; i.e. there is no net force or moment. Second, all forces must be within the cone of fiction. Third, it should be possible to increase the magnitude of the grasping force to prevent any displacement due to an arbitrary force, FEARING [1986].

For static grasping, only the gravity dependent terms will be used in this Chapter. Basically a solution is required to the undetermined relation given by Eq. 5.10. Before a solution is obtained, let us consider the three constraints imposed by the hand-object system.

5.4.1) First : Geometrical Constraints

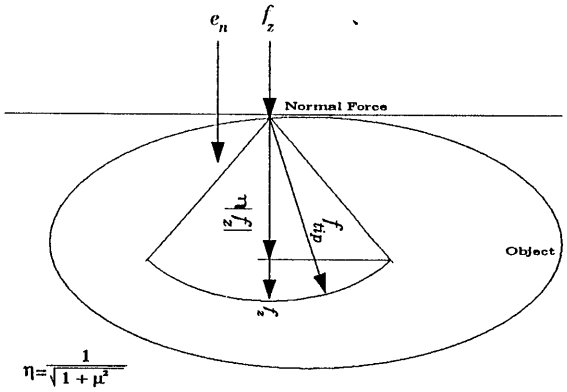
If the object shape is represented by a given geometric function, then the constraint in selecting the fingertip forces is restricted in computing the ones which will satisfy the constraints of the object shape. Because the normal and tangential forces of the *ith* fingertip exerted on the object are parallel and orthogonal to the inner normal vector respectively, we obtain the geometrical constraints of the fingertip force , as interpreted in Fig [5.2-a] :

$$\boldsymbol{e}_{ni} \cdot \boldsymbol{f}_{tipi} > 0 \qquad 1 \leq i \leq 4 \qquad (5.12)$$

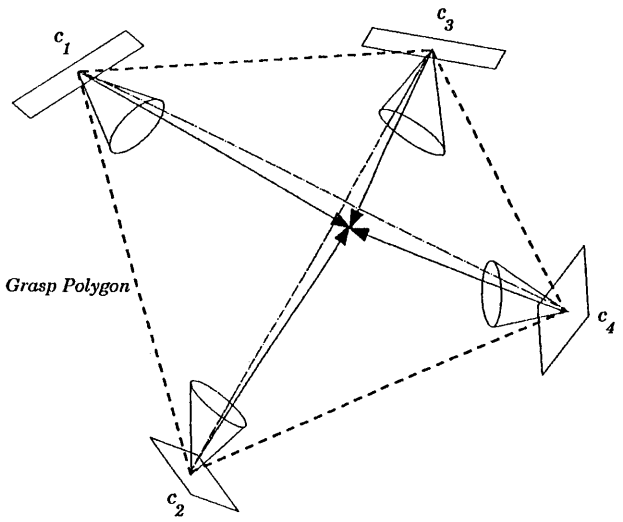
where $\boldsymbol{e}_{ni}$ is the normal from the *ith* point of contact, defined as inward direction from the outer object surface. The geometric constraints expressed by Eq. 5.12 ensure that : the force applied by the *ith* fingertip is acting in the same direction as a vector defining the shape of the grasped object. For each of the four contacts together in an object, the geometric constraints imposed will be those to keep normal forces in the same direction as the surface normals of the fingertips. This polygon constraint can be viewed from the four normal forces in Fig [5.2-b], AL-GALLAF and WARIWCK [1994-b].

5.4.2) Second : Frictional Constraint Nonlinearity

A characteristic of multifingered hands is that they rely on passive frictional contacts to transmit forces to the grasped objects, and the limitations of these must be accounted for. A consideration of the limitations of passive frictional contact is also necessary. It must be



a



b

Figure 5.2 : a : Static Frictional Constraints.
b : Frictional Cone at Points of Contacts to form a grasp polygon.

ensured that the magnitude of the tangential force must not exceed the product of normal force and coefficient of static friction, μf_z. Fig [5.2-b] illustrates the requirements of applying forces at each point of contact. That requirement is interpreted physically so that : *all* forces have to be within the frictional cone. For further understanding of this constraint, let us analyse one contact force. The applied force at the *ith* contact point is constrained as shown in Fig [5.3] by the maximum static frictional condition expressed by the following set of equations:

$$\boldsymbol{e}_{ni} \cdot \boldsymbol{f}_{tipi} \geq \frac{||\boldsymbol{f}_{tipi}||}{\sqrt{(1+\mu^2)}}$$

and

$$f_z \geq \frac{\sqrt{(f_x^2 + f_y^2 + f_z^2)}}{\sqrt{(1+\mu^2)}}$$

$$f_z^2 + f_z^2\mu^2 \geq (f_x^2 + f_y^2 + f_z^2)$$

$$f_x^2 + f_y^2 \leq -f_z^2\mu^2 \qquad (5.13)$$

Once the fingertips are brought in contact with the grasped object, a closed kinematic chain results, which is closed through the grasped object and opened or broken by removing a single member of the system which is often the grasped object.

If the unknown contact force vector on the object expressed in the contact coordinate frame is denoted by ${}^c\boldsymbol{f}_{tip}$, then the following vector for four fingers is expressed as :

$${}^c\boldsymbol{f}^T_{tip} = [\,{}^c\boldsymbol{f}_{tip1} \quad {}^c\boldsymbol{f}_{tip2} \quad {}^c\boldsymbol{f}_{tip3} \quad {}^c\boldsymbol{f}_{tip4}\,] \qquad (5.14)$$

Furthermore, the transform to solve contact forces from the contact coordinate frame for *ith* finger, to the reference object coordinate is found by, CHENG and ORIN [1991] :

$$F_b = \sum_{i=1}^{4} G_i {}^c f_{tipi}$$

$$F_b = G_1 {}^c f_{tip1} + G_2 {}^c f_{tip2} + G_3 {}^c f_{tip3} + G_4 {}^c f_{tip4} \qquad (5.15)$$

The limitation or constraint at contact points, as described graphically in Fig [5.3], is the friction cone centred at the contact point as a cone with quadratic surface. The use of quadratic inequality constraints would require the use of an optimization algorithm with quadratic inequality. However, since the method of quadratic nonlinear programming developed by GOLDFARD and ADNANI [1984] requires the restriction of the inequality to be linear, the nonlinear friction cone can be replaced by a piecewise linear friction pyramid that can be described by linear inequalities. Two obvious choices for this pyramid are shown in Fig [5.3]:

(*i*) The first choice is that which *circumscribes* the friction cone, hence $\mu^{-} = \mu$.

(*ii*) The second is that which is *inscribed* by the friction cone, hence $\mu^{-} = \frac{\sqrt{2}\ \mu}{2.}$

where μ is the coefficient of friction between the two contact surfaces.

In accordance with the friction which is present at the contact, where the contact normal is along the z direction, the friction force constraints of the circumcised cone may be expressed mathematically from Eq. 5.13 as:

$$\sqrt{({}^c f_x^{\,2} + {}^c f_y^{\,2})} \leq -\mu {}^c f_z \qquad (5.16)$$

where μ is the type of frictional material used.

The use of an inscribed or circumscribed pyramid of Fig [5.3] is an approximation, since it gives a conservative but linear set of constraints describing a friction cone. This gives the

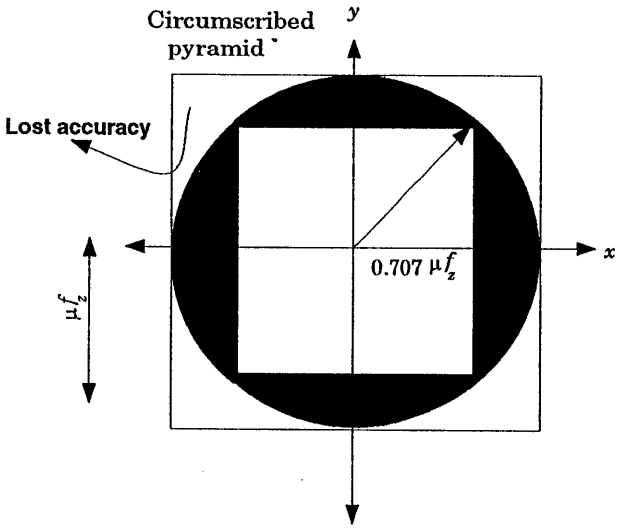


Figure 5.3 : Circumscribed and Inscribed Pyramids in Nonlinearity Approximation and Lost Accuracy.

following equations :

$$-{}^{c}f_{ix} + (\mu/\sqrt{2})\,{}^{c}f_{iz} \leq 0$$

$${}^{c}f_{ix} + (\mu/\sqrt{2})\,{}^{c}f_{iz} \leq 0$$

$$-{}^{c}f_{iy} + (\mu/\sqrt{2})\,{}^{c}f_{iz} \leq 0$$

$${}^{c}f_{iy} + (\mu/\sqrt{2})\,{}^{c}f_{iz} \leq 0$$

The friction force constraints may be further rewritten as :

$$\begin{bmatrix} -1 & 0 & -(\mu/\sqrt{2}) \\ 1 & 0 & (\mu/\sqrt{2}) \\ 0 & -1 & (\mu/\sqrt{2}) \\ 0 & 1 & (\mu/\sqrt{2}) \end{bmatrix} \begin{bmatrix} {}^{c}f_{xi} \\ {}^{c}f_{yi} \\ {}^{c}f_{zi} \end{bmatrix} \leq \begin{bmatrix} 0 \\ 0 \\ 0 \\ 0 \end{bmatrix} \qquad (5.17)$$

$$\boldsymbol{C}_{of}\,{}^{c}\boldsymbol{f}_{tipi} \leq 0$$

where $\boldsymbol{C}_{of}$ is the matrix coefficient of the friction constraints.

5.4.3) Third : Maximum and Minimum Torque Constraints

The third constraint in computing the fingertip forces is the constraint due to the physical limits in the hand actuation. Further constraints to be considered are the range within which a given joint produces a torque so that the maximum torque produced by a joint is within its limits. Hence the physical limits on the *ith* joint torques may be written as:

$$\tau_{imin} \leq \tau_{ai} \leq \tau_{imax} \qquad (5.18)$$

The fingertip forces ${}^{c}f_{tipi}$ for each finger are related to the joint torque vector τ_{ai} by the Jacobian transpose as expressed by :

$$\tau_{ai} = {}^{c}J_{i}^{T}\,{}^{c}f_{tipi} + \tau_{uncoi} \tag{5.19}$$

where ${}^{c}J_{i}^{T}$ is the transpose Jacobian for linear velocity of *ith* finger, using the origin of the contact coordinate frame as velocity reference point. τ_{uncoi} is the actuator torque vector to move the finger links in unconstrained motion.

Combining Eq. 5.18 with Eq. 5.19 gives :

$$\begin{aligned} {}^{c}J_{c}^{T}\,{}^{c}f_{tipi} &\leq (\tau_{max} - \tau_{unco})_i \\ -{}^{c}J_{c}^{T}\,{}^{c}f_{tipi} &\geq (-\tau_{max} + \tau_{unco})_i \end{aligned} \tag{5.20}$$

5.4.4) Equality and Inequality Constraints Formulation

Linear Equality Constraints :

The force balance equation for a static grasping is obtained by finding the contact force vector which satisfies the load balance distribution given by :

$$\begin{bmatrix} 1 & 0 & 0 & 1 & 0 & 0 & 1 & 0 & 0 & 1 & 0 & 0 \\ 0 & 1 & 0 & 0 & 1 & 0 & 0 & 1 & 0 & 0 & 1 & 0 \\ 0 & 0 & 1 & 0 & 0 & 1 & 0 & 0 & 1 & 0 & 0 & 1 \\ 0 & -r_{z1} & r_{y1} & 0 & -r_{z2} & r_{y2} & 0 & -r_{z3} & r_{y3} & 0 & -r_{z4} & r_{y4} \\ r_{z1} & 0 & -r_{x1} & r_{z2} & 0 & -r_{y2} & r_{z3} & 0 & -r_{y3} & r_{z4} & 0 & -r_{x4} \\ -r_{y1} & r_{x1} & 0 & -r_{y2} & r_{x2} & 0 & -r_{y3} & r_{x3} & 0 & -r_{y4} & r_{x4} & 0 \end{bmatrix} \begin{bmatrix} f_{x1} \\ f_{y1} \\ f_{z1} \\ f_{x2} \\ f_{y2} \\ f_{z2} \\ f_{x3} \\ f_{y3} \\ f_{z3} \\ f_{x4} \\ f_{y4} \\ f_{z4} \end{bmatrix} = \begin{bmatrix} f_x \\ f_y \\ f_z \\ m_x \\ m_y \\ m_z \end{bmatrix} \tag{5.21}$$

In Eq. 5.21 the object dynamic in static grasping will be due to the effect of gravity on the object given by $m_o g$ acting in the direction in which the object frame coincides with the gravity field. If the gravity field is acting against the Y axis fixed in the object, then the vector of object dynamics in static grasping will be :

$$\boldsymbol{F}_b^T = [0 \quad -m_o g \quad 0 \quad 0 \quad 0 \quad 0] \tag{5.22}$$

Once the hand changes its orientation of a Yaw, Roll, or Pitch by the action of a robot arm as has been achieved by STANSFIELD [1991], the gravity field effect on the grasped object-hand will also change even without changes in the fingers and contacts frames which remain fixed. This change in the gravity effect keeps some of the first three elements of $\boldsymbol{F}_b$ not of zero value, depending on the angles of rotations produced by the change in the hand orientation, thus :

$$\boldsymbol{F}_b^T = [f_x \quad f_y \quad f_z \quad 0 \quad 0 \quad 0] \tag{5.23}$$

In general, rotations of the robot arm can take place: this is common in industrial environments where a robot hand grasps an object and they are moved together by the action of a robot arm. If there is a change in the hand orientation, then the used force computation algorithm has to recalculate the fingertips forces to overcome the changes in the object dynamics due to another moving system, rather than to the effect of the object motion itself. This situation has led NAHON and ANGELES [1992] to recalculate the fingertips forces for a Salisburys type hand.

Furthermore, Eq. 5.21 is an undetermined problem which involves matrix inversion of $\boldsymbol{G}$ using either the generalized inverse $\boldsymbol{G}^+$, PENROSE [1955], or the pseudo inversion $\boldsymbol{G}^{-1}$, hence multiple solutions will exist. However such two way solutions give a fingertip

force vector which may not satisfy the force direction constraints or the physical limits of the hand.

One approach to overcoming this redundancy in solution is to employ optimization techniques. ROA [1984] has discussed the optimization of a quadratic defined objective function subject to linear inequality only. Before formulating the objective function, let us first look at the linear constraints.

Linear Inequality Constraints :

While considering the inequality terms of an optimization function, three main sources of inequality are of great importance in robotic hands: the geometric constraints, the frictional constraints and the maximum and minimum torque constraints. The geometric and frictional constraints are impeded in each other due to the rotation of the fingertip frames to accommodate the object contact surface.

Concatenating all the previously expressed constraints either at the contacts or within the hand maximum torque limit gives :

$$\Pi_i \, {}^{c}\boldsymbol{f}_{tipi} \leq \boldsymbol{C}_i$$

here Π is a concatenated matrix of each finger frictional and Jacobian inequalities for the entire hand. Put in general form this gives :

$$\Pi \, {}^{c}\boldsymbol{f}_{tip} \leq \boldsymbol{B}$$

$$\begin{bmatrix} \Pi_1 & 0 & 0 & 0 \\ 0 & \Pi_2 & 0 & 0 \\ 0 & 0 & \Pi_3 & 0 \\ 0 & 0 & 0 & \Pi_4 \end{bmatrix} \begin{bmatrix} {}^{c}\boldsymbol{f}_{1tip} \\ {}^{c}\boldsymbol{f}_{2tip} \\ {}^{c}\boldsymbol{f}_{3tip} \\ {}^{c}\boldsymbol{f}_{4tip} \end{bmatrix} \leq \begin{bmatrix} \boldsymbol{c}_1 \\ \boldsymbol{c}_2 \\ \boldsymbol{c}_3 \\ \boldsymbol{c}_4 \end{bmatrix} \qquad (5.24)$$

where Π_i $(1 \leq i \leq 4)$ is a composite matrix representing the contact and the finger kinematics constraints. The individual fingertip references are rotated in such a way that the contact frame is allied with the velocity reference point at the fingertip as shown diagrammatically in Fig [5.4].

The other source of inequality expressed by Eq. 5.19 is due to the physical limits of the actuators which has been included under the $\boldsymbol{B}$ vector in Eq. 5.24. To keep the joint torques within the physical limits of the actuators, maximum joint torque constraints are expressed as:

$$\tau_{imin} \leq \tau_{ai} \leq \tau_{imax} \tag{5.25}$$

where

$$\tau_a = \tau_{ucon} + \boldsymbol{J}^{T_c} \boldsymbol{f}_{itip}$$

This has the effect of increasing the dimensions of the problem. In Eq. 5.25, τ_{imax} is the maximum actuator torque vector for *ith* finger, and τ_{imin} is the minimum. The transpose of the Jacobian is to be expressed using the origin of the contact coordinate frame as the velocity reference point. At this stage we need to express Eq. 5.25 so that the final format is :

$$\begin{aligned} \boldsymbol{J}^{T_c} \boldsymbol{f}_{tipc} &\leq \tau_{max} - \tau_a \\ -\boldsymbol{J}^{T_c} \boldsymbol{f}_{tipc} &\geq -\tau_{max} + \tau_a \end{aligned} \tag{5.26}$$

The $\boldsymbol{B}$ vectors given by Eq. 5.24 are now changed to include the actuator limits by concatenating them with the frictional inequalities. In Eq. 5-24 $\boldsymbol{c}_1$, $\boldsymbol{c}_2$, $\boldsymbol{c}_3$, and $\boldsymbol{c}_4$ represent the concatenated friction and joint limits of the four fingers. For a single finger it can be expressed as :

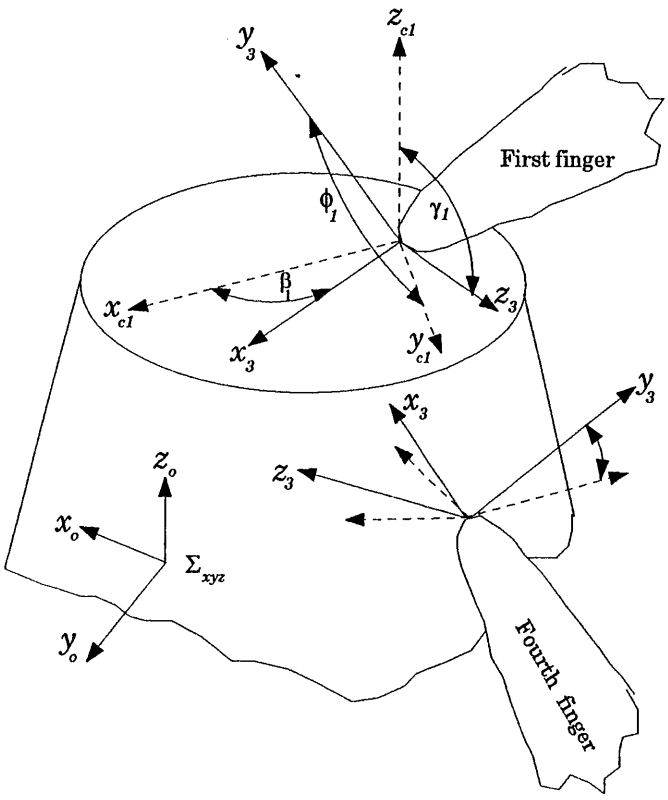


Figure 5.4 : Rotations of the Four Fingers at The Points of Contact.

$$c_i = \begin{bmatrix} 0 \\ 0 \\ 0 \\ 0 \\ \tau_{1imax} - \tau_{unco1} \\ \tau_{2imax} - \tau_{unco2} \\ \tau_{3imax} - \tau_{unco3} \\ -\tau_{1imin} + \tau_{unco1} \\ -\tau_{2imin} + \tau_{unco2} \\ -\tau_{3imin} + \tau_{unco3} \end{bmatrix} \tag{5.27}$$

where the τ_{unco1}, τ_{unco2}, and τ_{unco3} represent the torque produced by the finger joints to overcome the dynamic forces due to the hand Inertia M_h, centrifugal forces N_h, and the gravity, C_h of the finger links. Hence the inequality constraints including the frictional cone and limits in actuator torques have been expressed and formulated in matrix form. This main equation, Eq. 5.24, will be used in the coming section with an object function of optimization.

Object Function (Cost Function Under Computation) :

The solution to the inverse force equations Eq. 5.21 is not unique, but it can be chosen in an optimal manner by optimization of an objective function. All resolved redundancy by minimizing a performance index, is defined explicitly as a function of the joint variables, subject to the kinematic constraints relating joint and cartesian coordinates, ANDERSON and ANGELES [1989].

However, the criterion followed is to produce physical forces and to preserve the stability of grasping the object with the minimum force, so that no squeeze occurs to the object and no slipping at the contacts. Such a performance index will ensure the minimum requirement of the actuator energy. The approach taken here is to minimize the internal force to correspond to that of the component, of the solution that lies in the null

space of the grip transform, i.e. that which satisfies $\boldsymbol{G}\boldsymbol{f}_{tip} = 0$. The internal force was described earlier as the force that tends to crush the grasped object without producing any dynamical motion in the object.

The internal forces, as shown in Fig [5.5], can be minimized by minimizing the norm of actuator torques given by $\frac{1}{2}(\tau_a^T \tau_a)$. Here τ_a is a vector, of all the actuator torques in the system, found by appending all the torques in a single vector. The norm of the actuators torques has special configuration in the cost function $\Phi(\boldsymbol{f}_{tip})$. This is developed in the coming section.

The technique for minimizing the internal forces can be developed by writing the following standard quadratic objective function as, POWELL [1985] and LUENBERGER [1984] :

$$\Phi(\boldsymbol{f}_{tip}) = C^T \boldsymbol{f}_{tip} + \tfrac{1}{2} \boldsymbol{f}_{tip}^T \boldsymbol{W} \boldsymbol{f}_{tip} \tag{5.28}$$

where $\boldsymbol{f}_{tip}$ is a concatenated vector of all the four fingertip forces to be optimized, $\boldsymbol{W}$ is a weighting matrix chosen to satisfy certain criteria regarding the forces, and $\boldsymbol{C}^T \boldsymbol{f}_{tip}$ is a biasing force added to the computed fingertip forces.

5.4.5) Combined Cost $\Phi(\boldsymbol{f}_{tip})$ Function with the Constraints

An objective function determines the criteria of optimality for an underspecified problem. Since different applications for various multifingered robotic hands will have different criteria for optimality, there is no defined objective function for different tasks. The criteria followed here is the minimization of the norm of all the contact forces, which is valid for rigid contact. One approach for the minimization of the contact forces norms is the minimization of the grasp internal forces which are acting on the fingers in the grasp plane, as shown in Fig [5.5].

The need for the minimization of the internal grasp forces requires the minimization of the actuator torques. Thus, if the vector of all the actuator torques , $\tau_a \in \Re^{12}$, in the system is given by τ_a, then $\frac{1}{2}(\tau_a^T \tau_a)$ defines the actuator torque norm. The τ_a vector consists itself of two torques : the unconstrained torque τ_u to hold the hand links in addition to the torques needed to grasp the object, the $J_h^T f_{tip}$.

Let the hand Jacobian matrix for the velocity of the fingertips expressed in terms of the contact coordinates, be defined as, COLE *et al.* [1992] :

$$J_h = diag[\ J_1 \quad J_2 \quad J_3 \quad J_4\ ] \tag{5.29}$$

$$\begin{aligned} \Phi(f_{tip}) &= \tfrac{1}{2}(\tau_a^T \tau_a) \\ \tau_a &= \tau_u + J_h^T f_{tip} \\ \tau_a^T &= \tau_u^T + J_h f_{tip}^T \end{aligned} \tag{5.30}$$

Expanding $\Phi(f_{tip})$ gives :

$$\begin{aligned} \Phi(f_{tip}) &= \tfrac{1}{2}\tau_a^T\tau_a = \tfrac{1}{2}(\tau_u^T + J_h f_{tip})(\tau_u + J_h^T f_{tip}) \\ \tfrac{1}{2}\tau_a^T\tau_a &= \tfrac{1}{2}(\tau_u^T\tau_u + \tau_u^T J_h^T f_{tip} + J_h f_{tip} J_h^T f_{tip} + J_h f_{tip}\tau_u) \\ &= \tau_u^T J_h^T f_{tip} + \tfrac{1}{2} f_{tip}^T J_h J_h^T f_{tip} \end{aligned} \tag{5.31}$$

which can be further rewritten in a standard quadratic form as :

$$\Phi(f_{tip}) = C^T f_{tip} + \tfrac{1}{2} f_{tip}^T W f_{tip} \tag{5.32}$$

where C^T is given as $C^T = [\tau_{1u}^T J_1^T f_{tip} \quad \tau_{2u}^T J_2^T f_{tip} \quad \tau_{3u}^T J_3^T f_{tip} \quad \tau_{4u}^T J_4^T f_{tip}\ ]$ and W as :

$$W = J_h J_h^T \tag{5.33}$$

and $f^T_{tip} W f_{tip}$ as :

$$f^T_{tip} W f_{tip} = [f_{1tip} \quad f_{2tip} \quad f_{3tip} \quad f_{4tip}] \begin{bmatrix} J_1 J^T_1 & 0 & 0 & 0 \\ 0 & J_2 J^T_2 & 0 & 0 \\ 0 & 0 & J_3 J^T_3 & 0 \\ 0 & 0 & 0 & J_4 J^T_4 \end{bmatrix} \begin{bmatrix} f_{1tip} \\ f_{2tip} \\ f_{3tip} \\ f_{4tip} \end{bmatrix} \tag{5.34}$$

Put in matrix form :

$$\Phi(f_{tip}) = C^T f_{tip} + \tfrac{1}{2} f^T_{tip} W f_{tip} \tag{5.35}$$

This objective function is now expressed as a function of the object dynamic and hand parameters. The problem can now be generalised to :

$$\begin{aligned} &\textit{Optimize} \quad \Phi(f_{tip}) = C^T f_{tip} + \tfrac{1}{2} f^T_{tip} W f_{tip} \\ &\textit{subject to} \quad G f_{tip} = F_b \\ &\textit{and} \qquad \Pi f_{tip} \leq B \end{aligned} \tag{5.36}$$

Eq. 5.36 is a general form of quadratic defined objective function with linear inequality constraint, however, it also includes linear equality constraints. GOLDFARD and ADNANI [1984] have considered the numerical solution of quadratic defined objective functions with linear inequality only. Hence the solution of the above equation will require the reconfiguration of the problem so that the algorithm will also accommodate the equality constraint.

Internal Forces :

The internal grasping forces are those which are acting between the fingertips themselves. For a four finger hand design there are up to six internal forces acting between points of contacts on the grasp plan. Effectively, the internal grasping forces between pairs of fingers can be expressed as:

$$f_{ij} = (\boldsymbol{f}_i - \boldsymbol{f}_j) \cdot \boldsymbol{r}_{ij} \tag{5.37}$$

where $\boldsymbol{f}_i$ is the force exerted by *ith* finger, $\boldsymbol{r}_{ij}$ is the unit vector from the *ith* to the *jth* contact point, and f_{ij} is a specified scalar of internal grasping force. For the grasp plane shown in Fig [5.5], the six internal forces can be designated by:

$$\begin{aligned}
f_{41} &= (\boldsymbol{f}_4 - \boldsymbol{f}_1).\boldsymbol{r}_{41} &&= -f_{14} \\
f_{42} &= (\boldsymbol{f}_4 - \boldsymbol{f}_2).\boldsymbol{r}_{42} &&= -f_{24} \\
f_{43} &= (\boldsymbol{f}_4 - \boldsymbol{f}_3).\boldsymbol{r}_{43} &&= -f_{34} \\
f_{32} &= (\boldsymbol{f}_3 - \boldsymbol{f}_2).\boldsymbol{r}_{32} &&= -f_{23} \\
f_{31} &= (\boldsymbol{f}_3 - \boldsymbol{f}_1).\boldsymbol{r}_{31} &&= -f_{13} \\
f_{21} &= (\boldsymbol{f}_2 - \boldsymbol{f}_1).\boldsymbol{r}_{21} &&= -f_{12}
\end{aligned}$$

The internal force vector $\boldsymbol{F}^T = [f_{12}, f_{13}, f_{14}, f_{23}, f_{24}, f_{34}]$ given by $\boldsymbol{F} = \boldsymbol{G}\boldsymbol{f}_{in}$ has the following geometric characteristics. The load lines of the four fingertip forces $\boldsymbol{f}_i$ generally form a tetrahedron formed by the four contact points.

Internal force vector is the force which can be added to the manipulation or object driving force without disturbing equilibrium and can be used to modify the finger force to avoid sliding or breaking contact, PING and STEVEN [1992]. The internal forces once acting on the grasped object, produce a zero resultant force and keep the object in equilibrium.

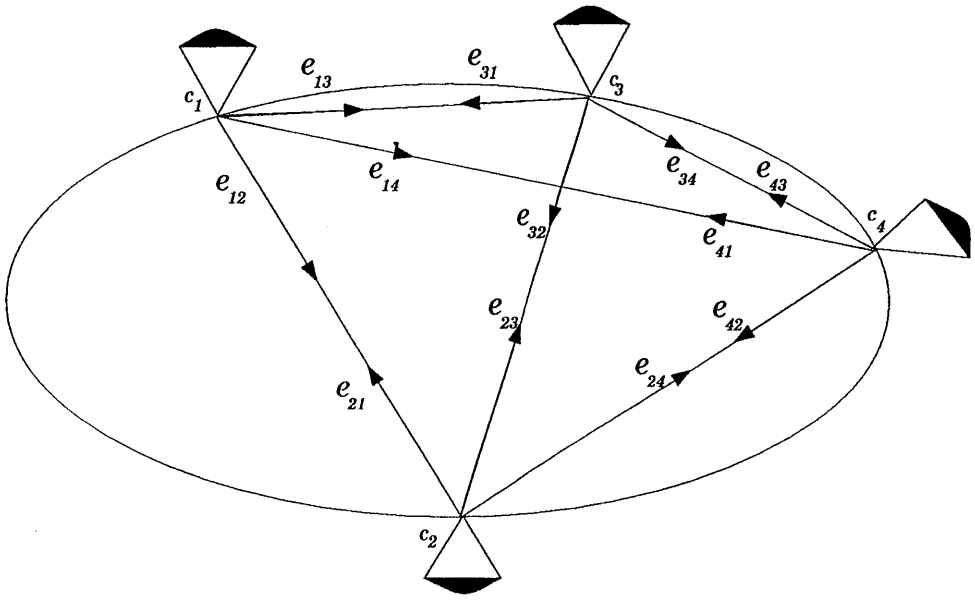


Figure 5.5 : A Four Fingered Hand Internal Force Vectors Representation.

The internal force is normally defined to be the vector in the null space of the grip transform G which does not contribute to the resultant motion of the object.

5.4.6) Internal Forces Optimization

The optimization of the grasp internal force necessitates the minimization of the side forces within the grasp plane. For a four fingered robot hand, up to six internal forces must be optimized. The interaction forces do not generate motions; they are needed for holding the object. The value of the interaction forces is determined by the task to be performed, YUN *et al.* [1993]. These six internal forces are responsible for the amount of squeeze within the grasped object. If a delicate object (soft material object) is to be grasped by a robot hand, the task then is to produce the minimum grasp forces by the hand. For the minimization of the grasp internal forces, the following formulation has been adopted, NAHON and ANGELES [1991]. If $W = E$, unity weighting matrix, and $C = 0$ the biasing torques are zero, hence $\Phi(f_{tip})$ is given by :

$$\Phi(f_{tip}) = \tfrac{1}{2} f_{tip}^{T} f_{tip} \tag{5.38}$$

Furthermore, if the f_{tip} vector solution is considered to consist of two solutions :

$$f_{tip} = f_{pA} + f_{hB} \tag{5.39}$$

where f_{pA} is the particular solution and f_{hB} is the homogenous solution (null space solution). The particular solution is found from the generated inverse of G as given in APPENDIX [A1] :

$$f_{pA} = G^{+} F_b \tag{5.40}$$

In Eq. 5.40 f_{pA} is the minimum norm solution. of the force equality constraints, DER-

VENTOS and DAVISON [1992]. After direct substitution of f_{tip} in the object and constraint equations, the problem is equivalent to the minimization of the homogenous solution. Subsituting f_{hB} in Eq. 5.38 gives :

$$\begin{aligned} &\text{minimize} && \Phi(f_{hB}) = \tfrac{1}{2}(f_{pA}+f_{hB})^T (f_{pA}+f_{hB}) && (5.41)\\ &\text{subject} && F_b = G(f_{pA}+f_{hB}) \\ & && Gf_{hB} = 0 \\ &\text{and} && \Pi f_{hB} \leq (B - \Pi f_{pA}) && (5.42) \end{aligned}$$

Expanding the objective function $\Phi(f_{hB})$ itself in terms of f_{pA} and f_{hB} gives :

$$\Phi(f_{hB}) = \tfrac{1}{2}(f_{pA}^T f_{pA} + f_{hB}^T f_{hB} + 2f_{pA}^T f_{hB}) \qquad (5.43)$$

However $f_{pA}^T f_{pA}$ gives a constant value, and $f_{hB}^T f_{hB}$ gives a null value since f_{pA} and f_{hB} are orthogonal solutions. Arranging the variables and the optimization of internal forces, can be viewed as the minimization of the homogenous solution f_{hB} only :

$$\begin{aligned} &\text{minimize} && \Phi(f_{hB}) = \tfrac{1}{2} f_{hB}^T f_{hB} \\ &\text{subject to} && G f_{hB} = 0 \\ &\text{and} && \Pi f_{hB} \leq (B - G f_{pA}) && (5.44) \end{aligned}$$

where B represents a varying quantity component depending on the hand posture. The method of solution has been by including the equality constraints in the GOLDFRAB and ADNANI algorithm. Hence the approach taken here is to initialize the algorithm at the equality-constrained minimum.

One solution of Eq. 5.44 has been discussed by LAWSON and HANSON [1974] for non

unity weighting matrix and non zero biasing torque as:

$$f_{pA} = W^{-1}G^{T}(G\,W^{-1}G^{T})^{-1}(F_b + G\,W^{-1}C) - W^{-1}C \qquad (5.45)$$

Direct substitution of all the above given variables gives:

$$f_{tip} = G^{T}(GG^{T})^{-1}F_b + \eta\lambda \qquad (5.46)$$

where η is the null space of the matrix G and λ is the vector for the minimum null space, Al-GALLAF *et al.* [1993-a].

Note that the dimensions of η and λ depend mainly on the value of the null-space of G. Therefore they have to be found for a particular grasp kinematic configuration. The final format of the problem is :

$$f_{tip} = f_{pA} + \eta\lambda \qquad (5.47)$$

where the λ vector is determined according to the optimization technique of the following format :

$$\begin{aligned} &\text{Optimize} \quad && \Phi(\lambda) = \tfrac{1}{2}\,\lambda^{T}\eta^{T}\eta\lambda \\ &\text{Subject to} \quad && \Pi\eta\lambda \le (B - \Pi f_{pA}) \end{aligned} \qquad (5.48)$$

Internal Forces Optimization Computation Aspects :

From the above optimization formula, Eq. 5.48, the problem of force optimization has been reduced to the computation of λ which is also to be multiplied by the null space matrix η. For a real time optimization of contact forces, the speed of convergence of the solution toward the optimized, is an issue that dominated the choice of any numerical

approach.

An important issue regarding the internal forces minimization is its relation with the fingertips forces decomposition into grasping and manipulation forces YOSHIKAWA and NAGAI [1991] as already described in Chapter One. The grasping forces described were added to satisfy the geometry and frictional constraints. The minimized internal forces using the optimization algorithm is another view of grasp mode scalar, (γ_1, γ_2, γ_3, γ_4) which is added to satisfy the grasping forces given by :

$$f_{tip} = f_g + f_m \tag{5.49}$$

where the internal forces are represented by the force vector f_g :

$$f_g = B_g h_g \tag{5.50}$$

and B_g is a matrix selected to satisfy the contact and geometrical constraint at the point of contact. YOSHIKAWA and ZHENG [1993] used the geometric means to search for a solution for formulating f_g, however this approach does not involve the existence of an optimal solution.

(5.5) EMPLOYMENT of NONLINEAR CONSTRAINTS FORCE OPTIMIZATION

5.5.1) Nonlinear Constraint Versus Linear Approximation

In the foregoing analysis the computation of the optimal fingertip forces for grasping an object was achieved by approximating the nonlinear mapping into a four sided, inscribed

or described pyramid. Such an approach uses an approximate model of the frictional cone which exists at the point of contact, already shown in Fig [5.3]. From a computational point of view the method is adopted in such a way as to blend both the linear inequality and equality constraint in the GOLDFARB and ADNANI quadratic optimization technique.

For an accurate modelling, the full nonlinear constraint will be investigated in this section. With reference to the frictional cone depicted in Fig [5.3], if an inscribed pyramid is adopted then a total of $\mu^2 f_z^{\,2}(2-\pi)$ area is lost in the approximation, and an area of $\mu^2 f_z^{\,2}(4-\pi)$ is lost if a circumscribed pyramind is used. For the four fingered robot hand, the four nonlinear constraints are expressed as :

$$\sqrt{({}^{c}f_{xi})^2 + ({}^{c}f_{yi})^2} \;\leq\; -\mu\, {}^{c}f_{zi} \qquad \text{for } i = 1 \text{ to } 4 \qquad (5.51)$$

Since the quadratic nonlinear programming algorithm does not deal with equality and inequality nonlinear constraints, the equality constraint has been augmented to the inequality constraint as represented by some relations. If the limits of the actuators torques are augmented with the object dynamics to give one vector expressed by the vector $\boldsymbol{U}^T_{lim}$ for the upper torque extreme and $\boldsymbol{L}^T_{lim}$ for the lower torque extreme, then :

upper torque extreme :

$$\boldsymbol{U}^T_{lim} = [\;\; \boldsymbol{F}_b \;:\;\; \tau_{max1j} \;\; \tau_{max2j} \;\; \tau_{max3j}\;] \in \Re^{18} \qquad j = 1 \text{ to } 3 \qquad (5.52)$$

lower torque extreme:

$$\boldsymbol{L}^T_{lim} = [\;\; \boldsymbol{F}_b \;:\;\; \tau_{min1j} \;\; \tau_{min2j} \;\; \tau_{min3j}\;] \in \Re^{18} \qquad j = 1 \text{ to } 3 \qquad (5.53)$$

The main concept in formulating the nonlinear constraints force optimization, is the augmentation of the grip transform with the hand Jacobian J_h. The inequality matrix is concatenated with the equality constraints under one matrix of the following form:

$$L_{lim} \leq \left[\begin{array}{cccc} E & E & E & E \\ S(r_1) & S(r_2) & S(r_3) & S(r_4) \\ \hline {}^cJ^T_1 & 0 & 0 & 0 \\ 0 & {}^cJ^T_2 & 0 & 0 \\ 0 & 0 & {}^cJ^T_3 & 0 \\ 0 & 0 & 0 & {}^cJ^T_4 \end{array}\right] {}^cf_{tip} \leq U_{lim} \qquad (5.54)$$

5.5.2) Objective Function of Optimization

The produced joint's torques must satisfy the defined constraints. There are a variety of objective functions that can be optimized while grasping an object rather than the internal forces. The objective function to be optimzed, can be the sum of two norm squares of the joint torque vectors.

There are other expressions often used in the literature for the effort exerted by the fingertips, such as norm of the force applied to the grasped object, absolute sum of the joint torques, and absolute sum of the normal components of the applied forces.

The performance index of joint torque norm square has been well used in the object load distribution problem to seek the minimization of energy consumption while grasping or manoeuvring the object, such as COI *et al.* [1992].

If the chosen objective function to be optimized is the same, to a certain extent , as adopted in the case of linear constraint minimization, which is the minimization of the

actuator torques expressed by $\frac{1}{2}(\tau_a^T \tau_a)$. Following the same simplification procedure in Eq. 5.30 to Eq. 5.35, this results in :

$$= [\,{}^c f_{1tip} \quad {}^c f_{2tip} \quad {}^c f_{3tip} \quad {}^c f_{4tip}] \begin{bmatrix} J_1 J^T{}_1 & 0 & 0 & 0 \\ 0 & J_2 J^T{}_2 & 0 & 0 \\ 0 & 0 & J_3 J^T{}_3 & 0 \\ 0 & 0 & 0 & J_4 J^T{}_4 \end{bmatrix} \begin{bmatrix} {}^c f_{1tip} \\ {}^c f_{2tip} \\ {}^c f_{3tip} \\ {}^c f_{4tip} \end{bmatrix} \tag{5.55}$$

Expanding Eq. 5.55 for the contact forces f_{x1} to f_{z4} results in :

$$\Phi(f_{tip}) = k_1 f_{x1}{}^2 + k_2 f_{y1}{}^2 + k_3 f_{z1}{}^2 + k_4 f_{x2}{}^2 + k_5 f_{y2}{}^2 + k_6 f_{z2}{}^2 + k_7 f_{x3}{}^2 + k_8 f_{y3}{}^2 + k_9 f_{z3}{}^2 + k_{10} f_{x4}{}^2 + k_{11} f_{y4}{}^2 + k_{12} f_{z4}{}^2 \tag{5.56}$$

where k_1 to k_{12} are constants determined by the fingers Jacobians at particular postures. For static grasping of an object $\Phi(f_{tip})$ remain constant due to the invariant of the finger Jacobians. However, once the object is in motion continuous updating of the objective function $\Phi(f_{tip})$ is required. For unity values of k_1 to k_{12}, the objective function is reduced to the summation of the square of the twelve contact forces of the hand given by:

$$\Phi(f_{tip}) = f_{x1}{}^2 + f_{y1}{}^2 + f_{z1}{}^2 + f_{x2}{}^2 + \text{- - - - - - - - - - - - } + f_{z4}{}^2$$

Put in another way :

$$\Phi(f_{tip}) = \sum_{j=1}^{4} (f_{xj}{}^2 + f_{yj}{}^2 + f_{zj}{}^2) \tag{5.57}$$

The major concern of the application of nonlinear constraints optimization approach is the reduction of the computational requirements, as will be further elaborated in Chapter

Seven. The computational requirements for the use of linear constraints optimization is determined by the structure of the grip transform G (on the points of contacts around the object), the structure of the null space η, and the object dynamics. The optimization using nonlinear constraints, is seeking a solution to the use of a nonlinear model of the contact, therefore finding a suitable solution for the hand object system with four nonlinear constraints is not a minor problem. For the time being let f_{Tri} be a vector of nonlinear constraints of the four fingertips contacts given by:

$$f_{Tri} = \begin{bmatrix} \sqrt{(f_{x1}^2 + f_{y1}^2)} \\ \sqrt{(f_{x2}^2 + f_{y2}^2)} \\ \sqrt{(f_{x3}^2 + f_{y3}^2)} \\ \sqrt{(f_{x4}^2 + f_{y4}^2)} \end{bmatrix} \tag{5.58}$$

Defining the E_e matrix to be composed from G the grip transform and J_h, such as:

$$E_e = \begin{bmatrix} G \\ \hline J^T{}_h \end{bmatrix} \quad \in \Re^{[18\times12]} \tag{5.59}$$

then E_e is bounded by the equality and inequality limits of the actuators as:

$$L_{lim} \leq E_e{}^c f_{tip} \leq U_{lim} \tag{5.60}$$

where L_{lim} and U_{lim} are vectors given by expanding Eq. 5.52 and Eq. 5.53 :

$$L^T{}_{lim} = [f_x \ f_y \ f_z \ m_x \ m_y \ m_z : \tau_{11} \ \tau_{12} \ \tau_{13} \ \tau_{21} \ \tau_{22} \ \tau_{23} \ \tau_{31} \ \tau_{32} \ \tau_{33} \ \tau_{41} \ \tau_{42} \ \tau_{43}] \in \Re^{18}$$

$$U^T{}_{lim} = [f_x \ f_y \ f_z \ m_x \ m_y \ m_z : \tau_{11} \ \tau_{12} \ \tau_{13} \ \tau_{21} \ \tau_{22} \ \tau_{23} \ \tau_{31} \ \tau_{32} \ \tau_{33} \ \tau_{41} \ \tau_{42} \ \tau_{43}] \in \Re^{18} \tag{5.61}$$

Thus the forces calculations can be expressed as, AL-GALLAF and WARWICK [1994-a]:

$$\text{Optimize } \Phi(\boldsymbol{f}_{tip}) = \sum_{j=1}^{4} (f_{xj}^{\,2} + f_{yj}^{\,2} + f_{zj}^{\,2})$$

$$\text{subject to } \boldsymbol{L}_{lim} \leq \boldsymbol{E}_e^{\,c}\boldsymbol{f}_{tip} \leq \boldsymbol{U}_{lim}$$

$$\text{and } \lambda_{Llim} \leq \boldsymbol{f}_{Tri} \leq \lambda_{Ulim} \qquad (5.62)$$

where λ_{Llim} is the lower limit in the nonlinear constraints, defined by the problem type, and determines the maximum force allowed to be applied considering the μf_z. Thus λ_{Llim} is given by :

$$\lambda^T_{Llim} = [\,\mu f_{z1} \quad \mu f_{z2} \quad \mu f_{z3} \quad \mu f_{z4}] \qquad (5.63)$$

and the upper limit of the constraints λ_{Ulim} is :

$$\lambda^T_{Ulim} = [\,0 \quad 0 \quad 0 \quad 0\,] \qquad (5.64)$$

Since the finger does not slide over the surface of the object itself, as in ZEXIANG *et al.* [1989], the $\boldsymbol{G}$ and η remain constants during the object motion and the computational requirement is mainly determined by $\boldsymbol{G}$ and $\boldsymbol{F}_b$. In terms of the optimization algorithm itself, the number of linear constraints is large for a four fingered hand due to the approximated frictional cone, by either a circumscribed or inscribed pyramid. On the contrary, for data to be fed to the nonlinear constraints optimization, it is necessary to have only the knowledge of the hand Jacobian $\boldsymbol{J}_h$ and the object dynamics (which are also needed for the linear constraints optimization) at each instance. From the previous analysis, it can be concluded that the employment of nonlinear constraints optimization in force computation will reduce the number of constraints and omit the need for constraints calculations outside the optimization algorithm itself, such as the calculation of

Π and $\boldsymbol{B}$ matrices for the linear constraints case. For further investigation of the computational flow, Fig [5.6-a] shows two flow charts used in both techniques which require the knowledge of the hand Jacobian $\boldsymbol{J}_h$.

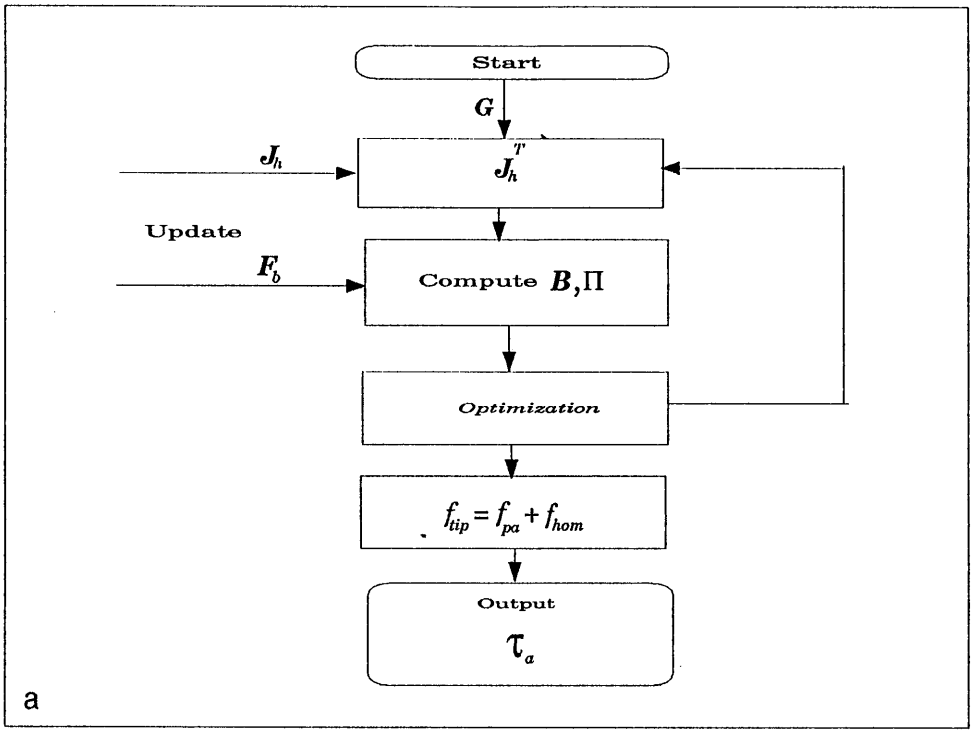
Furthermore, the employment of nonlinear constraints optimization will solve the twelve contact forces ($\boldsymbol{f}_{tip}$ vector) directly instead of solving the null space component vector $\eta\,\lambda$, Fig [5.6-b]. Thus we are reducing the time requirements for the addition and multiplication for computing the total contact forces $\boldsymbol{f}_{tip}$, and time for Π and **B** matrices.

Contrary to this, the use of nonlinear constraints optimization call certain internal defined functions which use the derivative and its approximation of the nonlinear constraints GILL *et al.* [1983], which can be time consuming especially when the solution is not converging very smoothly to an optimal function. The use of the linear and nonlinear constraints optimization algorithm have been based on formulating the force problem , and the use of the well known optimization functions defined in the NAG [1989].

Basically, the nonlinear constraints algorithm has been modified in such away as to deal both with equality ($\boldsymbol{F}_b = \boldsymbol{G}\boldsymbol{f}_{tip}$) with inequality constraints ($\boldsymbol{J}_h^T \boldsymbol{f}_{tip} \leq \boldsymbol{L}_{imit}$) and solving the twelve contact forces $\boldsymbol{f}_{tip}$ vector directly, instead of solving it through the adjustment of the null space vector.

(5.6) STATIC GRIPPING of OBJECT

Before discussing the fingertip force computation, let us consider the aspect of the controller structure for static grasping. Fig [5.7] shows the controller structure for grasping an object in a static mode using the linear constraint optimization. It is combined in the sense that two torques are generated the first to grasp the object based on internal forces



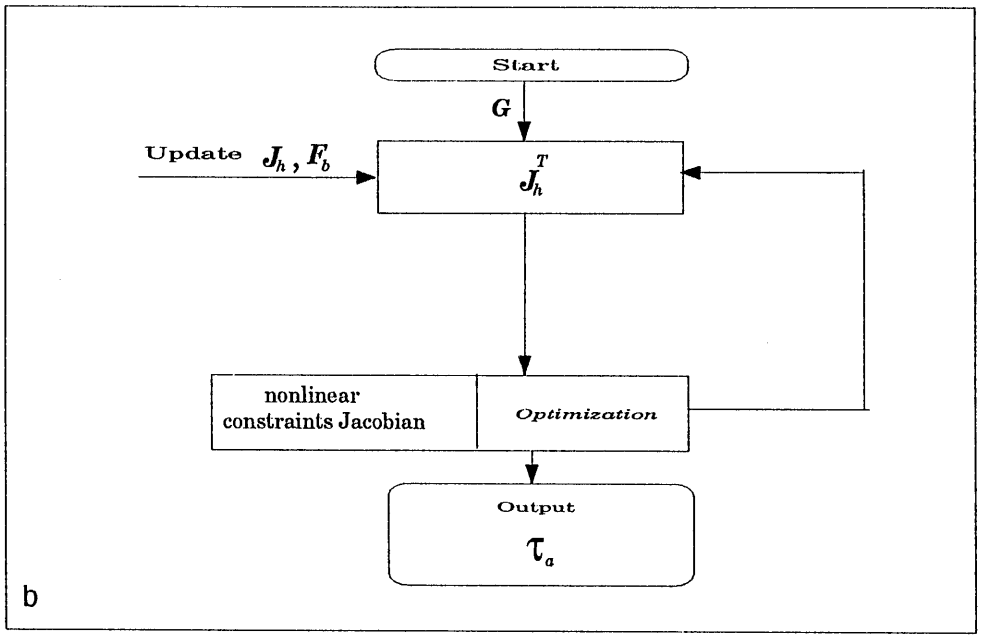


Figure 5.6 : a : Flow Chart for Internal Forces Optimization.
b : Flow Chart for Fingertips Forces Using Nonlinear Constraints Optimization.

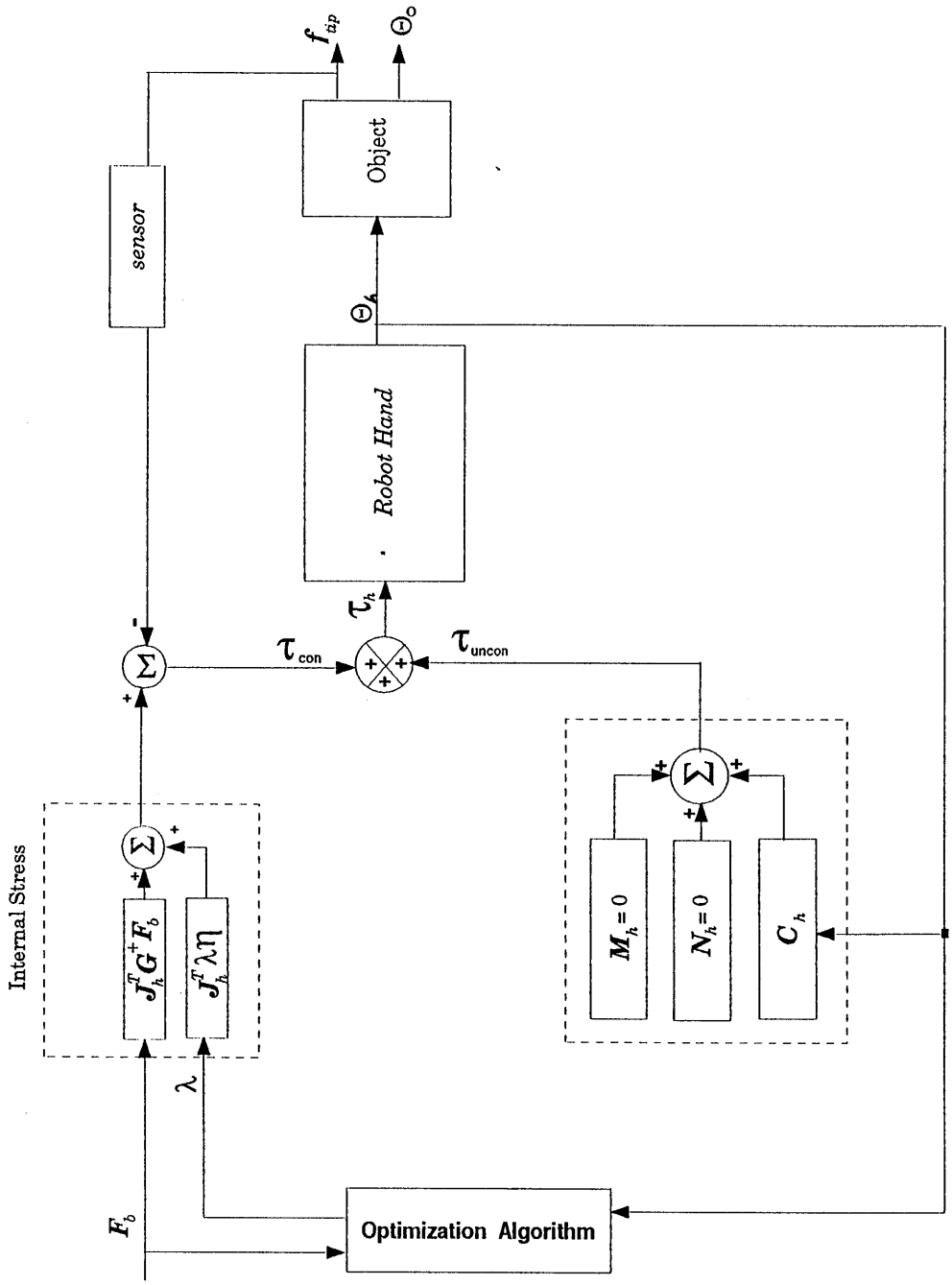


Figure 5.7 : Hybrid Controller for Static Grasping with Internal Forces Optimization.

optimization, the second to hold the links of the hand. In order to control the amount of stress on the object, the contact forces have to be enclosed in force feedback by sensing the normal force and the two associated frictional forces.

Since the motion parameters are all zero, the controller has to produce torques for overcoming the gravity effect in addition to torques for the object handling, through the generation of appropriate contact normal forces.

Contrary to this controller, Fig [5.8] shows the controller which has been based on the use of the nonlinear optimization algorithm. The controller has a similar structure unless the approach of generating the fingertips forces is different. Furthermore, the amount of stress on the object can be viewed by the decomposition of the contact forces into parallel and orthagonal components

The direction in which the gravity effect is acting is entirely dependent on the orientation of the frame attached to the object centre of gravity. If the hand is attached to a robot manipulator and the arm starts to change the orienation of the hand, the object orientation will also change, resulting in a change in which the object weight is acting on the object centre of gravity. However, for the time being we shall work under the assumption that the hand has not been changed in orientation and the gravity effect is only acting in the y direction.

Another issue for consideration in force distribution, is the orientation at which the fingertip is making contact with the grasped object. Before the application of the optimization algorithm, the fingers Jacobian J_1 to J_4 have to be expressed with respect to the point of contact frame. If the fingertip frame is making a given angle of rotation with the object surface, then this rotation is to be included in the corresponding finger Jacobian. These frame rotations will make sure the contact coordinate at the object surface and

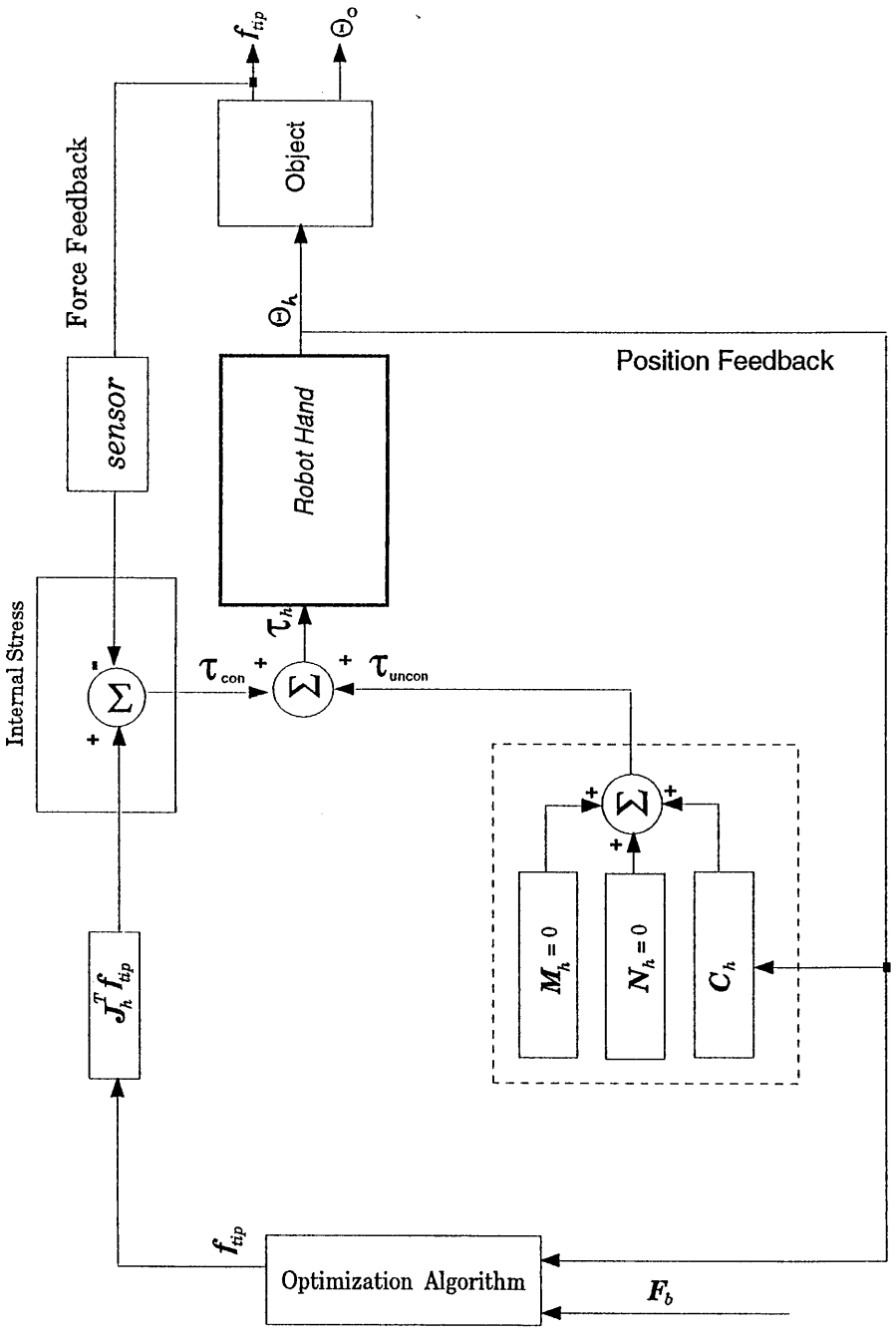


Figure 5.8 : Hybrid Controller for Static Grasping Using Non-Linear Constraints Qudratic Optimization.

the fingertip coordinate are of the same orienation irrespective of the object shape, as has been shown in Fig [5.4].

Defined Task :

As the robot hand changes its orientation with respect to the gravitational field, the force due to the object weight is no longer acting in one direction, however it is resolved into other force components which the fingertips have to compensate for. For static mode of grasping the orientation of the two frames remain fixed as is the case here, whereas the orientation changes as the fingers start to move the object under fixed orientation of the grasped object. The static object force vector F_b for the object grasped can be given by :

$$F_b^T = [0 \quad 0 \quad f_z \quad 0 \quad 0 \quad 0]$$

where

$$f_z = -g\, m_o \tag{5.65}$$

and m_o is the object mass and g is the gravity acceleration constant. For this analysis, the object mass has been chosen to be $0.05\,Kg$, thus of a weight $\cong 0.5\,N$, and the inertia characteristics are computed using Lagrange dynamics.

Assumption : For this application of optimization, the hand is oriented such that the palm is co-planar with the world x-y plane.

5.6.1) Results and Analysis

Two approaches of optimization to find the overall fingertips forces will be considered, we shall employ the use of internal forces optimization and the use of nonlinear inequality constraints optimization.

First : Linear Constraints and Internal Forces Optimization :

Let us consider the example of grasping an object of known mass distribution (the rectangular block presented above) and its action on a coordinate frame attached to its centre of gravity. Using the inverse kinematics model of the hand, the corresponding

contact locations are determined with the corresponding finger Jacobians J_i. Since the Jacobians are position dependent, the four fingers Jacobian with the corresponding rotating at the fingertip to accommodate the object surface have been computed.

Using the previous equations for calculating the fingertip forces which involve the use of the Π and B matrices and applying the optimization algorithm yields the corresponding null space solution to be added to the force calculated using the pseudo inversion of G. Thus the initial fingertip forces vector for grasping this rectangular block is given by:

Internal Forces	λ^T = [7.5, -2.9, -8.5, 6, 1 , -1.9]
Pseudo Inverse solution	$f_{pa}{}^T$ = [4.9, 0, -20.2, -14.9, 0, -152, 49.8, 0, 102, 49.8,0,52]
Internal Forces Vector	$f_{ho}{}^T$ = [- 9.5, 0, -5.27, 6.3,0,1.5, -0.49, 0,10.2, 3.66, 0,-6.5]
Fingertips Force Vector	$f_{tip}{}^T$ = [- 32, 5,- 195, -38, 0, - 110, 70,- 9,-190, 4,4, - 11]

It is clear if this force vector is back substituted in the grip transform, it will produce an opposing resultant object force that overcomes the gravitational effect on the object mass.

Geometric Constraints :

The first issue of analysing the results is the geometric constraints which have to be satisfied at each point of contact. For the designed grasping problem and from the object geometry, the four inward normals are expressed as :

Unit inward normal at first fingertip is	e^T_{n1}	[0 , 0 , -1]
second fingertip is	e^T_{n2}	[0 , 0 , 1]
third fingertip is	e^T_{n3}	[0 , 0 , -1]
fourth fingertip is	e^T_{n4}	[0 , 0 , -1]

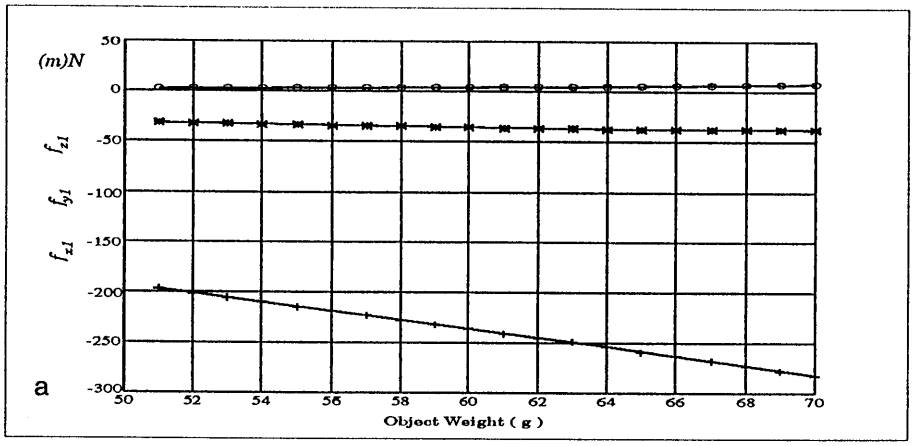
The dot product of the normal magnitude of the four fingertips forces by the inward normal gives forces which satisfy the geometric constraints given by Eq. 5.12.

Generated Fingertips Forces :

For further investigation of the used internal forces technique of calculating the fingertip force, the object weight has been changed linearly from [0.05 *Kg* to 0.07 *Kg*] which will result in an increase in the fingertips forces.

Fig [5.9] and Fig [5.10] show the corresponding four finger forces expressed within the frame attached to the points of contact to grasp the object. For instance, Fig [5.9-a] is the first fingertip forces where the f_1^z force component has a force magnitude which is greater in value than the resultant tangential forces, f_1^x and f_1^y. Furthermore, the optimizing mechanism has produced the solution for changes in m_o which also satisfy the geometric and friction constraints which exist at the point of contact.

Fig [5.9-b] also shows the second fingertip forces, in a similar way, the normal force component f_{2z} has a value greater than the two tangential forces and of direction similar to the f_{1z}, due to the orientation of the contact frame at the second point of contact. In the defined contact frame for the second finger, the f_z component is pointing upwards



*: x Force Component,
o : y Force Component,
+ : z Force Component.

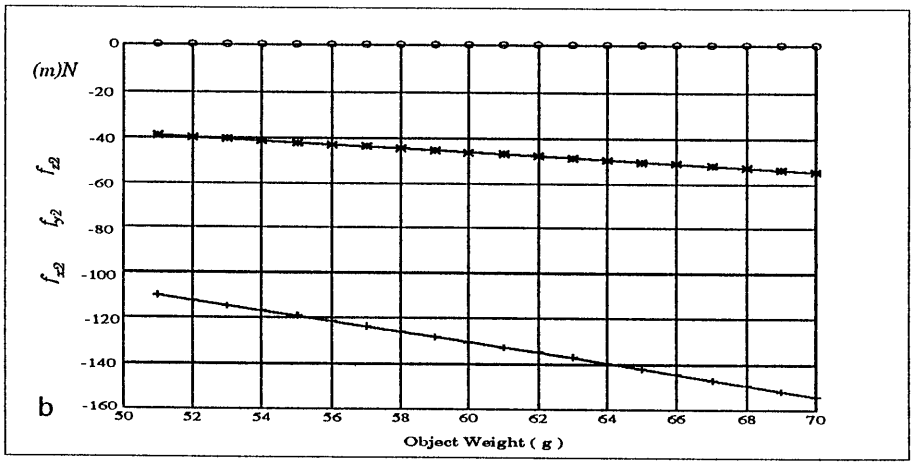
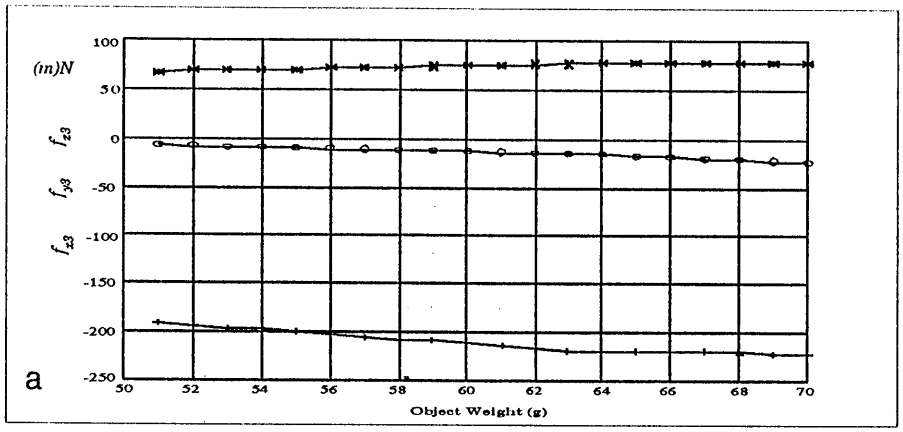


Figure 5.9 : a : The Contact Forces at First Finger Contact Frame Using Internal Forces Optimization.
b : The Second Finger Forces.



*: x Force Component,
o: y Force Component,
+: z Force Component.

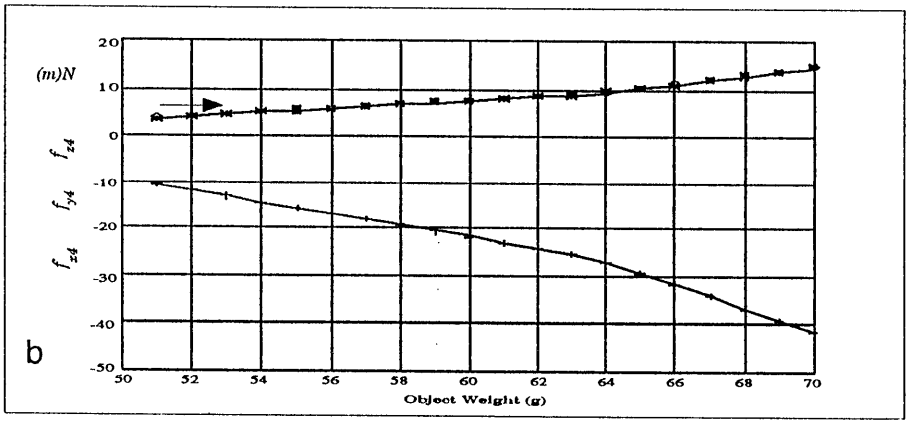


Figure 5.10 : a : Third Finger Contact Forces Using Internal Forces Optimization.
b : The Fourth Finger Forces.

——►> : f_{y4} closely corresponds to f_{x4} in plot-b .

and remains fixed even if the hand orientation is changed by wrist action.

The third finger contact forces are shown in Fig [5.10-a], due to the kinematic position and orientation of the third finger the contact forces have similar directions to the first finger. Finally, Fig [5.10-b] shows the contact forces at the fourth finger. The fourth finger contact frame is oriented with given angles due to its kinematic orientation with respect to the hand palm, as has been discussed in Chapter Three. With this contact frame orientation the normal force f_{4z} satisfies both the geometric and directional constraints.

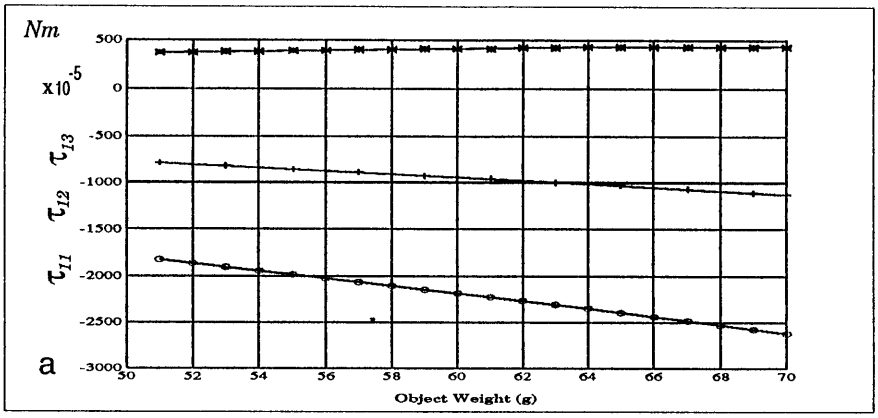
Generated Joint Torques :

Having considered the calculation of the fingertip forces, using Eq. 5.26 the fingertip forces are transformed to the corresponding joint torque .

The generated joint torques by the hand control mechanism is that which compensates for the finger dynamics (as given in APPENDIX [A5]) in addition to the objects weight. The generated torque by the actuators is calculated to be within the physical bounds of the actuators. The employment of the optimization technique will result in the minimum effort or minimum force to grasp the object. The effort of grasping can be increased by pre-multiplying the null space vector of the grasp transform by a constant K which results in increasing the internal forces f_{12}, f_{13}, f_{14}, f_{23}, f_{24}, and f_{34} acting on the object. The minimum effort to grasp the object is also important when the manipulation mechanism consists of a multi-arm system to grasp a single object.

Fig [5.11] shows the first and second fingers of the hand corresponding to the generated fingertip forces. The value of the generated torques have been bounded within the maximum torques generated by the actuators in the hand which is $0.12\,Nm$.

A similar approach, Fig [5.12] shows the corresponding third and fourth finger's generated



* : Proximal Joint Torque,
o : Medial Joint Torque,
\+ : Distal Joint Torque.

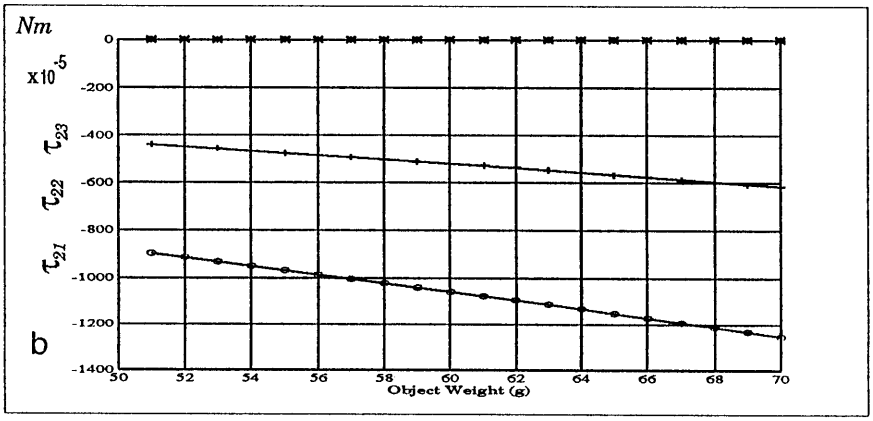


Figure 5.11 : a : First Finger Computed Torques.
b : Second Finger Computed Torques.

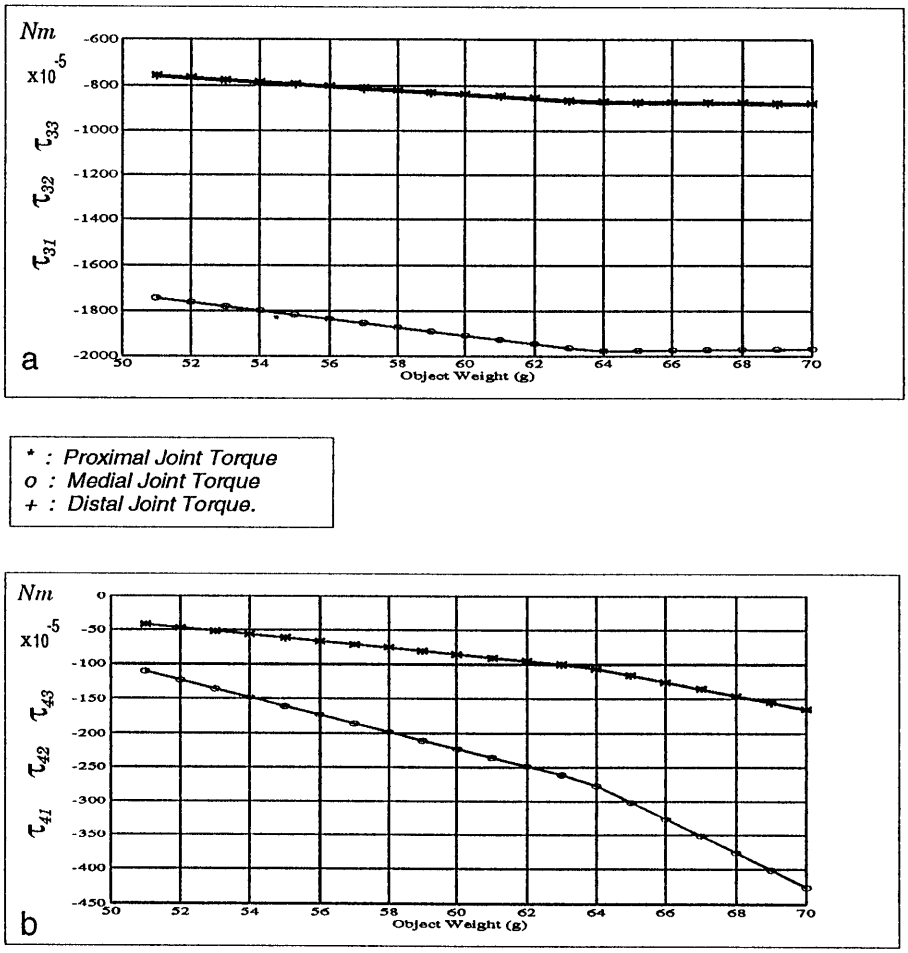


Figure 5. 12 : a : Computed Torques of the Third Finger.
b : Computed Torques of the Fourth Finger
(Using Internal Forces Optimization).

torques for producing the normal forces f_{3z} and f_{4z} respectively.

Fig [5.13-a] shows the corresponding magnitude of the internal forces vectors which are used to adjust the null space force vector of the grip transform. These internal forces have been the objective function of optimization procedure, unlike the case of nonlinear constraints. Although the magnitudes change as the object weight changes, the total force of the grasped object is a force that counteracts the disturbance force of gravity. The increase of the fingertip forces will certainly increase the objective function itself as shown in Fig [5.13-b] , since fingertip forces are related to the null space force vector magnitude.

Fig [5.14-a] shows the corresponding generated force by the fingertips. Since the objective function was to grasp the object in a static equilibrium , the resultant force is opposite to the force vector due to the gravity effect on the object. The sum of $\boldsymbol{F}_b$ and $\boldsymbol{G}\boldsymbol{f}_{tip}$ for static grasping is shown in Fig [5.14-b], where $\boldsymbol{F}_b - \boldsymbol{G}\boldsymbol{f}_{tip} \cong 0$.

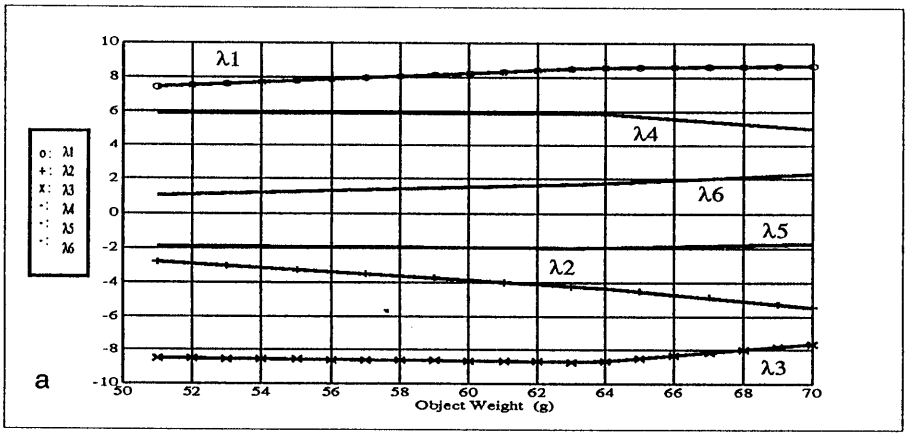
Second : Nonlinear Inequality Constraint Optimization Case :

Here we shall apply the same study case of fingertip forces computation, however, the technique used will be the computation using the nonlinear constraints optimization instead of optimizing the internal forces. The corresponding initial fingertips forces are :

$$\boldsymbol{f}^T_{tip} = [\ 8, 0, -225\ ,\ -18,\ 0,\ -170\ ,\ -5, 0,\ -113,\ \ 5,\ 0,\ -58\ ]$$

Geometric Constraints :

These are the same as for the linear constraints case, except that the second fingertip frame is pointing in the opposite direction to that of the internal forces method.



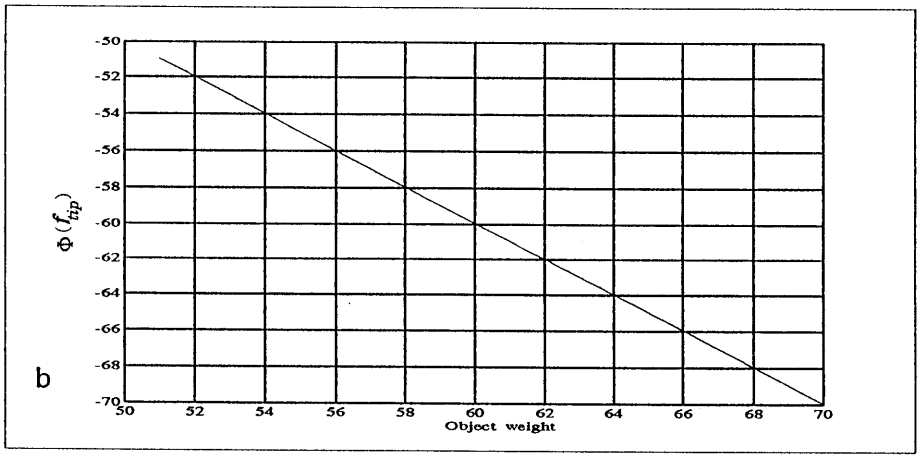
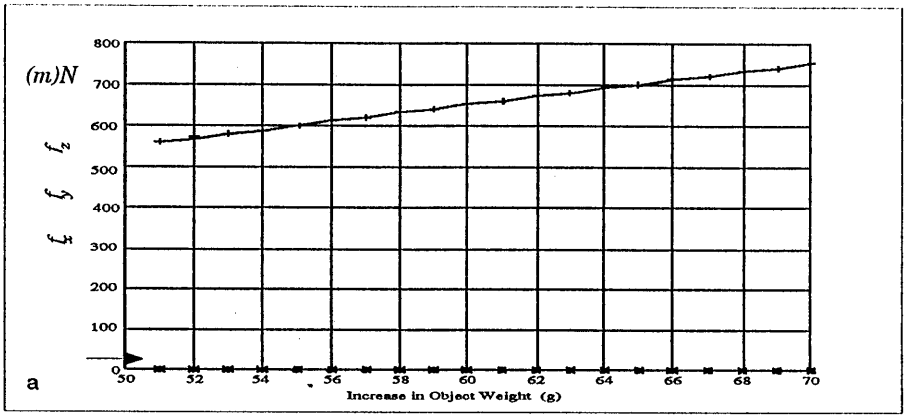


Figure 5.13 : a : Grasp Internal Forces Magnitudes.
b : Objective Function of Optimization.





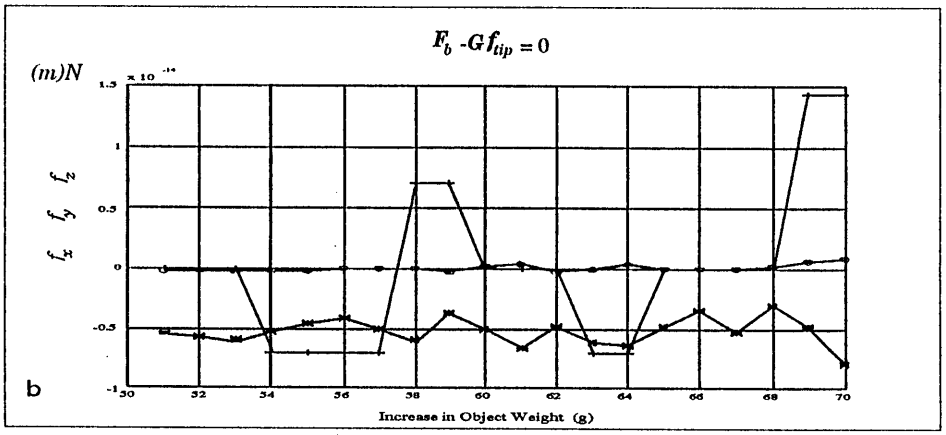


Figure 5.14 : a : The object Resultant Force Due to Joints Torques.
b : The Hand-Object Force in Equilibrium State.

——►>: f_y closely corresponds to f_x in plot-a.

Generated Fingertips Forces :

Fig [5.15] and Fig [5.16] show the corresponding results of applying the nonlinear constraints optimization of contact forces given by Eq. 5.62. For instance, Fig [5.15-a] represents the first fingertip forces at the points of contact for the same change in the weight of the grasped object from (0.05 to 0.07 *kg*). For this increase in the object acting resultant force , the corresponding fingertips forces also increase. Fig [5.15-b] is the second fingertip forces, the normal force f_{2z} is in the negative direction of the chosen frame at the second fingertip.

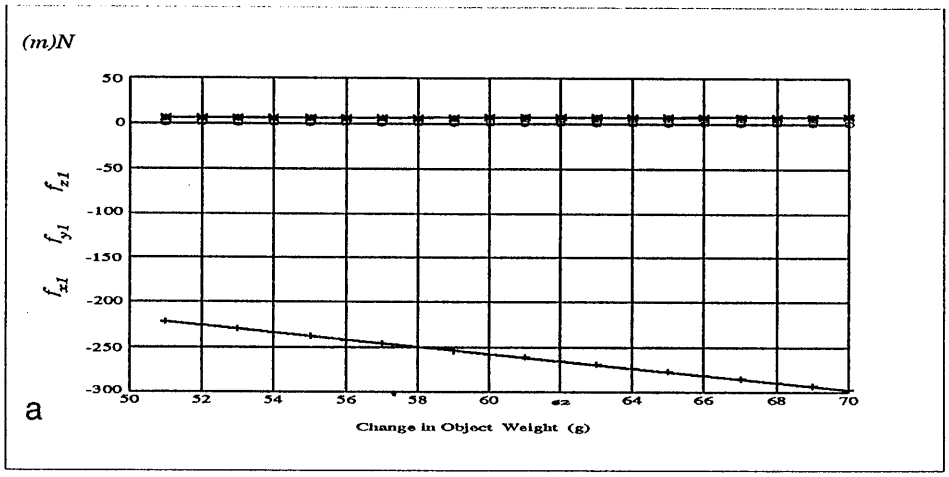
Fig [5.16] shows the corresponding fingertip forces for the third and fourth fingers in general. Combining these twelve forces will result in an object resultant force opposing in direction the force due to the object weight. From the shown curves, it is obvious that the normal force at each *ith* point of contact has a higher value than the two frictional forces which are determined by the frictional material.

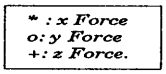
With respect to the geometric constraints at the four points of contact, the geometric constraints have been shown by the fact that the normal forces are in directions that coincide with the frame and correspond to the point of contact.

Generated Joints Torques :

The use of nonlinear inequality constraints has also ensured the generated torques to be within the maximum torques produced by the actuators and transformed to contact forces by the pressing action of the fingertips. For instance , Fig [5.17] shows the corresponding increase in the joint's generated torques by the first and second finger only. The corresponding generated torques for the third and fourth fingers are given in Fig [5.18]. The generated torques are within the bounds of the maximum torques the hand actuators can produce.

Back substituting these generated forces will generate an overall object resultant force that





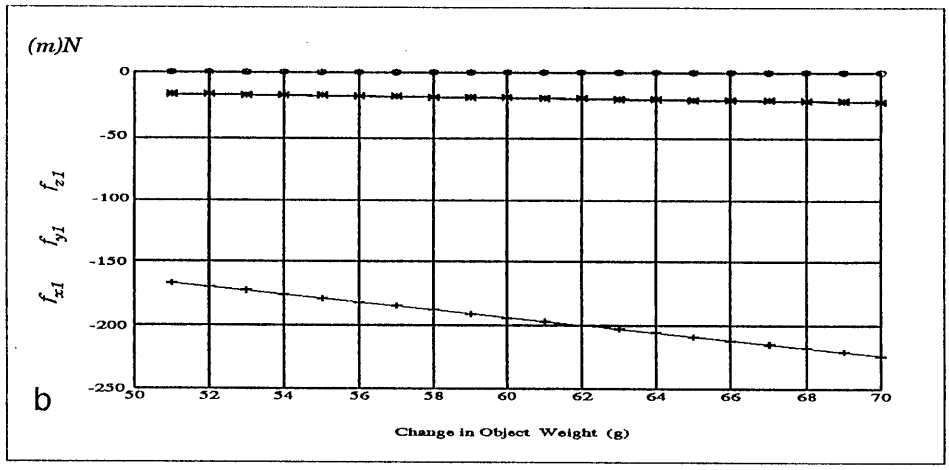
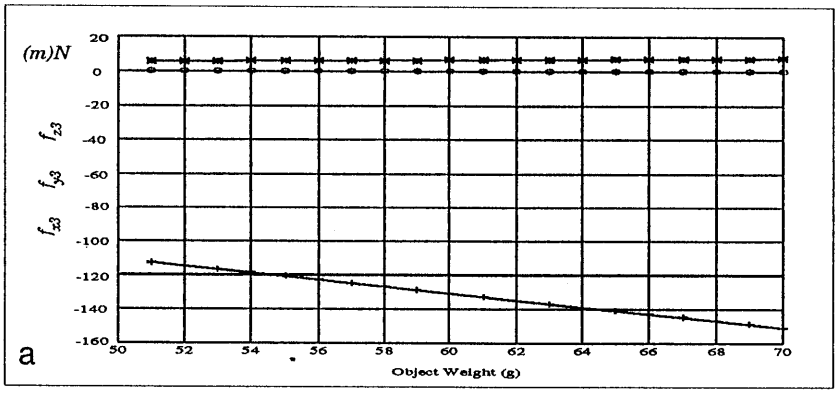


Figure 5.15 : a : First Finger Contact Forces Using Nonlinear Constraints Optimization.
b : Second Finger.



* : x Force Component,
o : y Force Component,
+ : z Force Component.

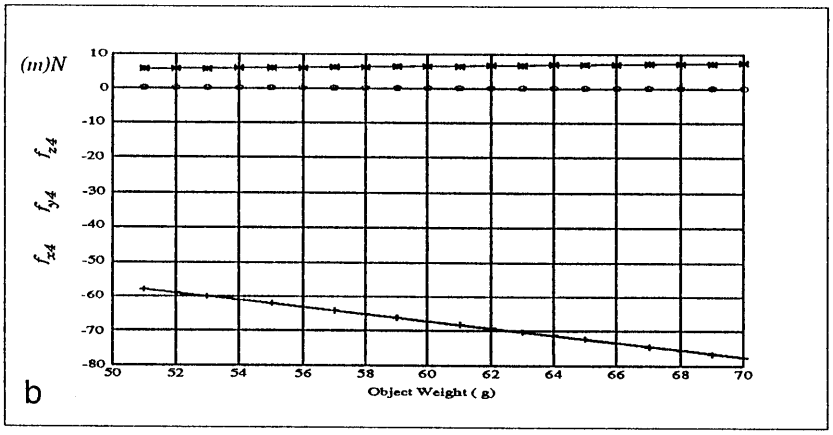
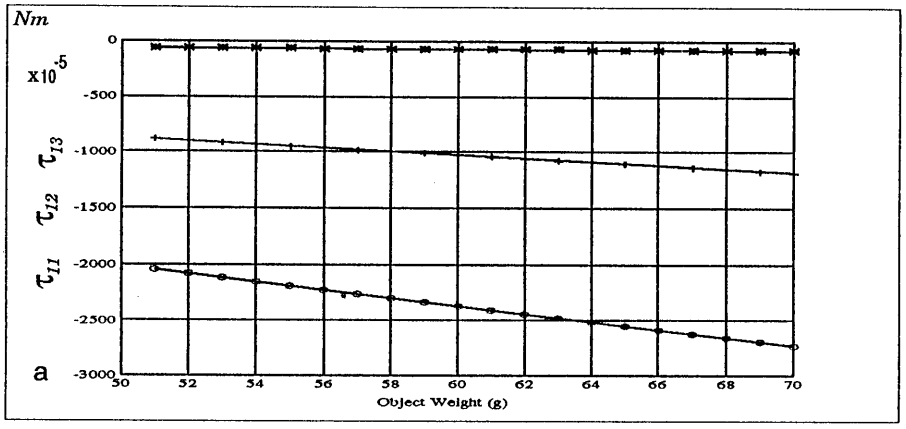


Figure 5.16 : a : Third Finger Contact Forces Using Nonlinear Constraints Optimization.
b : Fourth Finger.



* : Proximal Joint
o : Medial Joint
\+ : Distal Joint.

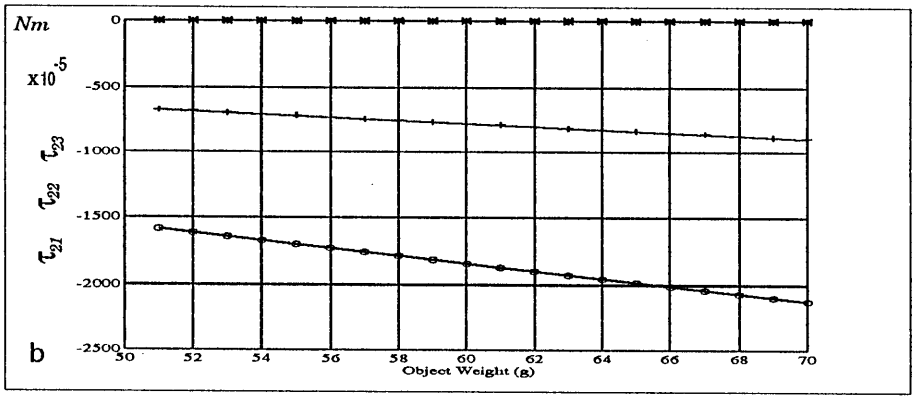


Figure 5.17 : a : Computed Torques by First Finger Using Nonlinear Constraints Optimization.
b : Torques of Second Finger.

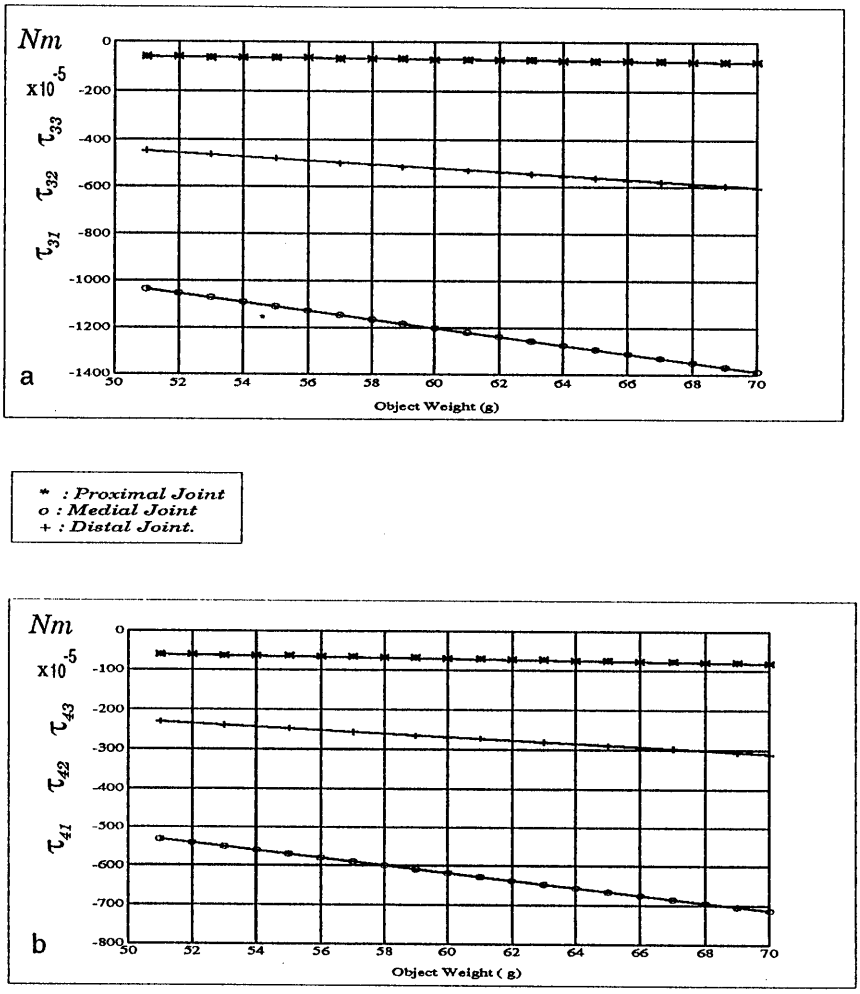


Figure 5.18 : a : Third Finger Computed Torques Using Nonlinear Constraints Optimization.
b : Fourth Finger.

compensates for the object weight using $F_b = GJ_h^{-1}\tau_a$ since the hand is not in singular configuration.

Fig [5.19-a] shows the objective function of optimization. Unlike the internal forces optimization, the objective function is higher in this case due to the fact that the sum square of contact forces are optimized rather than the internal forces.

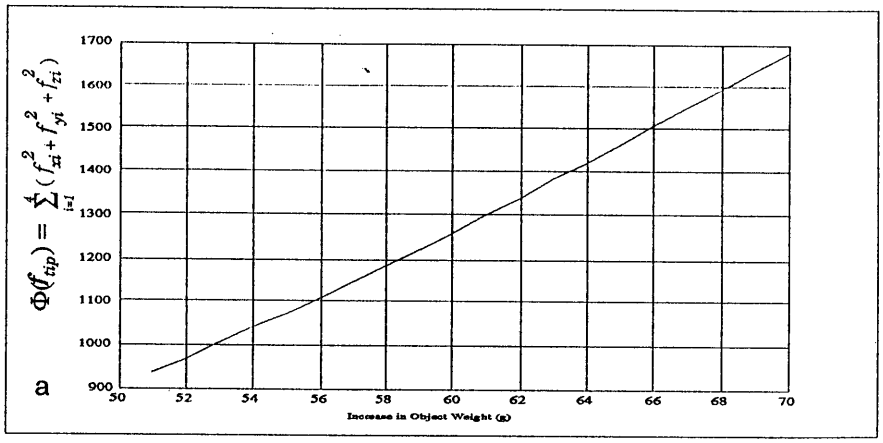
Fig [5.19-b] shows the corresponding resultant force vector due to the generated hand forces. It is the force vector that opposes the object dynamics that we would like to overcome. Fig [5.19-c] shows the corresponding resultant force-object vector which must be zero to achieve a static equilibrium.

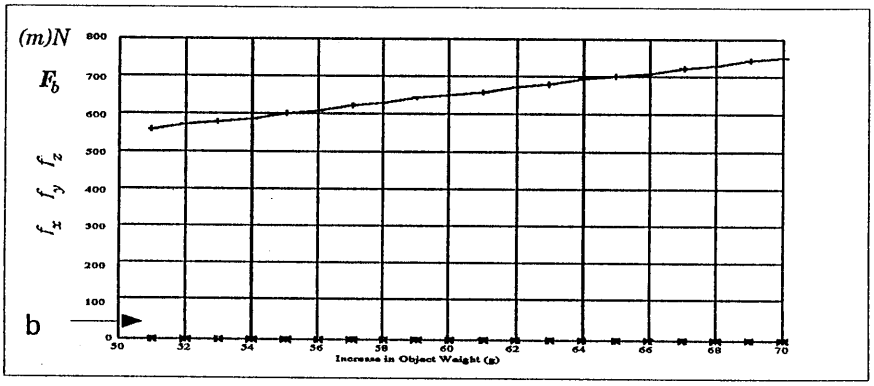
SUMMARY

Chapter Five has investigated in detail the concept of grasping and considered the basic requirements for object manipulation. The chapter started with grasping theory and the formulation of the grip transform from the defined type of contact. The grip transform is an important matrix in describing the nature of object displacement in multiple contact system.

The formulation of the grip transform has been used later in the chapter for developing two numerical techniques based on optimization for the calculation of the fingertip forces to keep the grasped object stable. The first techniques was the internal forces optimization for an approximated model of the four contacts, whereas the second was the employment of nonlinear constraints optimization.

Both techniques have proven their convergence to optimal solutions. From the number of constraints point of view, the nonlinear constraints have been shown to be fewer compared to the internal forces approach.





*: Fx Object Force
o: Fy Object Force
+: Fz Object Force

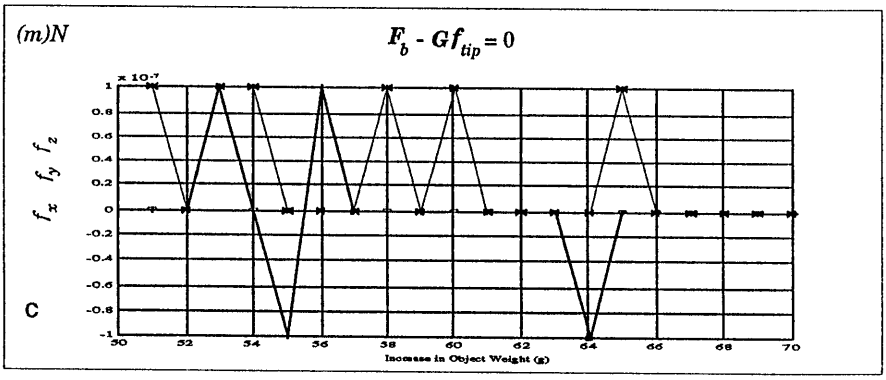


Figure 5.19 : a : Objective Function of Optimization.
b : Object Resultant Force Due to Fingertips Forces.
c : The Hand-Object Resultant Force Vector.

——►>: f_y closely corresponds to f_x in plot-b and c.

CHAPTER SIX

COORDINATED CONTROL and OPTIMIZATION of FINGERS DYNAMIC MANIPULATION FORCES

(6.1) INTRODUCTION

Chapter Four considered one class of robot hand control, basically the kinematic-based control, within which dynamic high speed terms of manipulation are not involved. However, operating a robot hand at a considerable speed, like shaking chemicals at high speed, will no doubt require dynamic based rather than kinematic based control.

For the case of motion with multiple contacts, application of contact forces must accommodate the resulting inertia forces when the object-fingers system is moving at a considerable rate. Generally, there are numerous potential applications for cooperating fingers motion. The purpose of this Chapter is to concentrate on the motion of all the fingers manipulating a single object, where closed dynamic chains are formed by the fingers and the objects through the hand palm.

Specifically, it is assumed that the fingers and the object are rigid, and that the contacts between them are point contacts with friction, that is, the positions and orientation of the fingertips relative to the object frame remain unchanged as the system configuration evolves. While applying the theory of force distribution and optimization to the object, the contact points are assumed to be fixed, hence it is only the hand kinematics and dynamics which change with progress manipulation in time.

This Chapter has been classified into six main sections. Section (6.2) presents the requirements of hand-object motion. Section (6.3) is concerned with the modelling of the hand-object dynamics for control purposes. Section (6.4) presents the derivation of the hybrid controller structure. The concept of applying a robust inverse of the entire hand Jacobian is further elaborated to avoid an ill condition hand Jacobian (for multiple contact system) is given in section (6.5). Since the concept of manipulation depends entirely on the frictional properties of the object surface and the fingertip geometric constraint, con-

siderable attention will be given to the physical limits of the friction forces. In a similar way two schemes of optimization will be applied as in Chapter Five, to grasp the object during motion, these are given in section (6.7). The first is the internal force, and the second is the use of nonlinear constraints optimization. Finally section (6.7) compares the two approaches of optimization.

(6.2) HAND-OBJECT MOTION

Basic Formulations for Coordinated Manipulation of an object :

Manipulation has been defined as how to impart force and position trajectories on grasped objects in any position or orientation, MICHELMAN and ALLEN [1993]. Furthermore, in dynamic coordinated manipulation of a single object using a multifingered robot hand, simultaneous position and force control of the fingers on the object are required as a condition for the dynamic stability of the object.

The basic formulation for the coordinated control of an object motion will be discussed within this sub-section. Coordinated manipulation with a four fingered robot hand is the computing of joint torques to produce motion. The interaction between each fingertip and the object will be restricted as before to frictional point type of contact. The vital assumption is that the contact point does not slip on the object as the object undergoes a motion.

Consideration of the manipulation of objects, where the interaction between the object and the fingers is a rolling contact, is an important issue when the object is manipulated at high speed. Basically, manipulation is considered as finding the appropriate joint torques in such a way that the object does not stray to slipping and forces do not crush the object . For moving a grasped object by motion of the links, dynamics of the two systems are significant since, once the object is in contact at the fingertips, the dynamic of object

will affect the dynamic of fingers and vice versa. Therefore, the joint torques are required not only to move the finger links, but extra torques are needed to account for the interaction of the object at the fingertips. This will be formulated analytically in section (6.3).

(6.3) OBJECT-HAND DYNAMICS

6.3.1) Cooperative Control for Robot Hands

So far in Chapter Four we developed a linear control law intending that a combined controller be used for each joint in the hand. While the damping of each control loop varied with the hand configuration, the joint perfomance was basically stable.

That type of control was based on the assumption that the coupling torque between the joints was small enough to be ignored. As a requirement for much more precise manipulation tasks, especially when the hand dynamics are large with respect to the object dynamics, more sophisticated controllers will be required. The dynamics terms of robot hands tend to dominate the overall motion and this must be compensated for.

The use of the advanced control approach based on the dynamic model of the hand-object system assumes the knowledge of the dynamic model when designing the controller. However, there are two main problems associated with such an approach. The first is concerned with real time computation for the four fingers which requires the use of high speed computational power. This problem can be solved by using a parallel computational system and making a few assumptions regarding the similarity in the kinematic and dynamic models of the fingers. This will be further discussed in Chapter Seven.

The second problem is concerned with certain terms which are not easily estimated such as the static and dynamic friction, which can have a great effect on the control of the hand. There are three basic approaches to having much improved control laws for hand

control, especially when dealing with constrained dynamics motion. These approaches are: the nonlinear cancelling, adaptive control as achieved by SWIFT *et al.* [1993], and the model-based control schemes. All three approaches make use of the dynamic models, but the third requires accurate models. For the first approach, the nonlinear cancelling methods increase the complexity of the control laws of the independent - joint controllers to compensate for dynamics and to account for non-linearities. Effectively, these methods cancel out the nonlinear terms given in Appendix [A5] that characterize the dynamics so that the resulting behaviour resembles that of a linear system.

Generally, advanced control of robots could be classified as either (Computed torque like), or (*Non-computed torque like*), where the computed torque would include robust control, adaptive control, learning control and so on, LEWIS *et al.* [1993].

However, before attempting to calculate the required torques for the designed hand computed torque cancelling controller, let us look at the other side of the problem , which is that we are dealing with constrained motion rather than free motion of the fingers. In constrained motion, the dynamics of one finger will affect the dynamics of the other fingers through the grasped object itself.

The hand-object system consists of a constrained mechanical system whose dynamical description can be derived using Lagrange's equations together with the constrained equations. Consider first the dynamics of the hand and the object separately:
For the hand:

$$(d/(\partial \dot{L}_h/\partial\theta)dt) - \partial L_h/\partial\theta)^T = \boldsymbol{M}_h\ddot{\Theta} + \boldsymbol{N}_h\dot{\Theta} + \boldsymbol{C}_h = \tau_a \qquad (6.1)$$

and for the object :

$$(d/(\partial \dot{L}_o/\partial u)dt) - \partial L_o/\partial u)^T = \boldsymbol{M}_o\ddot{u} + \boldsymbol{N}_o\dot{u} + \boldsymbol{C}_o = \boldsymbol{F}_b \qquad (6.2)$$

where L_h and L_o are the hand and object Lagrangians, respectively. M_i are the corresponding inertia matrices, N_i are the velocity-dependent forces, and C_i terms are the gravity and frictional forces. The object and hand Lagrangians are then linked together through constraints that represent the kinematics of the two bodies. From the force domain analysis the two dynamical equations are linked by:

$$(d/(\partial \dot{L}_h/\partial\Theta)dt) - \partial L_h/\partial\Theta)^T = J_h^T G^{-1}[(d/(\partial \dot{L}_o/\partial u)dt) - \partial L_o/\partial u)^T]$$

$$M_h\ddot{\Theta}_h + N_h\dot{\Theta}_h + C_h - J_h^T G^{-1}[M_o\ddot{u} + N_o\dot{u} + C_o] = \tau_h \qquad (6.3)$$

These vectorial differential equations are linked by some constraints which make these equations more manageable for control design and analysis, AL-GALLAF and WARWICK [1994-b]. This linkage is represented, as will be shown later, by velocity constraints, the direction of motion and forces normal. The velocity constraint can be stated analytically as :

$$\dot{J}_h\dot{\Theta}_h - G^T \begin{bmatrix} \upsilon_o \\ \\ \omega_o \end{bmatrix} = 0 \qquad (6.4)$$

Eq. 6.4 represents constraint in terms of the hand-object which has to be satisfied while manipulating an object. This constraint can physically be interpreted as : the fingertip velocities must equal the velocities at each point of contact with the object expressed in the contact coordinates.

The forces normal constraints can be stated as : the forces applied by the fingertips in the object surface normal will produce a resultant force on the object, as long as fingertip forces are expressed in the contact coordinates.

The hand object equation of mechanics , Eq. 6.3, can be simplified under the assumption that hand Jacobian J_h full row rank, allows explicitly to separate the two dynamics in terms of the independent variable u. Of great importance is the dynamic model of the hand which comprises the dynamic model of the four fingers. Appendix [A5] gives the derivation of the dynamic model of one finger based on the Lagrange equation of motion. This has been achieved using MATHEMATICA Package :

The dynamics of the *ith* finger in the hand can be written in the usual form including the frictional torques and the actuators torque :

$$M_i\ddot{\Theta}_i + N_i\dot{\Theta}_i + C_i + V\dot{\Theta}_i + K_i = \tau_{ai} - J_i^T f_{tipi} \qquad \Re^{[3\times 1]} \tag{6.5}$$

Here, as is common in the literature, $M_i \in \Re^{[3\times 1]}$ is the moment of inertia matrix of the *ith* finger ; $N_i \in \Re^{[3\times 1]}$ are the centrifugal and coriolis force terms, V_i is the vector of joints frictional modelling, and C_i is the gravitational force terms; τ_i is joint torque inputs and $J_i^T f_{tipi}$ is the vector of applied finger wrenches by the *ith* finger (due to the force $J^T{}_i f_{tipi}$ that the object is applying to the fingertip). K_i is a block diagonal matrix of the elastic constant of the joints-links transmission mechanism.

To simplify the use of symbols, the V vector will be considered as a part of N_i and the K_i as a part of C_i in Eq. 6.5.

Extra Dynamics :

Another important fact about robot hands is the extra dynamics due to the possible attachment of the hand to robot arms. Hence the orientation and position of the wrist has an effect in the hand dynamics (gravity effect), therefore an assumption has to be made while driving the hand dynamics.

The fact that the hand is assumed to be located with a given orientation horizontally means, the gravity effect will act on the links. The amount of torque required by the corresponding joints is totally dependent on the maximum acceleration, velocity and the corresponding finger links parameters (in particular the links masses m_1, m_2, m_3, and moment of inertia).

When a robot hand is positionally oriented in the three dimentional space, the fingers dynamics can be grouped together which results in what is referred to as the hand dynamics. The hand dynamics could be considered as a system where the inputs are the corresponding joints motion parameters and the corresponding outputs are the motion aspects of the four fingertips and the displacement of the grasped object. For non dynamic coupling hands, the resulting fingertips motion will be independent of each other. However, coupling among fingertips will appear once the hand is in the grasping mode of an object. This will be further discussed in the next section.

6.3.2) Group Dynamic of the Hand and Coupling Effects

The equation of motion for the hand-object system will be derived in this section. First, suppose that the joint driving torque is applied to the fingers while holding the object, and forces are exerted by the fingertips on the object surface at points of contacts. The joint driving torque that contributes to the object motion is represented by $\tau_c - J^T f_{tip}$.

Eq. 6.5 was the discrete dynamic model of the fingers separately, however, for describing the hand-object dynamics system, we need to concatenate the dynamics of the four fingers altogether, and work out the required torque to displace an object in the hand's working environment. Of great importance in the hand dynamics is the hand Jacobian matrix J_h which has to be calculated, since it relates the required joint torques τ_h to the required fingertip forces f_{tip} by :

Defining :

$$\Theta^T_h = [\,\Theta_1 \quad \Theta_2 \quad \Theta_3 \quad \Theta_4\,]$$

$$M_h = diag\,[\,M_1 \quad M_2 \quad M_3 \quad M_4\,] \qquad N^T_h = [\,N_1 \quad N_2 \quad N_3 \quad N_4\,]$$

$$C^T_h = [\,C_1 \quad C_2 \quad C_3 \quad C_4\,] \qquad \tau^T_h = [\,\tau_1 \quad \tau_2 \quad \tau_3 \quad \tau_4\,] \qquad (6.6)$$

J_h in the force domain is described at each point of contact with respect to the coordinate frame located at the hand palm frame in such a way that orthagonal axes coincide with the axes at the point of contact, where each finger J_i is expressed with respect to the finger roots. The dynamic equation of a four fingered robot hand is obtained by aggregating the four dynamics equations of the four fingers. Then, the overall hand dynamics can be grouped to yield, ZUOFENG *et al.* [1991] :

$$M_h \ddot{\Theta}_h + N_h \dot{\Theta}_h + C_h + V_h + K_i = \tau_h - J_h f^T_{tip} \qquad (6.7)$$

Physically Eq. 6.7 represents a torque vector of $\in \Re^{12}$ in the entire hand which is to be computed using the inverse dynamics of the hand. The torque vector will thus accommodate the dynamical motion parameters in addition to the forces acting at the fingertips of the hand due to the dynamics of the object.

As described in section (6.2.3), the main control objective is to manoeuvre the grasped object to track a given trajectory by specifying a set of joint torque inputs τ. There are also secondary objectives:

(*i*) The load distribution,

(*ii*) Force control computation so that the entire solution satisfies the frictional constraints, the geometric constraints of the object shape, and the physical limits of the hand actuation already presented in Chapter Five.

(6.4) OBJECT MOTION with CONTACT FORCES.

6.4.1) Equation of Motion for Hand-Object System

Computed-Torque Control :

Eq. 6.7 represents a highly coupled nonlinear system control, which is the entire hand. In the computed torque technique the effect of the dynamics nonlinearities are computed using the inverse dynamics model and are feed-forward joint control, as a varying voltage to the normal joints closed loop system. Hence the achievement of dynamic decoupling of the joints, MCKERROW [1991].

Meanwhile, by moving the inverse dynamic model into the main control loop, the control scheme needs to be fed with the joint positions, velocities , and acceleration of the joints.

Having considered the requirements for controlling the fingers based on their dynamical models, then the technique followed here is to cancel the nonlinear terms by computing the terms which are of time varying nature. Computed torque is one branch of multi-degrees of freedom control, which is the counterpart of the noncomputed-torque-link which appears in robust control, adaptive control, learning control, and so on.

Coordinated Dynamic Controller (Combined Torques)

A hand joint is required to generate two torques, one is responsible for the hand fingers links motion, and the other for grasping and generating a resultant force on the object under consideration. This combined torque is represented mathematically by, YOSHIKAWA and ZHENG [1993] :

$$\tau_h = \tau_{obj} + \tau_{hand}$$

The combining of two torques under two decoupled servos, the force servo and the position servo, has been called hybrid dynamic control by NAKAMURA [1991]. Generally speaking, the control system needs a feedback loop for each position control and force control.

In hybrid position-force control, the position control and the force control are decoupled in nature, and therefore their closed loops are designed independently. However, in this hybrid position and force control problem, they are coupled, and their dependence must be considered. For the practical implementation of joint torques control in manipulation of an object, further study of the synthesis of feedback control system must be undertaken.

Later in this chapter, aspects of the controller structure will be shown, which are based on the forces optimization as computing mechanism and not as a force feedback system. To maintain contact during manipulation the finger joint velocity and the object velocity $[\upsilon_o\ ;\ \omega_o]^T$ must fulfil the following velocity constraint :

$$\dot{\Theta}_h = J_h^{-1} G^T \begin{bmatrix} \upsilon_o \\ \omega_o \end{bmatrix} \tag{6.8}$$

Constrained Acceleration :

Eq. 6.8 suggests that the joint space trajectory of the hand obtained from the object space rate trajectory provided by the entire hand Jacobian is not singular. Having found the position and velocity of the joints, the last term is the joints acceleration $\ddot{\Theta}_h$.
The acceleration constraint is obtained by differentiating Eq. 6.8, this results in :

$$J_h\ddot{\Theta}_h + \dot{J}_h\dot{\Theta}_h = \dot{G}^T[\upsilon_o\ ;\omega_o]^T + G[\dot{\upsilon}_o\ ;\ \dot{\omega}_o]^T \tag{6.9}$$

In the case where the hand Jacobian is a non-singular matrix, it can also be expressed $\ddot{\Theta}_h$ as:

$$\ddot{\Theta}_h = \boldsymbol{J}_h^{-1}\boldsymbol{G}^T[\dot{\upsilon}_o\ ;\ \dot{\omega}_o]^T - \boldsymbol{J}_h^{-1}\dot{\boldsymbol{J}}_h\dot{\Theta}_h + \boldsymbol{J}_h^{-1}\dot{\boldsymbol{G}}[\upsilon_o\ ;\ \omega_o]^T \tag{6.10}$$

However, due to the fact that the fingertips do not slide (non sliding or rolling contact) over the surface of the grasped object, the Grasp transform parameters remain constant over the manipulation time and $\dot{\boldsymbol{G}}(t) = \boldsymbol{0}$. When the fingertips roll on the object, the control law will require an extra term that depends on the contact parameter to be included which involves the kinematic equations of contact as has been described by MONTANANA [1986].

Once the fingertips roll on the object, the right first term of Eq. 6.9 will not be zero and rolling analysis has to be included. From this assumption Eq. 6.10 can be simplified and rewritten as :

$$\ddot{\Theta}_h = \boldsymbol{J}_h^{-1}\boldsymbol{G}^T[\dot{\upsilon}_o\ ;\ \dot{\omega}_o]^T - \boldsymbol{J}_h^{-1}\dot{\boldsymbol{J}}_h\dot{\Theta}_h \quad \in \Re^{[12\times 1]} \tag{6.11}$$

Eq. 6.11 is interpreted as ; joint space acceleration of the mechanical hand expressed in rad/s^2 consists of points of contact acceleration transformed to joints by $\boldsymbol{J}_h^{-1}$.

$\boldsymbol{f}_{tip}$ for dynamic motion is given by, RAMADORAI *et al.* [1992]:

$$\boldsymbol{f}_{tip}(t) = \boldsymbol{G}^{+}\boldsymbol{F}_b(t) + \boldsymbol{f}_{hA}(t) \tag{6.12}$$

Due to the non-sysmetic structure of the grip transform, there is a redundancy in obtaining the fingertip forces to result in the desired object dynamics $\boldsymbol{F}_b(t)$. Furthermore, due to the use of the generalized inverse of $\boldsymbol{G}^{+}$, there is associated with it a vector which will not produce a force in the grasped object, and known as before the internal forces. Substituting back the value of $\ddot{\Theta}_h$ in Eq. 6.7 gives the following computed torque equ-

ation for manipulating a grasped object and moving the hand links together in the presence of internal forces, WALKER *et al.* [1991]:

$$\tau_h = J_h^T G^+ \begin{bmatrix} -m_o g \\ \omega_o \times I_o \omega_o \end{bmatrix} + J_h^T G^+ \begin{bmatrix} m_o E & 0 \\ 0 & I_o \end{bmatrix} \begin{bmatrix} \dot{v}_o \\ \dot{\omega}_o \end{bmatrix} + J_h^T \eta\lambda +$$

$$N_h + C_h + M_h [J_h^{-1} G^+ - \begin{bmatrix} \dot{v}_o \\ \dot{\omega}_o \end{bmatrix} J_h^{-1} \dot{J}_h \dot{\Theta}_h]$$

$$\tau_h = \tau_{obj} + \tau_{hand} \quad \in \Re^{[12 \times 1]} \tag{6.13}$$

This can be interpreted as the joint torques and consists of two components in accordance with Eq. 6.7. The first is a torque vector to grasp and manipulate the object, whereas the second is to move the hand links satisfying the motion constraint.

Regardless of how the fingertips are to be computed in Eq. 6.13, there exist optimization techniques, as in Chapter Five, for solving such redundant force problems during motion. One aspect of this optimization will be to find the minimum joint torque (based on internal forces optimization) for an object motion, hence the problem is reduced to the computation of the λ vector of Eq. 6.13.

To cope with modelling errors and disturbances that are inevitable in real applications, a control law has to be defined where a PID servo compensation is used. The control law is selected in such a way to keep the tracking error to a minimum. Then the overall

hand-object input torques become :

$$\tau_h = M_h J_h^{-1} [G^T \ddot{\Theta}_a - \dot{J}_h \dot{\Theta}] + N_h + C_h +$$

$$J_h^T G^+ \begin{bmatrix} m_o E & 0 \\ 0 & I_o \end{bmatrix} \begin{bmatrix} \dot{v}_o \\ \dot{\omega}_o \end{bmatrix} + J_h^T G^+ \begin{bmatrix} -m_o g \\ \omega_o \times I_o \omega_o \end{bmatrix} + J_h^T \eta\lambda \qquad (6.14)$$

where $\ddot{\Theta}_a = \left(\begin{bmatrix} \dot{v}_o \\ \dot{\omega}_o \end{bmatrix} + K_v \dot{e} + K_p e + K_i \int e \right) \quad \in \Re^{[12\times 1]}$

While the control law matrices are nondiagonal ones, this would result in a coupled control. Choosing the gain matrices as diagonal will make the closed-loop system keep the decoupled characteristics of the linearized system, TAO and LUH [1992]. Rewriting Eq. 6.14 in its general form with the object dynamics gives :

$$\tau_{hand} = M_h \ddot{\Theta}_c + N_h \dot{\Theta}_h + C_h \qquad (6.15)$$

where $\ddot{\Theta}_c = [J_h^{-1} G^T (\begin{bmatrix} \dot{v}_o \\ \dot{\omega}_o \end{bmatrix} + K_v \dot{e} + K_p e + K_i \int e) - J_h^{-1} \dot{J}_h \dot{\Theta}_h]$

The second is the torque to grasp the object and to define a manipulation force :

$$\tau_{obj} = J_h^T G^+ F_b \qquad \in \Re^{[12\times 1]} \qquad (6.16)$$

where $\ddot{\Theta}_c$ represent the constrained acceleration of the hand-object system. We have ended up with an equation that is composed of two main parts, where each term represents a generated joint torque to the grasped object. In addition, restoring

torques in according to a PID control law, will be generated if the object deviates from the described manipulation path in the three dimensional space.

The use of such control law for a robot hand has a non linearity cancellation term defined by $[N_h + M_h J_h^{-1} (G^T P \dot{X}_o - \dot{J}_h \dot{\Theta}_h) + J_h^T G^+ N_o]$. Also there are proportional, derivative, and integral error feedback terms to give the system decoupled linear error dynamics.

The computed torque for the constrained motion is subject to a number of issues concerning the cartesian defined task. For instance the derived equation for a four fingered hand will certainly pass through singular configuration of some of the fingers (since dealing with cartesian based motion). Furthermore, the object motion will be subjected to the hand working volume limits.

Two methods of choosing the contact forces are to be discussed. The optimization of internal forces using the linearized contact model, and, using the nonlinear constraints optimization. Furthermore, the use of nonlinear constraints to compute the required fingertip forces allows the addition of the internal forces vector. These internal forces are computed based on the decomposition of the entire contact force vector into orthagonal and parallel components.

6.4.2) Additional constraints for a coordinated motion

Main Dynamic and Kinematic Problems :

One problem associated with Eq. 6.14 is that the object defined motion might pass the fingers to a singular configuration, as in Chapter Three. At such configuration the hand Jacobian J_h determinant vanishes to zero and its inverse results in an undetermined solution, and contact forces might not satisfy the constraints. The main constrained equa-

tion of motion given by Eq. 6.14 has two main drawbacks :

(*i*) The first is a kinematic issue represented by the the possible approach of the fingers to a singular configuration due to the inversion of the hand Jacobian J_h, since the object motion is expressed in a cartesin based frame.

(*ii*) The second is dynamic constraint, represented by the fact that contact forces between the object and the grasped object must be preserved over the entire object dynamic motion.

Both issues will be discussed and possible solutions will be explored. Further consideration of the dynamic coordinated motion of the grasped object and the problem of some of the fingers being pushed into the area of singularity, hence the inverse of the hand Jacobian J_h is no longer a valid issue. Since the singular points of the fingers are found not only in the boundary of the workspace, but also in the middle of it, the singular points limit the trajectories that a finger should follow in solving inverse kinematics and inverse hand Jacobian J_h^{-1}. However, the most serious problem of singularity is not at singular points, which have zero volume in the workspace, but rather in the neighbourhood of singular points, which have finite volume.

(6.5) CARTESIAN ROBUST - SINGULARITY INVERSE of HAND JACOBIAN [RSI].

In this section, we introduce the concept of robust-singularity inverse, which is known as the RSI of the hand Jacobian. It is clear from the constrained dynamic acceleration equation of motion defined by Eq. 6.14 that : it is dependent on the evaluation of the inverse hand Jacobian J_h^{-1}. However, due to the fact that the fingertips are to pass

through some locations of singularities as developed in Chapter Three, a method of solution has to be employed for the computation of the hand Jacobian inverse even in the neighbourhood of singular points.

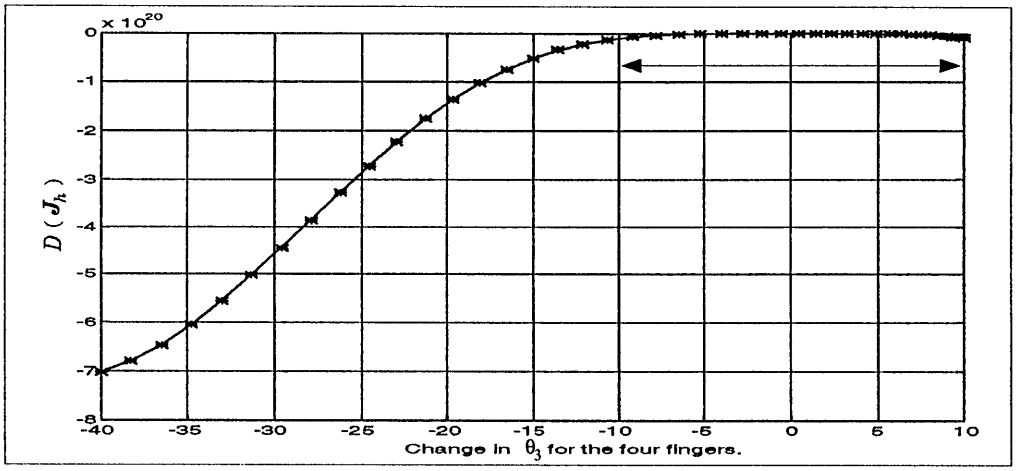
Furthermore, due to the closed kinematic structure of robot hands, the joint velocities used in Eq. 6.8 would be computed from the corresponding object velocity vector. Hence $\dot{\Theta}_h$ would be computed from $\dot{\Theta}_h = \boldsymbol{J}_h^{-1}\, \boldsymbol{G}^T [\, \upsilon_o : \omega_o]^T$ which also involves the use of the inverse hand Jacobian.

In addition, the corresponding forward hand Jacobian, which is a function of the four finger Jacobians, is a function of the joint space vectors that reaches a maximum value or gives multiple solutions at singularity. In summary, the problem of the hand Jacobian getting *ill-conditioned* during an object motion has the effect on the individual parameter acceleration equation represented by Eq. 6.14.

If the inverse within the ill-conditioned case is left unbounded, then using Θ_h in Eq. 6.14 will magnify the corresponding joint space error. The severity of the error can be reduced by having a much more robust inverse for the Jacobian matrix.

In Chapter Three it was shown that a finger will come to singular locations once the fingertip is fully straightened or folded back to the Z axis. Fig [6.1] shows the determinant function of the hand Jacobian for a given manipulation task involving the motion of all the hand joints. The manipulation task consists of moving the hand fingers in a continuous cyclic motion. The hand Jacobian becomes singular during the forward and backward motion as can be seen from the figure.

The determinant function approaches the zero value (indicating that the matrix is close to



Hand Links are Measured in mm in Obtaining this Function.

Figure 6.1 : Determinant Function of the Hand Jacobian with Change in the Distal Joints Position.

singular or at singular) at some defined range. Thus if a technique is employed to give a solution of the hand Jacobian at singular locations, then the manipulation task can be achieved. One approach is to employ the Generalised inverse of $\boldsymbol{J}_h$ using BOULLION function, BOULLION and ODELL [1971]. However, using the generalised inverse of $\boldsymbol{J}_h$ might result in solutions which are not homogenous with the solutions before and after the singular locations boundaries. The other approach is to employ what is known as the Robust Singularity Inverse where singularity robustness is defined as a property of inverse kinematics that allows us to provide continuous and feasible solutions even at or in the neighbourhood of singular points. The details of the RSI are presented in the Appendix [A1], meanwhile, the RSI can be defined as:

$$\boldsymbol{J}_h^R = (\boldsymbol{J}_h^T \boldsymbol{J}_h + \kappa_r \boldsymbol{E})^{-1} \boldsymbol{J}_h^T \tag{6.17}$$

where the κ_r is a scalar which determines the weighting between the exactness and the feasibility, and $\boldsymbol{E}$ is an identity matrix of $\in \Re^{[12 \times 12]}$ dimension.

The choice of the scalar κ_r determines the feasibility of the solution, furthermore the *exactness* and *feasibility* of solutions are contradictory requirements. The value of κ_r can be changed adaptively depending on the configuration of the hand itself, such that κ_r takes larger values in the neighbourhood of singular points and small values or zero outside the neighbourhood of singularity.

The manipulability measure already introduced in Chapter Three can be used as the evaluation factor over the hand motion. The measure of manipulability for a particular finger M becomes zero at singular points and takes positive values elsewhere. Since the measure of manipulability changes continuously as the hand moves its fingers it can be considered as a kind of distance from the singular locations. An approach to change the value of κ_r is based on the following equation:

$$\kappa_r = \begin{cases} \kappa_o \left(1 - \dfrac{M}{M_o}\right)^2 & \text{for} \quad \kappa_r < \kappa_o \\ 0 & \text{for} \quad \kappa_r \geq \kappa_o \end{cases} \tag{6.18}$$

where κ_o is the scale factor at singular points, and M_o is the measure of manipulabililty on the boundary of the neighbourhood of singular points. Basically it is necessary to vary the scalar κ_r in Eq. 6.17 so that it can be used in Eq. 6.18 for defining the RSI. This variation is based on how good the dexterity of the finger is.

In reality the effect of using the RSI is clear when the hand Jacobian is decomposed into the three bases matrices using SVD method. The SVD of a $\boldsymbol{J}_i$ for one finger is viewed as, DEO and WALKER [1992] :

$$\boldsymbol{J}_i = \boldsymbol{U}\Sigma\boldsymbol{V}^T \tag{6.19}$$

where Σ is the matrix representing the singular values of $\boldsymbol{J}_i$ and is expressed by:

$$\Sigma = diag\,[\sigma_1 \quad \sigma_2 \quad \sigma_3\,] \tag{6.20}$$

where $\sigma_1 \geq \sigma_2 \geq \sigma_3$ are the real singular values of $\boldsymbol{J}_i$. Furthermore, the pseudoinverse $\boldsymbol{J}^+$ can be computed as

$$\boldsymbol{J}^+ = \boldsymbol{V}\,\Sigma^+\,\boldsymbol{U}^T \tag{6.21}$$

where Σ^+ is $\in \Re^{[3\times3]}$ diagonal matrix with

$$\Sigma_{(i,i)} = 1/\,\sigma_i \qquad \text{if } \sigma_i \neq 0$$

$$= 0 \qquad \text{if } \sigma_i = 0$$

If Eq. 6.17 is redefined as :

$$\boldsymbol{J}^{R}_{h} = (\boldsymbol{J}^{T}_{h}\boldsymbol{J}_{h} + \boldsymbol{S})^{-1}\boldsymbol{J}^{T}_{h} \tag{6.22}$$

where $\boldsymbol{S} = diag[\,\boldsymbol{A}_1\ \boldsymbol{A}_2\ \boldsymbol{A}_3\ \boldsymbol{A}_4\,]$ and $\boldsymbol{A}_i = diag[\,\kappa_{ri}\ \ \kappa_{ri}\ \ \kappa_{ri}\,]$ *for* $i = 1$ *to* 4 and κ_i is determined from Eq. 6.18 for the *ith* finger. Further analysis using the SVD of Eq. 6.22 results in :

$$\boldsymbol{J}^{R}_{h} = \boldsymbol{V}\Sigma^{T}\boldsymbol{U}^{T}(\boldsymbol{U}\Sigma\Sigma^{T}\boldsymbol{U}^{T} + \boldsymbol{S}\,\boldsymbol{U}\,\boldsymbol{U}^{T})^{-1}$$

then $\boldsymbol{J}^{R}_{h}$ can be put as, Appendix [A1] :

$$\boldsymbol{J}^{R}_{h} = \boldsymbol{V}\left[\begin{array}{ccc|cccc} \frac{\sigma_1}{\sigma^2_1+\kappa_{r1}} & 0 & 0 & \cdot & & & \cdot \\ 0 & \frac{\sigma_2}{\sigma^2_2+\kappa_{r1}} & 0 & 0 & 0 & \cdots & \cdot \\ 0 & 0 & \frac{\sigma_3}{\sigma^2_3+\kappa_{r1}} & 0 & 0 & & \\ \hline & & & \frac{\sigma_4}{\sigma^2_4+\kappa_{r2}} & 0 & 0 & \\ \cdot & & & & & & \\ & & & & & & \\ \cdot & & & & & & \\ 0 & 0 & & & 0 & \frac{\sigma_{12}}{\sigma^2_{12}+\kappa_{r4}} & \end{array}\right]\boldsymbol{U}^{T} \in \Re^{[12\times 12]}$$

(6.23)

Thus, as singularity is approached the smaller singular values of $\boldsymbol{J}_i$ tend to go to zero resulting in very high singular values of $\boldsymbol{J}^{+}$. Also, when the singularity is reached, there is a discontinuous switch as the large singular values of $\boldsymbol{J}^{+}$ drop from a very high value to zero. From the developed results shown in Appendix [A1], the use of the RSI produces an error which can be computed as:

$$|| \dot{X} - J\dot{\Theta} || = \sqrt{(\Sigma [\kappa_r^2 / (\sigma_i^2 + \kappa_r)])} \qquad (6.24)$$

It is clear that for the pseudoinverse (when $\kappa_r = 0$), this error will be zero when the Jacobian has full row rank. The RSI will not suffer from the problem of discontinuous switching of solutions as the pseudoinverse does. As a singular value σ_i of J_i goes to zero, the term (σ_i / ($\sigma_i^2 + \kappa_r$) increses until it reaches a maximum at $\sigma_i = \alpha$ and then decreses to zero, thus there is no discontinuous jump in the solution. Using this concept of varying the κ_r factor, the RSI is a normal generalised inverse, however, it has an extra term which is adapted according to the dexterity measure of the finger.

6.5.1) Results and Analysis

Conventional Inverse :

Within this analysis, the same manipulation task for moving the object within the hand palm in a cyclic form will be used. Due to the linkage between one finger Jacobian singularity and the entire hand singularity some results of the already discussed RSI will be shown here. Fig [6.2] shows the corresponding condition number of the entire hand Jacobian J_h, which by itself is a function of the four fingers. Due to the rotation of some fingers Jacobian at points of contact, a finger Jacobian singularity will not change, however, what will change is the singular value which will drive a particular finger Jacobian to be zero determinant. Fig [6.3] shows the effect of the entire singularity due to the singularity of each finger Jacobian for one , two, three, and four fingers.

Although the four fingers Jacobian are concatenated, there is no change in the associated condition number. In a similar way, Fig [6.4] shows the corresponding determinate function of one, two, three, and four fingered hands. In addition to this, due to the cyclic nature of the defined task, two main zero determinant function of J_h are evident from

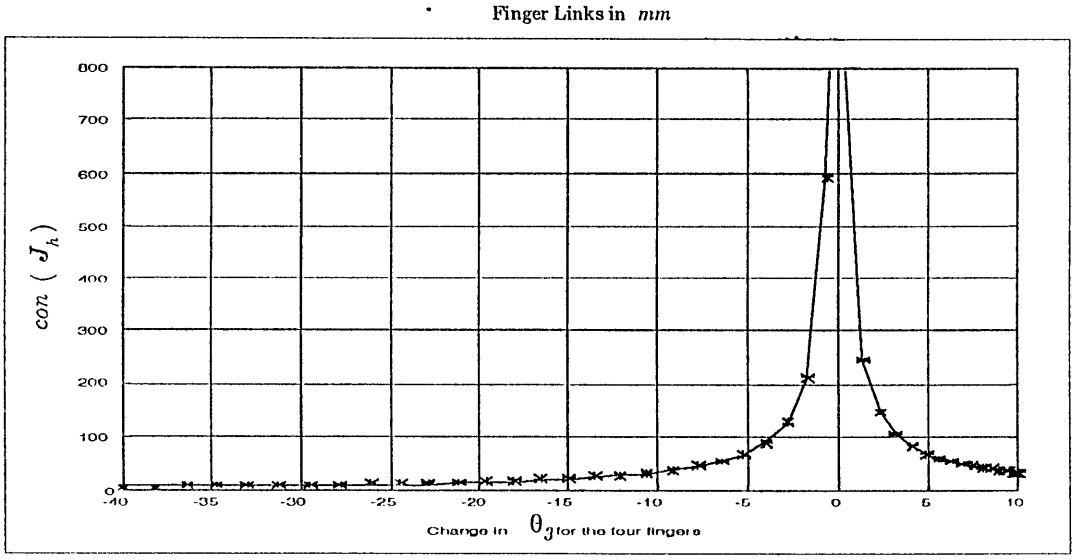


Figure 6.2 : Another View of an Ill Conditioned Task, the Condition Number.

Hand Links in mm

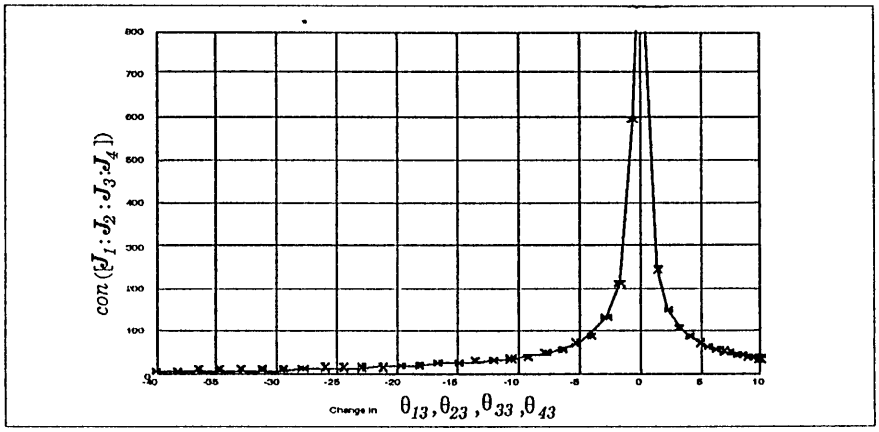
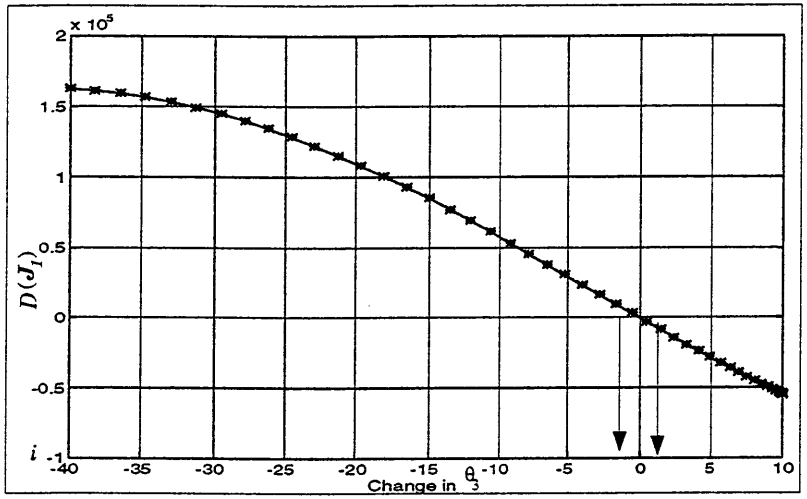
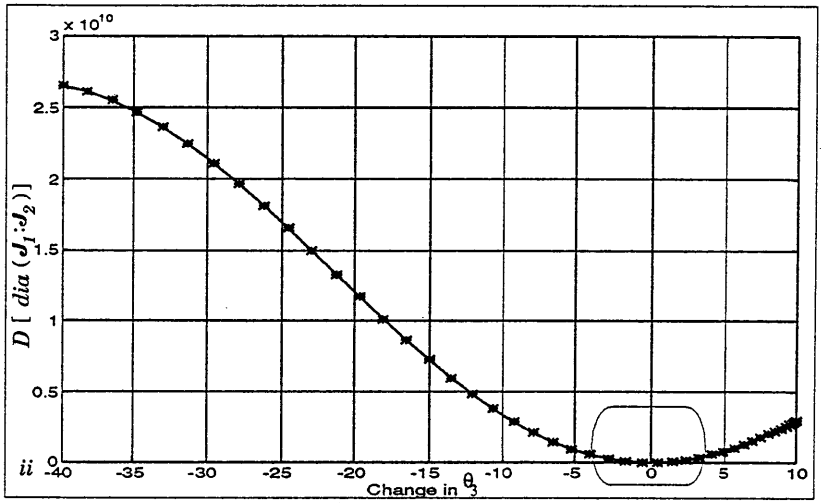
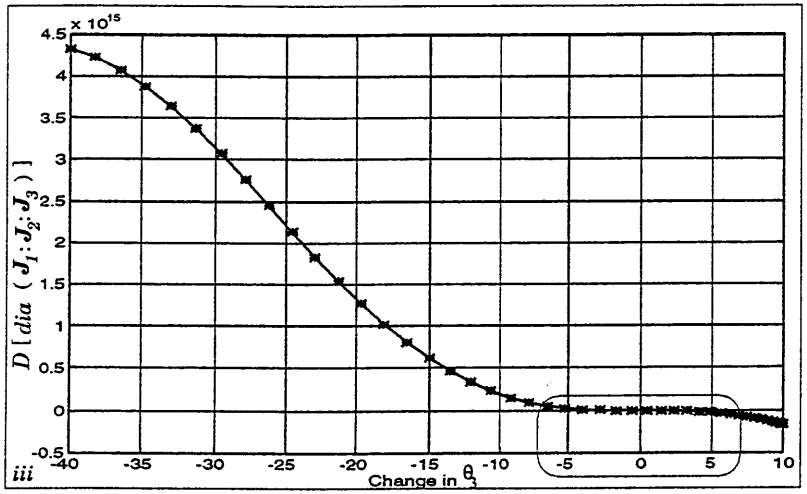


Figure 6.3 : The Condition Number of Jacobian for Four Fingers.

Hand links are in mm unit







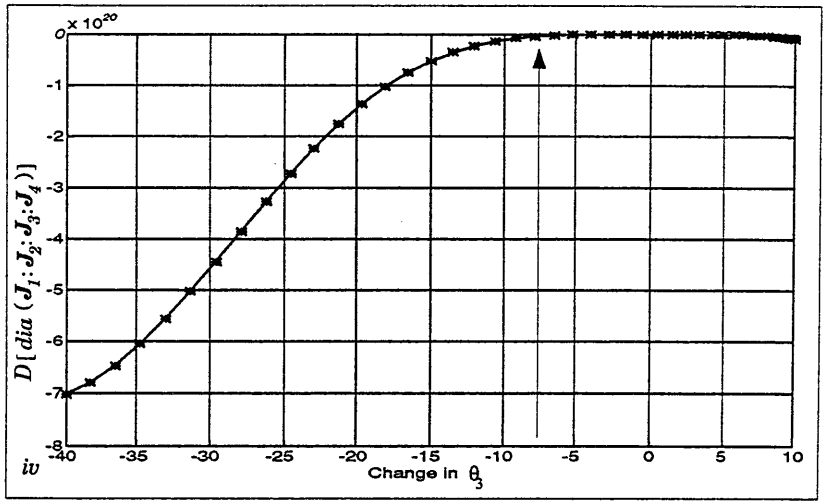


Figure : 6.4 : The Determinant Function of *i* : One Finger, *ii* : Two Fingers,
iii : Three Fingers *iv* : Four Fingers.

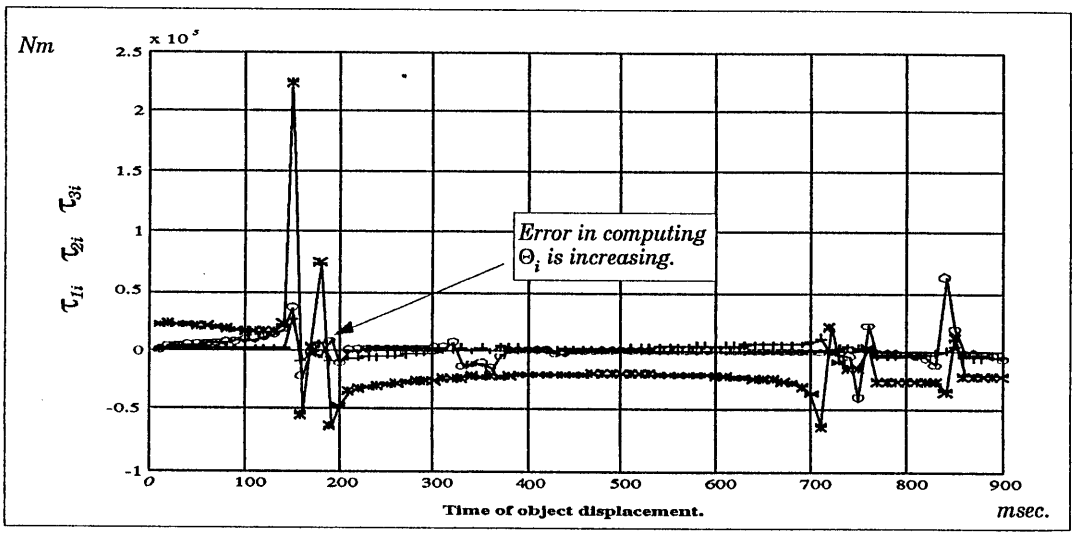
the grasp to occur. One during the forward motion and the other during the backward motion.

If the singularity problem inherent in any cartesian based motion is left without being overcome, then the corresponding displacement, velocity, or joint torques will approach an infinite value, limiting the system performance. Fig [6.5] shows the simulation of the constrained inverse dynamic problem for the constrained motion (*further analysis will be given later*) for moving a finger over the defined period of time. The distal joint angle of the third joint has to pass through the zero value (*which is the singular configuration*). Due to the requirement of the inverse Jacobian in the dynamic model, the inverse falls at the singular configuration resulting in a sharp rise in joint torques.
This discontinuity is totally undesired, since it results in the error being carried out for both position and velocity and application of high value of joint torques to the finger. Furthermore, it is clear from Fig [6.5] that the period during which a sudden rise in the computed torque has occurred is spread over 10 *msec.* units of time at each end of the total dynamic manipulation time.

The control must smooth this sudden change in the computed torque. The method employed is to invert the hand Jacobian matrix using the Robust Inverse Singularity *RSI* technique presented at the beginning of this section. Use of this approach would require the rescaling of the workspace within which the finger is to be moved. In Chapter Three it was found that the manipulation space was dropped to zero only in and at the boundary of singular locations, therefore the performance can be improved by reconstructing the inverse itself at the presence of singularity.

Variable Scale Factor :

The properties of the singularly robust inversion with the variable scale factor κ_r are



o : *Proximal Joint,*
* : *Medial Joint,*
+: *Distal Joint.*

Figure 6.5 : Total Constrained Torques of *ith* Finger To Move an Object Using Normal Inverse.

further examined for the four fingers. Using the same trajectory motion described in the last section, the ratio of manipulability, (M/M_o) is shown in Fig [6.6].

Fig [6.6-a] shows the manipulability ratio when the error of computed $\dot{\theta}$ and θ are carried out over the entire task. Fig [6.6-b] shows the graph of the ratio (M/M_o) drops to zero value at the singular configuration only in accordance with the rule described by Eq. 6.18 when the computing of θ is not carried out.

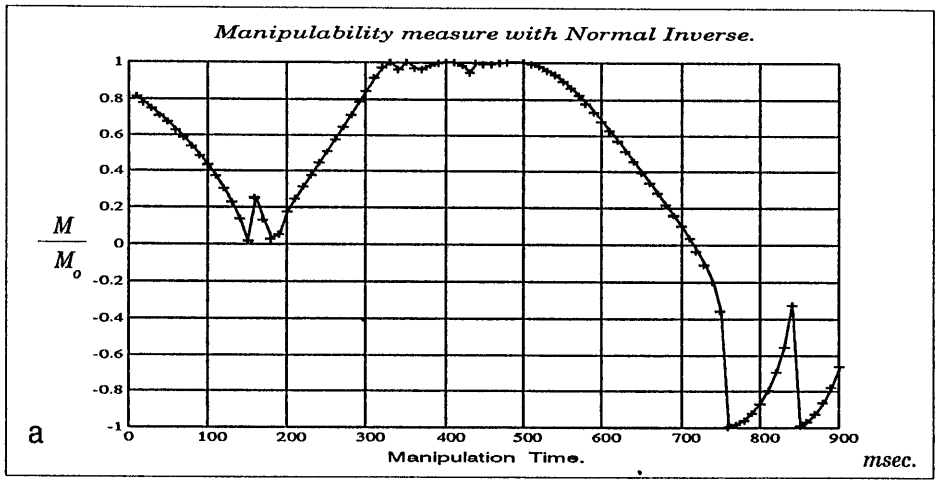
Fig [6.7-a] shows the κ_r / κ_o scaling factor used in Eq. 6.22 when the error is carried out. Also shown in Fig [6.7-b] is the ratio of κ_r / κ_o where the ratio is 380 in the neighbourhood of singularity and zero elsewhere. In these computations the neighbourhood of singularity is chosen to be – 30° to + 30°.

Making κ_o variable using this scheme will ensure the resulting inversion of the hand Jacobian J_h to be defined even when it is singular.

Fig [6.8] shows the effect of the variable scale factor in inverting J_h and the computed joint torques. In Fig [6.8] the required differential changes in $\partial\Theta_3$ is solved using RSI for differential changes in cartesian object position, and used to compute the constrained torque to produce the object cartesian motion.

The rapid shot in the value of torque shown in Fig [6.8-a] (during the interval 100 to 200 *msec.*) and how it has been smoothed with the employment of variable scaling factor κ_o is clear from the graph. As κ_o is approaching zero as in Fig [6.7-b], the inverse moves smoothly to a generalized inverse rather than RSI.

In a similar way Fig [6.9] shows the corresponding changes in a finger joint space vector in *rad* computed using the RSI of the hand Jacobian for the object motion. The RSI has produced a solution used to move the corresponding fingertip even within singular



$$\frac{[L_3 \text{Cos}(\theta_2 + \theta_3) + L_2 \text{ Cos}(\theta_2) + L_1]}{[L_3 \text{Cos}(\theta_{o3} + \theta_{o2}) + L_2 \text{Cos}(\theta_{o2}) + L_1]}$$

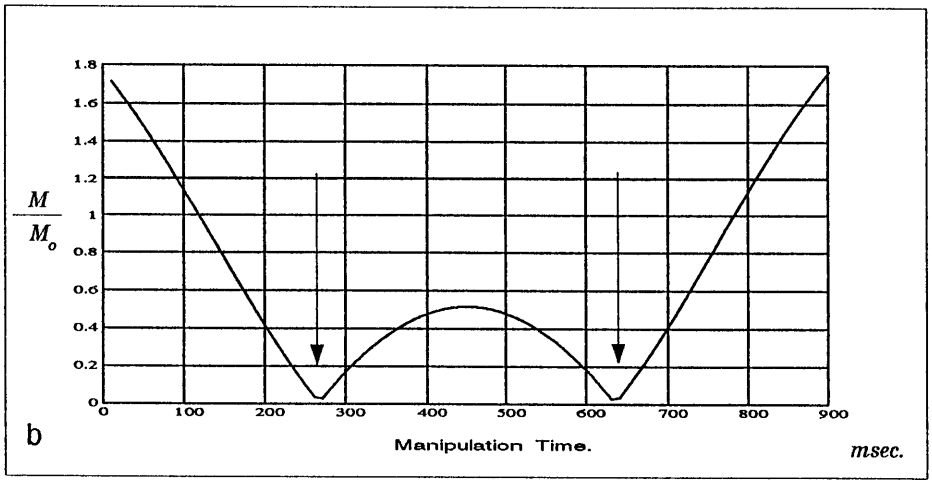
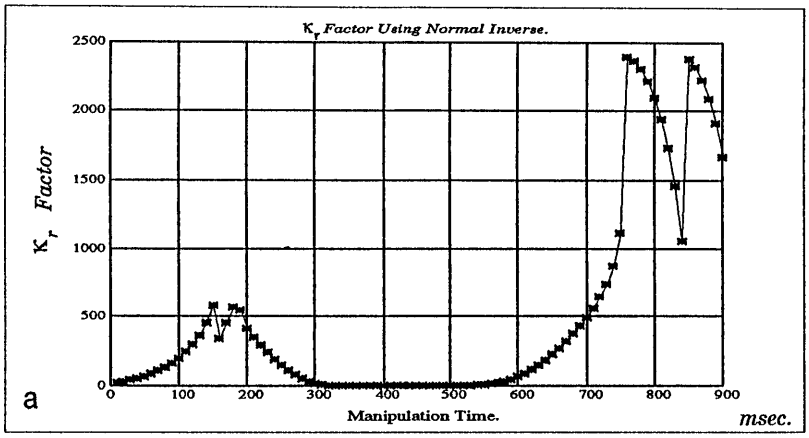


Figure 6.6 : Ratio of Manipulation Measure :
a : Using Normal Inverse where Error is Carried Out .
b : Using RSI Based On Manipulability Measure.



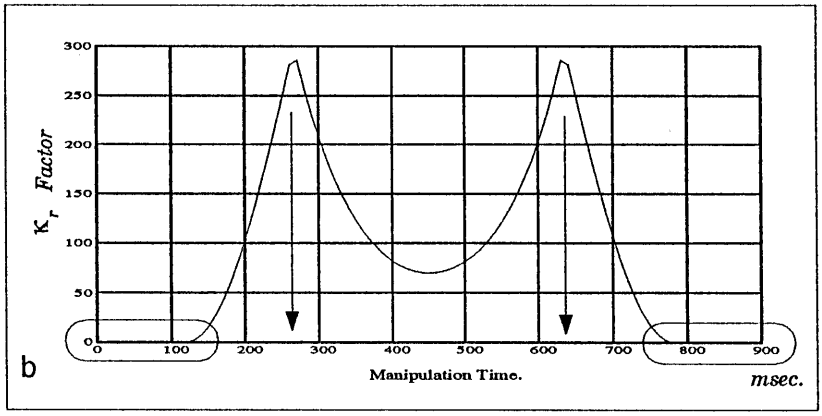
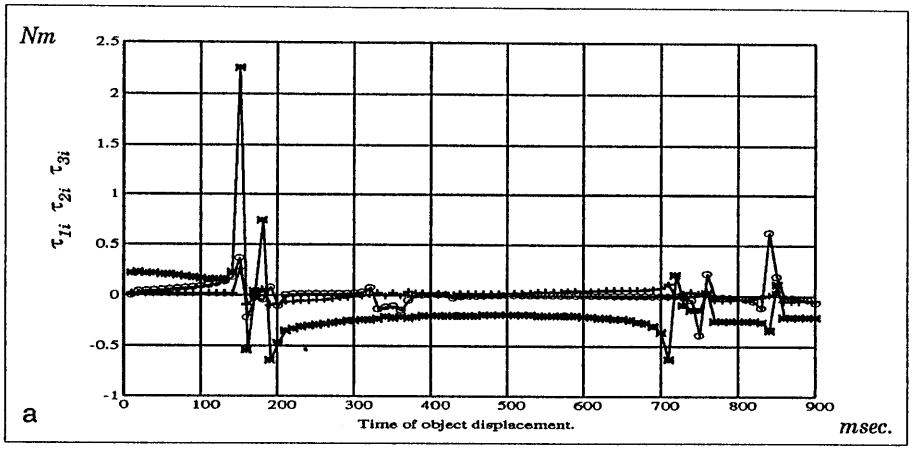


Figure 6.7 : Value of κ_r Factor as :
a : Error Carried Out.
b : Where Error is Not Carried Out.



o : Proximal Joint,
** : Medial Joint,*
+: Proximal Joint.

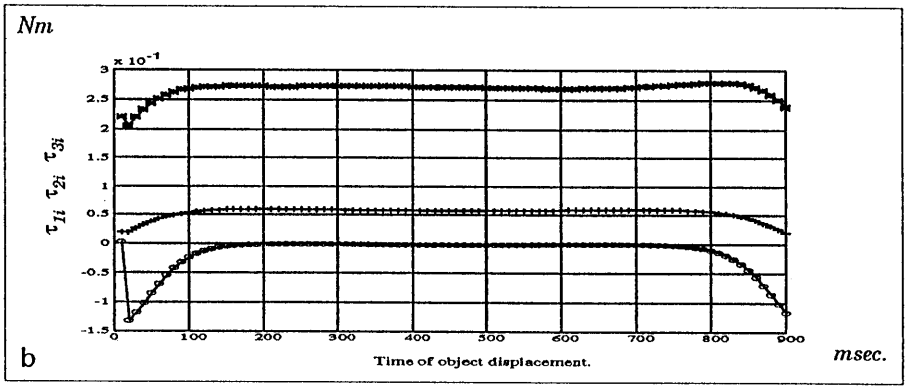
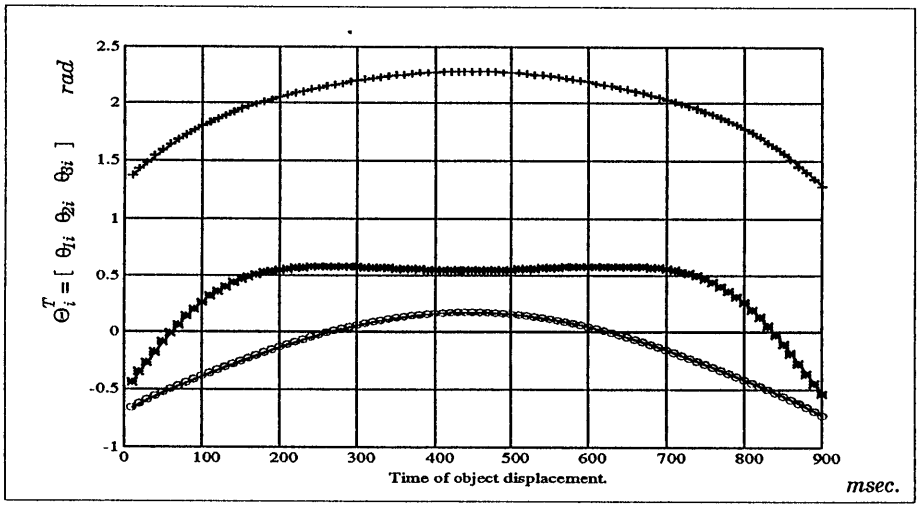


Figure 6.8 : Comparision of Two Unconstrained Torques For One Finger
a : Normal Inverse of Jacobian where Error is Carried Out.
b : In Using RSI For the Multiple Contact.



o : Distal Joint,
** : Medial Joint,*
+ : Proximal Joint.

Figure 6.9 : Joint Positions For Fingertips Cartesian Motion Using RSI in the Multiple Contact.

configuration. Furthermore, the medial joint displacement reaches a near constant value due to the fact that the effect of singularity is reduced to a minimum.

The employed technique of avoiding the effect of singularity has a drawback, the method is quite expensive in terms of the required computation time. This increase in the computation time is due to the fact that a modified generalised inverse has been used. The generalised inverse requires the computation and multiplication of the Jacobian transpose J_h^T with the Jacobian itself, and invert the result. The use of the RSI would require, in addition to this, another vector to be added to the inversion which represents the effect of the variable factor κ_r.

The mechanism of changing the value of κ_r in Eq. 6.22 gives a solution which is effective only when the finger is at singularity. Compared to a similar approach of the use of (damped least-squares) solution used by WAMPLER [1986], hence a reduced computation is required. The reduced computation is due to the fact that a generalized inversion is used (with less computation time) outside the singularity region, and a robust singularity inverse is performed only within the ill-condition of J_h, whereas the damped least square solution will be used with a constant κ_r factor even outside singularity.

Having considered the aspects of variable scale factor used in the inverse operation, here the computational requirements are further analysed and compared with conventional existing inverse techniques.

In accordance with the computational requirements, as discussed by NAKUMARA [1992], using RSI over the conventional inverse result in a great deal of arithmetic to be computed. Such computations are time consuming, especially for real time applications.

(6.6) DYNAMIC FORCES COMPUTATION USING OPTIMIZATION

6.6.1) Constraints Formulation in the Coordinated Motion

Internal Forces Optimization During the motion:

Under assumption 2 of section (6.22), the force balance equation for grasping during dynamic motion can be expressed using the grip transform in the following way:

$$\boldsymbol{F}_b(t) = \boldsymbol{G}\,\boldsymbol{f}_{tip}(t) \tag{6.25}$$

where the $\boldsymbol{F}_b(t)$ is the vector of the time varying object dynamic.

However, due to the object motion following a defined trajectory over time $\theta(t)$, and the $\boldsymbol{B}(t)$ vector are time dependent.

$$\Pi(t) = \begin{bmatrix} \boldsymbol{F}_{ri} \\ \hline \boldsymbol{J}^T{}_h(t) \end{bmatrix} \tag{6.26}$$

Expanding the above inequality constraint equation in a similar way as done in Chapter Five:

$$\Pi(t)\boldsymbol{f}(t)_{tip} \leq \boldsymbol{B}(t) \tag{6.27}$$

The $\boldsymbol{c}_i(t)$ vectors are the inequality constraints which take the following format:

$$\boldsymbol{c}_i(t) = \begin{bmatrix} 0 \\ 0 \\ 0 \\ 0 \\ \tau_{imax} - \boldsymbol{M}_i\,\ddot{\Theta}_i + \boldsymbol{N}_i\dot{\Theta} + \boldsymbol{C}_i \end{bmatrix} \tag{6.28}$$

Eq. 6.28 accounts for the physical limits in the joint torques for producing the object defined motion by including the finger dynamics which change during the object motion. The

equation also reveals the fact that, once the object is in a static mode, the hand motion parameters such as the inertia M_h, centrifugal force N_i will be zero and the generated joint torque is that which compensates only for the gravity effect parameters, as has been investigated in Chapter Five.

An important issue for consideration, which is not apparent in the static mode of grasping, is the motion dependence in the defined task. While the robot hand changes its configuration to track the object motion, the Jacobians of the individual fingers change as the motion progresses. This change puts another constraint on the object contact coordinate, since it requires the computation of the individual Jacobians as expressed at the *ith* point of contact. Hence the direction cosine is computed only at the beginning of the task since the points of contact do not change, it is only the orientation of the contact point that changes.

Optimization of Dynamic Internal Forces :

Using the same development as in Chapter Five for calculating the null space components of the Grip transform G which is based in the computation of the internal forces, then the function to be optimized is given by :

$$\begin{aligned} &\textit{Optimize} && \Phi(f(t)_{tip}) = C^T f(t)_{tip} + \tfrac{1}{2} f(t)_{tip}{}^T W f(t)_{tip} \\ &\textit{subject to} && G f(t)_{tip} = F_b(t) \\ &\textit{and} && \Pi(t) f(t)_{tip} \leq B(t) \end{aligned} \qquad (6.29)$$

The C^T force vector adds a biasing fingertip force if the object is to push against an externally acting force, e.g. an environmental force.

Following the same development outlined in Chapter Five for optimizing the internal forc-

es, we are left with the following formulation for the dynamic case:

$$\begin{aligned} &\textit{Optimize} && \Phi(\lambda) = \tfrac{1}{2}\lambda\eta\eta\lambda \\ &\textit{Subject to} && \Pi(t)\eta\lambda \leq (\boldsymbol{B}(t) - \Pi(t)\,\boldsymbol{f}(t)_{PA}) \end{aligned} \tag{6.30}$$

For dynamic manipulation, an important issue regarding the internal forces optimization, is their relation to the fingertip forces decomposition, into grasping and manipulation forces, presented by YOSHIKAWA and NAGAI [1991] and described in Chapter One. The grasping forces described were added to satisfy the geometry and frictional constraints. The optimized internal forces using optimization algorithm is the other view of the grasp mode scalar which is added to satisfy the grasping forces as given by :

$$\boldsymbol{f}_{tip} = \boldsymbol{f}_g + \boldsymbol{f}_m \tag{6.31}$$

where the internal forces are represented by $\boldsymbol{f}_g$:

where $$\boldsymbol{f}_g = \boldsymbol{B}_g \boldsymbol{h}_g \tag{6.32}$$

and $\boldsymbol{B}_g$ is a matrix selected to satisfy the contact and geometrical constraint at the point of contact. When employing non linear constraints optimization, the grasping forces are blended within the manipulation forces, since the calculated fingertip forces are already satisfying the geometric and frictional contact constraints. As the object progresses in its motion the $\boldsymbol{B}_g$ matrix will reach a stage where the contact constraints will not be satisfied, and hence the grasping mode of ($\gamma_1\ \gamma_2\ \gamma_3$ and γ_4) has to be updated.

Fig [6.10] illustrates the hybrid controller structure expressed by Eq. 6.14 and which has been based on the employment of nonlinear optimization of the internal forces. The controller has been considered under the assumption that, the required cartesian object

motion parameters are defined. Since the motion is based on cartesian coordinates, the hand inverse kinematics are used with reference to a fixed frame in the work location.

In the figure, the control structure adds two types of torque vectors at the summing junction *A*. The computed torque technique is used to compute the inverse dynamic of the whole hand. Also shown in Fig [6.10] are the internal forces which must be optimized to produce the minimum effort to move the object. Due to the equilibrium of forces, the defined object motion parameters will produce a cartesian force proportional to the object mass. Also shown in the figure is the cartesian error which is generated by the difference between the object motion and the real fingers position.

In the controller structure of the cartesian based hand motion, either using the linear or nonlinear optimization technique, it requires the actuating of appropriate joint motors for changes in the fingertips forces, due to the object dynamics. At each sampling period the computation complexity of multiple contact object motion, is not as the case of computing variables for a robot arm controlled in cartesian base. This is due to the dynamic of the object in producing an effect on the fingers during the object motion .

6.6.2) Employment of Nonlinear Constraints Optimization During the Motion :

In the previous section optimization of internal forces based on the linearised model of the contacts has been investigated. Another approach is to employ the nonlinear constraints optimization in the dynamic manipulation, hence to define an optimal criterion during the object motion.

Computation of the fingertip forces and hence the object resultant forces using a linearised model of the contact is enforced by ignoring some areas of the friction cone model at the point of contact. It also has the disadvantage of conatenating the $\Pi(t)$ and $\boldsymbol{B}(t)$ matrix

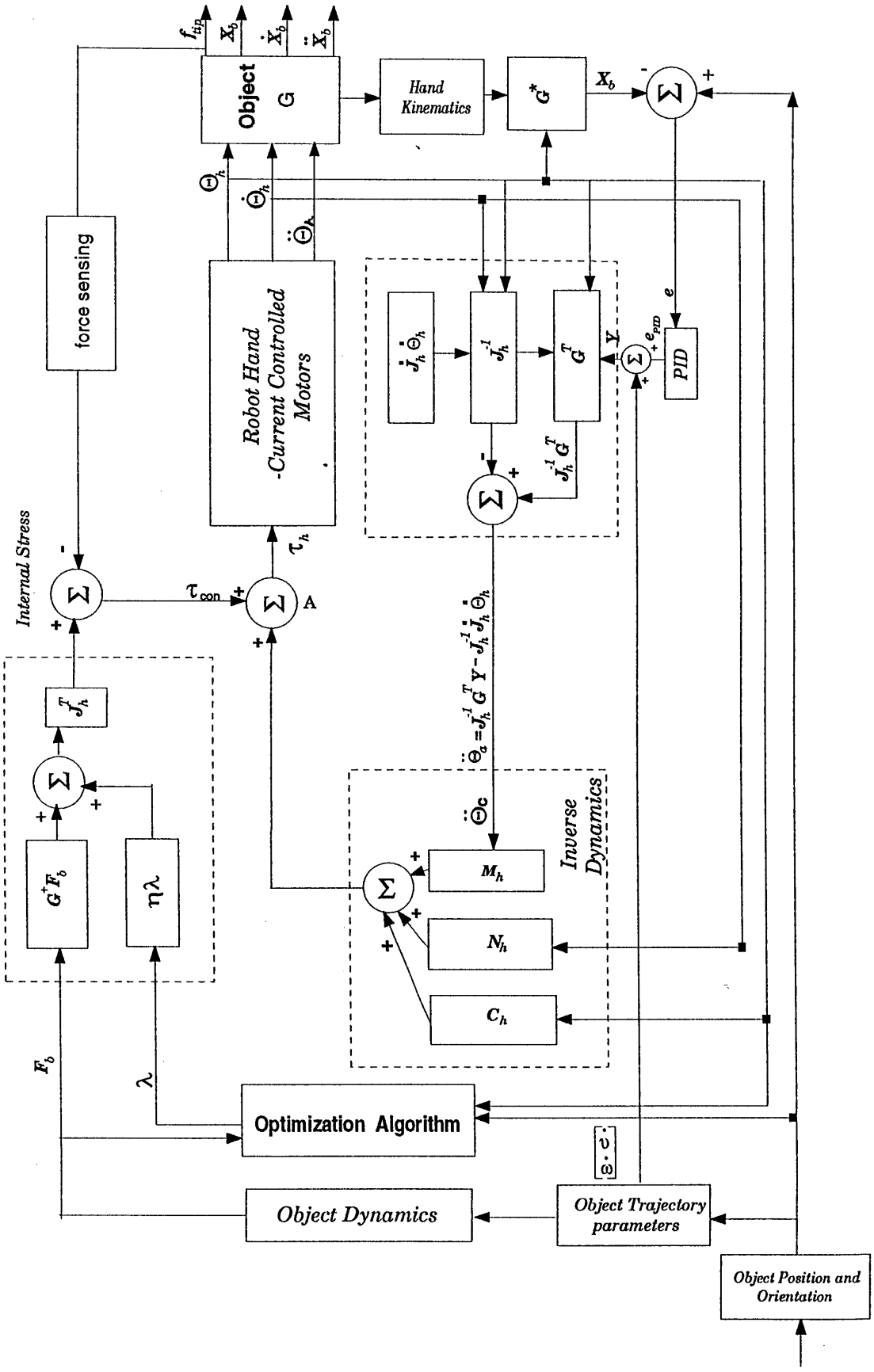


Figure 6.10 : Manipulation Forces Control Based On Internal Forces Optimization with Computed Torque Control Scheme.

and vector respectively in the optimization, which is time consuming. Another approach to solving the same problem is to model the contact as a purely nonlinear model of a cone, and solve the contact forces within this cone for keeping the object under consideration in a stable grasp.

Force optimization of nonlinear constraints is done by the optimization of the real contact forces $f_{x1}, f_{y1}, \ldots f_{z4}$ instead of the optimization of dummy variables, λ vector, as in the linear constraint problem which has been discussed by COI *et al.* [1992], when they used the *force ellipsoid* to formulate the optimal load distribution of two robot arms. Having this in consideration, the control strategy based on the optimized contact forces themselves and finding a suitable solution for the hand object system with four nonlinear constraints is not a trivial task for dynamic motion.

In section (6.6.1) the force control strategy has been based on optimization of the contact forces by the optimization of the grasp internal forces, and the controller structure shown in Fig [6.11] has resulted. Within this section the employment of nonlinear constraint will be used in the optimization scheme.

Define the $\boldsymbol{E}(t)_e$ matrix to be composed from $\boldsymbol{G}$ the grip transform and $\boldsymbol{J}_h(t)$, such as:

$$\boldsymbol{E}(t)_e = \begin{bmatrix} \boldsymbol{G} \\ \hline \boldsymbol{J}_h^{\,T}(t) \end{bmatrix} \tag{6.33}$$

then $\boldsymbol{E}(t)_e$ is bounded by the time varying equality limits as:

$$\boldsymbol{L}(t)_{lim} \leq \boldsymbol{E}(t)_e \leq \boldsymbol{U}(t)_{lim} \tag{6.34}$$

where $\boldsymbol{L}(t)_{lim}$ and $\boldsymbol{U}(t)_{lim}$ are dynamic based vectors given by:

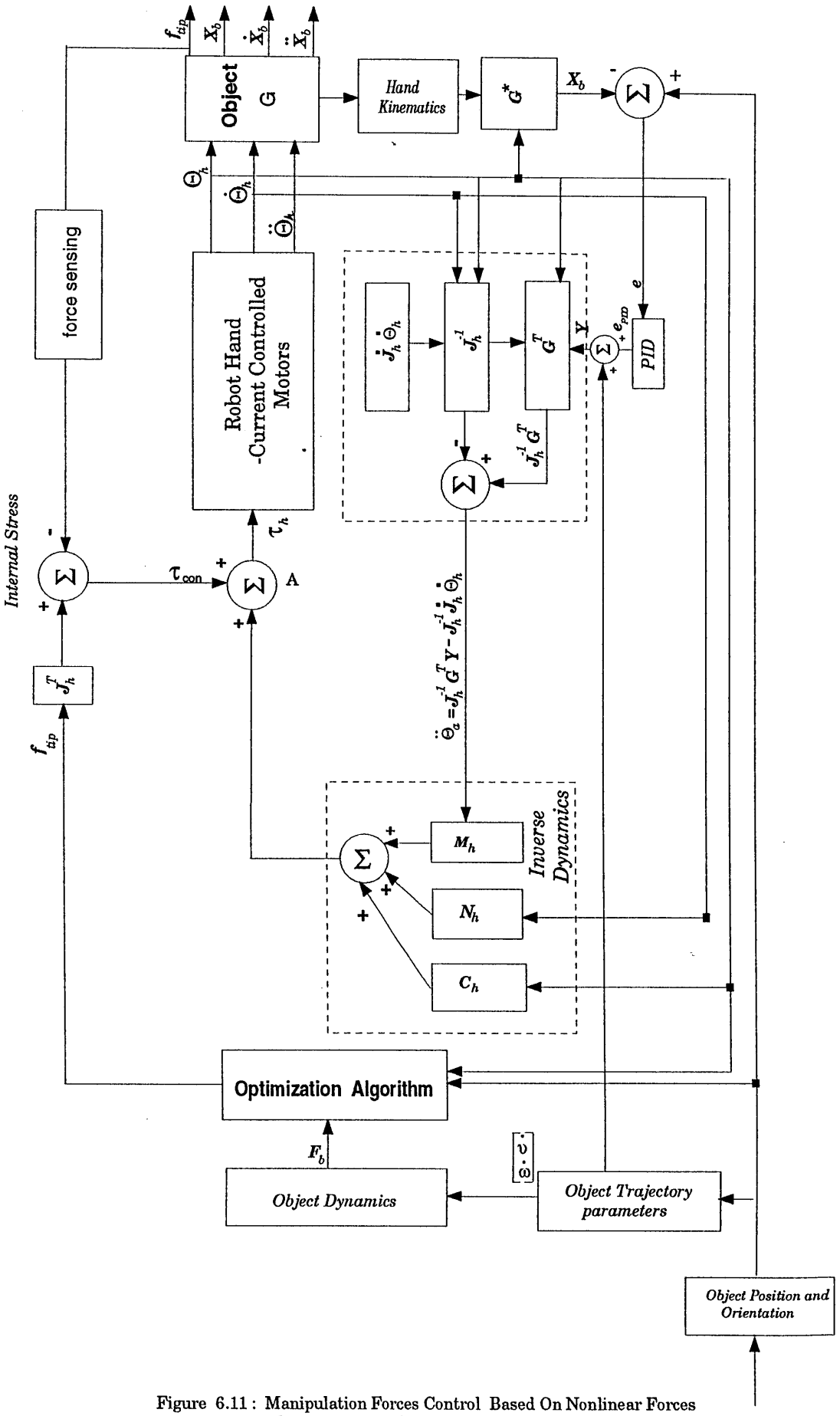


Figure 6.11 : Manipulation Forces Control Based On Nonlinear Forces Optimization with Computed Torque Control Scheme.

$$\boldsymbol{L}^T(t)_{lim} = [f_{bx}\ f_{by}\ f_{bz}\ \ m_{bx}\ \ m_{by}\ \ m_{bz}\ \ (\tau_{in1j} - \tau_{yn1j})\ (\tau_{in2j} - \tau_{yn1j})\ \ (\tau_{in3j} - \tau_{yn1j})] \in \Re^{18}$$

$$j = 1 \text{ to } 3$$

$$\boldsymbol{U}^T(t)_{lim} = [f_{bx}\ f_{by}\ f_{bz}\ \ m_{bx}\ \ m_{by}\ \ m_{bz}\ \ (\tau_{ax1j} - \tau_{yn1j})\ (\tau_{ax2j} - \tau_{yn1j})\ (\tau_{ax3j} - \tau_{yn1j})]^T \in \Re^{18}$$

$$j = 1 \text{ to } 3 \qquad (6.35)$$

The forces calculations expressed in Chapter Five can be rewritten in the following form for the dynamics case as, AL-GALLAF and WARWICK [1994-a] :

$$\begin{aligned} &\textit{Optimize} \quad \Phi(\boldsymbol{f}_{tip}) = \sum_{j=1}^{4} (f^2_{xj} + f^2_{yj} + f^2_{zj}) \\ &\textit{subject to} \quad \boldsymbol{L}(t)_{lim} \leq \boldsymbol{E}_e(t) \leq \boldsymbol{U}(t)_{lim} \\ &\textit{and} \qquad\quad \lambda_{lim} \leq \boldsymbol{f}_{Tri} \leq \lambda_{lim} \end{aligned} \qquad (6.36)$$

The employment of the nonlinear constraints optimization simplifies the controller structure for a cartesian based motion. This can be seen from the controller structure shown in Fig [6.12]. In the Figure the inverse dynamic model with constrained acceleration of the entire hand is the same as that adopted in section (6.4.1). What has been changed is the computation of the forces at contacts.

6.6.3) Results Analysis

Within this section some simulation results obtained for the object motion with optimal contact forces will be presented.

Defined Manipulation Task. :

In order to illustrate the concept of object manipulation, a task has been defined and involves the motion of an object within the workspace of the Cybhand. A spherical object of defined mass and inertia parameters is required to be moved in a cyclic motion given

by the following sinuosodial changes in its position with respect to the hand palm:

$$\boldsymbol{X} = \begin{bmatrix} 32 - 114\,sin\,(h)t \\ 100 - 50\,sin\,(h)t \\ -165 + 70\,sin\,(h)t \\ 0 \\ 0 \\ 0 \end{bmatrix} \in \Re^6 \quad \text{in } mm \qquad (6.37)$$

In accordance with Eq. 6.37 , the cartesian path of the object is cyclic with respect to the palm frame, hence such a cartesian path will be associated with cartesian velocities and acceleration expressed as three element position vector with no change in the object orientation.

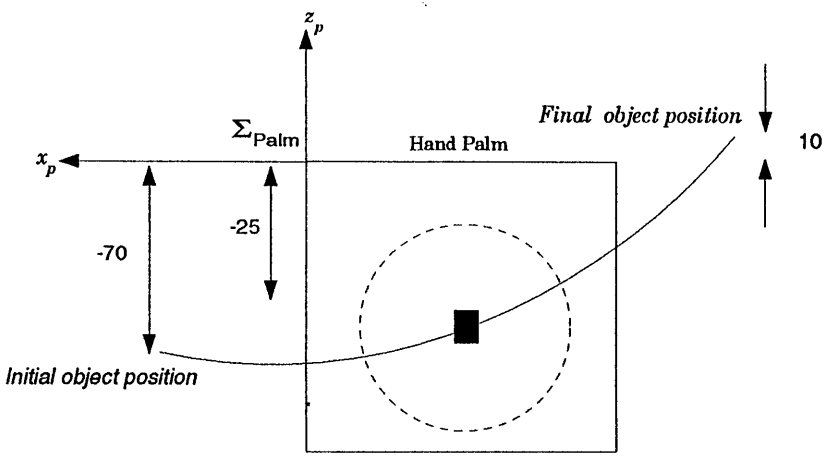
Fig [6.12] shows the corresponding cyclic path of the object to be moved. In Fig [6.12-a] the object direction of motion from bottom to top is in the Z direction. Fig [6.12-b] shows the the object motion from a plan view where the cyclic motion is in X and Y directions.

Inverse Dynamic For One Finger :

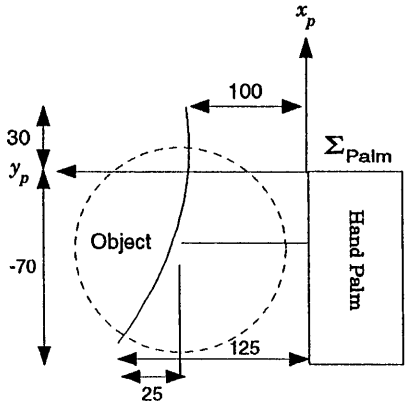
First the analysis of the manipulation task, the inverse dynamic response of one finger, will be investigated. The computed joint space parameters (position, velocity, acceleration) of a finger will be used to show the unconstrained motion of one finger using the inverse dynamic model of the finger. The inverse dynamic has been based on the use of a finger Lagrange.

Unconstrained Joint Torques :

Fig [6.13] shows the required joint torques required to move one finger for the defined manipulation task using the inverse dynamic model of one finger. For instance, Fig [6.13-a] shows the gravitational torques required by the three joints in one finger. Because



a



b

Measurements in mm unit.

Figure 6.12 A Defined Manipulation Task. Object Centre Follows a Path with An Optimality Function.
a : Front View. b : Top View.

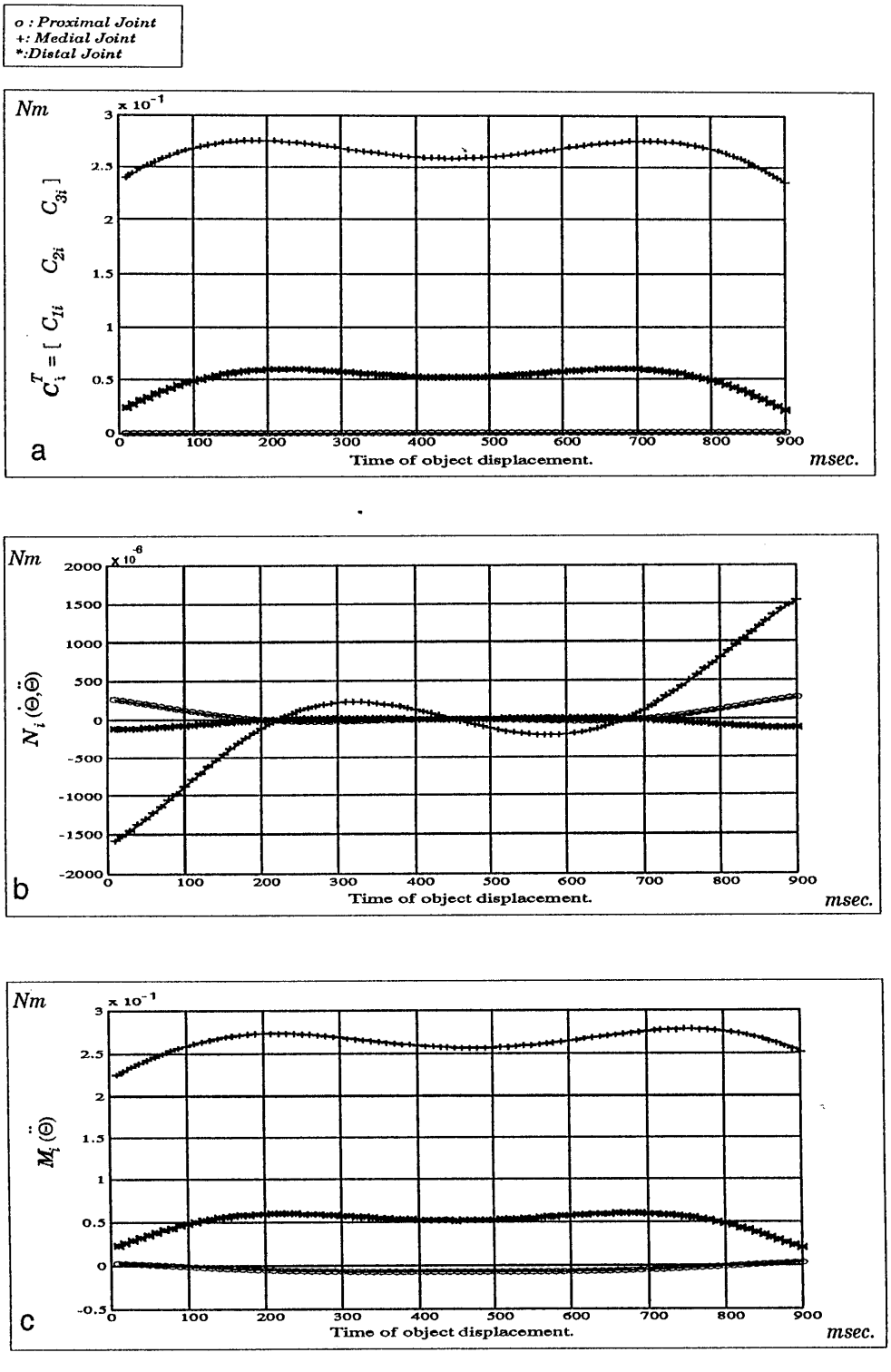


Figure 6.13 : Inverse Dynamic of One Finger (Unconstrained Motion):
a : Gravity Effect.
b : Centrifugal and Coriolis Torque.
c : Inertia Torque.

in this analysis the hand orientation remains horizontal, the proximal joint requires zero torque to overcome the gravity effect, whereas the the medial and distal joints require a certain amount of torque to overcome gravity.

In a similar way, the centrifugal forces effects are shown in Fig [6.13-b], whereas the inertia terms and their dependence on the joint acceleration are shown in Fig [6.13-c]. Similar results are obtained for the other fingers in the hand.

Fig [6.14] shows the corresponding velocity computed using RSI for three joints trajectories in one finger. Due to the fact that all the fingers have to start and stop motion at the same moment of time as a requirement of manipulation, the other three fingers all have the same joint space parameters of motion. Therefore, their fingertips locations with respect to the hand fixed palm frame are different due to their kinematics relation, presented in Chapter Three.

When the closed dynamic system represented by the object-hand motion occurs (fingers in contact with object), the acceleration of the joints are constrainred. Fig [6.15] shows the corresponding constrained acceleration of the one finger, Eq. 6.11. As the constrained acceleration expressed by Eq. 6.11 needs the hand Jacobian to be inverted, the effect of singularity is quite clear. Fig [6.15-a] shows the computed acceleration when the normal inverse is used where the acceleration is corrupted due to the singularity problem.

Fig [6.15-b] has the same acceleration when the RSI has been employed rather than the normal inverse. Since the motion of the entire hand has to pass the distal joints through zero value of joint angle, (*thus within singularity*) the result of this singularity is the peak in acceleration.

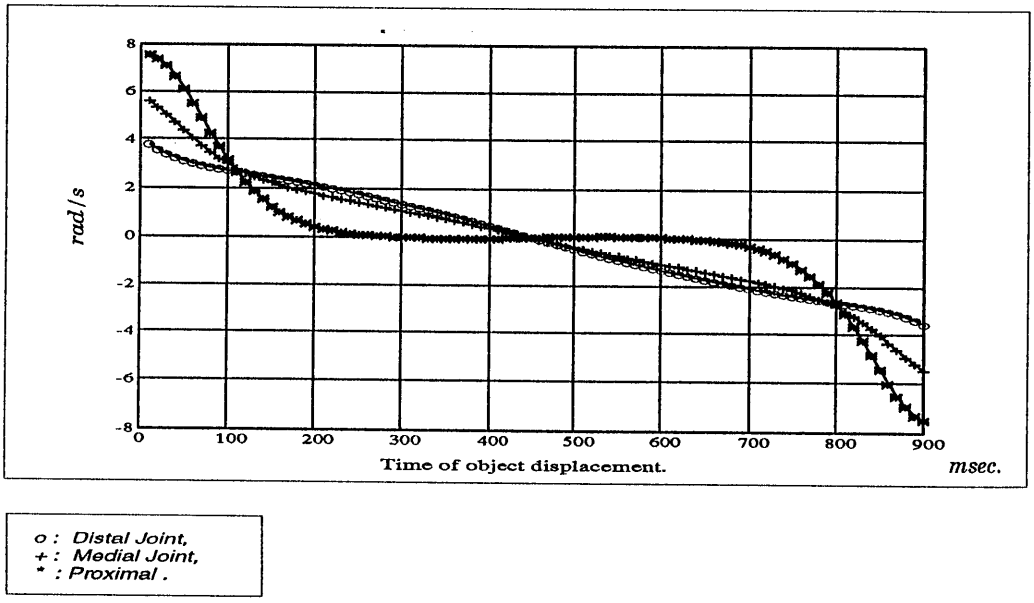
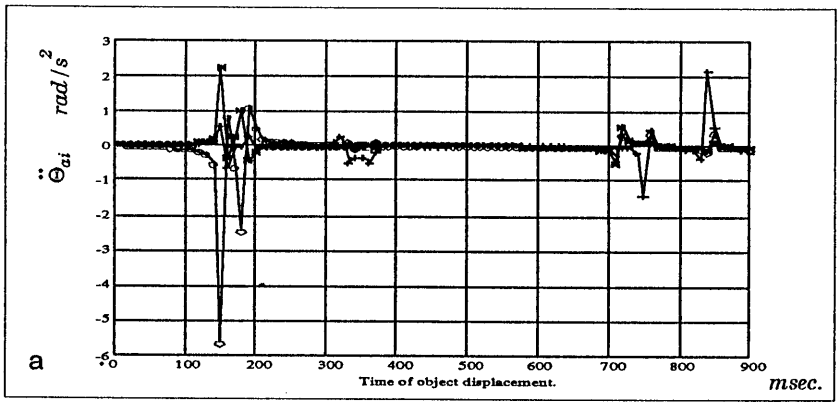


Figure 6.14 : Joint Velocities Expressed in rad/s Using RSI Inverse Hand Jacobian



$$\ddot{\Theta}_{ai} = J_h^{-1}[G^T \begin{bmatrix} \dot{v}_o \\ \dot{\omega}_o \end{bmatrix} + e_{PID} \dot{J}_h \dot{\Theta}_h]$$

o : Proximal Joint,
* : Medial Joint,
+: Distal Joint.

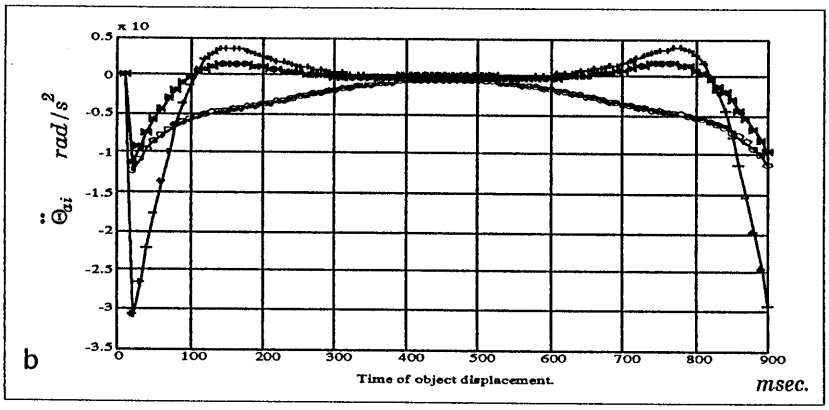


Figure 6.15 : a : Constrained Joints Accelerations Using Normal Inverse of Hand Jacobian.
b : Using RSI.

Constrained Motion Torques :

Fig [6.5] has shown the corresponding generated torque for the constrained motion case due to the singularity problem. The generated torque for the joints were corrupted and hence cannot be applied to the hand mechanical servo system, as that will produce a very large joint space motion.

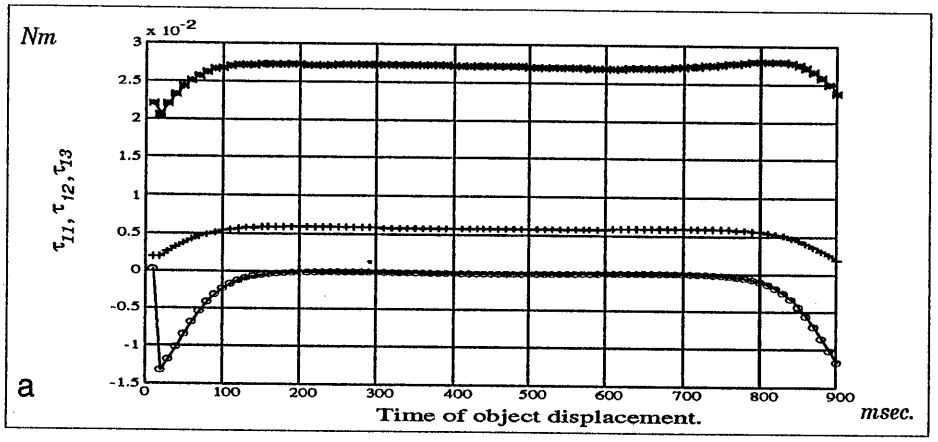
Fig [6.16] shows the corresponding torques for moving the two fingers all together, even within the location of singularity. The application of the RSI has reduced the peak of the computed torque. For instance, Fig [6.16-a] shows the corresponding computed torques due to the computed constraint acceleration for moving the first finger. The object must be grasped during motion while the two fingers must move in the same direction. Fig [6.16-b] shows the corresponding computed torques for moving the second finger. The four fingers have similar torqures ensuring the direction of object motion.

Fingertips Location Using RSI :

The corresponding fingertip positions of the four fingers with respect to the hand palm frame due to the computed torques are shown in Fig [6.17] and Fig [6.18]. In Fig [6.17] the first and second fingertips displacement with respect to the hand palm coordinate are shown. Due to the kinematic structure of the fingers, the corresponding positions are different in terms of their position with respect to the hand palm reference. Fig [6.18] shows the corresponding position of the fingertips for the third and fourth fingers. From the structure of the grip transform, it can be seen that the fingertips actually move with the points of contact as the object is displaced in the cartesian frame.

Optimization of Forces :

In the last sub-section the concept of generating the required joints torques for the fingers motion has been presented. Within this sub-section the aspects of generating the fingertip



o : Proximal Joint,
* : Medial Joint,
+: Proximal Joint.

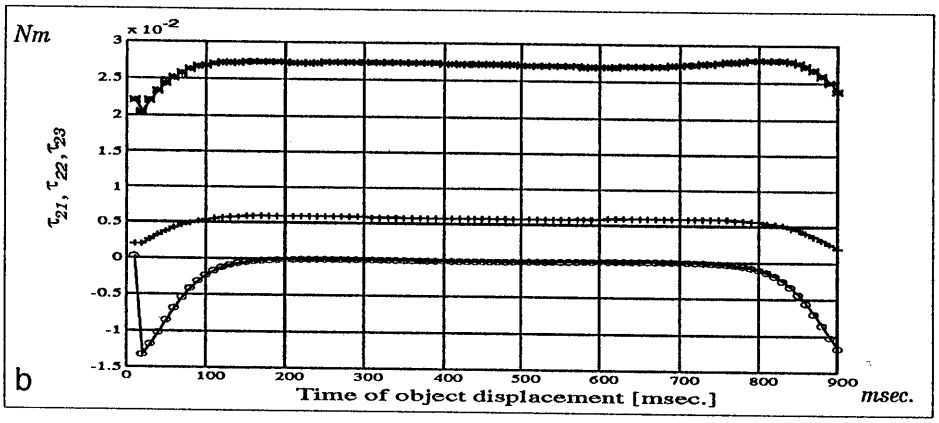


Figure 6.16 : Similar Constrained Computed Torques of Two Fingers Using Different Scaling Factor in RSI.
a : First Finger. b: Second Finger.

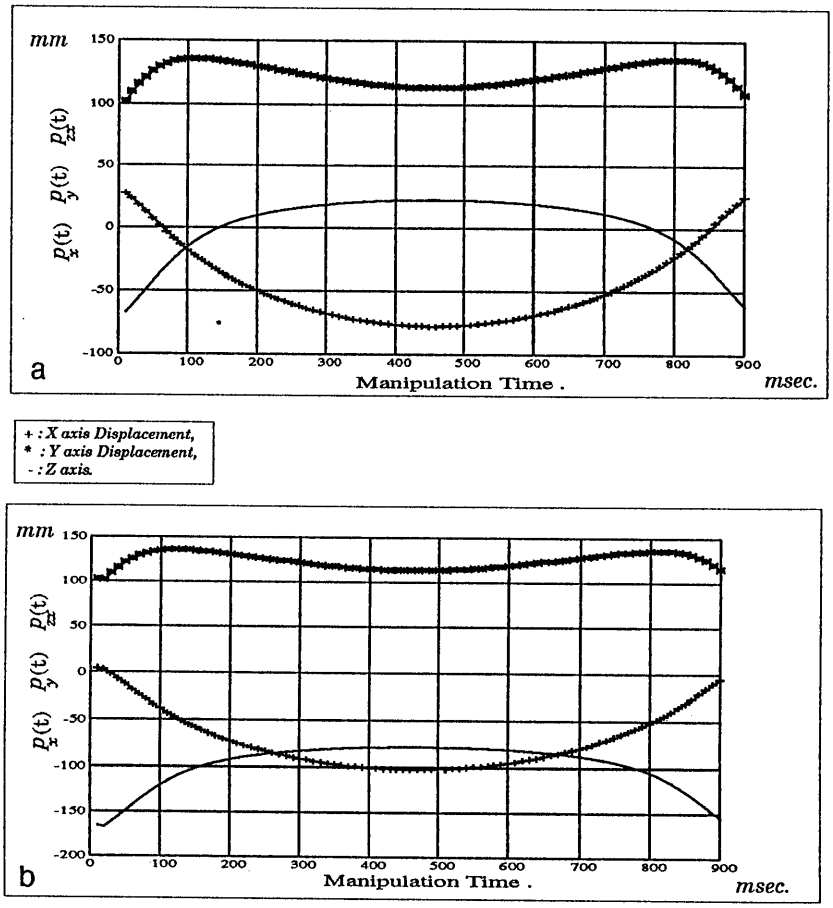


Figure 6.17 : Fingertips Displacement In Hand Palm Coordiante
Using RSI with Different Scaling Factor.
a : First Finger. b : Second Finger.

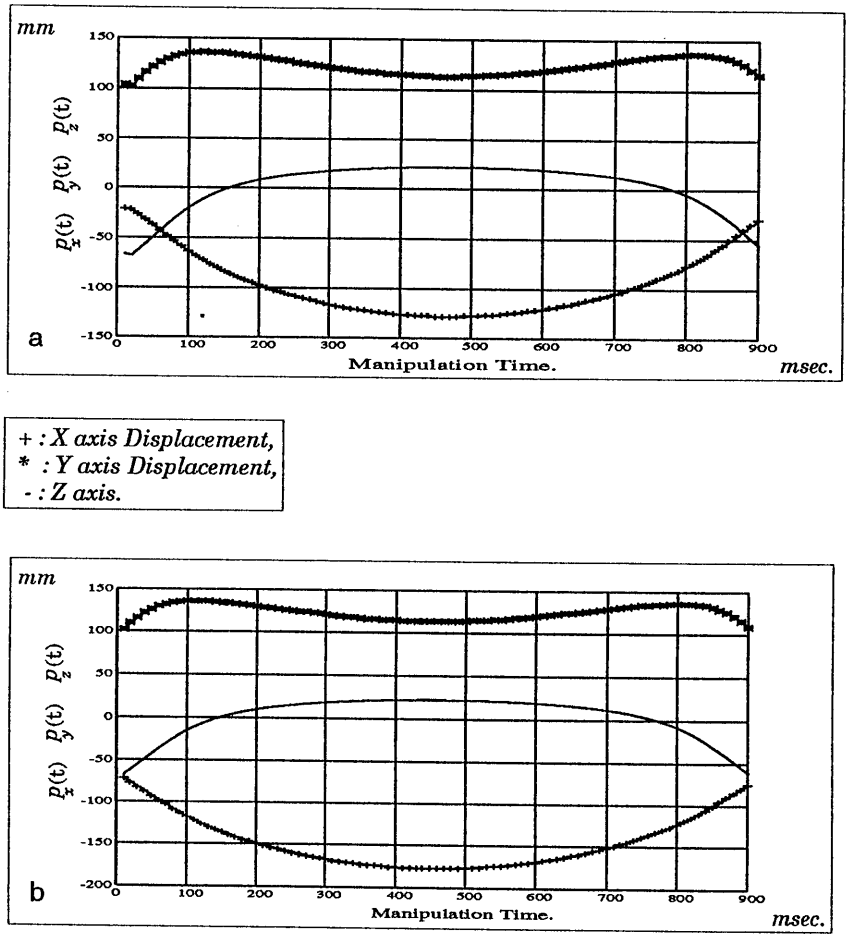


Figure 6. 18 : The Corresponding Fingertips Displacements Using RSI.
a : Third Fingertip
b : Fourth Fingers.

forces at the four fingertips will be analysed, based on the use of optimization techniques. As has been indicated in Chapter Five, two approaches of optimization have been adopted, the first is the extension of the use of internal forces optimization and the second the use of nonlinear inequality constraints optimization. Both solutions will be analysed and compared in terms of formulation , computational requirements and the continuity of solution.

(*i*) *Linear Constraints Optimization* :

For the analysis of the torque vector computation in achieving a defined manipulation task, this section illustrates the use of the internal forces minimization for moving a grasped object by the fingertips prehension. Here the main requirement is to keep the object in track while ensuring the contact forces do not stray from the frictional limits. The torque vector of calculation of the hand is divided in accordance with Eq. 6.14, into two main parts. The first is constraint with the inverse dynamic of the hand which has been based on computed torque technique. The second is the ability of the hand to generate torques that are of importance in keeping the fingertips in contact with the object surface, which is represented by optimization.

(*ii*) *Internal Forces* :

Since the whole concept of linear constraints quadratic optimization is the optimization of the internal force vector, Fig [6.19] shows the six internal forces which have been computed during the manoeuvre of the object. Further multiplication of this internal force vector by a scalar will have the effect of increasing the grip on the object which might cause damage if the object is not rigid.

Fingertip Forces :

Fig [6.20] shows the corresponding real fingertip forces (normal and frictional) of the first

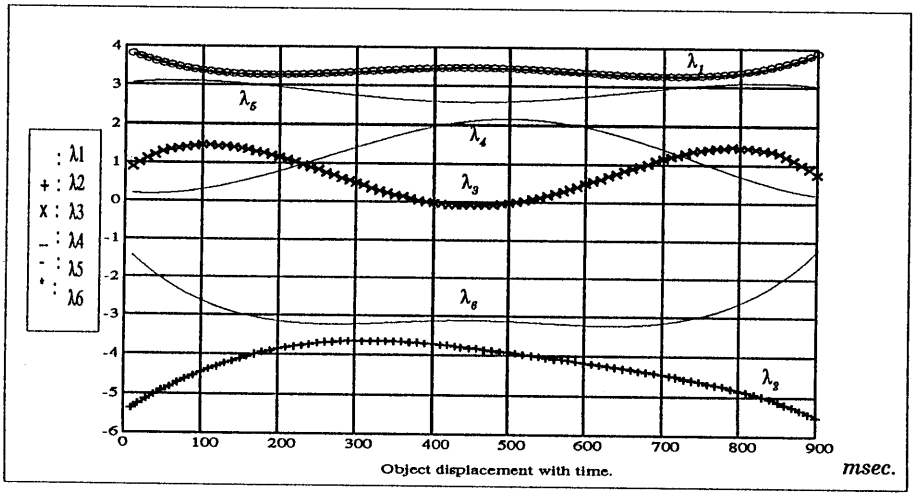
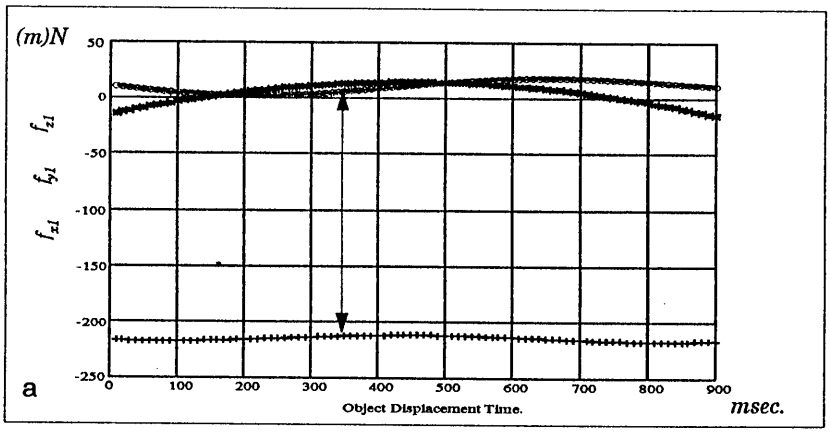


Figure 6.19 : Internal Forces Vector Used with the Null Space of the Grasp Transform.



** : x Force Components,*
o: y Force,
+: z Force.

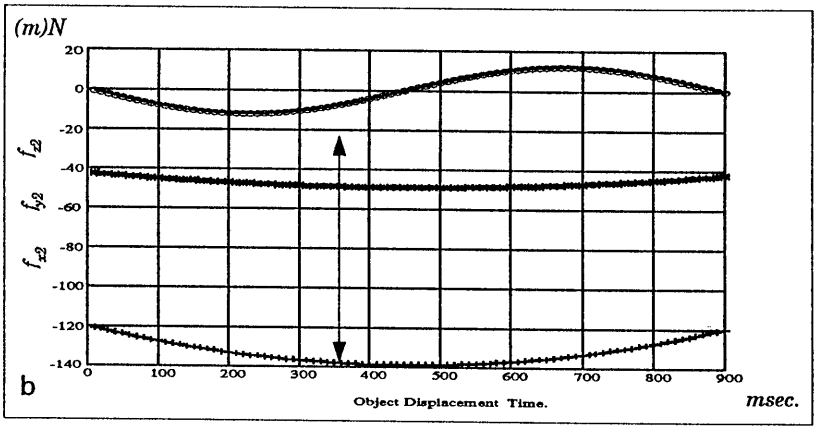


Figure 6.20 : a : First Finger Force Vector Using Internal Forces Optimization.
b : Second Finger.

and second fingers, while Fig [6.21] shows the fingertip forces for the third and fourth fingers. Using a similar argument, the normal forces f_{3z} and f_{4z} are normal to the frames attached at each contact point.

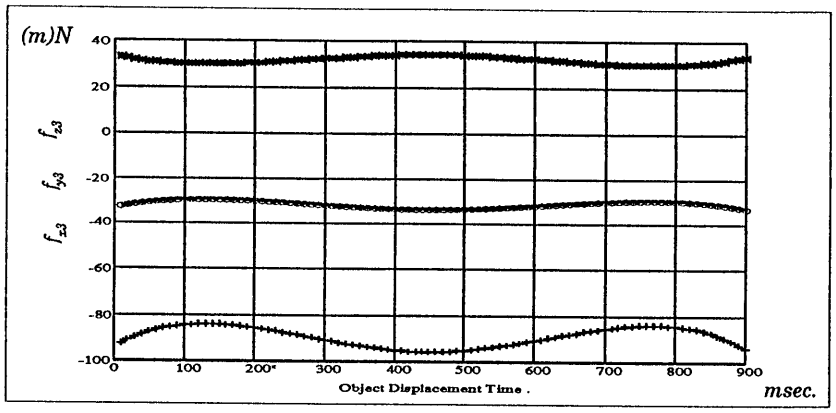
The normal force at the contact frames has greater value than the corresponding frictional forces at each fingertip, thus satisfying the frictional constraints. Furthermore, the normal and frictional forces satisfy the geometric constraints imposed by the fact that the first fingertip normal force should be in an opposing direction with respect to the second finger due to the orientation of the frames at each fingertip.

Since the required motion of the object is cyclic in nature, the corresponding forces should also be cyclic, ensuring that when grasping the object in a forward movement, the same forces are used for the reverse movement.

Fig [6.22] shows the corresponding objective function to be optimized, the sum of squared internal forces. The objective function has taken a cyclic shape with one maximum and one minimum due to the cyclic cartesian motion of the grasped object.

However, there is a comment in the shape of the objective function obtained which represents the summation of the squared fingertip forces. The objective function has reached a minimum and maximum for the same object displacement in the forward and return of the object.

The use of internal forces optimization in robot hands will optimize the magnitude of these internal forces, hence, the cost function shown in the figure represents the summation of these internal forces magnitude rather than the real forces themselves. Due to the requirement of the hand to grasp the object against the gravity effect at zero time of



* : x components of force,
o : y components,
+: z components.

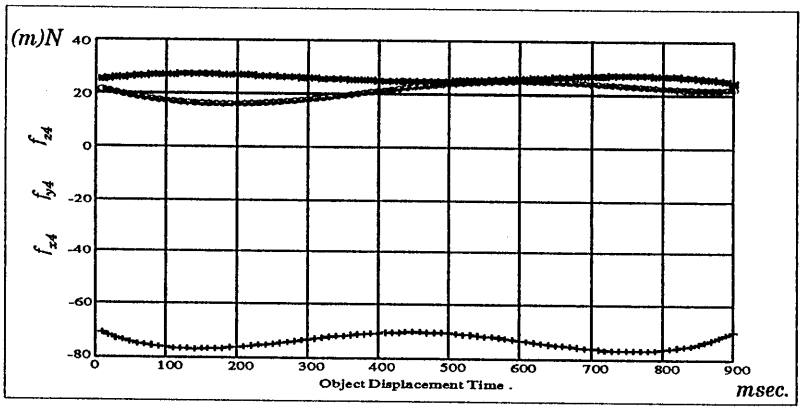


Figure 6.21 : a : x y z Force Components of Third Fingertip.
b : Fourth Fingertip.

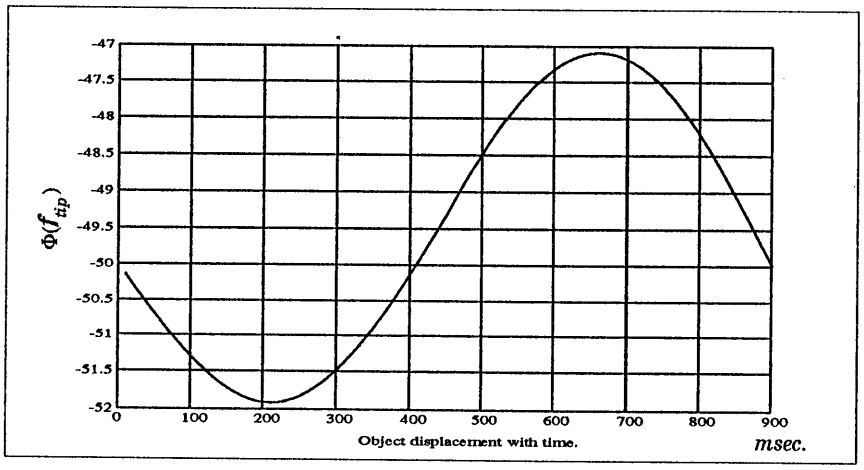


Figure 6.22 : The Objective Function to be Optimized, (*Internal Forces Method*).

manipulation, the graph shows that at zero time there are internal forces of magnitude $-50.2\,mN$, required to grasp the object.

The cost function shows it has reached a minimum and maximum at a repetitive time, indicating that, although the object dynamic after the middle of the task is similar to the first half, the computed internal forces could be different, while the constraints are still active.

Fig [6.23] shows the corresponding object dynamic force vector F_b. It is clear from the graph that the object dynamic is dominated by the object weight. However, there are also the inertial forces which the hand has to overcome. The resultant object force vector generated by the hand itself is shown in Fig [6.24-a], where, if this force vector were added vectorially to the object dynamics, the motion would result in the entire force system of the hand-object satisfying a zero resultant force as shown in Fig [6.24-b].

Joint Torques :

Fig [6.25] and Fig [6.26] show the corresponding finger joint torques which are responsible for the generation of the fingertip forces.

The torque generated to allow the fingers to grasp the object has to be added to the torque generated to move the hand links, especially when the hand is to move the fingers at high speed, where the centrifugal and coriolis force of the object and the links are to be accounted for. These combined torques are the result of decoupled torques which will be acting at a particular joint during the motion.

(iii) Nonlinear Constraints Optimization :

Within this sub-section we discuss the employment of nonlinear inequality constraints for

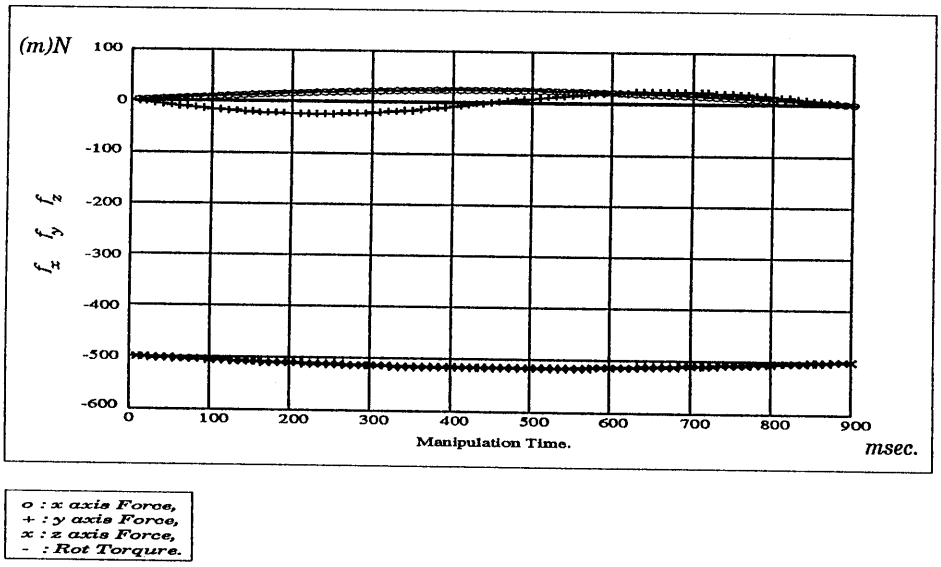
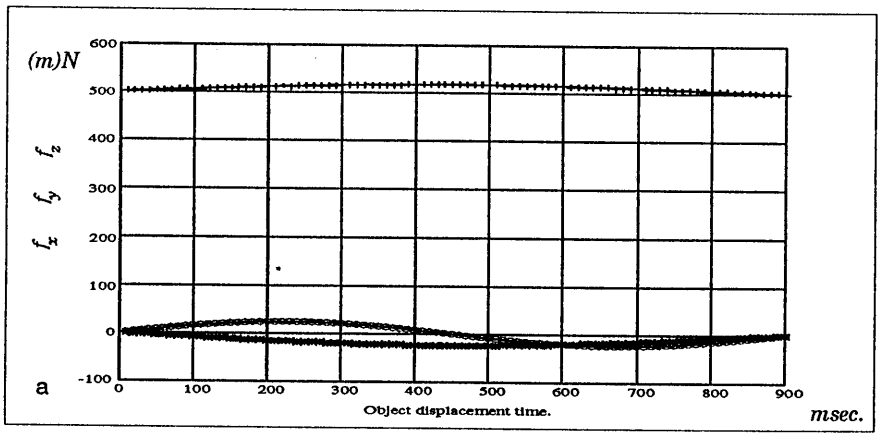


Figure : 6.23 : Corresponding Object Resultant Force Due To the Defined Trajectory.



o : x axis Force,
+ : y axis Force,
x : z axis Force,
- : Rot Torqure.

$$F_b - G f_{tip} = 0$$

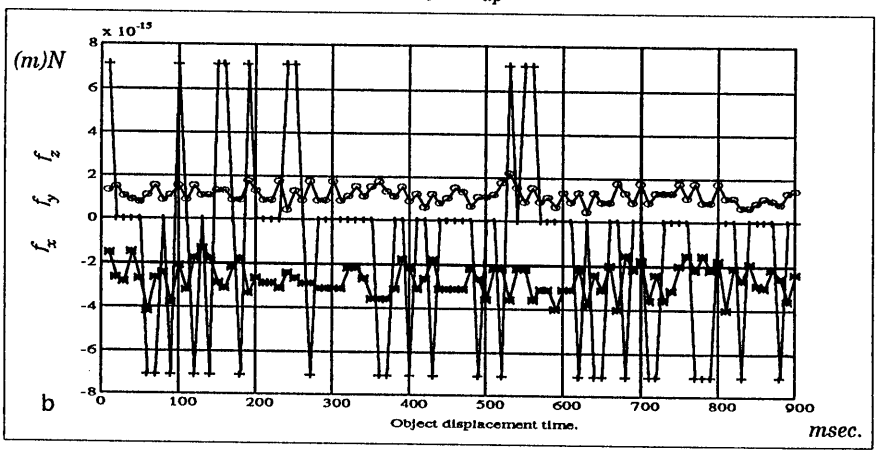
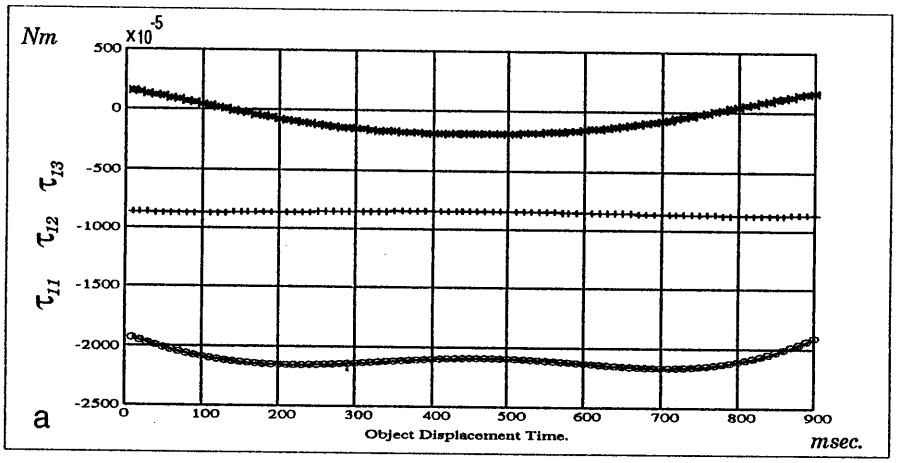


Figure 6.24 : a : Resultant Force of Object Due to Fingertips Forces.
b : Object - Hand Resultant Force Vector.



* : Proximal Joint,
o : Medial Joint,
\+ : Distal Joint.

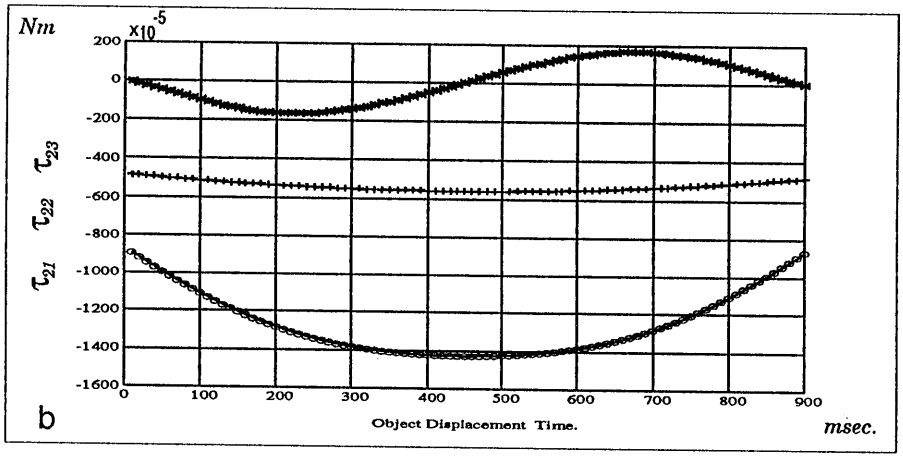
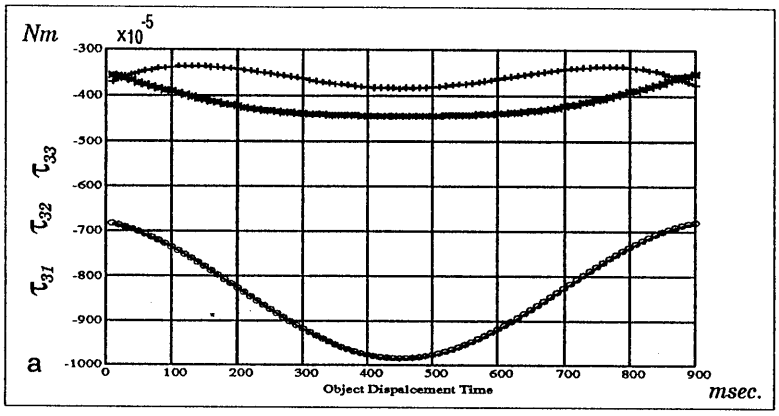


Figure 6.25 : a : First Finger Joints Torques Using Internal Forces Optimization.
b : Second Finger Torques.



* : Proximal Joint,
o : Medial Joint,
\+ : Distal Joint.

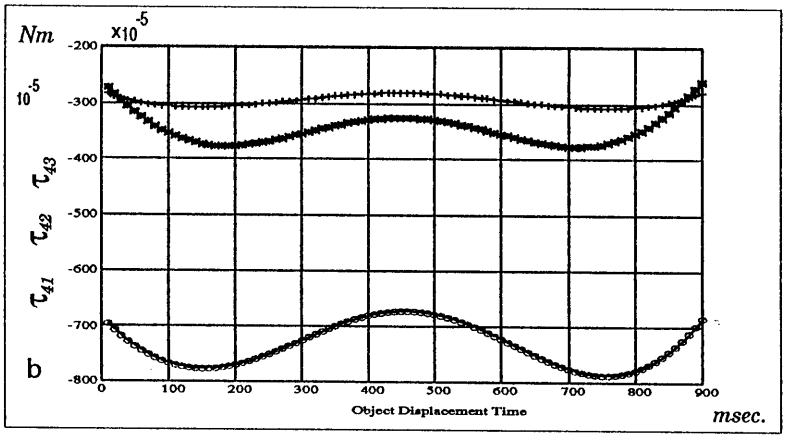


Figure 6.26 : a : Computed Torques for the Third Finger.
b : Fourth Finger.

calculating manipulation forces.

Using the same analysis done for the internal forces optimization , we analyse the force to grasp an object during object motion. However, instead of calculating the internal forces which are added to the pseudo-inverse solution to generate the appropriate fingertip forces, the fingertip forces are computed directly by optimizing the suitable forces which will satisfy both the equality and nonlinear inequality constraints already discussed.

Fingertip Forces :

Fig [6.27] shows the corresponding real fingertip forces (normal and two frictional) of the first and second fingers , while Fig [6.28] shows the opposing fingertip forces for the third and fourth fingers. The normal forces in both fingers, f_{1z} and f_{2z}, have a magnitude of greater value than the corresponding frictional forces at each fingertip, thus satisfying the frictional constraints imposed by each contact. The direction of the normal forces f_{1z} and f_{2z} are opposite due to the rotation of contact frames at each contact point.

Fig [6.28] shows a similar description, of the generated fingertip forces for both the third and fourth fingers. First the normal forces f_{3z} and f_{4z} are of greater magnitude than the corresponding frictional forces f_{3x} f_{3y} f_{4x} and f_{4y}, meanwhile of similar direction of application at the object surface. The direction of the normal forces in all the fingers do satisfy the constraints imposed by the directional norms.

Fig [6.29-a] shows the corresponding cost function of optimization which represents the summation of square fingertip forces. The cost function approaches a maximum value at the middle of the manipulation task, indicating the increase of required forces at this point. Furthermore, the cost function has similar behaviour during the first and second phases of manipulation. For the manipulation task to start at zero time the cost function is not zero due to the requirement of the hand to apply an amount of force to grasp

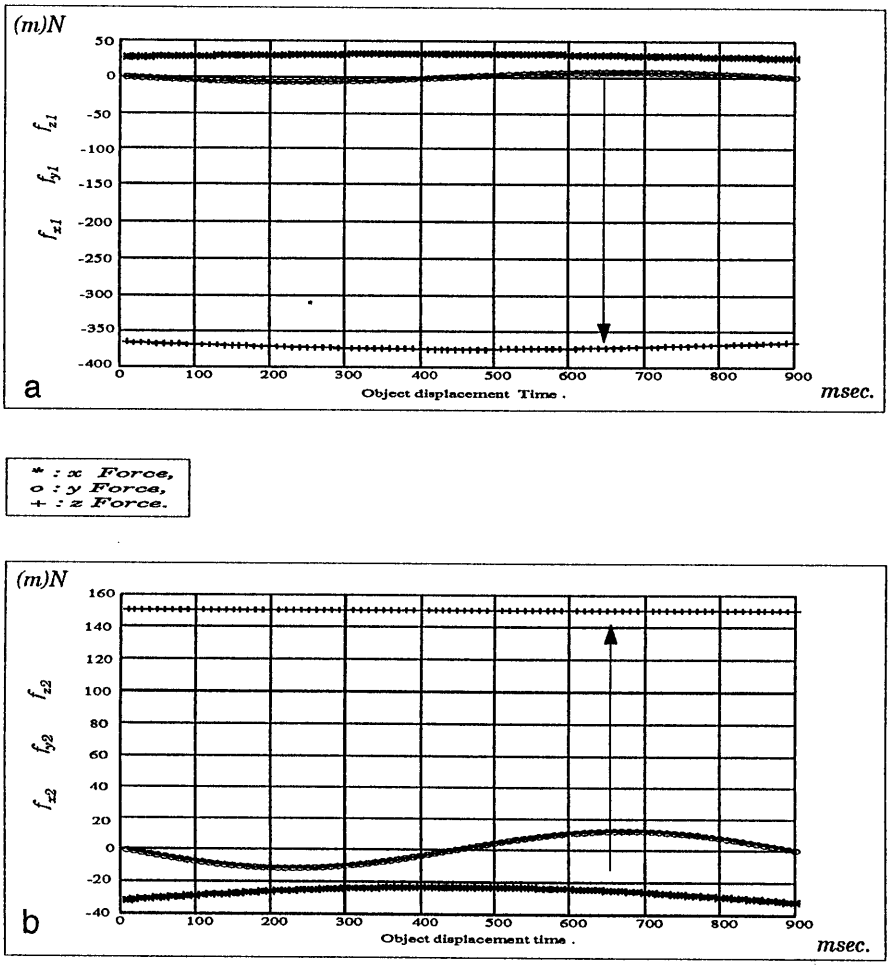


Figure 6.27 : a : First Finger Contact Forces.
b : Second Finger Contact Forces x y z Components.

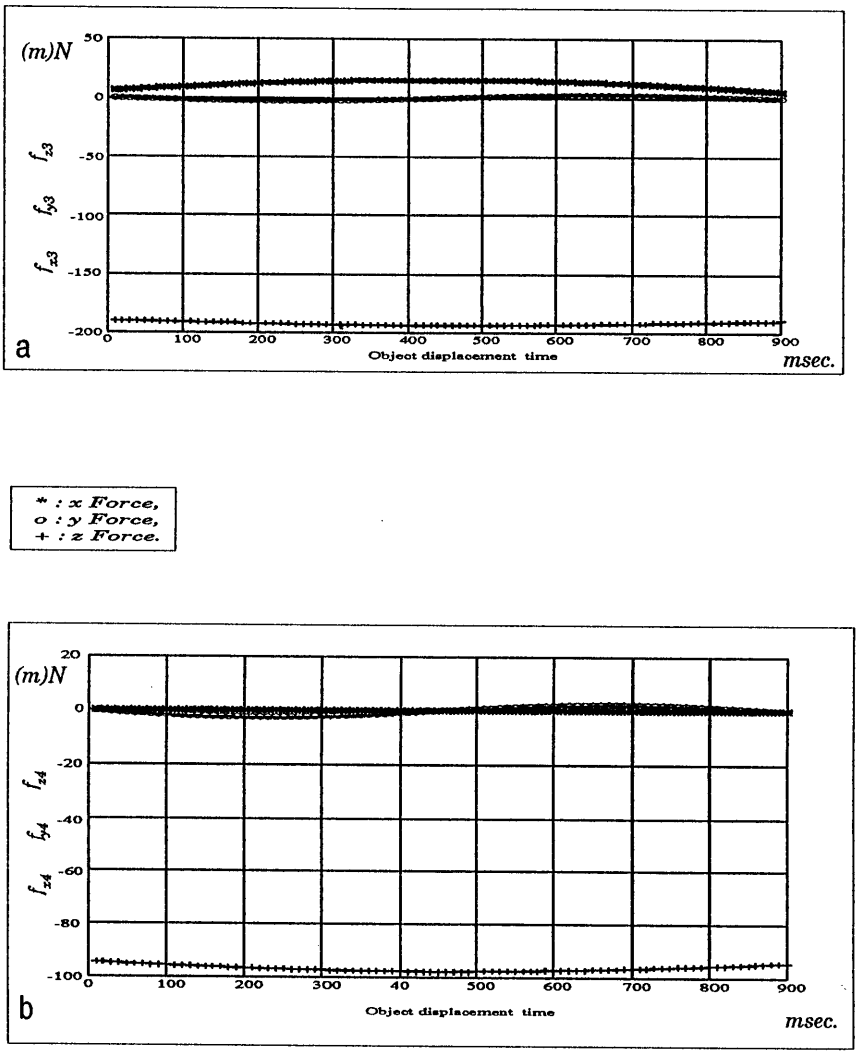
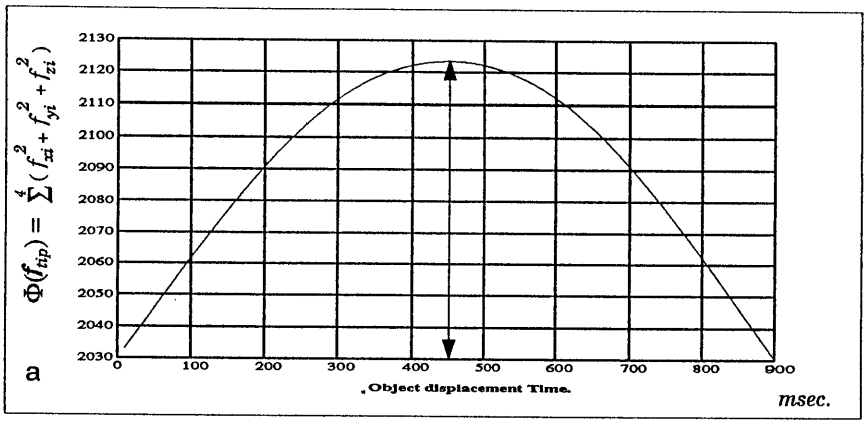
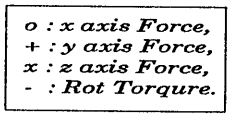


Figure 6.28 : a : Third Fingertip Forces.
b : Fourth Fingertip Forces.





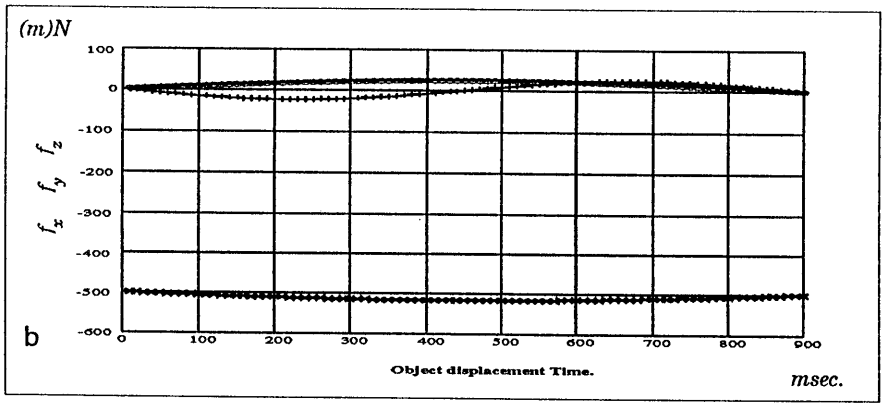


Figure 6.29 : a : Objective Function of Optimization for Nonlinear Constraints.
b : Corresponding Object Resultant Force Due To the Defined Trajectory.

the object against gravity.

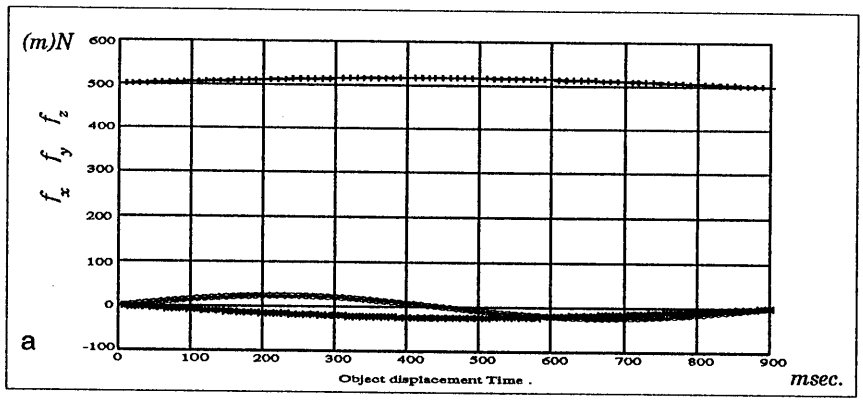
Fig [6.29-b] shows the object resultant force due to the object motion. It is clear from the graph that there is a biasing force added in the Y direction, defining the force due to the object weight. Thus the hand forces have compensated for the object weight in addition to the dynamic forces due to its motion. Fig [6.30-a] shows the corresponding generated resultant force of the object due to the motion, which is similar to the one obtained for the internal forces optimization. Fig [6.30-b] is the vector of resultant force in the hand-object, since the resultant force is to be zero, the six dimensional resultant force vector is zero, similar to the internal forces optimization method.

Joint Torques :

Fig [6.31] to Fig [6.32] show the corresponding finger joint torques which are responsible for the generation of the fingertip forces. For instance, Fig [6.31] is the torques produced by the first and second fingers in the hand compensating for the grasped object dynamics during the entire manipulation task. Unlike force computation using internal forces optimization, due to the symmetric nature of the task, the generated torques are symmetric around the middle of the task where the object reaches its maximum motion. The other observation is that torques generated by the proximal joints in both fingers nearly oppose each other. In a similar way, Fig [6.32] illustrates the generated torques in the third and fourth fingers in total. The generated torques are bounded within the maximum torques produced by the hand actuators.

(6.7) COMPARISON BETWEEN LINEAR and NONLINEAR FORCE OPTIMIZATION

In the last Section both linear and nonlinear constraints optimization techniques have been used to compute the fingertip forces without mentioning any aspects of the computational



o : x axis Force,
+ : y axis Force,
x : z axis Force,
- : Rot Torqure.

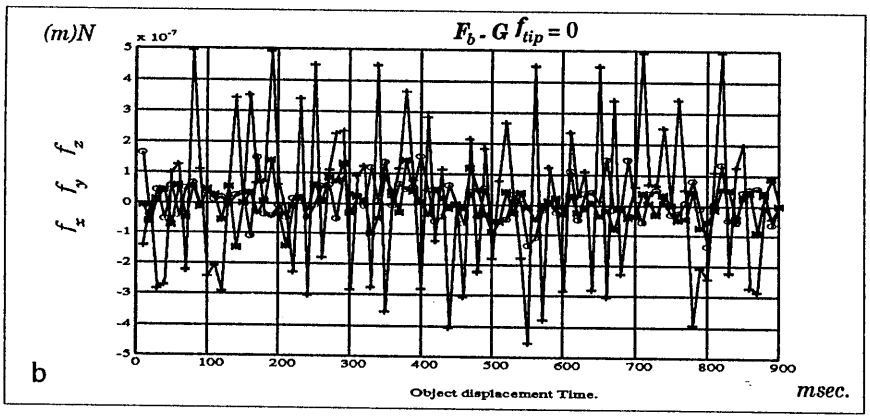
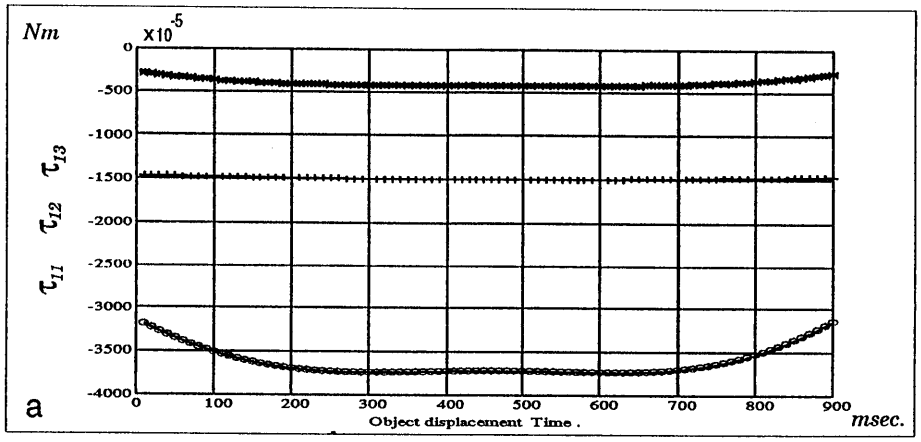


Figure 6.30 : a : The Object Resultant Force Due to Fingertips Forces.
b : The Entire Hand-Object Resultant Force = Zero.



* : *Proximal Joint Torque,*
o : *Medial Joint,*
\+ : *Distal Jont.*

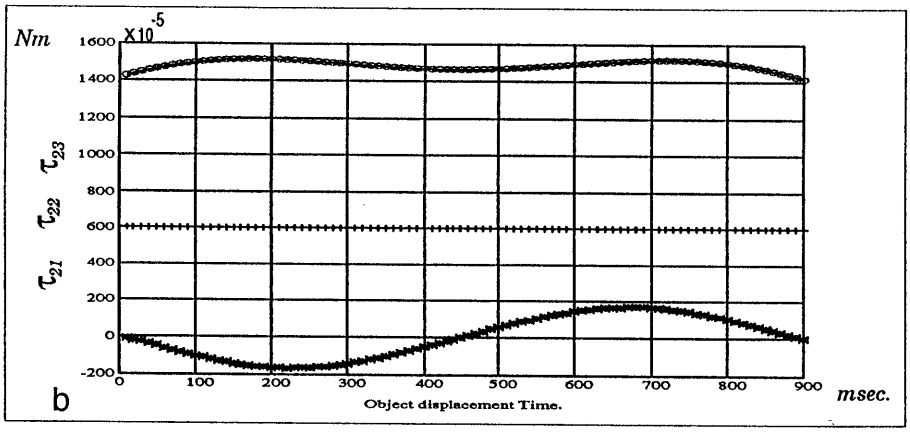
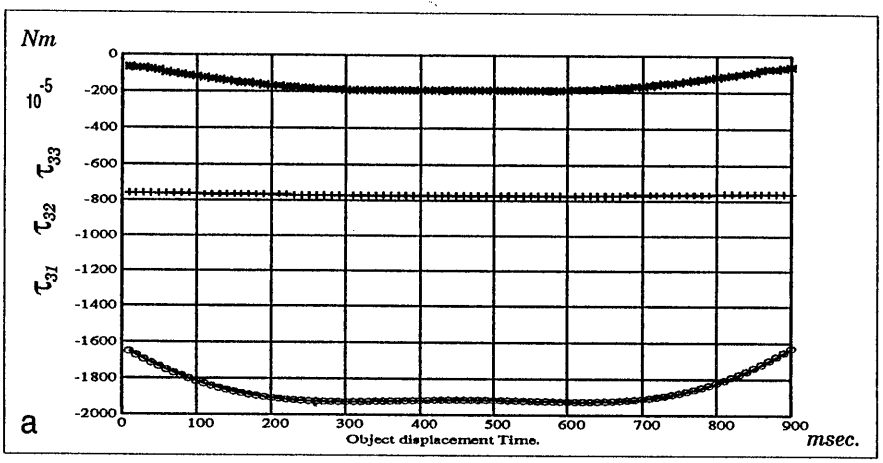


Figure 6.31 : a : First Finger Computed Torques.
b : Second Finger Torques.



* : *Proximal Joint,*
o: Medial Joint,
+: Distal Joint.

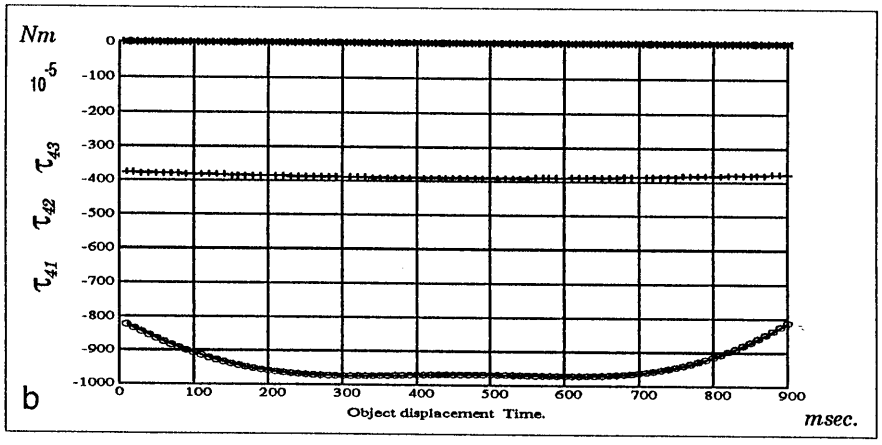


Figure 6.32 : a : Third Finger Computed Torques,
b : Fourth Finger.

comparison between the two approaches. Within this section requirements for formulating the optimization variables in terms of the hand Jacobian and the object dynamics will be investigated and compared in terms of the required arithmetical operations.
The issues of comparison between the employment of the linear and nonlinear optimization algorithms is the speed of convergence to an optimial solution and the continuity of solutions. Speed of convergence to an optimal solution is mainly determined by the number of constraints to be solved, whereas the continuity of solution is determined by the numerical algorithm itself and the nature of the objective function to be optimized.

If the obtained fingertip forces for a smooth variation in the object dynamics is discontinuous, this will result in the change of the joint torques over all the hand for small variations in the object dynamics. Table [6.1] shows the computational requirements for both the linear constraints and nonlinear constraints optimization formulations. The requirements for internal forces optimization has been dropped to more than the half using the nonlinear optimization approach.

Operation	*Linear Optimization*		Total	*Nonlinear Optimization*		Total
	Addition	*Multiplication*		*Addition*	*Multiplication*	
f_{pA}	60	72	132	0	0	0
$\lambda\eta$	60	72	132	0	0	0
F_b	6	9	15	6	9	15
$f_{pA}+f_{pA}$	12	0	12	0	0	0
$B-\Pi f_{pA}$	28	50	78			
J_h	12	32	44	12	32	44
$J_h^T f_{tip}$	6	72	78	6	72	78
Total	491			132		

Table [6.1] : Computational requirement for linearized friction cone and nonlinear optimization approach without including *householder* rotations and for non zero *null space* matrix of G.

Both techniques minimize the contact forces applied by the fingertip prehension in the object, however the computational aspects of the first method (internal forces optimiz-

tion) is more intensive due to the use of inverse of the Jacobian matrices of the all fingers to formulate the linear constrains outside the optimization algorithm.

Regarding the speed of convergence to an optimal solution, the number of constraints determines how far the numerical method has to fulfil the inequalities.

SUMMARY

Chapter Six has focused on the development of controller design which includes the dynamic effect of the hand-object system. It started with the Lagrange formulation for the combined hand-object system linked through the grip transform. The full dynamic model of the hand has been developed as a basic model for manipulation by a multi-fingered robot hand.

Due to the nature of motion and the dependence of friction forces to keep the object stable even during high speed manipulation, two main issues have been of importance. First, a kinematic problem represented by the approach to singularity of the entire hand Jacobian, and second, the need to keep contact by fingertips during object motion.

The first has been solved using RSI for the multiple contact system with different measure of manipulability for each chain, whereas the contact problem has been based on the use of optimization using both internal forces optimization and nonlinear constraints optimization.

CHAPTER SEVEN

PARALLEL COMPUTATION APPROACH OF ROBOT HANDS

(7.1) INTRODUCTION

A major problem in effectively realizing advanced manipulation schemes for a multifingered robotics system has been the difficulty of implementing the kinematic and dynamic relations required for dynamic coordination in real time. This problem is accentuated by the increasing structural and task complexities of the next generation of robots under development. Coordination of multiple-finger systems operating in higher speed regimes, while making and breaking contact with the environment, places stringent computational demands on the control system.

Determination of the Inertia, Coriolis and Centripetal terms in addition to the Gravity terms as presented earlier involves a considerable amount of computation as has been discussed by CHEN *et al.* [1988] and JAVAHERI and Orin [1991]. In case of robot hands holding an object, another task arises: the control of the constrained motion of the object by the computation of fingertips forces.

Chapter Six has discussed the concept of computing torques for constrained coordinated motion of the fingers; although using such complicated control law is a requirement, the direct application of such control is not feasible for real time implementation. CHENG and ORIN [1991], and CHARLES and SAKON [1990] investigated the constrained equation by subdividing the entire equation into inverse dynamics and force distribution problems and solved them separately by intensive computations. However, relationships exist between these two main issues which have to be investigated.

This chapter presents the employment aspects of transputer based control for the coordinated control used in the manipulation of an object grasped by a four fingered robot hand. The main concern of the transputer is how different processors in the network communicate the variables. This chapter does not deal with the physical implementations

aspects, it deals with how dynamic and kinematic operations can be simplified for parallel processing.

Chapter seven has been divided into six sections. Section (7.2) presents the problems associated with a constrained motion dynamics. Section (7.3) investigates the computational complexity of the Lagrange dynamics associated with the four finger, whereas the dynamics and kinematics issues are dealt with in sections (7.4) and (7.5), respectively. Finally section (7.6) investigates the used optimization schemes.

(7.2) NATURE of PARALLEL PROCESSING

Within Chapter Six the constrained motion of a robot hand has been developed, where the computational cost of the overall dynamic parameters cannot be performed using a single processor system. There are several control algorithms of computation for articulated system control that would involve the inclusion of the dynamic model of the overall hand such as ZEXIAWG *et al.* [1989] and SCHNEIDER and ROBERT [1992]. However, there are several associated associated that need to be resolved prior to practical implementation. These are :

(*i*) Greater computing power is required to enable the on-line implementation of certain control laws which cannot be achieved using a single processing unit. Although simplified or customized dynamic formulations have been used extensively as done by PAUL [1981] and ZOMAYA and MORRIS [1989], even the simplified modelling suffers from computational deficiency arising from the large amount of multiplications and additions which hamper their on-line implementation.

(*ii*) The constrained nature of motion of an object within the hand palm requires the on-line application of force computation which might involve optimization technique due to

changes in object dynamics.

(*iii*) The dynamic model must be simplified in a way that makes the grouping of dynamic parameters direct and systematic.

(*iv*) Most robot hands have a three degrees of freedom kinematic structure of each finger, thus the possibility for the finger to be in singular is very high without the approach being avoided. This would require the employment of advanced inversion algorithms in real time which are numerically time intensive.

(*v*) Robots hands are devices which are usually attached to robot arms, hence the gravitational force effect in the dynamics of the hand will be orientation dependent ; this adds extra orientation parameters to the complexity of the dynamics.

Since a numerical nonlinear constraint optimization approach has been adopted for calculating the fingertip forces for a manipulation task, the optimization algorithm itself can be sub-divided into a number of sub-tasks for implementation in parallel processing machines.

(7.3) ASPECTS of PARALLEL COMPUTATION of the HAND DYNAMICS.

In Chapter Six the concept of object manipulation and displacement within the hand palm has been presented. For very fine manipulation and high speed of operations the dynamic model of the hand is of great significance that has to be accounted for in applied control. Furthermore, in the coordinated motion of the fingers, modelling of the hand-object subsystems have been treated as if they are one dynamic system coupled through the points

of contacts ; this adds further complications because of the object dynamics and forces acting at fingertips.

While discussing the manipulation of an object using the potential of parallel processing machines, the control law defined by Eq. 6.14 is to be implemented in a real time basis. The problem can be defined as: the coordinated unconstrained motion of the hand fingers, thus τ_{hand} , in addition to the constrained motion which involve the fingertips forces and the corresponding torques, τ_{object} . This section will concentrate on the concept of parallel computation of the hand dynamics: whereas the computational requirements for the force optimization implementation will be discussed in section (7.6).

The parallel issue of one finger dynamics is much simpler than the dynamics computation for a six degrees of freedom robot due to the fewer degrees of freedom. The entire hand dynamics consisting of the individual fingers can be simplified because relationships among the fingers's kinematic structure exist which can be utilized. Such kinematic structure suggests that one finger dynamics will be sufficient to be used for the entire hand as long as the fingers start and end motion at the same time and the fingers are of similar dynamic parameter, which is the case in this research.

Furthermore, from a kinematics point of view, the location of the fingers would suggest that finger Jacobians would be similar regardless of the rotation needed at each point of contact.

Parallel Scheme :

The solution of the dynamic problem incurs a heavy computational load. This computation of the highly coupled dynamic equations has always produced a bottleneck in real-time advanced dynamic control of the links. Parallel processing techniques can now be used to

reduce the determination time for models of a highly mathematical nature.

This subsection presents the aspects of a parallel processing scheme which allows us to execute control computation in the minimum time on a multi-transputer system. Key points for parallel processing on a general transputer system are : how to decompose the computation complexity into several small parts called tasks (*and subtasks*) and how to allocate or schedule the tasks to these individual processors through task time schedule.

7.3.1) Computational Modules of Euler - Lagrange Equation of Motion.

Since the finger dynamics have all been based on the use of the Euler-Lagrange equation of motion as derived in Appendix [A5], the computation issues would start from this formulation.

An investigation of the E-L equations of motion confirms a certain amount of parallelism with a large amount of sequentialism in the flow of computation, LEE [1993]. The functional decomposition separates the inertial, coriolis, centrifugal and gravity terms into parallel form. Added to this there will be torques to overcome the object dynamics represented by $J_h^T f_{tip}$.

Fig [7.1] shows the computational flow and data dependence of the E-L equations for one finger in the hand. All blocks represent computational modules, with the object being computed listed in the block, alonge with the number of computations required by the dynamic modules.

The figure shows that the gravitational, coupling forces (*coriolis and centrifugal*), and inertial terms can be computed in parallel without any major dependencies on data from the other terms except for the $U_k(\partial T_o^k)^T/(\partial\theta_i)$, which is used for computing both

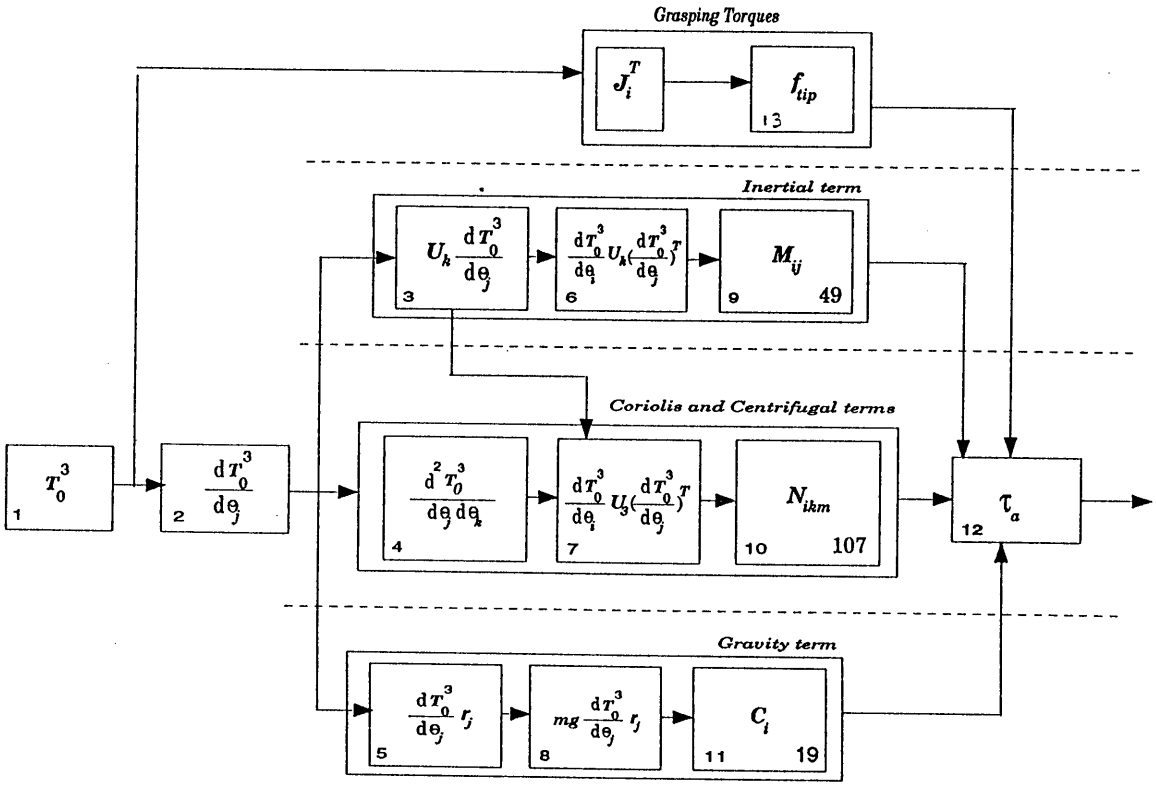


Figure 7.1 : One Finger Euler-Lagrange Equation of Motion Computational Flow, and four levels of parallelism.

the coupling and inertial terms. The main bottleneck in this algorithm is the computation of the coupling terms like $(\partial^2 \boldsymbol{T}_o^{\,k})/(\partial\theta_i\partial\theta_k)$ and $[(\partial^2 \boldsymbol{T}_o^{\,k})/(\partial\theta_j\partial\theta_k)]\boldsymbol{U}_k[(\partial \boldsymbol{T}^k{}_o)/(\partial\theta_j)^T]$ which exhibit a highly sequential flow of computation rather than parallelism.

A major concern of this equation is the computation of the hand inertia matrix $\boldsymbol{M}_h$, which by itself consists of the individual finger's inertial matrices.

The main distinction between the configurations employed is how the task is classified, that is, the amount of work carried out by each processor and the overhead caused by the communication between the separate transputers in the network. In order to evaluate the feasibility for real time operation, the computational requirements for setting hand inverse dynamics and force distribution problems will be investigated separately.

7.3.2) The Computational Investigation

Off-Line and Online :

Broadly speaking there are three main intensive computations in object manipulation. The first is what was discussed earlier, the hand dynamics, the second is the kinematics which includes the Jacobian formulation, its differential, and its inverse and the third is the computation of forces distribution which could include optimization.

1 : Hand Dynamics :

Having considered this, there are a few terms which can be computed offline before an on-line computation starts. Further investigation of one finger dynamics suggests that there is a simplification in the model that can be used, as there are zero elements in one finger inertia matrix. Due to the dynamic structure of the finger these zero terms are given in Eq. 7.1 :

$$M_1 = \begin{bmatrix} D_{111} & 0 & 0 \\ 0 & D_{122} & D_{123} \\ 0 & 0 & D_{133} \end{bmatrix} \tag{7.1}$$

The other expression in one finger dynamics are the coriolis and centripetal terms:

$$\boldsymbol{H}_i = \begin{bmatrix} H_{11} & H_{21} & H_{31} & H_{41} \\ H_{12} & H_{22} & H_{32} & H_{42} \\ H_{13} & H_{23} & H_{33} & H_{43} \end{bmatrix} \tag{7.2}$$

For simplification, let us open the individual terms and explore the corresponding computational operation required. The corresponding computational requirements for the hand inertia, Centripetal, Coriolis and gravity are given in Table [7.1], Table [7.2] and Table [7.3] respectively.

Operations Count (OC)				
Term	***Operation per Term***			
	Multiplications		Additions	
	On Line	*Off Line*	*On Line*	*Off Line*
D_{11}	8	18	6	0
D_{12}, D_{21}	0	0	0	0
D_{13}, D_{31}	0	0	0	0
D_{22}	1	6	1	0
D_{23}, D_{32}	1	5	1	0
D_{33}	0	2	0	0
Total	10	31	8	0

Table [7.1] : Inertial Terms and the Number of Computation.

Operations Count (OC)				
Term	Operation per Term			
	Multiplications		Additions	
	On Line	*Off Line*	*On Line*	*Off Line*
H_{11}	16	19	10	0
H_{22}	12	19	9	0
H_{33}	9	8	5	0
Total	37	46	24	0

Table [7.2] : Coriolis & Centripetal Terms and the Number of Computations.

Operations Count (OC)				
	Operation per Term			
Term	Multiplications		Additions	
	On Line	*Off Line*	*On Line*	*Off Line*
C_1	0	0	0	0
C_2	3	8	3	0
C_3	1	3	1	0
Total	4	11	4	0

Table [7.3] : Gravitational Effects Terms and the Number of Computations.

2- Hand Kinematics :

Hand Jacobian: The second computational complexity of the algorithm is the kinematics which includes the Jacobian $\boldsymbol{J}_h$, its inverse $\boldsymbol{J}_h^{-1}$, and its derivative $\dot{\boldsymbol{J}}_h$.

The hand Jacobian can be simplified by looking at the individual fingers Jacobian, since some terms will drop to zero due to the kinematic structure of particular

fingers. Here the Jacobian of the first and third fingers is different from those of the second and fourth due to the chosen point of contact frame.

$$J_1 = J_3 = \begin{bmatrix} J_{11} & 0 & 0 \\ 0 & J_{22} & J_{23} \\ 0 & 0 & J_{33} \end{bmatrix} \quad \text{and} \quad J_2 = \begin{bmatrix} 0 & J_{12} & 0 \\ J_{21} & 0 & J_{23} \\ 0 & 0 & J_{33} \end{bmatrix} \tag{7.3}$$

3- Forces Optimization :

For the internal forces that consist of two main matrices, the first is the frictional constraints and the second the Jacobian which has been discussed above. The other part of the linear constraints is the corresponding finger Jacobian J_i which changes as the object undergoes a manipulation motion.

On-line Computation:

The on-line computations are discussed next, starting with the requirements for the linear optimization. The object dynamics can be rewritten in a simplified form rather than the one defined in matrix.

The use of the matrices in the constrained dynamic equation is totally time consuming while seeking fast computational requirements. One approach is to expand the terms in non matrix forms and omit the zero elements in the equations. For the linear optimization case, extra computations are required to formulate the problem as the fingers move with the grasped object.

Since the generalized inverse of the grip transform changes with time as the object dynamics changes, Table [7.4] shows the computational requirements for the $G^{+}F_b$ assuming the elements of the G matrix are obtained for non zero points of contacts.

Of great importance in the computation for the linear optimization is the null space vector representing the internal forces of the grasp. Also assuming non zero elements of the null space matrix of the grasp transform, the computational requirements are represented in Table [7.4].

The computation requirements of $\eta\lambda$ are mainly dependent on the structure of the null space matrix η which is dependent on the grasp transform, thus depending on the points of contacts around the object. Conversion from contact forces to the joint torques is achieved by a number of operations which are also summarised in Table [7.4].

Thus the computational requirements for the total constrained part of the Eq. 6.14 is totally determined by the G^+, η, F_b and the corresponding resulting internal forces magnitude λ. This is summarized in Table [7.4].

Operation	F_b		G^+F_b		$\eta\lambda$		$f_{pA}+f_{hB}$		$J_h{}^T f_{tip}$	
Calcuation	A	M	A	M	A	M	A	M	A	M
Linear Constraint	6	9	60	72	60	72	12	0	6	18
Total	M = 161		A = 144							
Nonlinear	6	9	0	0	0	0	0	0	6	18
Total	M = 99		A = 72							

Table [7.4] : On line Computational Requirements for the Linear and Nonlinear Constraints.

What has been formulated in terms of the computational requirements is the determination of the corresponding joint torques. In addition to this, for the use of the linear constrained type optimization, the problem is to be formulated in order that the Π and **B** matrices can be passed to the optimization algorithm. Table [7.5] show the corresponding

computational requirements of the problem formulation at each instance. The difference between force computation based on internal forces computation and nonlinear constraints can be seen as quite obvious.

While dealing with internal forces optimization, a number of matrix multiplication such as $\eta\lambda$ *and* $\boldsymbol{B} - \Pi \boldsymbol{f}_{PA}$ will increase the arithmetic needed. However, by employing the nonlinear optimization, this amount of computation is reduced. This reduction can be seen from Table [7.5].

The entire on-line *major* computation for the constrained and unconstrained motion of the four fingered hand holding a single object is shown in Table [7.5].

Terms	Add	Sub	Multi	Div	Total
Hand Dynamics M_h, N_h, C_h	144	0	204	0	348
Hand Kinematics J_h $\dot{J}_h$	3	18	8	18	47
Object Dynamics F_b	6	0	9	0	15
$G^T F_b$	60	0	72	0	132
Null Space $\eta\lambda$	60	0	72	0	132
Tips to Joints $J_h^T f_{tip}$	6	0	18	0	24
Formulation LinC1.	0	0	50	0	50
LinC2.	0	28	50	0	78
Final τ_h	48(36*)	0	0	0	48(36*)
Total LC	327	46	483	18	874
Nonlinear Constraints	213	18	293	18	542
Total NC	249	18	293	18	578

Table [7.5] : On-line Total Computational Requirements for Linear and Nonlinear Constraints by Treating Fingers with Different Dynamics.

* *for the nonlinear case.*

There are a number of computations which need to be performed in parallel. Listing them in order : The dynamic model of the hand which by itself consists of the dynamic model of the fingers, Jacobian computation at each sampling period, Inverse Jacobian, the force computation algorithm, object trajectory and the Newton-Euler formulation of the object dynamics and, finally, the constraints requirements for implementing optimization.

However, due to the kinematic and dynamics structure of the cybhand, the use of one finger dynamics or Jacobian is enough for other fingers in the hand, as long the fingers start and end their motion from the same initial values.

For instance, the second finger Jacobian has a different fingertip axis due to the location of the fingertip fame which opposes the other fingers. Furthermore, the gravitational effect or vector of the fourth finger C_4 is different from the rest of the fingers due to the orientation of the fourth finger by a defined rotation angle.

The computation of the described foregoing hand dynamic terminology with the optimization algorithm can be divided into five essential tasks which are relative to each other.

Task 1: Arrangement into 18 subtasks representing the effective and coupling inertia terms.

Task 2 : Arranged into 12 subtasks for the Coriolis and Centripetal terms.

Task 3 : Division into 12 subtasks representing Gravitational terms which add up to a total of all subtasks.

Task 4 : Deals with Jacobians, its differential in addition to the inverse hand Jacobian J_h^{-1}.

Task 5 : Is the computation of the Linear and nonlinear constraints to be utilized for the optimization algorithm.

Such subdivision is shown in Fig [7.2].

(7.4) HAND DYNAMICS

Aspects of Parallel Computation of Hand Dynamics :

The first three tasks of the parallel computations are the computation of the inertia (task1), centripetal and coriolis forces (task2), and the gravitational forces (task3).

Task 1 : Task 1 can be further subdivided into 4 subtasks representing the Effective and Coupling Inertia terms. Inputs to this task are the elements of the constrained acceleration coming from another task. Outputs from this task are the computed inertia torques of the hand.

Task 2 : Is subdivided into 3 subtasks representing the Coriolis and Coupling terms. The inputs are the joint space velocities, whereas outputs are the velocity dependent terms to be added to the outputs of Task 1.

Task 3 : Is further subdivided into 2 subtasks representing the Gravitational terms. Inputs are joint space vectors and outputs are torques added to results of task2.

(7.5) PARALLEL COMPUTATION of the HAND JACOBIAN and its INVERSE

Task4 : 1 *Hand Jacobian* :

In principle the inverse hand Jacobian J_h^{-1} is an essential factor in the computation of the contact forces and the relating of cartesian displacement of fingertips to their joint space vectors. Inversion of J_h is generally computationally expensive and difficult to implement in real-time, furthermore, if the hand Jacobian is ill-conditioned then advanced inverse computation to avoid this singularity would be even more computationally expensive.

The formulation of the entire hand Jacobian, which is based in PAUL's algorithm pre-

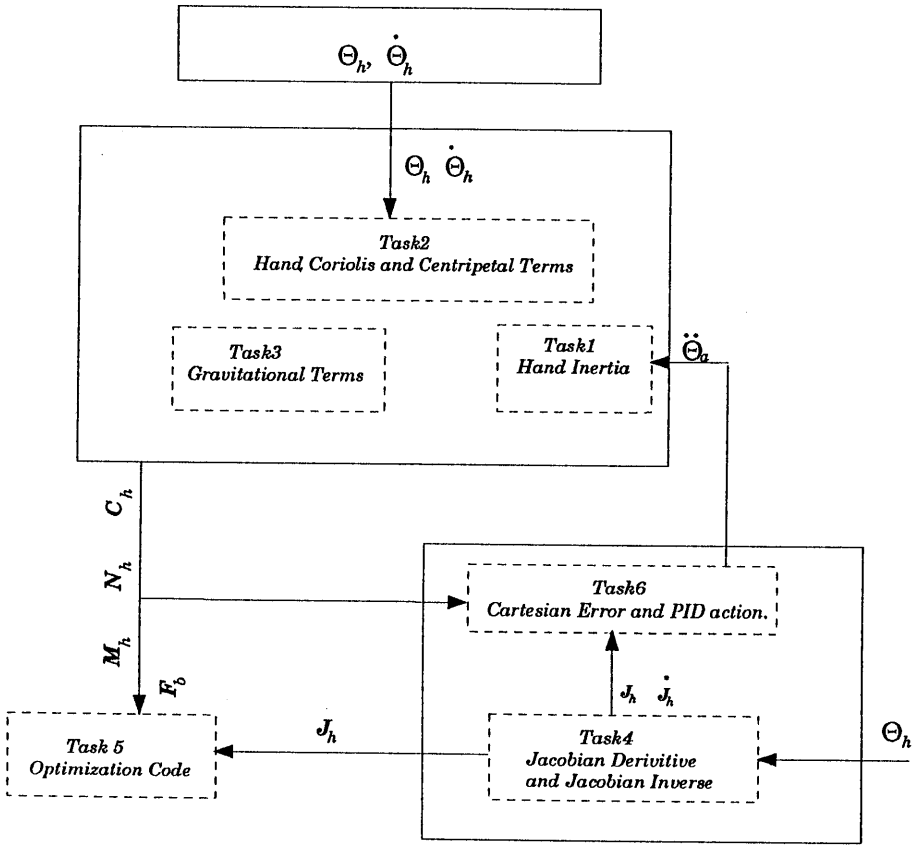


Figure 7.2 : Sub-division of the Constrained Equation of Motion into Six Sub-Tasks with Inter-Communication.

sented in Chapter Thee, would be extremely difficult to be implemented in real time if expressed as concatenated matrix form. Due to the involvement of the all the fingers in motion (*to start and end at the same instant*), the formulation can be simplified. There is an extra matrix of rotation at each fingertip describing the orientation of the fingertip frames with respect to the object surface as a requirement for formulating the optimization of contact forces. From the hand kinematic design, for an object motion within the hand palm, all fingers will have similar motion parameters, hence the computation of one finger Jacobian will be used for the other three fingers, provided an extra computation is required for rotating the fingertips frames. These extra rotations represent the reconfiguration of finger Jacobian elements for each finger, thus terms will be displaced in the matrix.

Using the same procedure given in Chapter Three, provided that the algorithm would require an extra matrix for each finger, hence :

$$A^3 d_i = [-n_x p_y + n_y p_x]\, i \quad [-o_x p_y + o_y p_x]\, j \quad [-a_x p_y + a_y p_x]\, k$$

$$A^3 \delta_i = n_z i \quad o_z j \quad a_z k$$

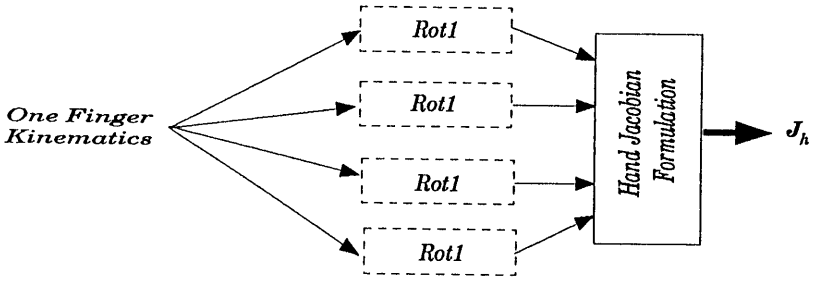
$$A^3_i = {}^0A_3\, ROT_i \qquad 1 \le i \le 4 \tag{7.4}$$

Parallel aspects of Jacobian would be the individual formulation of one finger which will be used to formulate the entire hand Jacobian through the appropriate consideration of fingertip rotations, as shown in Fig [7.3-a].

Task4 : 2 Inverse Hand Jacobian :

The other source of computational complexity in real time is the inverse of the hand Jacobian, especially when the matrix is in singular configuration and RSI technique is used instead of conventional inverse. To compute the inverse of the hand Jacobian Gaussian

Task 4 -1



Task4 - 2

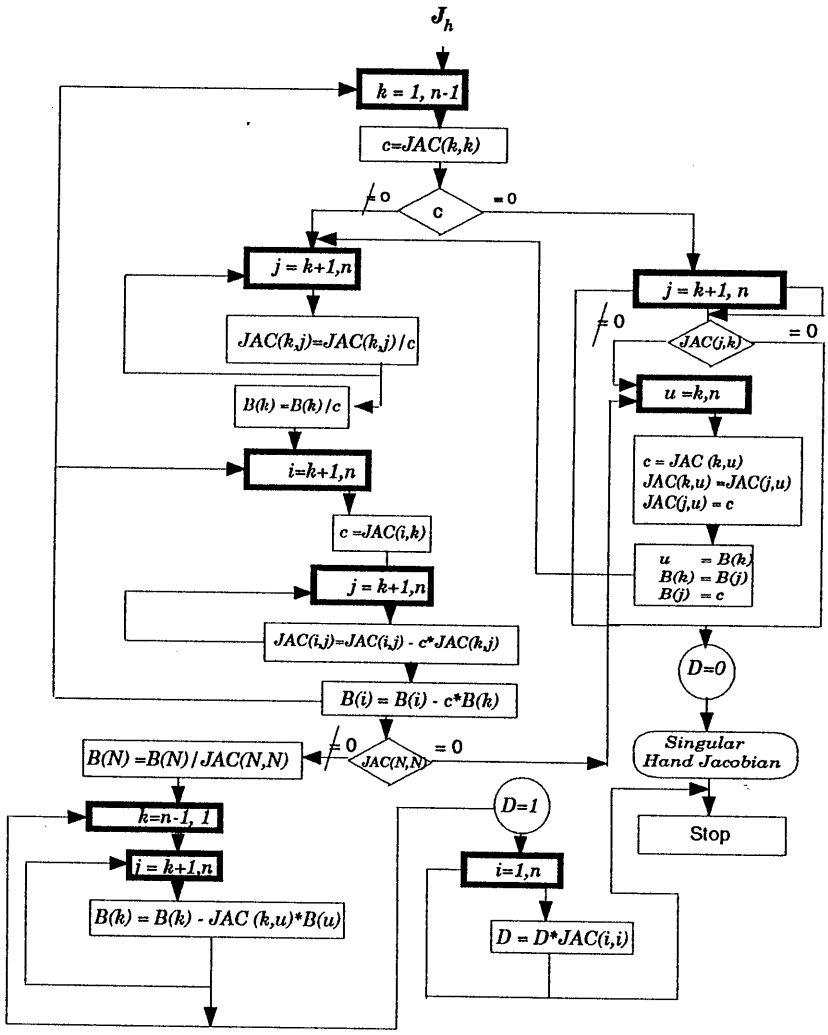


Figure 7.3 : Configurartion of Task4.
a : Simplifications in Computing the Entire Hand Jacobian
b : Gaussian Elimination and Its Support to Parallelism.

Elimination Method is adopted for its support of parallelism. Further simplification of applying GEM can be achieved by considering the fact that some elements of J_h are zero due to the kinematic structure of the fingers.

Parallel Gaussian Elimination Method :

The Gaussian Elimination Method, where a flow chart is shown in Fig [7.3-b], is used to solve a linear system of equations. For the parallel implementation of the algorithm we need to invert a $\Re^{[12\times12]}$ matrix corresponding to the four Jacobians of the four fingers. Since the hand Jacobian matrix J_h does not depend on the type of contact, the complexity in inverting it is determined by the number of fingers in the hand. The GAUSSIAN ELIMINATION method is a general algorithm for inverting an $\Re^{[12\times12]}$ matrix, hence a parallel implementation of the algorithm can be achieved.

(7.6) ASPECTS of PARALLEL REQUIREMENTS for LINEAR and NONLINEAR CONSTRAINTS OPTIMIZATION.

Task 5

The problem of involving numerical methods of optimization for the force computation is certainly another source of complication to be achieved in real time, thus it is time expensive. Within this section the requirements of constraint computation for the linearized constraints case and nonlinear frictional cone limits applied in Chapter Five and Chapter Six are discussed in such a way for parallel implementation.

7.6.1) Aspects of Parallel Linear Constraint Optimization

The main concern in using this approach is the processing time necessary to compute the general inverse of the grip transform G. This is computationally intensive for evaluating the particular solution if the fingertips slip over the object surface. For the non slipping fingertips $\dot{G}(t) = 0$, hence G^{-1} is computed at each instant of the manipulation task.

For dynamic computation of forces and at the beginning of each sampling period, the Jacobian changes in addition to the changes in the dynamic motion of the object, hence the constrained equation presented in Chapter Five or the optimization of the grasp internal forces is given by :

$$\Pi\eta\lambda \leq (\boldsymbol{B} - \Pi \boldsymbol{f}_{pA}) \tag{7.5}$$

where vector $\boldsymbol{B}$, which has already been discussed in Chapter five, has to be computed and updated accordingly. Within this section, the aspects of dividing such computations are discussed in a parallel format, rather than as a sequential implementation. The kinematic terms of computing Eq. 7.5 have already be discussed in Task 4, hence terms from this task can be used directly and what would remain is the object dynamics. Another issue of employing the internal forces optimization is the calculation of the real fingertip forces by adding the puesdo inverse solution to the null space solution.

Further Reduction :

Having considered the two main assumptions that : (*i*) The kinematic deign of the entire hand allows the fingers to have similar kinematics relations ; (*ii*) The dynamic structure of the finger links and the motion parameters (*position, velocity and acceleration*) are the same for each joint in each finger. Hence the kinematic and dynamic model of one finger can be employed to describe the dynamic behaviour of the entire hand for computing the required torque.

Furthermore, the Jacobian computation in real time for one finger can be used for describing the Jacobian of the entire hand $\boldsymbol{J}_h$ as long as the rotations at each fingertip are considered by the hand controller. If the fingertip rotations are made by a right angle (axes are shifted in orientation), then what will distinguish one finger Jacobian from another is the displacement of the Jacobian elements without change in the Jacobian matrix ele-

ments numerical values. For other than right angle rotations of fingertip frames, there will be extra elements appearing in the Jacobian matrix itself, representing the angle of rotation of the *ith* fingertip to the previous fingertip frame.

7.6.2) Aspects Implementing of the Nonlinear Constraints

Taking into consideration the number of arithmetical multiplications, the nonlinear equation is seen to be simpler, since it is formulated with only the object Newton-Euler dynamics, where it does not involve the pesudo-inverse of the Grip transform.

A further look at the nonlinear formulation would suggest that one computational complexity is in concatenating the grip transform (*which is a invariant matrix*) with the hand Jacobian. The computation of the hand Jacobian has already been discussed in task 4, hence what remains is the concatenating of the grip transform and the hand Jacobian.

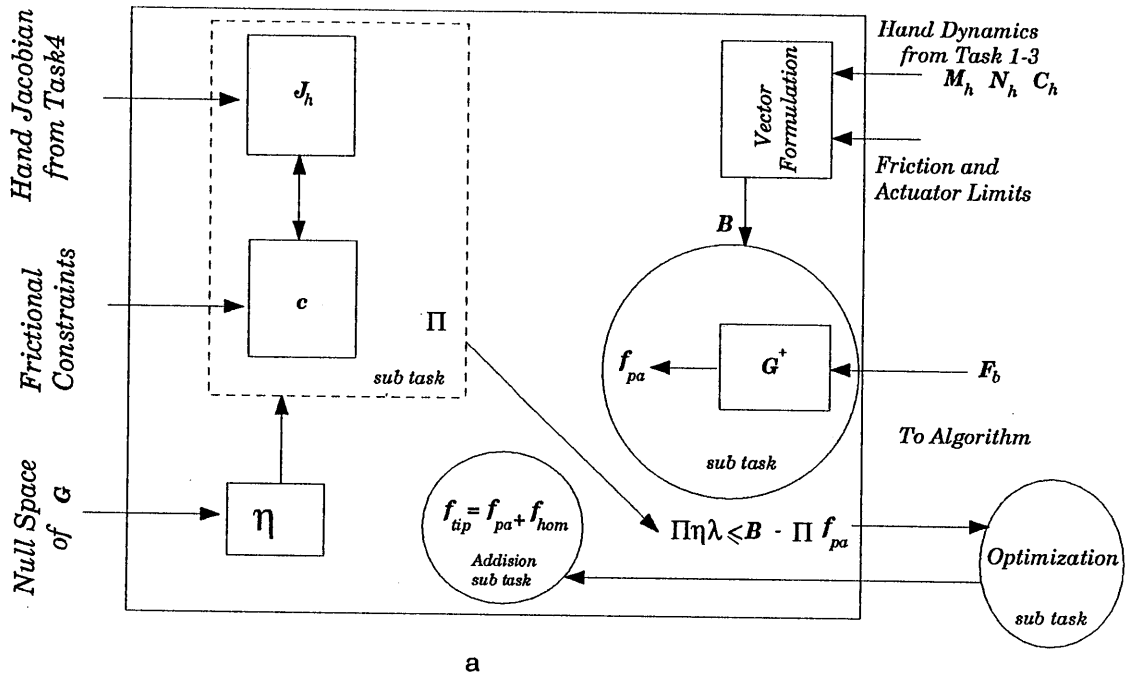
After the fingertip forces have been computed using optimization, these forces have to be converted to joint torques using the Jacobian transpose of the individual fingers. The input to this subtask will be the formulated hand Jacobain from task-4, whereas the output will be the computed torques required to grasp the object as shown in Fig [7.4-b].

SUMMARY

Generally this chapter has concentrated on the aspects of computing the hand-object equation formulated in Chapter Six. Due to the nature of the problem, parallel computation is the most feasible due to the dependence of various terms of this equation on each other.

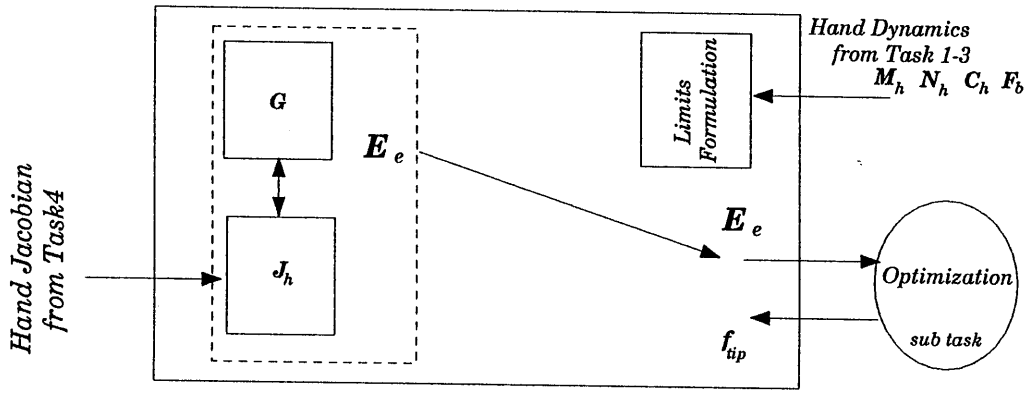
Further discussed in this chapter is the concept of using one finger dynamics and kinematics to formulate the entire hand dynamics and the kinematics used for torques and

Task 5-1 : Linear Constraints Internal Forces Optimization



a

Task 5-2 : NonLinear Constraints Optimization



b

Figure 7.4 : Task 5 : Possible Optimization Variables Formulation.
a : Linear Constraints.
b : Nonlinear Constraints.

Jacobian computations where certain conditions are satisfied.

It has been shown that the use of nonlinear constraints optimization has the advantage of reducing the arithmetical force computation over the use of internal forces optimization.

Finally the chapter considers the hand-object equation of motion as a problem which can be broken into smaller subtasks ; interconnection is established between these various smaller tasks if a parallel scheme of computation is implemented.

CHAPTER EIGHT

CONCLUSIONS REMARKS and FURTHER RESEARCH.

(8.1) INTRODUCTION

Robotics and automated systems play a significant role today and in the future in industrial locations, medical, remote manipulation, BRUNO [1992], manipulation in space, NAGASHIMA and NAKAMURA [1992] and under sea environment exploration.

Although robot hands play an important role in today's and future manipulation, they are not capable of performing works and useful tasks by themselves unless they are instructed and managed in a well structured manner.

In particular, robot hands start to be of significant use in automated environments where an object path is specified from a much higher level of control. This high level of control of object motion could either be obtained from a camera based vision system connected to a tele-operation mechanism, or defined object parameters of motion. In either case, manipulation is tendered by a number of issues, some of which have been elaborated within this thesis.

This thesis has addressed three of the issues regarding aspects of hybrid position-force control on a grasped workpeice by including the dynamic effect of both the mechanical hand and the grasped object for static grasping and dynamic manipulation.

Three main Issues :

(*i*) The employment of force feedback of the four fingers based on differential tendon tension sensing .

(*ii*) Use of nonlinear constraints of the frictional force cone in the computation of fingertip forces to produce stable grasp for static grasping and dynamic manipulation. The calculation has been achieved by optimizing the grasp contact forces. Results are then compared with internal forces optimization already proposed by NAKAMURA *et al.*

[1989] and, NAHON and ANGELES [1992].

(*iii*) Use of the dexterity measure of the finger Jacobians to define a strategy for inverting the entire hand Jacobian (*for the multiple contact system*) using a robust singularity inversion. The hand Jacobian is employed in the hybrid dynamic controller structure.

Furthermore, the above three concepts could not have been discussed unless the kinematic and dynamic models of the robot hand are available. Hence, the research has also looked at the following side issues:

(*i*) The mechanical design and the construction of a four fingered robot hand (cybhand), the derivation of the kinematics and dynamic modelling of the hand, and the definition of a strategy for control.

(*ii*) A brief discussion on the implementation of the constrained dynamic problem of the hand-object motion using the potential of a transputer parallel computation hardware structure.

The exploration of these three main issues, certainly, has wide the spectrum for further research in the mechanics of manipulation.

(8.2) THE HAND DESIGN.

One aspect of this research work was the design and the implementation of a four fingered robot hand. The hand has been designed with position control in all joints, and force control in the distal joints. The design of a four finger hand increases the control complexity, meanwhile, it has been shown that it increases the grasp quality measure by a considerable amount.

Although the use of tendon and remotely actuating the hand is one aspect of hands design, the development of fast and high driving torques direct-drive actuators are becoming popular as a substitute to the use of indirect drive mechanism. Hence, further research activity in the hand driving mechanisms, will undoubtly involve the use of direct drive system as a substitute for tendons. The finger design based on Flexible Micro-actuator by KOICHI *et al.* [1991] shows the future perspective of using flexible actuation in robot hands. However, the question of modelling such flexible devices from dynamics and kinematics points of view remains for further research.

(8.3) HAND KINEMATICS AND DYNAMICS.

8.3.1) Kinematics and Dynamics Relations

The work in hand research and the derivation of the all kinematic relations have been achieved using the conventional DENAVIT HARTENBERG relations. Although the use of the DENAVIT HARTENBERG transformation matrices to describe the hand-object motion parameters is not an obvious task in multi-fingered robots hands due to the parallel nature of contact motion, they have shown the possibility to have a full kinematic and dynamic models of the hand-object system which are of great importance for control.

The computation of the direct (*forward*) and inverse Jacobian plays a major role in the hand forces computation and advanced control in avoiding the singularity.

8.3.2) Hand Jacobian and the Dexterity Measure

The kinematic relations have led to the derivation of the Jacobian matrix of the whole hand which later played an important role in cartesian based motion of an object. For a three jointed finger, it was an easy task to obtain and visualize the dexterity measure of the finger. However, for higher degrees of freedom finger design, the dexterity measure is not a trivial task and hence other measures have to employed such as the configuration

space and the Global Task Space Manipulability Ellipsoid developed by CHIACCHIO *et al.* [1991].

Use of the Quaternion Algebra :

It would be useful and convenient in further research to consider different kinematic modelling techniques as alternatives to the homogeneous transformations employed within this research. Of these techniques is the dual-number quaternion algebra as in ROBERTS [1990], which treats rigid body translations and rotations in a convenient manner. Later dynamic modelling and parallelism could be applied to speed up the inverse kinematics and dynamics of the hand system.

Since the research has also considered the use of computed torque techniques for hand-object motion, that requires the development of one finger dynamic model and hence the dynamic model of the entire hand. A one finger dynamic model has been derived using the Lagranigan equation of motion which indeed has been verified by the Mathematica Software Package. The development of the dynamic model for one finger was achieved by considering the customized model of the finger as already discussed by PAUL [1981] and ZOMAYA, as in WARWICK [1993]. Furthermore, the model has been arranged in such way as to ease the possible implementation in a parallel architecture machine, where one finger kinematics and dynamics are enough to describe the entire hand dynamics as long as certain conditions are satisfied.

(8.4) EMPLOYMENT of FORCE FEEDBACK.

Pure force control on an object is an important issue in any grasping, whereas combined position and force hybrid feedback are essential for an objects dynamic manipulation. Force control based on force feedback has been employed in the four fingers of the hand design. The amount of force to be applied to an object can be controlled by controlling the

torque produced by the driving pulley of the controlled joint.

This aspect of research has shown the force control on an object by controlling the amount of strain a tendon produces on a beam. The amount of strain produced has been shown to be a function of the physical structure of the sensor. The use of force feedback would require the force control law to overcome the frictional present at the actuator, friction due to the tendon routing and tendon hysteresis.

Equivalent Rotational Stiffness :

The angular displacement of the controlled joint in force control is proportional to the amount of force to be applied to the object by a constant which is known as the Equivalent Rotational Stiffness. This constant has been derived for the designed force feedback system which is entirely a function of the tendon layout and routing around the strain gauge transducer. Future research in force sensing and control is to consider other techniques of force sensing rather the use of strain gauges which exhibit the thermal drift problem.

(8.5) FORCE COMPUTATION and OPTIMIZATION.

The force control on an object and the problem of controlling an overall associated force of an object have been addressed within this thesis. A new technique has been shown to be effective that involves the optimization of contact forces on an object, rather than optimizing a grasp internal forces.

Less Number of Constraints :

The optimization algorithm has been based on blending the linear equality constraints with the nonlinear inequality constraints of the frictional cone either for static or dynamic cases. The defined methodology has proven its ability to converge to an optimal solution

with less computation time.

The use of nonlinear constraints optimization has reduced the arithmetic required, as compared to the internal forces optimization. Although optimization and numerical force computation gave reasonable results for both static and dynamic cases, these techniques may require a considerable amount of time, especially when the algorithm is to search for an optimal solution. The used optimality technique has been compared with the internal forces optimization for the case of a four fingered robot hand.

Hence, one approach to speed up the computational requirements of the optimization algorithm could be implemented in parallel fashion, added to the fact that, this algorithm supports parallelism in the data flow.

(8.6) CONSTRAINED DYNAMICS and the SINGULARITY PROBLEM.

Manipulation of an object requires the overall hand joints to be both controlled in position and force coordinated mechanism. This thesis has looked at object motion considering the physical constraints represented by the maximum torque produced by the actuators, the frictional constraints at the points of contacts and the geometric constraints of the normal force direction at the object surface.

Singularity in the Multiple Contact :

An important aspect of cartesian based motion of the hand-object system is the singularity problem in the multiple contact system which occurs to the hand Jacobian. A method of solution has been employed which takes into account the singularity problem by extracting the *ill conditioned* areas and use them to define the robust singularity inverse (RSI) . The method has shown the possibility of using advanced force position control scheme even

in singular conditions. However, the price paid is the computational complexity of using these advanced inversion methods.

Employed Assumptions :

The singularity problem has been addressed based on three main assumptions regarding the trajectories of the joint space vectors stated as : (*i*) The physical lengths of the fingers link are identical, *i.e* finger lengths are equal due to identical kinematic structure. (*ii*) The joint space vectors of the four fingers are also equal and the four fingers start their motions at the same instant with the same joint displacements. (*iii*) The entire hand Jacobian J_h is a block diagonal matrix, thus all the off diagonal elements are zero. Such assumption are constraints from the kinematics point of view, since the velocity at the points of contacts has to be similar to the velocity of the fingertips.

Non Identical Joint Displacements :

Using the singular value decomposition theory, for the RSI of the Jacobian matrix, once the joints were identical in their motion, a similar result was obtained to the case when the one finger dexterity measure was used for the entire hand.

When the three assumptions are not met, the entire dexterity measure, will be a function of the individual joint positions, and the lengths of the finger links, in the entire hand. For this case, the manipulability measure of one finger, cannot be employed for the all the fingers. Hence, the individual fingers' manipulability measures are used in the RSI, as has been clarified using the singular value decomposition theory. The use of this theory, in particular Eq. 6.23, has shown that : the *individual dexterity* measures can describe how a finger is close to a singular posture.

Non identical joint displacements produce a complicated measure of dexterity, especially

when the fingertips are displaced at different velocities. Such complications increase with the number of fingers being used.

Future research would be the parallel implementation of this inversion computation scheme with today's advanced computing powers. The use of RSI does not necessitate the use of a finger dexterity measure of the finger determinant function. However, it can be based on various measures, such as *Task ellipsoid*, the *force and velocity ratios* of the task, or *Global Task Space Manipulability Ellipsoid* GTSME for multiple contact used by CHAIACCHIO *et al.* [1991].

(8.7) PARALLEL COMPUTATION of HAND DYNAMICS.

Having considered the computational complexity of the constrained dynamic motion of the hand-object system, such a method of control (*especially when using the full PID control law*) cannot be achieved using single processor computation. Hence two approaches of producing fast computation can be done, the employment of DSP or the use of transputer based parallel computation hardware. The use of transputers has been emphasized here due to the fact that : parallelism is more easily achieved using trasputers than any other form of current computer hardware.

Although the research work addressed the computational requirements for the constrained problem, another important issue of consideration is the design of fast interfaces between parallel processor systems and the hand control unit. This would require the building of electronic circuitry that establish a channel between the parallel computation and spreads data to the appropriate servo system.

(8.8) GENERAL AREAS of RESEARCH.

The generation of manipulation based on robots hands will be utilized in application.

This includes the application of robot hands in industry, medicine domestic, space, and under sea environments.

With regard to the use of robot hands in industrial environments, this would include the need to develop user programming languages that are applicable to the nature of manipulation under parallel contacts. Unlike programming languages for conventional robots arms, the programming language is to include the fact that the object motion is constrained rather than free of the fingertips. The programming language has also to consider the complex kinematics of the hand.

With regard to the employment of robot hands in remote and tele-operations, such as in underwater and space environments, this would necessitate a slave robot hand motion being translated to the master hand through camera based sensors in addition to a data glove. A vision based system would translate the operator hand motion to a remotely located robot hand motion. Image processing and extraction of motion parameters are not trivial and would need further investigation.

The use of robot hands in medical environments is a further challenge. The operation and control of robot hands in these environments would require hands of much more compliant materials, and the challenge of control is also a non trivial issue.

Similarly, one of the most challenging long-term problems in general robotics is the efficient control of multiple - robot systems. Control problems of multi-robot systems are similar to concerned with the manipulation of a common object grasped by a robot hand. However, the problem could be simplified due to the fact there are no frictional constraints to be preserved during the object motion. Furthermore in this context, the demand for massive computing power is obvious.

APPENDIX A1

GENERALIZED, PSEUDO and ROBUST - SIGULARITY INVERSE RSI

In robotics, for a non symmetric matrix $G \in \Re^{m \times n}$ and $X \in \Re^{n \times m}$, the following equations are used to define a generalized inverse, a reflexive generalized inverse, and pseudoinverse of G BOULLIONl and ODELL [1971] :

Generalized Inverse :

$$GXG = G \tag{A1.1}$$

$$XGX = X \tag{A1.2}$$

$$(GX)^T = GX \tag{A1.3}$$

$$(XG)^T = XG \tag{A1.4}$$

Eq. A1.1 up to Eq. A1.4 are known as the PENROSE conditions, PENROSE [1955].

Pseudo Inverse :

A pseudo-inverse of a matrix $G \in \Re^{m \times n}$ is a matrix $X = G^+ \in \Re^{n \times m}$ satisfying Eq. A1.1 to Eq. A1.4 .

Properties of Pseudo Inverse Properties :

(1) $(G^+)^+ = G$

(2) $(G^T)^+ = (G^+)^T$

(3) $G^+ = (G^T G)^+ G^T = G^T (G G^T)^+$

(4) G^+G, GG^+, $E - G^+G$ and $E - GG^+$ are symmetric and idempotent.

(5) If $G \in \Re^{n \times n}$ is symmetric and idempotent, then for any matrix $B \in \Re^{m \times n}$, the following equation holds :

$$G(B\,G)^+ = (B\,G)^+ \tag{A1.5}$$

(2.2) *Least-Squares Solutions Theory and its use in robotics.*

For a linear equation $\mathbf{X} \in \Re^n$ where

$$\mathbf{GX} = \mathbf{Y} \tag{A1.6}$$

where $\boldsymbol{G} \in \Re^{m \times n}$ and $\mathbf{Y} \in \Re^m$, the general form of the least-squares solutions is given by

$$\mathbf{X} = \boldsymbol{G}^+\boldsymbol{Y} + (\boldsymbol{E} - \boldsymbol{G}^+\boldsymbol{G})\boldsymbol{z} \tag{A1.7}$$

where $\boldsymbol{z} \in \Re^n$ is an arbitrary vector, and $\boldsymbol{E}$ is an identity matrix. The minimum norm solution among all the solutions is :

$$\mathbf{X} = \boldsymbol{G}^+\boldsymbol{Y} \tag{A1.8}$$

The least-squares solution is the $\mathbf{X}$ that minimizes the error norm - namely :

$$min \; || \; \boldsymbol{Y} - \boldsymbol{G}\mathbf{X} \; ||$$

where $||*||$ denotes the Euclidean norm of a vector *.

Robust Sigularity Inverse RSI

In this section, we introduce another type of matrix inversion for the Jacobian matrix. Here the singularity robustness is defined as a property of inverse kinematics that allows us to provide continuous and feasible solutions even at or in the neighbourhood of singular points.

$$\boldsymbol{J}_h^{RSI} = (\boldsymbol{J}_h^T \boldsymbol{W}_1 \boldsymbol{J}_h + \boldsymbol{W}_2)^{-1} \boldsymbol{J}_h \boldsymbol{W}_1^T \tag{A1.9}$$

where $\boldsymbol{W}_1$ and $\boldsymbol{W}_2$ are two weighting matrices. However $\boldsymbol{W}_1$ and $\boldsymbol{W}_2$ are generally represented as :

$$\boldsymbol{W}_1^T = \boldsymbol{N}_r^T \boldsymbol{N}_r \quad \text{and} \quad \boldsymbol{W}_2 = \kappa_r \boldsymbol{N}_\Theta^T \boldsymbol{N}_\Theta \tag{A1.10}$$

$\boldsymbol{N}_r$ and $\boldsymbol{N}_\Theta$ should be determined depending on the task, the physical limits of joints, and the *dynamic characteristics* of joints. The scalar κ_r determines the weighting between the *exactness* and the *feasibility* of the matrix inversion.

When N_r and N_Θ are identity matrices, then W_1 and W_2 are identity, the RSI of the Jacobian matrix is defined as:

$$J_h^R = (J_h^T J_h + \kappa_r E)^{-1} J_h^T \tag{A1.11}$$

or

$$J_h^R = J_h^T (J_h J_h^T + \kappa_r E)^{-1} \tag{A1.12}$$

The solution by the RSI belongs to the orthogonal complements as the solution by the pseud oinverse. The κ_r constant is used as an adjustment factor chosen to satisfy the system physical limits.

Related Relations of RSI :

In terms of the SVD, the RSI is :

$$\begin{aligned} J_h^R &= J_h^T (J_h J_h^T + \kappa_r E)^{-1} \\ &= V\Sigma^T U^T (U\Sigma\Sigma^T U^T + \kappa_r U U^T)^{-1} \\ &= V\Sigma U (U(\Sigma\Sigma + \kappa_r E)^{-1} U^T) \\ &= V\Sigma^T U^T (U(\Sigma\Sigma^T + \kappa_r E)^{-1} U^T) \\ &= V(\Sigma^T(\Sigma\Sigma^T + \kappa_r E)^{-1} U^T \end{aligned} \tag{A1.13}$$

However, $\Sigma\Sigma^T$ matrix represents the sequare terms of the Jacobian singular values. Multiplying $(\Sigma\Sigma^T + \kappa_r E)^{-1}$ by Σ^T results in :

$$J_h = V Q_r U^T \tag{A1.14}$$

where $Q_r = diag\,[\,q_1 \;\; q_2 \;\; q_3 \;\; q_4\,]$ and q_j are given as :

$$q_j = \frac{\sigma_i}{\sigma_i^2 + \kappa_{rj}} \qquad \begin{array}{l} for\ i = 1\ to\ 12, \quad j = 1\ to\ 4 \\ for\ i = 1,4,7,10 \end{array}$$

terms, which are robust interms of σ_i get zero value.

APPENDIX A2

DERIVATION of RELATION BETWEEN APPLIED FINGERTIP FORCE and SENSED VOLTAGE.

Within this appendix the relation between an applied torque at the fingertip and the generated voltage due to strain in the cantilever beam is presented. The derivation starts by considering the relation between the tendon tension T acting in a pulley of $\Re_p$ radius generating an amount of torque acting at the centre of the pulley of τ value and expressed as:

$$\tau = \Re_p \, T \tag{A2.1}$$

Using relations from Chapter Two, that due to the tension in the upper and lower tendons there are acting vertical forces in the beam itself, a force for one beam is :

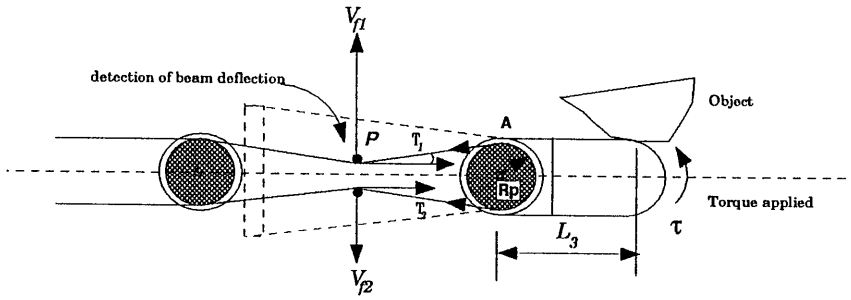
$$\begin{aligned} V_f &= 2 \, T_1 \, sin(\beta_1) \\ &= 2 \, (\tau / \Re_p) \, sin(\beta_1) \end{aligned} \tag{A2.2}$$

In accordance to Fig [A2-1] and Fig [A2-2], the strain ε acting in a beam of known physical dimensions due to an applied edge force can be expressed by :

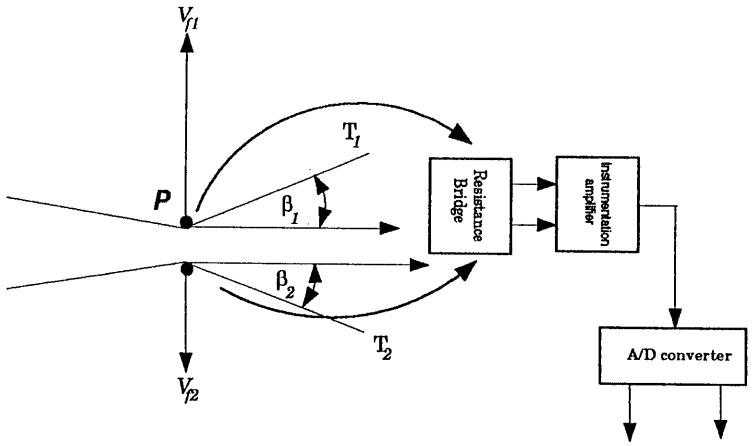
$$\varepsilon = \frac{6 \, V_f \chi}{E_s \, W \, t^2} \tag{A2.3}$$

where E is the Young's modules of the beam material expressed in N/m^2.

Substituting V_f from Eq. A2.2 in Eq. A2.3 gives an expression for the change strain

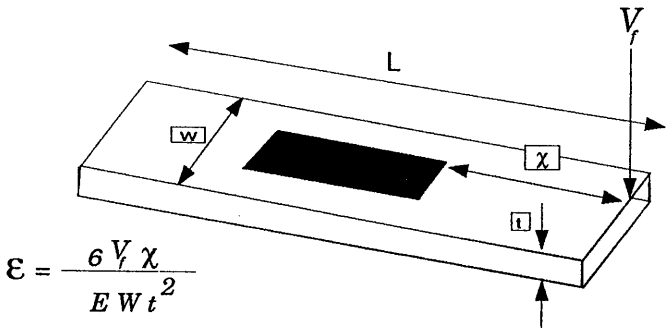


a

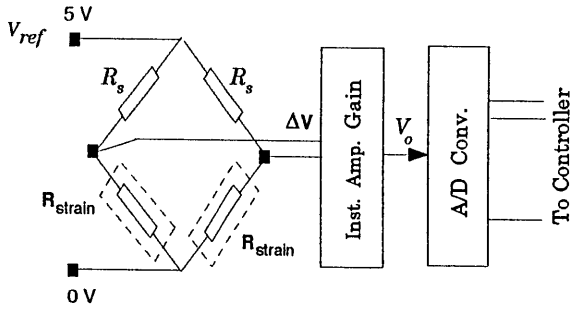


b

Figure A2.1 a : Physical Mechanism of Force Sensing at the Fingertip.
b : Conversion from Forces to Digital Signal for Force Feedback.



a



b

Figure A2.2 : a : Strain Acting on a Catilevel Beam and the Associated Physical Parameters.
b : Strain Bridge.

in terms of the applied torque and the physical structure of the transducer.

Change in strain =

$$\varepsilon = (6(\, 2(\tau / \Re_p)\, sin(\beta)\,)\, \chi) / (E_s\, W\, t^2) \qquad \text{(A2.4)}$$

Once an amount of strain is acting in the beam structure, there will change in the material resistor, either the resistance to increase or decrease by an amount of ΔR.

The change in the resistor bridge gives :

$$\Delta R = 2\, R_{nom}\, \varepsilon$$

$$= 2\, R_{nom} \frac{12\, \tau\, sin(\beta)\, \chi}{\Re_p\, E_s\, W t^2} \qquad \text{(A2.5)}$$

which can be written as :

$$\Delta R = \kappa\, \tau \qquad \text{(A2.6)}$$

where $\kappa = 24\, R_{nom} sin\,(\beta)\, \chi / (\Re_p\, E_s\, W\, t^2)$

If G_a is the instrumentation amplifier gain, hence V_o can be written as:

$$V_o = G_a\, V_{ref}\, \kappa\, \tau \qquad \text{(A2.7)}$$

The torque τ acting at the driving pulley of the distal joint is related to the force applied at a particular location in the fingertip. Let this location be L_3, which the physical length of the distal link, where the velocity reference point is expressed as discussed in Chapter Three.

Eq. A2.7 can be written in terms of that acting force as:

$$V_o = G_a V_{ref}\, \kappa\, F_a\, L_3 \qquad \text{(A2.8)}$$

which expresses force acting in a normal direction (*the case for grasping*) to a measurable voltage suitable for feedback control.

Substituting of all the physical constants of the sensor given in Table [A2] in Eq. A2.8 :

Physical Parameter	Symbol	Value	Unit
Young's Modulus	E_s	196×10^9	N/m^2,
Beam width	W	6	*mm*
Distal Pulley Radius	$\Re_p$	6	*mm*
Beam thickness	t	0.2	*mm*
Strain Gauge Location	χ	2	*mm*
Angle of Tendon	β	30	Deg
Distal Link Length	L_3	40	*mm*
Total Beam Length	L	10	*mm*
Instr. Amplifier Gain	G_a	800	
Reference Voltage	V_{ref}	5	*V*

Table [A2] : Physical Constants of the Sensor Structure.

Using the above constants gives $\kappa = 0.0425$ *V/Nm*.

Substituting the value of the constant κ and the associated parameters in Eq. A2.8 gives a relation for sensing the amount of force to be applied to an object surface. This quantity is used later for closing the loop in force control of the distal joints.

$$V_o = 6.80 \; F_a \qquad \text{(A2.9)}$$

APPENDIX A3-1

COMPUTATION of FINGER JACOBIAN DETERMINANT FUNCTION

This appendix is related to Chapter Three where it shows how the determinant function of a finger is derived from the first principles. Since the finger determinant function plays an important role in the robust singularity inversion of the Jacobian, a careful derivation has been followed by determining the Jacobian matrix co-factors.

The finger Jacobian has been found in Chapter Three as :

$$\boldsymbol{J}_{\Theta} = \begin{bmatrix} -s_1\Psi & -c_1(L_3s_{23} + L_2c_2) & -c_1L_3s_{23} \\ c_1\Psi & -s_1(L_3s_{23} + L_2s_2) & -s_1L_3s_{23} \\ 0 & L_3c_{23} + L_2c_2 & L_3c_{23} \end{bmatrix} \qquad \text{(A3.1.1)}$$

Applying the rules of algebra, the determinant function of the matrix in Eq. A3.1.1 can be found by:

(*i*) *First co-factor* CF_1:

$$\begin{aligned} CF_1 &= -s_1\Psi[-s_1(L_3s_{23} + L_2s_2)L_3c_{23} + s_1L_3s_{23}(L_3c_{23} + L_2c_2)] \\ &= -s_1\Psi L_2L_3[s_1(s_{23}c_2 - c_{23}s_2)] \end{aligned} \qquad \text{(A3.1.2)}$$

From standard trigonometry,

$$sin(\theta_2+\theta_3) = sin(\theta_2)cos(\theta_3) + cos(\theta_2)sin(\theta_3) \qquad \text{(A3.1.3)}$$

and

$$cos(\theta_2+\theta_3) = cos(\theta_2)cos(\theta_3) - sin(\theta_2)sin(\theta_3) \qquad \text{(A3.1.4)}$$

Applying these two relations to Eq. A3.1.2 gives

$$CF_1 = -s^2{}_1 \Psi L_2 L_3 s_3 \qquad \text{(A3.1.5)}$$

(ii) Second co-factor CF_2 *of* Eq. A3.1.1:

$$CF_2 = c^2{}_1 L^2{}_3 \Psi s_{23} c_{23} + L_2 L_3 c^2{}_1 s_2 \Psi c_{23} \qquad \text{(A3.1.6)}$$

(iii) Third co-factor CF_3 *of* Eq. A3.1.1:

$$CF_3 = -c^2{}_1 L^2{}_3 s_{23} c_{23} \Psi - L_2 L_3 c^2{}_1 c_2 s_{23} \Psi \qquad \text{(A3.1.7)}$$

By adding CF_2 *to* CF_3 that gives :

$$CF_4 = L_2 L_3 c^2{}_1 s_2 \Psi c_{23} - L_2 L_3 c^2{}_1 c_2 s_{23} \Psi \qquad \text{(A3.1.8)}$$

Adding CF_1 to CF_4 gives :

$$D = -\Psi L_2 L_3 s_3 . \qquad \text{(A3.1.9)}$$

The result of determinant function computation is thus $D = -\Psi L_2 L_3 s_3$ which is a function of the second link L_2, third link L_3 and the $\sin(\theta_3)$ of the third joint angular position.

APPENDIX A3-2

DEVELOPMENT of SYMBOLIC SINGULAR VALUES of J_Θ

In Chapter Three three graphs representing how singular values of one finger Jacobian were changing as function of a defined manipulation task. Within this appendix, the symbolic format of the singular values are obtained for the purpose of further study and analysis in which of the values drop to zero resulting in singular matrix. MATHEMATICA software has been used for the development of the expressions. Due to the relation among

the terms in one finger Jacobian, these expressions are presented for the kinematically designed hand:

if $U^T J_\Theta V = diag\,[\,\sigma_1,\ \sigma_2,\ \sigma_3\,]$ *then*

$V^T(J_\Theta{}^T J_\Theta)V = diag\,[\sigma_1^2,\ \sigma_2^2,\ \sigma_3^2]$ *and*

$U^T(J_\Theta J_\Theta{}^T)U = diag\,[\sigma_1^2,\ \sigma_2^2,\ \sigma_3^2]$

representing the right and left singular vectors of J_Θ.

The singular values and the matrix determinant are related together by the relation that:

$$D(J_\Theta) = \sigma_1 \sigma_2 \sigma_3 \qquad \text{(A3.2.1)}$$

Which indicates the fact , the determinate (*an important factor in matrix inversion*) will approach zero, as far one the singular values is zero value.

The eigenvalues of $J_\Theta J_\Theta{}^T$ are the squared singular values of J_Θ.

Applying MATHEMATICA to $J_\Theta{}^T J_\Theta$ for eigenvalues determination, this gives the following three singular values :

First and Third Fingers, AL-GALLAF and WARWICK [1994-d] :

$$\sigma_1 = \Psi^2$$

$$\sigma_2 = \frac{(L_2^2 + 2L_3^2 + 2L_2L_3C_3 + \chi^2)}{2}$$

$$\sigma_3 = \frac{(L_2^2 + 2L_3^2 + 2L_2L_3C_3 - \chi^2)}{2}$$

$\chi = \sqrt{(L_2^2 + 2L_3^2 + 2L_2L_3C_3 + 2L_2L_3S_3)}$ and Ψ as defined earlier in Chapter Three.

It is evident from the above three equations σ_1 and σ_2 never approaches zero, while σ_3 is the one responsible for the singularity when θ_3 is zero. Then θ_3 is zero in value, thus the finger is stretched, the first terms in σ_3 will be subtracted from $L_2^2 + 2L_3^2 + 2L_2L_3C_3$ resulting in zero value. Then θ_3 is not zero, there will be an additional term given by

$2L_2L_3S_3$ that moves σ_3 away from zero.

Second Finger Fingertip Frame Rotation:

For the purpose of aligning the second fingertip frame with the object surface, the fingertip frame is rotated by a defined angle depending in the shape of the object contact location (as elaborated in Chapter Five). This rotation will undoubtedly changes the elements of second finger Jacobian, and hence there might be changes in the location of the singular values of the matrix $\boldsymbol{J}_2$ itself.

For the purpose of investigating this issue which will be used in Chapter Six for the inversion of the hand Jacobian $\boldsymbol{J}_h$, the singular values of $\boldsymbol{J}_2$ have been computed using for the rotated fingertip frame of the second finger. Hence the singular values are :

$$\sigma_1 = \Psi^2$$

$$\sigma_2 = \frac{(L_2^2 + 2L_3^2 + 2L_2L_3C_3 + \chi^2)}{2}$$

$$\sigma_3 = \frac{(L_2^2 + 2L_3^2 + 2L_2L_3C_3 - \chi^2)}{2}$$

which reveals that the singular values of the second finger are of smaller values to the first and third fingers.

Fourth Finger:

Although the fourth fingertip has been rotated by a given angle for aligning it with the object surface frame, however the determinant function also drops to null value once θ_3 is zero.

APPENDIX A4 -1

DERIVATION of the EQUIVALENT ROTATIONAL STIFFNESS of FORCE SENSOR

Within this Appendix the formula for the equivalent rotational stiffness $k_{s\Theta}$ will be derived from the geometric structure of the force sensor and the location of the driving pulley itself. There are a number of techniques which can be employed to compute the physical equivalent rotational stiffness, where the method adopted here is to draw a relation between the displacement of the driving pulley and the corresponding deformation of the stain gauge beam shown in Fig [A4-1-1-a].

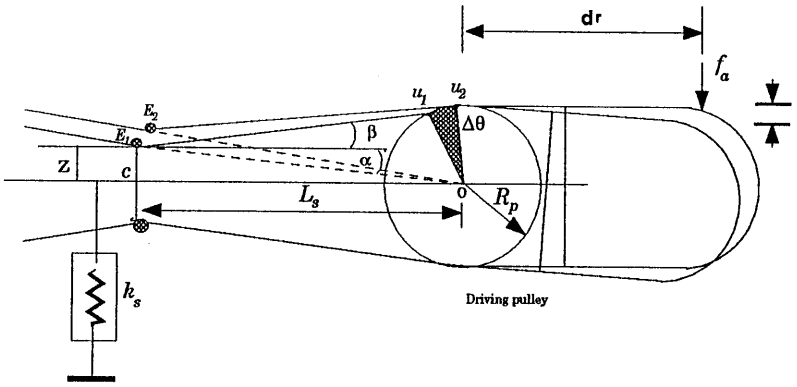
The physical meaning of the rotational stiffness can be experienced when a force is applied to the fingertip, there will be a restoring torque as the angular displacement increases from an initial position.

Let k_s and $k_{s\Theta}$ be the *Y*- directional sensor stiffness, as shown in Fig [A4-1-1], and the equivalent rotational stiffness of the sensor around the driving pulley with radius $\Re_p$, respectively.

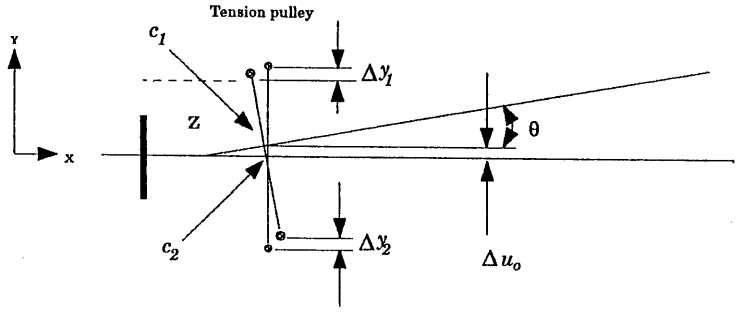
The general definition of stiffness for both linear and rotational systems can be written as, with reference to Fig [A4-1-1] :

$$V_{f1} = k_s \Delta y \qquad \text{(A4.1.1)}$$

$$\tau = k_{s\Theta} \Delta\theta \qquad \text{(A4.1.2)}$$



a



b

Figure A4.1.1 : Further Analysis of the Sensor.
a : Angular displacement and Y directional displacement of the sensor.
b : Sensor deformation for an applied torque.

where V_{fl} is the y-directional force acting on the sensor beam, and Δy, $\Delta\theta$ are the y-directional displacement and the θ -directional angular displacement, respectively. However the formula for τ and V_{fl} has already been expressed in Chapter Two as :

$$\tau = \Re_p(T_1 - T_2) \tag{A4.1.3}$$

$$V_{fi} = 2T_i \sin(\beta) \tag{A4.1.4}$$

Equating Eq. A4.1.2 and Eq. A4.1.3, gives :

$$K_{s\Theta}\Delta\theta = \Re_p(T_1 - T_2) \tag{A4.1.5}$$

From Eq. A4.1.4 T_1 and T_2 can be expressed as $T_i = V_{fi}/(2 \sin(\beta))$. Substituting T_i in Eq. A4.1.5 result in :

$$k_{s\Theta}\Delta\theta = \Re_p(V_{f1} - V_{f2})/(2 \sin(\beta)) \tag{A4.1.6}$$

$$k_{s\Theta}\Delta\theta = \Re_p k_s \Delta Y/(2 \sin(\beta)) \tag{A4.1.7}$$

Eq. A4.1.6 reveals that : to compute the rotational stiffness $k_{s\Theta}$ would require the knowledge of the differential change, ΔY in the vertical position of the cantilever beam itself, as illustrated in Fig [A4-1-1-b].

With reference to Fig [A4-2-1-b], let Δu_o and Δy_1 and Δy_2 be the y-directional displacements at point C and the tension pulleys, respectively. The following geometrical relations exist for describing the vertical movement of the location where the tendon is acting on the beam :

$$\Delta y_1 = \Delta y_o - Z\theta^2 \tag{A4.1.8}$$

$$\Delta y_2 = \Delta y_o + Z\theta^2 \tag{A4.1.9}$$

where θ and the distance Z are the deflection angle due to V_{fi} and the half length of the sensor arm, respectively.

Assuming a sufficiently small deflection angle to keep Δy_o greater than $Z\theta^2$, we obtain:

$$\Delta y \cong \Delta y_i \quad (i = 0, 1, 2) \tag{A4.1.10}$$

For expressing the rotation stiffness of the driving joint, it is needed to express the changes at the driving pulley to deformation of the sensor beam.
Furthermore, in Fig [A4-1-1-a] the triangles E_1OE_2 and u_1Ou_2 are having similar geometric relation thus, taking the relationship between Δy and Δθ into consideration, we can rewrite Eq. A4.1.7 as :

$$k_{s\Theta} = [(cos\alpha - sin\alpha\ sin\beta\ tan(\alpha+\beta))k_s] \ /\ (8\ sin\beta\ sin(\alpha+\beta)) \tag{A4.1.11}$$

however the value k_s which is the beam stiffness has been expressed in Chapter Two as :

$$k_s = (WE_s(t/L)^3)\ /4 \tag{A4.1.12}$$

$$k_{s\Theta} = \frac{(cos\alpha - sin\alpha\ sin\beta\ tan(\alpha+\beta))k_s}{8\ sin\beta\ sin(\alpha+\beta)} \tag{A4.1.13}$$

From Eq. A4.1.13, it is clear that $k_{s\Theta}$ is proportional to $(t/L)^3$ and thus $k_{s\Theta}$ can be changed substantially by the parameter (t/L) which is dependent on the sensor physical dimensions. Using the physical structure of the sensor described in Chapter Two, and working under the case when the beam sensor is having a stiffness value of $2352\ N/m$, we are left with a numerical value of the equivalent rotational stiffness as:

$$k_{s\Theta} = 102.2\ Nm/rad$$

APPENDIX A4–2

For the CYBHAND, the numerical values of the actuator parameters are obtained from the data sheets in addition to experimental verification. The parametric data for the motor unit are listed in Table [A4-1].

Parameter	Symbol	Value	Unit
Terminal Voltage	V_{termi}	15	V
Shaft moment of inertia	J_a	35×10^{-7} **	$kg.m^2$
Electrical Time constant	τ_e	0.12×10^{-3}	sec
Shaft damping	B_a	15×10^{-8}	$Nm/\ rad/s$
Back emf constant	k_b	3.5	$v/\ 1000\ rpm$
Armature inductance	L	10×10^{-3}	H
Armature Resistance	R	120	Ω
Torque Constant	k_i	33×10^{-3}	Nm/A
Frictional torque	f_m	0.094×10^{-3}	Nm
Link frictional Torque	f_{ml}	93×10^{-3}	Nm
Gear Ratio	n	1/400*	
No-load rated speed	K_e	320**	rad/s
Rated shaft torque	T_r	425×10^{-3}	Nm

Table [A4.1] : Parameters of the Motor.

* : This gear ratio is seen at the motor shaft, hence the motor motion will be reduced by 1/400. ** : At the output of the motor shaft before gearing. f_m is the average friction torque which exists in each actuator., whereas f_{ml} is the friction torque which exists in each assembly and must be overcome.

APPENDIX A5

SYMBOLIC DERIVATION of ONE FINGER LAGRANGIAN MECHANICS

What is of great concern in coordinated manipulation of an object is the dynamic model of the hand which by itself consists of the dynamic model of all four fingers. For the purpose of studying the dynamics of the entire hand dynamics, *Lagrangian Mechanics* provides a useful tool for multiple degrees of freedom system. The derivation has been based on the support of the MATHEMATICA Package.

From the Lagrangian mechanics point of view, the system dynamics behaviour is described in terms of work and energy using generalized coordinate. The joint variables are defined by $(\theta_1, \theta_2, \theta_3)$, and the mass of the links (m_1, m_2, m_3). Using the kinematic relation already defined in Chapter Three, this gives:

$$ {}^0T_1 = \begin{bmatrix} c_1 & 0 & s_1 & L_1c_1 \\ s_1 & 0 & -c_1 & L_1s_1 \\ 0 & 1 & 0 & 0 \\ 0 & 0 & 0 & 1 \end{bmatrix} \quad {}^1T_2 = \begin{bmatrix} c_2 & -s_2 & 0 & L_2c_2 \\ s_2 & c_2 & 0 & L_2s_2 \\ 0 & 0 & 1 & 0 \\ 0 & 0 & 0 & 1 \end{bmatrix} \quad {}^2T_3 = \begin{bmatrix} c_3 & -s_3 & 0 & L_3c_3 \\ s_3 & c_3 & 0 & L_3s_3 \\ 0 & 0 & 1 & 0 \\ 0 & 0 & 0 & 1 \end{bmatrix} \quad \text{(A5.1)} $$

Lagrange's equation of motion for a conservative system is $\tau^T = [\ \tau_1 \quad \tau_2 \quad \tau_3\ ]$, where

$$ \tau_i = (d\,[\,\partial L / \partial \dot{\theta}_i\,] / dt) - \partial L / \partial \theta_i \qquad \textit{for } i = 1 \textit{ to } 3 \qquad \text{(A5.2)} $$

where θ_i's are generalized coordinates variables, τ is a three vector of generalised torque,

and L is the Lagrangian operator. The Lagrangian function is used to drive the equations of motion for one finger and is defined in terms of the kinetic energy K and the potential energy P. Since Lagrangian is the difference between the kinetic and potential energies of a system, then :

$$L = K - P \tag{A5.3}$$

The dynamics equations (Generalised torques τ_{a1} , τ_{a2} , τ_{a3}) which are applied to the corresponding joints of (θ_1, θ_2, θ_3) are computed from Eq. A5.1 :

$$\begin{aligned} \tau_{a1} &= d[\partial L / \partial \dot{\theta}_1] / dt - \partial L / \partial \theta_1 \\ \tau_{a2} &= d[\partial L / \partial \dot{\theta}_2] / dt - \partial L / \partial \theta_2 \\ \tau_{a3} &= d[\partial L / \partial \dot{\theta}_3] / dt - \partial L / \partial \theta_3 \end{aligned} \tag{A5.4}$$

Applying the Lagrange-Euler formulation to the Lagrangian function L of the finger gives the necessary generalized torques τ_{a1}, τ_{a2}, τ_{a3}. The torques in Eq. A5.4 can be interpreted as a sum of the torques due to the kinetic and potential energies present within the system.

KINETIC ENERGY :

In general, the kinetic energy of the *ith* link in the finger of mass dm located at ${}^{i}\boldsymbol{r}_i$ is expressed as:

$$K_1 = \tfrac{1}{2}\, T_r [(\partial \boldsymbol{T}_1 / \partial \theta_1)\, \boldsymbol{U}_1\, (\partial \boldsymbol{T}_1 / \partial \theta_1)^T \dot{\theta}_1 \dot{\theta}_1] + \tfrac{1}{2} J_{a1} \dot{\theta}_1^2 \tag{A5.5}$$

$$\begin{aligned} K_2 = \tfrac{1}{2}\, T_r [&(\partial \boldsymbol{T}_2 / \partial \theta_2)\, \boldsymbol{U}_2\, (\partial T_2 / \partial \theta_1)^T \dot{\theta}_1 \dot{\theta}_1 + (\partial \boldsymbol{T}_2 / \partial \theta_2)\, \boldsymbol{U}_2\, (\partial \boldsymbol{T}_2 / \partial \theta_2)^T \dot{\theta}_1 \dot{\theta}_2 \\ &+ (\partial \boldsymbol{T}_2 / \partial \theta_2)\, \boldsymbol{U}_2\, (\partial \boldsymbol{T}_2 / \partial \theta_1)^T \dot{\theta}_1 \dot{\theta}_2 + (\partial \boldsymbol{T}_2 / \partial \theta_2) \boldsymbol{U}_2\, (\partial \boldsymbol{T}_2 / \partial \theta_2)^T \dot{\theta}_1 \dot{\theta}_2] + \tfrac{1}{2} J_{a2} \dot{\theta}_2^2 \end{aligned} \tag{A5.6}$$

$$K_3 = \tfrac{1}{2}\, T_r [(\partial \boldsymbol{T}_3 / \partial \theta_3) \boldsymbol{U}_3 (\partial \boldsymbol{T}_3 / \partial \theta_1)^T \dot{\theta}_1 \dot{\theta}_1 + (\partial \boldsymbol{T}_3 / \partial \theta_3) \boldsymbol{U}_3 (\partial \boldsymbol{T}_3 / \partial \theta_2)^T \dot{\theta}_1 \dot{\theta}_2$$

$$+ (\partial \boldsymbol{T}_3/\partial\theta_3)\boldsymbol{U}_3(\partial \boldsymbol{T}_3/\partial\theta_3)^T \dot{\theta}_1\dot{\theta}_3$$

$$+(\partial \boldsymbol{T}_3/\partial\theta_3)\boldsymbol{U}_3(\partial \boldsymbol{T}_3/\partial\theta_1)^T \dot{\theta}_1\dot{\theta}_1 + (\partial \boldsymbol{T}_3/\partial\theta_3)\boldsymbol{U}_3(\partial \boldsymbol{T}_3/\partial\theta_1)^T \dot{\theta}_2\dot{\theta}_1 + (\partial \boldsymbol{T}_3/\partial\theta_3)\boldsymbol{U}_3(\partial \boldsymbol{T}_3/\partial\theta_2)^T \dot{\theta}_2\dot{\theta}_2$$

$$+ (\partial \boldsymbol{T}_3/\partial\theta_3)\boldsymbol{U}_3(\partial \boldsymbol{T}_3/\partial\theta_3)^T \dot{\theta}_2\dot{\theta}_3 + (\partial \boldsymbol{T}_3/\partial\theta_3)\boldsymbol{U}_3(\partial \boldsymbol{T}_3/\partial\theta_1)^T \dot{\theta}_3\dot{\theta}_1 +$$

$$+ (\partial \boldsymbol{T}_3/\partial\theta_3)\boldsymbol{U}_3(\partial \boldsymbol{T}_3/\partial\theta_3)^T \dot{\theta}_3\dot{\theta}_3] + \tfrac{1}{2} J_3^2 \dot{\theta}_3^2 \qquad \text{(A5.7)}$$

where T_r in Eq. A5.5 to Eq. A5.7 is the trace operator on a matrix and J_{ai} is the *ith* link actuator inertia. Hence the total kinematic energy of the finger is then found as:

$$K = (K_1 + K_2 + K_3) + K_{actu} \qquad \text{(A5.8)}$$

In addition to the kinetic energy of the links of the fingers, we add to this the kinetic energy of the actuators within one finger which is represented by :

$$K_{actu} = \tfrac{1}{2}(J_{a1}\dot{\theta}_1^2 + J_{a2}\dot{\theta}_2^2 + J_{a3}\dot{\theta}_3^2) \qquad \text{(A5.9)}$$

where J_{ai} are the moment of inertia of the joint actuators. In a number of cases the inertia of the actuators are of significant value in that they reduce the inertia resulting from the finger links motion.

Potential Energy Of One Finger :

If the gravity vector is expressed as : $\boldsymbol{g}^T = [g_x \; g_y \; g_z \; 0]$, then the corresponding potential energy of one finger is :

$$\begin{aligned} P_1 &= -m_1 \boldsymbol{g}^T \boldsymbol{T}_1 \boldsymbol{r}_1 \\ P_2 &= -m_2 \boldsymbol{g}^T \boldsymbol{T}_2 \boldsymbol{r}_2 \\ P_3 &= -m_3 \boldsymbol{g}^T \boldsymbol{T}_3 \boldsymbol{r}_3 \end{aligned} \qquad \text{(A5.10)}$$

The total potential energy of the *ith* finger is the summation of the three potential energies which can be expressed as :

$$P = P_1 + P_2 + P_3$$

$$P = -\sum_{i=1}^{3} m_i \boldsymbol{g}^T \boldsymbol{T}_i \boldsymbol{r}_i \qquad \text{(A5.11)}$$

Using Eq. A5.9 and Eq. A5.11 the Lagrange formula of Eq. A6.3 can be written as:

$$L = K_1 + K_2 + K_3 + K_{actu} - (P_1 + P_2 + P_3) \qquad \text{(A5.12)}$$

Using the notation by PAUL [1981]:

$$L = \sum_{i=1}^{3} \tfrac{1}{2} [\sum_{j=1}^{1} \sum_{k=1}^{1} T_r [(\partial T_i / \partial \theta_i) \boldsymbol{U}_i (\partial T_i / \partial \theta_k)^{\mathrm{T}}] \dot{\theta}_j \dot{\theta}_k + J_{ai} \dot{\theta}_i^2 - m_i \boldsymbol{g}^T \boldsymbol{T}_i r_i^1] \qquad \text{(A5.13a)}$$

Through appropriate manipulation of terms we arrive at the following relation:

$$\tau_{ia} = \sum_{j=i}^{3} \sum_{k=1}^{i} T_r [(\partial \boldsymbol{T}_j / \partial \theta_k \boldsymbol{U}_i \partial \boldsymbol{T}_j / \partial \theta_i)^T] \ddot{\theta}_k + \sum_{i=1}^{3} \sum_{k=1}^{j} \sum_{m=1}^{j} T_r [(\partial^2 \boldsymbol{T}_j / \partial \theta_k \partial \theta_m) \boldsymbol{U}_j (\partial \boldsymbol{T}_j / \partial \theta_i)^T] \dot{\theta}_k \dot{\theta}_m$$

$$- \sum_{j=1}^{3} m_i \boldsymbol{g}^T (\partial \boldsymbol{T}_j / \partial \theta_i)^j \boldsymbol{r}_j + J_{ai} \ddot{\theta}_i^2 \qquad \text{(A5.13b)}$$

which can be further rewritten in standard form as, WARWICK [1993] :

$$\tau_{ia} = \sum_{j=1}^{3} M_{ij} \ddot{\theta}_j + J_{ai} \ddot{\theta}_i^2 + \sum_{j=1}^{3} \sum_{K=1}^{3} N_{jk}^{i} \dot{\theta}_j \dot{\theta}_k + C_i \qquad \text{(A5.14)}$$

where $$M_{ij} = \sum_{L=max(i,j)}^{3} T_r [\partial \boldsymbol{T}_L / \partial \theta_j \boldsymbol{U}_L (\partial \boldsymbol{T}_L / \partial \theta_i)^T] \qquad \text{(A5.14.a)}$$

$$N_{jK}^{i} = \sum_{L=max(i,j)}^{j} \sum^{j} T_r [(\partial^2 T_L / \partial \theta_j \partial \theta_K) \boldsymbol{U}_L (\partial T_L / \partial \theta_i)^T] \qquad \text{(A5.14.b)}$$

$$C_i = -\sum_{L=i}^{3} m_L \boldsymbol{g}^T (\partial \boldsymbol{T}_L / \partial \theta_i) \boldsymbol{r}_L^L \qquad \text{(A5.14.c)}$$

The main concern in Eq. A5.14 is that it is expressed as a function of the two differential operators the $(\partial \boldsymbol{T}_L / \partial \theta_i)$ in case of inertia computation terms and $(\partial^2 \boldsymbol{T}_L / \partial \theta_j \, \partial \theta_K)$ for the centrifugal and coriolis case. For the intension of simplifying this equation, it can be

simplified in terms of the inertial and centrifugal forces.

Paul's have developed the partial derivatives given by Eq. A5.15 to simplify the computation needed in performing $(\partial \boldsymbol{T}_L / \partial \theta_i)$.

$$(\partial \boldsymbol{T}_L / \partial \theta_i) = \boldsymbol{T}_L^{\mathrm{L}} \Delta_i \tag{A5.15}$$

Since all three joints in one finger are revolute, the differential translation rotation vectors are defined for the *ith* frame in the finger :

$$\begin{aligned}
{}^{L}d_{ix} &= -{}^{i-1}\eta_{Lx}\,{}^{i-1}p_{Ly} + {}^{i-1}\eta_{Ly}\,{}^{i-1}p_{Lx} \\
{}^{L}d_{iy} &= -{}^{i-1}o_{Lx}\,{}^{i-1}p_{Ly} + {}^{i-1}o_{Ly}\,{}^{i-1}p_{Lx} \\
{}^{L}d_{iz} &= -{}^{i-1}a_{Lx}\,{}^{i-1}p_{Ly} + {}^{i-1}a_{Ly}\,{}^{i-1}p_{Lx} \\
{}^{L}\delta_i &= {}^{i-1}\eta_{Lx} i + {}^{i-1}o_{Lz} j + {}^{i-1}a_{Lx} k
\end{aligned} \tag{A5.16}$$

hence Δ_i^L is the standard differential operator of rotation and translation in $\boldsymbol{T}_L$ coordi nates with respect to the differential change of the *ith* joint which can be rewritten as :

$$\Delta^L_i = \begin{bmatrix} 0 & -\delta^L_{iz} & \delta^L_{iy} & d^L_{ix} \\ \delta^L_{iz} & 0 & -\delta^L_{ix} & d^L_{iy} \\ -\delta^L_{iy} & \delta^L_{ix} & 0 & d^L_{iz} \\ 0 & 0 & 0 & 0 \end{bmatrix} \tag{A5.17}$$

Hence M_{ij} can be expressed in terms of this differential operator as :

$$M_{ij} = \sum_{L=max(i,j)}^{3} T_r \left(\Delta_i^L \boldsymbol{U}_L \Delta_i^{L\,T}\right) \tag{A5.18}$$

What is needed in Eq. A5.17 is the knowledge of the $\Delta^L_i \in \Re^{(4\times4)}$ pseudo-inertia matrix for link i. If the total mass of the *ith* link is located at ${}^{i}\boldsymbol{r}^T = [x\ y\ z\ 1]$ which

is the coordinates in *ith* frame of the centre of gravity of the *ith* link, then U_L, the pseudo inertia matrix, can be expressed as:

$$U_L = \begin{bmatrix} (-u_{xx}+u_{yy}+u_{zz})/2 & u_{xy} & u_{xz} & m_L x_L \\ u_{xy} & (u_{xx}-u_{yy}+u_{zz})/2 & u_{yz} & m_L y_L \\ u_{xz} & u_{yz} & (u_{xx}+u_{yy}-u_{zz})/2 & m_L z_L \\ m_L x_L & m_L y_L & m_L z_L & m_L \end{bmatrix} \qquad \text{(A5.19)}$$

where the u_{ii} are the moment of inertia terms and U_{ij} are the cross-product of inertia of the corresponding link in the finger design.

Here an assumption is made regarding the cross-product inertia terms, for simplifying the computation, the products inertia are assumed to be zero.

Let the moment of inertia terms and first moments to be designated as :

$$\begin{aligned} \beta^L_{11} &= (-u_{xx}+u_{yy}+u_{zz})/2 & \beta^L_{14} &= m_L x_L \\ \beta^L_{22} &= (u_{xx}-u_{yy}+u_{zz})/2 & \beta^L_{24} &= m_L y_L \\ \beta^L_{33} &= (u_{xx}+u_{yy}-u_{zz})/2 & \beta^L_{34} &= m_L z_L \\ \beta^L_{44} &= m^L \end{aligned} \qquad \text{(A5.20)}$$

Effective and Coupling Inertia Terms :

Having expressed $(\partial T_L / \partial \theta)_i$ by Δ^L_i and U_L by much simplified pseudo inertia matrix, then by direct substitution of Δ^L_i in Eq. A5.14 gives the inertia terms as :

$$M_{ij} = \sum_{L=max(i,j)}^{3} T_r [\Delta^L_i U_L \Delta^{L\,T}_i] \qquad \text{(A5.21)}$$

By application of Eq. A5.20, assuming the off-diagnal inertia terms are zero in Eq. A5.17,

using the simplification adopted by ZOMAYA [1992], and by the aid of MATHEMATICA Package, then Eq. A5.21 can be expanded as :

$$
\begin{aligned}
M_{11} &= 1/3\, m_1 L_1^{\,2} + m_2 L_1^{\,2} + m_2 L_1 L_2\, C_2 + 1/3 L_2^{\,2} m_2\, C_2^{\,2} + \; m_3 L_1^{\,2} + 2 L_1 L_2 m_3\, C_2 \\
&\quad + m_3 L_2^{\,2}\, C_2^{\,2} + \; m_3 L_2 L_3\, C_2 C_{23} + \; 1/3 m_3 L_3^{\,2}\, C_{23}^{\,2} \; + m_3 L_1 L_3\, C_{23} \\
M_{12} &= 0 \qquad\qquad M_{13} = 0 \qquad\qquad M_{21} = 0 \\
M_{22} &= 1/3 m_2 L_2^{\,2} + m_3 L_2^{\,2} + L_2 L_3 m_3\, C_3 + 1/3 L_3^{\,2} m_3 \\
M_{23} &= 1/3 m_3 L_3^{\,2} + \; 1/2 L_2 L_3 m_3\, C_3 \qquad M_{31} = 0 \\
M_{32} &= 1/3 m_3 L_3^{\,2} + \; 1/2 L_2 L_3 m_3\, C_3 \qquad M_{33} = 1/3 m_3 L_3^{\,2}
\end{aligned}
\tag{A5.22}
$$

where M_{ii} is the effective inertia at the *ith* joint in the finger.

and M_{ij} is the coupling inertia between the *ith* and *jth* joints in one finger. Futhermore, M_{33} represents the inertia of the link itself , since the third link in the finger is not connected to other further links.

For this finger design, 9 inertial terms of the matrix $\boldsymbol{M}$ are to be evaluated, but due to the symmetry structure of the inertia matrix ($M_{ij} = M_{ji}$) the number reduces to 6 terms.

Coriolis and Centripetal Terms :

The velocity related coefficient in the Coriolis ($\dot{\theta}_i, \dot{\theta}_j$) and centrifugal terms ($\dot{\theta}_{ii}^{\,2}$) are of great importance when an object is manipulated at high speed of motion. There are a number techniques used to develop these velocity dependent terms. However, we shall employ the algorithm adopted by ZOMAYA [1992] where the double differential term in Eq. A5.14-b, the $(\partial^2 \boldsymbol{T}_L / \partial\theta_j\, \partial\theta_k)$, are approximated by differential rotation and translation. This can be stated as :

$$(\partial^2 \boldsymbol{T}_L / \partial\theta_j\, \partial\theta_k) = \boldsymbol{T}_L\, \Delta_j^L\, \Delta_k^L$$

Hence the Coriolis and Centripetal terms of Eq. A5.14 were stated as:

$$N_{jK}^{i} = \sum_{L=max(i,j)}^{j} \sum^{j} T_r \left[(\partial^2 \boldsymbol{T}_L / \partial\theta_j \partial\theta_K) \, \boldsymbol{U}_L \, (\partial \boldsymbol{T}_L / \partial\theta_i)^T \right] \qquad \text{(A5.23)}$$

In Eq. A5.21, a further simplification could be done by premultiplying and postmultiplying by T_L and T_L^T respectively, since this will cause the trace operation to remain unchanged, affecting the rotation part only. Thus Eq. A5.22 is expressed as:

$$N_{jk}^{i} = \sum_{L=max(i,j,k)}^{3} T_r \left[\Delta_j^L \Delta_K^L \, \boldsymbol{U}_L \, \Delta_i^{LT} \right] \qquad \text{(A5.24)}$$

What we are after is the expansion of Eq. A5-23 in terms of $\Delta_j^L \Delta_K^L \, \boldsymbol{U}_L \, \Delta_i^{LT}$ and dropping the terms which are off diagonal in the pesudo-inertial matrix. Once again by the application of MATHEMATICA software and through the simplification of the terms we arrived at terms which are velocity dependent as:

$$N_{11} = [-\tfrac{1}{2} L_1 L_2 m_2 S_2 - \tfrac{1}{3} L_2^2 m_2 C_2 S_2 + L_2 L_3 m_3 C_{23} S_2 - L_2 m_3 \Psi S_2 +$$

$$\tfrac{1}{6} L_3^2 m_3 S_{23} C_{23} - \tfrac{1}{2} L_3 m_3 \Phi S_{23}] 2\dot{\theta}_1 \dot{\theta}_2 + [\tfrac{1}{6} L_3^2 m_3 C_{23} - \tfrac{1}{2} L_3 m_3 \Psi S_{23}] 2\dot{\theta}_1 \dot{\theta}_3$$

$$N_{22} = [-\tfrac{1}{2} L_2 L_3 m_3 S_3] \dot{\theta}_3^2 + [-\tfrac{1}{2} L_2 L_3 m_3 S_3] 2\dot{\theta}_2 \dot{\theta}_3 + [\tfrac{1}{2} L_1 L_2 m_2 S_2 + \tfrac{1}{3} L_2^2 m_2 C_2 S_2 -$$

$$\tfrac{1}{2} L_2 L_3 m_3 C_{23} S_2 - \tfrac{1}{6} L_3^2 m_3 S_{23} C_{23} + \tfrac{1}{2} L_3 m_3 \Psi S_{23}] \dot{\theta}_1^2$$

$$N_{33} = [\tfrac{1}{2} L_3 m_3 \Psi S_{23} - \tfrac{1}{6} L_3^2 m_3 S_{23} C_{23}] \dot{\theta}_1^2 + [\tfrac{1}{2} L_2 L_3 m_3 S_3] \dot{\theta}_2^2 \qquad \text{(A5.25)}$$

Gravitational Loading Terms :

The third term in the dynamic equation of a finger is the vector of gravitational loading

acting in the fingers links, which is important for static grasping of an object. The gravity term can be expressed as:

$$C(\Theta) = \partial P(\theta) \partial\theta \tag{A5.26}$$

With reference to Eq. A5.14.c, the gravity terms loading is given by $-\sum_{L=i}^{3} m_L$ $\boldsymbol{g}^T(\partial \boldsymbol{T}_L / \partial\theta_i)\boldsymbol{r}^L{}_L$. If $(\partial \boldsymbol{T}_L / \partial\theta_i)$ is designated by $\boldsymbol{U}_{ij}$ then by expanding this equation gives :

$$\begin{aligned} C_1 &= -(m_1 \boldsymbol{g}^T \boldsymbol{U}_{11}{}^1\boldsymbol{r}_1 + m_2 \boldsymbol{g}^T \boldsymbol{U}_{21}{}^2\boldsymbol{r}_2 + m_3 \boldsymbol{g}^T \boldsymbol{U}_{31}{}^3\boldsymbol{r}_3) \\ C_2 &= -(m_2 \boldsymbol{g}^T \boldsymbol{U}_{22}{}^2\boldsymbol{r}_2 + m_3 \boldsymbol{g}^T \boldsymbol{U}_{32}{}^3\boldsymbol{r}_3) \\ C_3 &= -(m_3 \boldsymbol{g}^T \boldsymbol{U}_{33}{}^3\boldsymbol{r}_3) \end{aligned} \tag{A5.27}$$

The matrix $\boldsymbol{U}_{ij}$ is to be evaluated using :

$$\begin{aligned} \boldsymbol{U}_{ij} &= {}^0\boldsymbol{T}_{j-1}\, \boldsymbol{Q}\, {}^{j-1}\boldsymbol{T}_i \qquad \text{for } j \le i \\ &0 \qquad\qquad\qquad\qquad \text{for } j > i \end{aligned} \tag{A5.28}$$

where $\boldsymbol{Q}$ is a matrix of partial derivative defined as :

$$\boldsymbol{Q} = \begin{bmatrix} 0 & -1 & 0 & 0 \\ 1 & 0 & 0 & 0 \\ 0 & 0 & 0 & 0 \\ 0 & 0 & 0 & 0 \end{bmatrix} \tag{A5.29}$$

Further application of Eq. A5.27 give:

$$\begin{aligned} C_1 &= 0 \\ C_2 &= \tfrac{1}{2} g L_2 m_2 C_2 + \tfrac{1}{2} g L_3 m_3 C_{23} + g L_2 m_3 C_2 \\ C_3 &= \tfrac{1}{2} g L_3 m_3 C_{23} \end{aligned} \tag{A5.30}$$

REFERENCES

Allen A. J. and Mitchell R. J., [1986]. " Cybernetics Computerised Learning of Interactive Design ," *IEE Colloquim on the use of personal computers in control systems analysis*, London.

Al-Gallaf E., Allen A., and Warwick K., [1992]. "Multifingered Robot Hands, in " *Robotic Systems*' , S. G. Tzafestas (ed.), Kluwer, pp. 542-550.

Al-Gallaf E., Allen A., and Warwick K., [1993-a]. "A Survey of Multi-fingered Robot Hands : Issues and Grasping Achievements," *International Journal of Mechatronics*, vol. 3, no 4., pp. 465-49.

Al-Gallaf E., Allen A., and Warwick K., [1993-b]. " Dextrous Hands: Issues Relating To a Four-Finger Articulated Hand," *International Journal of Mechatronics*, vol. 3, no.3, pp. 329-342.

Al-Gallaf E., Allen A., and Warwick K., [1991]. " Evaluation of a Direct Drive Approach in Multi-fingered Robotics Hands", *IEE Colloquium on Robot Actuators*, London, pp. 7/1-7/4.

AL-Gallaf E. and Warwick K., [1994-a]. " Compliance Motion Within an Optimal Contact Force", *Proceedings of the Tampere International Conference on Machine Automation*, pp.159-172, Tampere, Finland.

AL-Gallaf E., and Warwick K., [1994-b]. " Optimal Manipulation Forces

Distribution for Controlling an Object Motion in a Four Fingered Robot Hand (cyb-Hand), " *Proceedings of the IEE International Control-94 Conference*, Warwick University, UK.

AL-Gallaf E, [1994-c]. " A Four Fingered Robot Hand Design, Control and Programming ", *Technical Report in a Four Fingered Hand*, Dept. of Cyberentics, University of Reading.

AL-Gallaf E. and Warwick K., [1994-d]. " Cybhand : A Four Fingered Robot Hand", *IMACS International Symposium on Signal Processing, Robotics and Neural Networks*, Lille , France, pp. 590-593.

Anderson K. and Angeles J. , [1989] " Kinematic Inversion of Robotic Manipulators in the Presence of Redundancies, " *The International Journal of robotics research*, vol. 8, no.6, pp. 80-97.

Asada H., Kanade T., and Takeyama I., [1983]. "Control of a Direct-Drive Arm," *ASME. Transactions. of Journal of Dynamic Systems, Measurement, and Control*, no. 105, pp. 136-142.

Bejczy A. K., [1974]. " Robot Arm Dynamics and Control," *NASA-JPL Technical Memorandum*, pp. 33-669.

Biccgi A. and Prattichizzo D., [1992]. "New Issues in the Kineto-Statics, Dynamics, and Control of Whole-Hand Manipulation, " *Proceedings of the IMACS/SICE Inter. Symposium on Robotics, Mechatronics and Manufacturing Systems*,

Kobe, Japan, pp. 677-683.

Boullion T. L., and Odell , P. L., [1971]. " Generalized Inverse Matrices, " *Wiely-Interscience*, New York.

Bruno M. J., [1992]. "Man-Equivalent Telepresence Through Four Fingered Human-Like Hand System," *Proceedings of the IEEE International Conference on Robotics and Automation*, Nice, France, pp. 843-848.

Burdick J. W., [1992]. " A Recursive Method for Finding Revolute-Jointed Manipulator Singularities," *Proceedings of the IEEE International Conference on Robotics and Automation*, Nice, France, pp. 448-453.

Casalino G., Aicardi M., and Cannata G., [1992] . "Recent Advances in Grasp Planning Task Representation and Learning Hybrid Control for Dexterous Manipulation," *Proceedings of the IMACS SICE International Symposium on Robotics, Echatronics and Manufacturing Systems*, Kobe, Japan, pp. 663-670.

Charles H. and Sakon K. [1990], "Optimal Force Distribution for the Legs of a Walking Machine with Friction Cone Constraints," *IEEE Tran. on Robotics and Automation*, vol. 6, no.1, pp. 73-85.

Cheng F. I. and Orin D E., [1990]. "Algorithm for Optimal Force Distribution - The Compact-Dual LP Method", *IEEE Transaction on Robotics and Automation.* vol. ra-6, no.2, pp. 178-187.

Cheng F. I. and Orin D. E., [1991]. " Efficient Formulation of the Force Distribution Equations for Simple Closed-Chain Robotic Mechanisms," *IEEE Transaction on Systems, Man, and Cybernetics*, vol. smc-21, pp. 25-32.

Chen C. L., Lee C. S., and House. S. H., [1988]. "Efficient Scheduling Algorithms for Robot Inverse Dynamics Computation on a Multiprocessor System," *IEEE Transaction on Systems, Man, and Cybernetics*, vol. 18, no.5, pp. 729-743.

Chiacchio P., Chiaverini S., Sciavicco L., and Siciliano B., [1991]. "Global Task Space Manipubility Ellipsoid for Multi-Arm Systems," *IEEE Transaction on Robotics and Automation*, vol. ra-7, pp. 678-685.

Cole A. B., Hsu A, P., and Sastry S. S., [1992]. " Dynamic Control of Sliding by Robot Hands for Regrasping," *IEEE Transactions. on Robotics and Automation*, vol. ra-8, no.1, pp. 42-52.

Coi M.H., Lee B.H., and Ko M.S., [1992]. "An Application of Force Ellipsoid to the Optimal Load Distribution for Two Cooperating Robots", *Proceedings of the IEEE International Conference on Robotics and Automation*, Nice, France, pp. 461-466.

Crowder R. M., [1991-a]. " Local Actuation of Multijointed Robotic Fingers ," *Proceedings of the IEE International Control-91 Conference*," vol. 1, no. 332, pp. 48-52.

Crowder R. M., [1991-b]. "A Manipulator For Glove-Box Operations", *International Journal of Mechatronics*, vol. 1, pp 37-58.

Cutkosky M. R., [1989]. " On Grasp Choice, Grasp Models, and the Design of Hands for Manufacturing Tasks, *IEEE Transactions on Robotics and Automation*, vol. 5, no.3, pp. 269-279.

Cutkosky M. R., [1986]. "Robotic Grasping and Fine Manipulation", Boston, MA: Kluwer.

Cutkosky M. R. and Kao I., [1989]. "Computing and Controlling the Compliance of a Robotic Hand" , *IEEE Transactions on Robotics and Automation,* vol. ra-5, pp. 151-165.

Daniel G., and Hsia S., [1988]. "Universal six-joint robot controller, " *IEE Control Systems Magazine*, pp.31-36.

Doll T. J. and Scneebeli H. J., [1988]. "The Karlsruhe hand," *IFAC Symp. on Robot Control*, Germany, pp. 37/1- 37/6.

Denavit J. and Hartenberg R. S., [1955]. A Kinematic Notation for Lower Pair Mechanisms Based on Matrices," *Journal of Applied Mechanics*, pp. 215-211.

Deo. A. S. and Walker I. D., [1992]. " Robot Subtask Performance with Singularity Robustness using Optimal Damped Least-Squares," *Proceedings. of the IEEE International Conference on Robotics and Automation*, Nice, France, PP. 434 - 441.

Derventos C. A. and Davison E.J., [1992]. " Robust Motion/Force Control Cooperative Multi-Arm Systems," *Proceedings of the IEEE International Conference on Robotics and*

Automation, Nice, France, pp. 2230-2237.

Elosequi P., Daniel R. W., and Sharkey P.M., [1990]. "Joint Servoing for Robust Manipulator Force Control, " *Proceedings of the IEEE International Conference Robotics and Automation*, pp. 246-25.

Fearing R. S., [1986]. "Simplified Grasping and Manipulation with Dextrous Robot Hands," *IEEE Journal of Robotics and Automation*, vol. ra-2, no.4, pp. 188-195.

Fu K. S., Gonzalez R.C., and Lee C.S., [1987]. " Robotics Control, Sensing, Vision, and Intelligence, " *McGraw- Hill International Editions*, Singapre.

Gilbert E. G. and Ha I. J., [1984]. "An Approach to Nonlinear Feedback Control with Applications to Robotics," *IEEE Transactions on System, Man, Cybernetics*, vol. smc -14, no. 6, pp. 879-884.

Gill, P. E., Murray W., Saunders M. A., and Wright M. H., [1983], " User's Guide for Sol/N P SOL, *Report Sol 83-12, " Department of Opertional Research, Stanford Unviersity*, Califorina 94305.

Goldfarb D. and Idnani A., [1983]. "A Numerically Stable Dual Method for Solving strictly Convex Quadratic Programs, " *Math. Program.*, 27, pp. 1-33.

Grupen R. A., Henderson T. C., and McCammon I. D., [1989]. " A Survey of General Purpose Manipulation, " *International Journal of Robotics Research*, vol. 8, pp. 38-62.

Hanafusa H. and AsadA H., [1977]. "Stable Prehension by a Robot Hand with Elastic Fingers, " *Proceedings of the 7th International Symp. on Industrial Robots*, Tokyo, pp. 361-368.

Hollerbach J. and Narasimhan S., [1986]. "Finger Force Computation without the Grip Jacobian", *Proceedings of the IEEE International Conference on Robotics and Automation*, San Francisco, pp. 871-875.

Hollerbach J., Hunter I., Lang J., Umans S., and SEPE R., [1993]. "McGill / MIT Direct Drive Motor Project," *Proceedings of the IEEE International Conference on Robotics and Automation*, Atlanta , Georgia, pp. 611-617.

Hunt K. H., Samuel A. E. and McAreeP.R., [1991]. " Special Configurations of Multi-Fingere Multi-Freedom Grippers - A Kinematic Study," *International Journal of Robotics Research*, vol. 10, no.2, p. 123-134.

Jacobsen S. C., Wood J. E., Knutti D. F., and Biggers K. B., [1984]. " The Utah/MIT Dextrous Hand : Work in progress, " *International Journal of Robotics Research*, vol. 3, pp. 21-50.

Jacobsen. S.C., [1986], "Design of the Utah/MIT dexterous hand," *Proceedings of the IEEE International Conference on Robotics and Automation*, San Francisco. CA, pp. 1520-1532.

Javaheri M. A. and Orin D., [1991]. "Parallel Algorithms for Computation of the Manipulator Inertia Matrix," *The International Journal of Robotics Research*, vol.

10, no.2, pp. 162-172.

Kao I., M. and Cutkosky M., [1992]. "Quasistatic Manipulation with Compliance and Sliding,, " *International Journal of Robotics Research*, vol. 11, pp. 20-40, February .

Kaneko M., Yokoi K. and Tanie K., [1990]. "On a New Torque Sensor for Tendon Drive Fingers", *IEEE Transactions on Robotics and Automation*, vol. 6, no.4, pp. 501- 507.

Kaneko. M. Pasetsch W. and Tolle. H., [1992]. " Input-Dependent stability of joint torque control of Tendon-driven robot hands", *IEEE Transactions on Industrial Electronics*, vol.39, No.2, pp. 96-104 .

Kasahara, H., [1993] . "Parallel Processing of Robot Control and Simulation," found in " *Parallel Computation Systems for Robotics: Algorithms and Architectures*," Edited by A. Fijany and A. Bejczy, pp.77-93, World Scientific.

Kerr J. and Roth B., [1986]. "Analysis of Multifingered Hands", *International Journal of Robotics Research*, vol. 4, pp. 3-17.

Kieffer J., [1992]. " Bifurcations and Isolated Singularities in the Inverse Kinematics of Linkages and Manipulators," *Proceedings of the IEEE International Conference on Robotics and Automation*, Nice, France, pp. 428-433.

Klema V.C. and Lanb A. J., [1980]. " The Singular Value Decomposition: Its

Computation and Some applications", *IEEE Transactions on Automatic Control,* vol. AC-25, no.2, pp. 164-176.

Koichi S. L., Shichi L. and Tanaka H., [1991]. "Applying a Flexible Microactuator to Robotic Mechanisms," *Proceedings of the IEEE International Conference on Robotics and Automation,* pp. 21-26.

Krigman D., Siegel D. and Gerpheide G., [1985]. " Computational Architecture for the UTAH-MIT Hands", *Proceedings of the IEEE on Robotics and Automation*, pp. 918-924.

Kvikels N. and Fassams P., [1984]. "Microprocessors Implementation of PID Controllers and Lead-Lag Compensators", *IEEE Transactions on Industrial Electronics*, vol. IE-31, no.1, pp. 79-85.

Kumar V. R. and Waldron K.J., [1988]. " Force distribution in closed kinematic chains, " *IEEE Transactions on Robotics and Automation*, vol.4, no.6, pp. 657-663.

Kumar V. R., [1993]. "A Compact Inverse Velocity Solution for Redundant Robots," *The International Journal of Robotics Research*, vol. 12, no.1, pp. 45-54.

Laroussi K., Hemami H. and Goddard R., [1988]. " Coordination of two planar robots in lifting, " *IEEE Journal of Robotics and Automation*, vol.4, no.1, pp. 77-85.

Lathrop, R. H., [1985], "Parallelism in Manipulator Dynamics," *International Journal of Robotics Research*, vol.4, no.2, pp. 80-102.

Lawson C. L. and Hanson R. J., [1974], " Solving Least Squares Problems, " Englewood, Clifls, NJ : Prentice-Hall.

Lee C. S., [1993]. " Parallel Algorithms and Architectures for Inverse Dynamics Computation", found in *"Parallel Computation Systems for Robotics: Algorithms and Architectures,"* Edited by A. Fijany and A. Bejczy, pp.77-93, World Scientific.

Lee S. G., and Chang, P. R., [1988]. " Efficient Parallel Algorithm for Robot Forwards Dynamics Computation, " *IEEE Transactions on System, Man, and Cybernetics*, vol. smc-18, no.2, pp. 238-251.

Lewis F. L ., Abdallah, C. T. and Dawson D. M., [1993]. "Control of Robot Manipulators", *Macmillan Publishing Company*, New York, USA.

Luenberger D. G., [1984]. "Introduction to Linear and Nonlinear Programming " Second Edition, *Addison-Wesley Publishing Company*, Reading, UK.

Luh, J. Y. and Lin C. S., [1982]. "Scheduling of Parallel Computation for a Computer Controlled Mechanical Manipulator," *IEEE Transactions on Systems, Man, and Cybernetics*, vol. smc-12, no.2, pp. 214-234.

Luh J. Y., Walker M. W., and Paul R. P. ,[1980]. " On-line Computational Scheme for Mechanical Manipulators," *Transactions ASME J. Dynamic Systems*, vol. 102, pp. 69-76.

Luh J.Y., [1983]. "Conventional Controller Design of Industrial Robots - A Tutorial,

" *IEEE Transactions on System, Man, and Cybernetics*, vol. smc-13, no. 3, pp. 298-316.

Maekawa H., Tanie K., Komoriya K., Kaneko M., Horiguchi C., and Sugawara T., [1992]. " Development of a Finger-Shaped Tactile Sensor and its Evaluation by Active Touch," *Proceedings of the IEEE International Conference on Robotics and Automation*, Nice, France, pp. 1327-1334.

Markenscoff X., Luqun Ni. and C.H. PAPADI Mitrious, [1990]. "The Geometry of Grasping," *The International Journal of Robotics Research*, vol. 9, no. 1, pp. 61-74.

Mason M. T. and Salisbury J. K., [1985]. "Robot Hands and the Mechanics of Manipulation," Cambridge, MA : MIT Press.

McAree P., Samuel A. and Hunt K., [1991]. "A Dexterity Measure for the Kinematic Control of a Multifinger, Multifreedom Robot Hand" , *The International Journal of Robotics Research*, vol. 10, pp. 439-453.

Mckerrow P. J., [1991]. " Introduction to robotics, " Addison-Wesley, Singapore.

Michelman P. and Allen P., [1993]. " Compliant Manipulation with Dextrous Robot Hand," *Proceedings of the IEEE International Conference on Robotics and Automation*, Atlanta , Georgia, pp. 711-716.

Mishra B. and Silver N., [1989]. " Some Discussion of Static Gripping and its Stab ility, " *IEEE Transactions on System, Man, and Cybernetics*, vol. smc-19, pp.

783-796, July/August .

Montanan D., [1986]. " Tactile sensing and kinematics of contact," *Ph.D. Thesis, Division of Applied Sciences*, Harvard University.

NAG, [1989]. " Library in documentation of the Numerical Analysis Group," *University of Reading*, Computer Service.

Nagashima F. and Nakamura Y., [1992]. " Efficient Computation Scheme for the Kinematics and Inverse Dynamics of a Satellite-Based Manipulator," *Proceedings of the IEEE International Conference on Robotics and Automation*, Nice, France, pp. 905-912.

Nagai K. and Yoshikawa T., [1993]. " Dynamic Manipulation - Grasping Control of Multifingered Robot Hands," *Proceedings of the IEEE International Conference on Robotics and Automation*, Atlanta , Georgia , pp. 1027-1033.

Nakamura Y., Nagai K. and Yoshikawa T., [1987]. " Mechanics of Coordinated Manipulation by Multiple Robotic Mechanisms, " *Proceedings of the IEEE International Conference in Robotics and Automation* , pp. 991-998.

Nakamura Y., Nagai K. and Yoshikawa T., [1989]. " Dynamic and Stability in Coordination of Multiple Robotic Mechanisms," *The International Journal of Robotics Research*, vol.8, no.2, pp. 44-61.

Nakamura Y., [1991]. " Advanced Robotics ; Redundancy and Optimization," Addison-Wesley Publishing, USA.

Nahon M. A. and Angeles J., [1992]. " Real-Time in Parallel Kinematic Chains under Inequality Constraints, " *IEEE Transactions on Robotics and Automation* , vol. ra-8, no. 4, pp. 439-450.

Nahon M. A. and Angeles J., [1991]. "Optimization of Dynamic Forces in Mechanical Hands," *ASME Journal of Mechanical Design*, vol. 113, pp. 167-173.

Narasimhan S., Siegal D. and Hollerrach J. M., [1989]. " CONDOR : An Architecture for Controlling the UTAH-MIT Dexterous Hand", *IEEE Transactions on Robotics and Automation*, vol. ra-5, no.5, pp. 616-627.

Nguyen V. D., [1989]. " Constructing Stable Grasps, " *The International Journal of Robotics Research*, vol. 8, no.1, pp 26-37.

Ogata K., [1987] . " Discrete-Time Systems", *Prentice-Hall International*, USA.

Okada T., [1979]. " Object-Handling System for Manual Industry, " *IEEE Transactions on System, Man, and Cybernetics*, vol. smc-9, no.2, pp. 79-89.

Orin D. E., Chao H. H., Olson K. W., and Schrader W. W., [1985], " Pipeline/Parallel Algorithms for the Jacobian and Inverse Dynamics Computations," *Proceedings of the IEEE International Conference on Robotics and Automation*, pp. 785-789.

Park Y. and Starr G., [1989]. "Finger Force Computation for Manipulation of An Object by A Multifingered Robot Hand, *"Proceedings of the IEEE International Conference in Robotics and Automation*, pp. 930-935.

Penrose R. , [1955]. " A Generalized Inverse for Matrices, " *Proceedings Cambridge Phil. Soc. 51* : 406-413.

Ping H., and Steven S., [1992]. " Coordinated Control of Multiple Manipulator Systems - Experimental Results," *Proceedings of the IEEE International Conference on Robotics and Automation*, France, Nice, pp. 2199-2204.

Paul R. P., [1981]. "Robot Manipulators: Mathematics, Programming, And Control," *MIT Press*, Cambridge, USA.

Ponce J., Sullivan S., Boissonnat J., and Merlet J., [1993]. " On Characterizing and Computing Three - and Four - Finger Force-Closure Grasps of Polyhedral Objects," *Proceedings of the IEEE International Conference on Robotics and Automation, Atlanta , Georgia*, pp. 821-827.

Powell M.J.D., [1985]. "On the Quadratic Programming Algorithm of GOLDFRAB and IDNANI, " *Mathematical Programming Study*, vol. 25, North-Holland, pp.46-61.

Ramadorai A. K., Tran T. J. and Bejczy A. K., [1992]. " Task Definition, Decoupling and Redundancy Resolution by Nonlinear Feddback in Multi-Robot Object handling, " *Proceedings of the IEEE International Conference on Robotics and Automation*, Nice, France, pp. 467- 474.

Rao S. S., [1984] , " Optimization Theory and Applications", New Delhi, India

Richard D.K., Chmielewski T. A., and Negin M. [1989], Robot Engineering; An Integrated Approach, : *Prentice-Hall Press*, USA.

Roberts K., [1990]. "Coordinating a Robot Arm and Multi-finger Hand Using the Quaternion Representation", *Proceedings of IEEE International Conference in Robotics and Automation*, pp. 1252-1257.

Rohling R. N. and Hollerbach J., [1993]. " Optimized Fingertip Mapping for Tele-operation of Dextrous Robot Hands," *Proceedings of the IEEE International Conference on Robotics and Automation*, Atlanta, Georgia, pp. 769 - 775.

Romdhane L. and Duffy J., [1990]. " Kinestatic Analysis of Multifingered Hands, " *The International Journal of Robotics Research*, vol. 9, no.6, pp. 3-18.

Russell R. A., [1990]. "Robot Tactile Sensing, " *Prentice Hall Press*, Australia.

Salisbury J. K., [1984]. " Design and Control of an Articulated Hand, " *Proceedings of the First International Symposium on Design and Synthesis*, Tokyo.

Salisbury J. K. and Craig J. J., [1982]. "Articulated Hands : Force Control and Kinematic Issues ," *The International Journal of Robotics Research*, vol. 1, no.1, pp. 4-17.

Salisbury J. K., [1982]. " Kinematic and Force Analysis of Articulated Hands,"

Ph.D. Thesis, Department of Mechanical Engineering, Stanford University.

Salisbury J., [1983]. " Interpretation of Contact Geometries From Force Measurements, " *Proceedings of the 1st International Symposium on Robotics Research,* MIT Press, Cambridge, Massachusetts.

Samson C., Borgne M., and Espiau B., [1991]. " Robot Control : Task Definition Approach," *Clarendor Press,* Oxford, UK.

Sarkar N., Yun X., and Kumar V., [1993]. " Dynamic Control of 3-D Rolling Contacts in Two-Arm Manipulation", *Proceedings of the IEEE International Conference on Robotics and Automation,* Atlanta , Georgia , pp. 978- 983.

Schneider S.A. and Robert H. Jr., [1992]. " Object Impedance Control for Cooperative Manipulation: Theory and Experimental Results", *IEEE Transactions on Robotics and Automation,* vol. ra-8, no.3, pp. 383-394.

Shimoga K. B. and Goldenberg A. A., [1992]. " Soft Materials for Robottc Fingers," *Proceedings of the IEEE International Conference on Robotics and Automation,* Nice, France, pp. 1300-1305.

Stansfield S. A., [1991]. "Robotic Grasping of Unknown Objects A Knowledge-Based Approach, " *International Journal of Robotics Research,* vol. 10, pp. 314-326.

Sugano S. and Kato I., [1987]. " Wabot-2 : Autonomous Robot With Dexterous Finger-Arm Coordination Control in Keyboard Performance, " *Proceedings of IEEE Inter-*

national Conference in Robotic and Automation, pp. 90-97.

Swift D. C., Kaufman H. and Cummings S. T., [1993]. "Direct Model Reference Adavtipe Control of a Puma Manipulator ", *Proceedings of the IEEE International Conference on Robotics and Automation*, Atlanta , Georgia , pp. 346-351.

Tao J. M., and Luh J. Y. S ., [1992]. " Robust Position and Force Control for a System of Multiple Redundanti-Robots," *Proceedings of the IEEE International Conference on Robotics and Automation*, Nice, France, pp. 2211-2216.

Venkatavaman S.T. and Djaferis T. E., [1987]. " Multivariable Feedback Control of the JPL/Stanford hand, " *Proceeding of the IEEE on Robotics and Automation*, pp. 77-82.

Wampler C. W., [1986]. " Manipulator Inverse Kinematic Solutions Based on Vector Formulations and Damped Least-Squares Methods," *IEEE Transactions on System, Man, Cybernetics*, vol. smc -16, no.1, pp. 93-101.

Walker I. D. , Freeman R. A. and Marcus S.I., [1991]. " Analysis of Motion and Internal Loading of Objects Grasped by Multiple Cooperating Manipulators, " *The Inter. Journal of Robotics Research*, vol. 10, no. 4, pp. 396-409.

Warwick K. , [1993] . "Robotics : Applied Mathematics and Computational Aspects," *Clarendon Press*, Oxford.

Wolfram S., [1988]. "Mathematica : A System for Doing Mathematics by Computer," *Addison Wesley*, USA.

Yoshikawa T. and Nagai K., [1991]. "Manipulating and Grasping Forces in Manipulation by Multifingered Robot Hands, " *IEEE Transactions Robotics and Automation*, vol. ra-7, pp. 67-77.

Yoshikawa T., and Zheng X., [1993]. " Coordinated Dynamic Hybrid Position/Force Control for Multiple Robot Manipulators Handling One Constrained Object," *International Journal of Robotics Research*, vol. 12, no. 3, pp. 219-230.

Young P. G. and Starr G.P., [1989]. " Finger Force Computation for Manipulation of an Object by a Multifingered Robot Hands," *Proceedings of the IEEE International Conference on Robotics and Automation*, pp. 930-935.

Young P. G., and Starr G. P., [1990]. "Optimal Grasping Using a Multifingered Robot Hand ", *Proceedings of the IEEE International Conference in Robotics and Automation*, pp. 689-694.

Yun X., Kumar V., Sarkar N. and Paljug E., [1992]. "Control of Multiple Arms with Rolling Constraints," *Proceedings of the IEEE International Conference on Robotics and Automation*, Nice, France, pp. 2193-2198.

Yokokohji Y. and Yoshikawa T., [1992]. " Bilateral Control of Master-Salve Manipulators for Ideal Kinesthetic Coupling, " *Proceedings of the IEEE International Conference on Robotics and Automation*, Nice, France, pp. 849-858.

Yun X., [1993]. "Object handling using two arms without grasping, " *The International Journal of Robotics Research*, vol. 12, no. 1, pp. 99-106.

Zexiang L., Hsu P. Li and Sastry S., [1989]. "Grasping and Coordinated Manipulation by a Multifingered Robot Hand," *International Journal of Robotics Research*, vol. 8, no.4, pp. 33-50.

Zexiang Li. and Sastry S., [1988]. " Task-Oriented Optimal Grasping by Multifingered Robot Hands, " *IEEE Transactions on Robotics and Automation*, vol. ra-4, pp. 32-43 .

Zuofeng L., Tran T.J. and Bejczy A. K., [1991]. " Dynamic Workspace Analysis of Multiple Cooperating Robot Arms, " IEEE Transactions on Robotics and Automation, vol.7, no.5, pp. 589-596.

Zomaya, A. Y. and Morris A. S., [1989]. " On the Complexity Reduction of the Coriolis and Centripetal Effects of a 6-dof Robot Manipulators," in Robot Control : Theory and Applications, Edited by K. Warwick, *Peter Peregrinus Ltd.*, pp. 71-81.

Zomaya, A. Y. and Morris A. S., [1993]. " Transputer Networks for Fast Robot Dynamics", in Robotics: Applied Mathematics and Computational Aspects", Edited by K. Warwick, *Clarendon Press*, Oxford, pp. 335-353.

Zomaya A. Y. [1992], " Modelling and Simulation of Robot Manipulators: A Parallel Processing Approach, *World Scientific Publishing*, Singapore.